Loughborough University

This item was submitted to Loughborough University as a PhD thesis by the author and is made available in the Institutional Repository (https://dspace.lboro.ac.uk/) under the following Creative Commons Licence conditions.

creative commons

COMMONS DEED

Attribution-NonCommercial-NoDerivs 2.5

You are free:

- to copy, distribute, display, and perform the work

Under the following conditions:

Attribution. You must attribute the work in the manner specified by the author or licensor.

Noncommercial. You may not use this work for commercial purposes.

No Derivative Works. You may not alter, transform, or build upon this work.

- For any reuse or distribution, you must make clear to others the license terms of this work.
- Any of these conditions can be waived if you get permission from the copyright holder.

Your fair use and other rights are in no way affected by the above.

This is a human-readable summary of the Legal Code (the full license).

Disclaimer

For the full text of this licence, please go to:
http://creativecommons.org/licenses/by-nc-nd/2.5/

BLDSC no:- DX 176076

LOUGHBOROUGH
UNIVERSITY OF TECHNOLOGY
LIBRARY

AUTHOR/FILING TITLE

THORNLEY, J.M.

ACCESSION/COPY NO.

0400738775

VOL. NO. | CLASS MARK

06 DEC 1999

1

30 MAR 2000

FOR REFERENCE ONLY

14 APR 2000

18 MAY 2000

27 JUN 1997

0400738775

BADMINTON PRE
18 THE HALFORD
SYSTON
LEICESTER LE7
ENGLAND
TEL: 0533 6029
FAX: 0533 6956

BLDSC no:- DX 176076

LOUGHBOROUGH
UNIVERSITY OF TECHNOLOGY
LIBRARY

AUTHOR/FILING TITLE

THORNLEY, J.M.

ACCESSION/COPY NO.

0400738775

VOL. NO. | CLASS MARK

date due

18 FEB 1997
LOAN 3 WKS. + 3
UNLESS RECALLED
AC 13751

20 MAR 1997

27 JUN 1997

21 MAY 1997

27 JUN 1997

26 JUN 1998

20 MAR 1998

24 APR 1998
12 JUN 1998

1 DEC 1998

26 MAR 1999

18 NOV 1999

0400738775

BADMINTON PRE
18 THE HALFORD
SYSTON
LEICESTER LE7
ENGLAND
TEL: 0533 6029
FAX: 0533 6956

BLDSC no:- DX 176076

LOUGHBOROUGH
UNIVERSITY OF TECHNOLOGY
LIBRARY

AUTHOR/FILING TITLE

THORNLEY, J.M.

ACCESSION/COPY NO.

0400738775

VOL. NO.	CLASS MARK	
	LOAN COPY	
~~14 JAN 1994~~	- 1 JUL 1994	15 DEC 1995
9 FEB 1994	30 JUN 1995	23 MAY 1996
7 MAR 1994	30 JUN 1995	14 JUN 1996
12 MAY 1994	30 JUN 1995	- 6 NOV 1996
	15 NOV 1995	

0400738775

BADMINTON PRE
18 THE HALFORD
SYSTON
LEICESTER LE7
ENGLAND
TEL: 0533 6029
FAX: 0533 6956

METHODS OF APPLICATION OF PIEZOELECTRIC MULTILAYER ACTUATORS TO HIGH-SPEED CLUTCHING, USING DISPLACEMENT AMPLIFICATION.

by

J. K. Thornley, B.Sc. (Physics)

A DOCTORAL THESIS
SUBMITTED IN PARTIAL FULFILMENT OF THE REQUIREMENTS
FOR THE AWARD OF
THE DEGREE OF DOCTOR OF PHILOSOPHY,
of the Loughborough University of Technology
January, 1993.

© by J. K. Thornley

Aug 93
0400 73877
W9920222

SUMMARY.

The suitability of electromagnetic actuating devices for application to machines with ever more demanding response time specifications is discussed, with the proposal that piezoelectric actuator technology can produce practical devices with faster response times than solenoids, for example. This thesis discusses and validates the proposition that the performance of piezoelectric ceramic actuators makes them viable devices for inclusion in high-speed machine applications, where rapid clutching using two-state actuation is required. Further, techniques are devised and explored for the design and application of these devices using displacement amplifying structures, which lead to the utilisation of engineering methods of relatively low precision. This is highly advantageous as to date, the piezoelectric multilayer actuator has usually been associated with high precision engineering.

Applications of piezoelectric ceramic technology are reviewed, and the mechanical and electrical properties of these materials are discussed. Literature covering applications of piezoelectric actuators in relation to clutches, motors and positioners is also reviewed. This data search revealed many devices or systems where the displacement amplification of piezoelectric actuators was exploited in some way, but failed to show any devices where the high efficiency of these amplifying structures was either primary or even necessarily achieved. Indeed, it was concluded that in the absence of such applications or methodologies, a fruitful area of research might be to explore these methodologies. This work is a core element of this thesis.

Using two basic topologies, devices producing efficient transformation of high-force, small movement two-state actuation, to larger movement with lower force, have been designed (using flexural hinge methods), manufactured, tested and analyzed. Hydraulic transformers have been briefly investigated and ultimately rejected on the grounds of comparative complexity. For any displacement amplifying or transforming device, applications for these systems are widely varying, but criteria for advantageous employment of the piezoelectric approach, as opposed to electromagnetic, are established.

Design techniques which are partially analytical and partially experiential are proposed, which in practice exhibit adeptness for producing well-optimised designs. These methods are incorporated into special purpose structure-designer computer programs. Several design examples are detailed, and their performance analyzed in comparison with the modelling techniques and design program predictions.

The application of these displacement amplifiers is discussed by example, to two discrete motion machines, both of which have been designed specifically to demonstrate the possibilities of using piezoelectric technology to regulate discrete motion drives. It is shown that the speed of response of the devices is such, that the concept of zero-velocity clutching with the intention of minimising wear, is feasible.

ACKNOWLEDGEMENTS.

The author wishes to express his thanks and appreciation to his Director of Studies, Dr. T.G.King and his Supervisor, Dr. M.E.Preston, both of The University of Technology at Loughborough, for their consistent and helpful support for the duration of this research project.

Technical support from Mr. V.Roulstone, Mr. A.Pearson and Mr. J.Robins of the Department of Mechanical Engineering in the construction of test equipment, has been greatly appreciated, as has photographic services from Mr. K.Topley.

Acknowledgement is also due to Mr. P.Norton, along with Mr. J.A.Guy and his staff for providing valuable support in the area of electronics instrumentation and construction.

Finally, thanks are due to Dr. G.Sweeney for his involvement with the Specially Promoted Programme in the Design of High-Speed Machinery.

DECLARATION.

This is to certify that I am responsible for the work submitted in this thesis and that the original work is my own, except where due reference to previous work has been acknowledged. I also certify that neither this thesis, nor the original work contained therein has been submitted to this or any other institution for a higher degree.

CONTENTS

1 **INTRODUCTION.** 1
1.1 HIGH-SPEED MACHINES. 1
1.2 LIMITATIONS OF SOLENOIDS. 1
1.3 DISCRETE MOTION DRIVES. 4

2 **PIEZOELECTRICITY AND ITS APPLICATION IN ACTUATORS.** . . 6
2.1 THE PHENOMENON OF PIEZOELECTRICITY. 6
2.2 APPLICATIONS OF DIRECT PIEZOELECTRICITY. 7
2.3 THE CONVERSE PIEZOELECTRIC EFFECT. 8
2.4 RECENT APPLICATIONS OF PIEZOELECTRIC ACTUATORS. 10
2.4.1 Optical Alignment Actuator. 10
2.4.2 Bimorphs and Unimorphs. 11
2.4.3 Stacks. 12
2.4.4 A Piezoelectric Print Head. 13
2.4.5 A Rotary Wave Motor. 14
2.4.6 A Piezoelectric 'Inchworm' Drive. 15
2.5 CHARACTERISTICS OF PIEZOELECTRIC MATERIALS. 15
2.5.1 Compliance: S^E. 16
2.5.2 Dynamic Operation. 17
2.5.3 Hysteresis and Non-Linearity. 19
2.5.4 Creep. 19
2.5.5 The d_{33} Coefficient. 20
2.5.6 Temperature Response. 20
2.6 MECHANICAL LOADING. 22
2.7 ELECTRICAL DRIVE SYSTEMS. 27
2.7.1 Simple Drives. 27
2.7.2 Digital Drives. 29
2.7.3 Linear Drives. 30
2.8 MOUNTING CONSIDERATIONS. 32
2.9 DISCUSSION. 33

3 **HIGH SPEED ACTUATORS : A LITERATURE REVIEW.** 34
3.1 TECHNIQUES. 34
3.2 CHARACTERISATION AND MODELLING. 35
3.3 SPECIFIC APPLICATIONS. 35
3.3.1 Displacement/Force Controllers. 36
3.3.2 Wave Motors. 37
3.3.3 Inchworms (Rotary/Translational) 37
3.3.4 Inertial Pulse Caterpillars. 38
3.3.5 Impulse Transfer Devices. 38
3.3.6 Bi-Stables. 39
3.3.7 Clutches or Brakes. 39
3.4 GENERAL PAPERS AND REVIEWS. 39

3.5 DISCUSSION OF REVIEW FINDINGS. 40

4 FEASIBILITY OF DIRECT PIEZOELECTRIC CLUTCHING. 42
4.1 DIRECT ACTION PIEZOELECTRIC CLUTCHING. 42
4.2 MECHANICAL AMPLIFIERS AND ACTUATOR REQUIREMENTS. 46
4.3 AN APPRAISAL OF THE CLUTCHING FUNCTION. 48
4.4 CANDIDATES FOR DISPLACEMENT AMPLIFYING SYSTEMS. 49
4.4.1 Simple Lever (Direct Output). 50
4.4.2 Simple Lever (Transverse Output). 52
4.4.3 Compressive Flexural Bridge. 53
4.4.4 Snap Action Toggle (Bi-Stable Device). 55
4.4.5 Hydraulic Amplifier. 62
4.5 MISCELLANEOUS DISPLACEMENT AMPLIFIER DESIGNS. 65
4.5.1 Piezoelectric Electronic Jacquard Actuator. 65
4.5.2 High-Gain Compound Amplifiers. 66
4.6 ACTUATOR REQUIREMENTS. 68
4.6.1 Selection of Actuator. 68
4.6.2 Specification. 70
4.7 OBSERVATIONS. 71

5 A PIEZOELECTRIC CLUTCHING ELEMENT. 73
5.1 OVERVIEW. 73
5.2 THE CLUTCHING APPLICATION. 73
5.3 DEVICE DESIGN. 74
5.3.1 Overview. 74
5.3.2 Design Techniques. 75
5.3.3 Materials. 76
5.3.4 Design Method. 77
5.3.5 Finite Element Analysis. 78
5.3.5.1 Static Analysis. 78
5.3.5.2 Dynamic Analysis. 80
5.3.6 Fabrication. 80
5.4 PERFORMANCE. 81
5.4.1 Static. 81
5.4.2 Dynamic. 84
5.4.3 Device Damping. 85
5.5 FATIGUE STUDIES. 86
5.5.1 Loading. 87
5.5.2 Fatigue Under Repeated Stress. 88
5.5.3 Endurance Test. 91
5.5.4 Results. 92
5.6 DISCUSSION. 92

6 THE DESIGN OF SIMPLE BEAM DISPLACEMENT AMPLIFIERS. 94
6.1 INTRODUCTION. 94
6.2 THE GENERIC SOLUTION. 94
6.3 DESIGN METHODOLOGY. 95
6.3.1 Output Force / Displacement Characteristics. 96

6.3.2 Choice of Actuator. 97
6.3.3 Choice of Material and Billet Thickness. 97
6.3.4 Solution of l_1, l_2, w_1, w_2. 98
6.3.5 Solution of a_1, a_2. 99
6.3.6 Solution of d, e_1, e_2. 103
6.4 MATERIAL AND TOPOLOGICAL LIMITATIONS. 106
6.5 ASSESSMENT OF MAXIMUM ATTAINABLE EFFICIENCY. 107
6.6 REAL STRUCTURES. 111
6.7 TEST CASES. 115
6.7.1 Example 1: 0.1 mm Output. 115
6.7.2 Example 2: 0.2 mm Output. 121
6.7.2.1 Static Performance. 122
6.7.2.2 Dynamic Performance. 128
6.7.2.3 Mechanical Damping. 131
6.7.2.4 Electrical Response Control. 137
6.8 OBSERVATIONS. 139

7 THE DESIGN OF FLEXURAL BRIDGE DISPLACEMENT AMPLIFIERS. 143
7.1 INTRODUCTION. 143
7.2 SEMI-ANALYTICAL MODEL. 144
7.2.1 Analytical Solution. 144
7.2.2 Testing the Semi-Analytical Model. 150
7.3 ITERATIVE SOLUTION. 152
7.3.1 Basic Algorithm. 152
7.3.2 Iteration Algorithms. 153
7.4 THE DESIGNER PROGRAM. 157
7.4.1 Method. 158
7.4.2 Program Performance. 160
7.4.3 A Test Case. 163
7.4.3.1 Finite Element Modelling. 165
7.4.3.2 Real Device Performance. 166
7.5 OBSERVATIONS. 167

8 PULSE RESPONSE MODELLING. 169
8.1 INTRODUCTION. 169
8.2 DISCRETE TIME MODELLING. 170
8.3 MODEL APPLICATION. 177
8.4 OBSERVATIONS. 186

9 APPLICATIONS. 189
9.1 A PIEZOELECTRICALLY CONTROLLED DISCRETE-MOTION MACHINE. . 189
9.1.1 Basic Design. 189
9.1.2 Design Considerations. 190
9.1.2.1 Clutch Face. 190
9.1.2.2 Clutching Energy Loss. 191
9.1.2.3 Inertial Loading. 194
9.1.2.4 Inertial Load Limit. 196

9.1.2.5 Actuators And Sensors. 197
9.1.2.6 Electronics. 197
9.1.3 Evaluation & Observations. 201
9.2 A ROTARY MICRO-POSITIONING INDEXER. 205
9.2.1 Prior Art. 205
9.2.2 Basic Design. 207
9.2.3 Revised Mechanical Design. 209
9.2.4 Electrical Design. 212
9.2.5 Performance. 215
9.2.6 Evaluation and Observations. 215

10 CONCLUSIONS AND FUTURE WORK. 217
10.1 CONCLUSIONS. 217
10.2 FUTURE WORK. 223

11 APPENDIX 1. 225
11.1 COMPLIANCE OF A TAPERED BEAM. 225
11.1.1 Analytical Modelling. 225
11.1.2 Finite Element Verification. 228
11.2 COMPLIANCE OF AN ELLIPTICAL BEAM. 230
11.2.1 Analytical Modelling. 230
11.2.2 Finite Element Verification. 234

12 APPENDIX 2: BEAM DESIGNER PROGRAM LISTING. 236

13 APPENDIX 3: 'DISTIME' PROGRAM LISTING. 254

14 APPENDIX 4: BRIDGE DESIGNER PROGRAM LISTING. 276

15 APPENDIX 5: CUSTOM INSTRUMENTATION. 292
15.1 GENERAL PURPOSE TEST AMPLIFIER. 292
15.2 LOW-PASS FILTER. 294

16 PLATES. 298

17 REFERENCES. 307

18 PUBLICATIONS. 313

LIST OF FIGURES

Figure 1: Stereo Phonograph 'Pick-up'. 7
Figure 2: Series Connected Ceramic Pick-up Element. 8
Figure 3: Cross-section of Tubular Ceramic Accelerometer Element. 9
Figure 4: Electric Field Inducing Expansion of a Piezoelectric Material. 10
Figure 5: Optical Aligning and Translating Actuator. 11
Figure 6: Bimorph and Unimorph Topologies. 11
Figure 7: Stacked Ceramic Actuator. 12
Figure 8: Piezoelectric Dot-matrix Printing Head (Single element). 13
Figure 9: Piezoelectric Ceramic Powered Rotary Motor. 14
Figure 10: Operation of the 'Inchworm' Motor. 16
Figure 11: Typical Hysteresis Behaviour of a Soft Piezoelectric Actuator. 19
Figure 12: Temperature Dependency of the Piezo Effect for a Typical Material. 21
Figure 13: Non-Isodynamic Loading of a Multilayer Actuator. 22
Figure 14: Coupling Efficiency versus κ. 26
Figure 15: Circuit Diagram of a Simple Drive System. 27
Figure 16: Voltage and Current Waveforms for the Simple Drive Circuit. 28
Figure 17: Ideal Voltage and Current Curves. 29
Figure 18: A Bi-directional Constant Current Circuit. 30
Figure 19: Bimorph Shape Required to Generate Larger Forces. 47
Figure 20: Simple Lever Displacement Amplifiers. 51
Figure 21: An Example of a Simple Lever Amplifier (Transverse). 52
Figure 22: Static Modes of Deformation of a Flexural Hinge. 53
Figure 23: Basic Concept for the Flexural Bridge Amplifier. 54
Figure 24: Operating Principle of a Snap Action Toggle. 56
Figure 25: Force/Displacement Characteristics. 57
Figure 26: Model of a bistable mechanism. 58
Figure 27: Static Internal and Output Force. 58
Figure 28: A Sample Output Trace from the Discrete Time Model. 61
Figure 29: A Hydraulic Displacement Amplifier. 63
Figure 30: Hydraulic Amplifier (Cross-Section). 64
Figure 31: A Piezoelectric Electronic Jacquard. 65
Figure 32: A Two-stage Displacement Amplifier. 67
Figure 33: High-efficiency Two-stage Amplifier. 67
Figure 34: Relative Energy Densities of Differing Piezoelectric Actuator Groups. 70
Figure 35 : Clutching Element Schematic. 75
Figure 36 : Finite Element Mesh Half Structure Shown. 79
Figure 37: Finite Element Mesh Bridge Structure Detail. 79
Figure 38: First ten resonant modes of the Strip-Clutch. 81
Figure 39: Static Compliance Test Jig. 83
Figure 40: Displacement against excitation voltage. 83
Figure 41 : Test-rig for the examination of the velocity/time profile of the Strip-Clutch. 84
Figure 42: Dynamic response; Output Bridge Velocity for an undamped

structure. 85
Figure 43: Output Bridge Velocity for a damped structure. 87
Figure 44: Endurance Limits For a Typical Titanium Alloy and Mild Steel. . . . 89
Figure 45: Generic Master Diagram for the Fatigue Life of Steels. 90
Figure 46: Schematic of the Endurance Test Experiment. 91
Figure 47: Idealised Amplifier. 96
Figure 48: Geometry of flexors at full drive. 100
Figure 49: Solution of d and e values. 106
Figure 50: Finite Element Mesh for Actuator Stall-Loading Tests. 108
Figure 51: Local Deformations of the Half-Plate. 109
Figure 52: Distortion Wave-Fronts for 3 Materials with a Tokin NLA-5x5x10 Actuator. 109
Figure 53: Finite Element Mesh for Edge Loading. 111
Figure 54: Graph showing Vertical Compliance of Hinge Anchor. 112
Figure 55: Actuator and Structure Stiffness with Actuator Length. 113
Figure 56: Effect of Host Width on Hinge Anchor Stiffness. 114
Figure 57: Family of solutions for the 100 μm amplifier (Example 1). 116
Figure 58: Relationship of mass function against efficiency for the 100 μm amplifier. 116
Figure 59: Screen Dump of the Beam Designer Program; Example 1. 118
Figure 60: Two views of the 100 μm Amplifier Monolith. 119
Figure 61: Output Displacement (mm) against Drive Voltage. 119
Figure 62: Deviation of Span and Zero for Increasing Static Load. 120
Figure 63: Screen Dump of the Beam Designer Program; Example 2. 122
Figure 64: Perspective View of the 200 μm Amplifier. 123
Figure 65: Results of the Static Tests for Example 2. 124
Figure 66: Finite Element Mesh used to model Example 2. 125
Figure 67: Finite Element Mesh showing Free Extension. 126
Figure 68: Finite Element Mesh showing Stalled Extension. 126
Figure 69: Diagram showing Stress Levels during Free Extension. 127
Figure 70: Diagram showing Stress Levels during Stalled Extension. 128
Figure 71: Modes and Frequencies of Vibration for Example 2. 129
Figure 72: Schematic of the Test Rig used for Determination of Time Domain Response. 130
Figure 73: The Time-Domain Response of the actuator, with No Additional Mechanical Damping. 131
Figure 74: Test Rig used for Frequency Domain Analysis. 132
Figure 75: Frequency Domain Plot for the Undamped Structure. 133
Figure 76: Time Domain Response of a Mechanically Damped Amplifier. 133
Figure 77: Frequency Domain Response of a Mechanically Damped Amplifier. 134
Figure 78: The Effect of adding more Damping. 134
Figure 79: The Neutral Axis of the Amplifier Output Beam (Ex.2). 135
Figure 80: Removal of Material from the Output Beam (Ex.2). 136
Figure 81: Shift of Resonant Frequency due to Optimisation. 136
Figure 82: The Time-Domain Response of the actuator, with No Additional Mechanical Damping. 138
Figure 83: Response to a 360 Hz bandwidth limited drive. 139
Figure 84: Response to a 360 Hz bandwidth limited drive. 138

Figure 85: Response to a 260 Hz bandwidth limited drive. 140
Figure 86: A Combination of Electrical and Mechanical Control. 141
Figure 87: Operation at a Repetition Rate of 200 Hz. 142
Figure 88: Semi-symmetrical Model of the Flexural Bridge Structure. 143
Figure 89: Finite Element Model Response to the 4 Test Cases. 151
Figure 90: Iteration Parameter Network for the Half-Bridge Structure. 153
Figure 91: Nature of the ΔE Curve. 157
Figure 92: Screen-shot from the Flexure Bridge Designer Program. 160
Figure 93: Finite Element Mesh Used to Evaluate Input Parameters. 161
Figure 94: The Program's Design Solution for the 110 μm Amplifier. 162
Figure 95: Perspective View of the 100 μm Bilateral Flexure Amplifier. 163
Figure 96: The Constrained Design Solution for the 100 μm Bilateral Amplifier.164
Figure 97: Finite Element Mesh used for Verification. 165
Figure 98: Uniaxial Finite Element Model of a Piezoelectric Multilayer Actuator. 171
Figure 99: Model of the Electromechanical Interaction of an idealised Piezoelectric Element. 173
Figure 100: Flow chart for the "Distime" Impulse Response Model. 174
Figure 101: A Typical Set of Traces produced by the 'Distime' Impulse Model. 178
Figure 102: Maximum Theoretical Departure Velocities. 179
Figure 103: The use of a Matching Component for Impulse Transfer. 180
Figure 104: Simple Velocity Limit Model for the Impulse Actuator. 181
Figure 105: Impulse Response Predicted by Simple Analytical Second Order Model. 182
Figure 106: Maximum End Face Velocities for the NLA 5x5x18 Actuator (Analytical). 183
Figure 107: Departure Velocities Predicted by the 'Distime' Model for Differing Values of Series Resistance 184
Figure 108: Scatter Graph of Peak Currents against Maximum Velocity. 185
Figure 109: Graph showing the Dependence of Velocity on Series Resistance and Inductance. 186
Figure 110: Relationship between Velocity and Series Resistance for Inductance of 22.5 μH. 187
Figure 111: Relationship between Velocity and Peak Inrush Current. 187
Figure 112: Mechanical Layout for the Discrete Motion Machine. 190
Figure 113: View of the Clutch and Anvil Arrangement. 191
Figure 114: Displacement, Velocity and Acceleration experienced by a component undergoing Simple Harmonic Motion. 192
Figure 115: In-elastic collision model. 193
Figure 116: Lift profile for a cycloidal cam with dwell. 195
Figure 117: System Diagram for the Discrete Motion Machine. 198
Figure 118: System timing diagram for the EPLD. 199
Figure 119: The EPLD equivalent circuit. 200
Figure 120: Circuit Diagram of the Control Board containing the EPLD. 202
Figure 121: Piezoelectric Driver Board Circuit Diagram. 203
Figure 122: Basic Design of the Rotary Micropositioner. 206
Figure 123: Diagram showing the original clutch and extension assembly. 206
Figure 124: Two Views of the Original Extending and Clamping Mechanism. . 207

Figure 125: Sequencing of the Clamps and Extender. 208
Figure 126: One of the Clamping Amplifiers. 210
Figure 127: Textual Output from the Beam Designer Program. 210
Figure 128: Step Size Variation. 211
Figure 129: Perspective View of the Extender Mechanism. 211
Figure 130: Circuit Diagram of the IBM PC Interface Board. 213
Figure 131: Schematic of the Rotary Micropositioner Control System. 214
Figure 132: An Encastred Tapered Beam. 225
Figure 133: Von Mises Stress Distribution for a Tip Vertical Unit Load. 229
Figure 134: Magnified Beam Displacement. 230
Figure 135: Magnified Beam Displacement. 231
Figure 136: Von Mises Stress Distribution for a Tip Vertical Unit Load. 232
Figure 137: An Encastred Elliptical Beam. 233
Figure 138 : Beam Compliance for various e and a values. 235
Figure 139: Test Amplifier Power Output Stage. 293
Figure 140: Precision Voltage Reference. 293
Figure 141: Power Supply for the Test Amplifier. 294
Figure 142: Drive Signal Conditioning Circuit. 295
Figure 143: 6 th Order Butterworth Active Filter. 296
Figure 144: Calibration Curve for the Filter Circuit. 296

LIST OF PLATES

Plate 1: Component Parts of the Hydraulic Amplifier. 299
Plate 2: Assembled Hydraulic Amplifier. 299
Plate 3: A Complete Strip-Clutch Element, shown with a scale reference. 300
Plate 4: Strip-Clutch Element mounted on a jig for preliminary slip tests. 300
Plate 5: A Scanning Electron Micrograph of Zone 4 of the Strip-Clutch. 301
Plate 6: Two Simple Beam Amplifiers (200μm Output). 301
Plate 7: The Bilateral (200μm Output) Flexure Bridge Amplifier. 302
Plate 8: Bilateral Amplifier Compliance Measurement. 302
Plate 9: Simple Beam Amplifier on the Test Apparatus. 303
Plate 10: Complete Static Test Apparatus. 303
Plate 11: Discrete Motion Machine complete with Drive Electronics. 304
Plate 12: Detail showing; Motor, Slot Cam, Rocker, Opto-switches and Strips. 304
Plate 13: One Strip-Clutch mounted on the Machine Carriage. 305
Plate 14: Mechanics for the Rotary Micro-positioner. 305
Plate 15: Close-up of the Clutching and Extending Mechanism. 306

1 INTRODUCTION.

1.1 HIGH-SPEED MACHINES.

For more than 200 years, the role of the electro-mechanical actuator has been conspicuously dominated by the electromagnetic coil in its various forms. Solenoids and motors of diverse topological varieties have been designed and exploited with a high degree of success in many fields, from acoustics to automotive traction. The use of such devices is prominent in the area of high-speed machines (particularly with the growth in the integrated approach to machine design involving electronic and software control), but as faster actuation times are required for new machine designs, the speed limitations of the electromagnetically based device have become problematic. Typical electrical time constants are commonly in excess of several milliseconds (with additional mechanical responses varying according to application).

The emergence of *Helenoids* and *Colenoids* [1] has demonstrated that it is possible to produce larger 'solenoids' with response times normally associated with much smaller devices but, these response times are typically in the range of several milliseconds, and there is a limit which it is not possible to transcend in terms of response speeds.

1.2 LIMITATIONS OF SOLENOIDS.

1.2.1 Electrical Speed.

The speed limitations inherent in the design of solenoid type actuators stem from two facets of their nature. In the context of high speeds, the least serious of these is the fact that they possess self inductance. Driven from a finite resistance, the limit of the speed of response is governed by a first order lag with a time constant τ given by;

$$\tau = \frac{L}{R_L + R_D} \tag{1}$$

(where L is the self inductance of the solenoid, R_L is the effective resistance of the solenoid and R_D is the resistance of the drive system). The time constant can be reduced by increasing R_D or R_L, or decreasing L, but this generally requires increasing the voltage from which the device must operate, to maintain a particular drive current.

For an application with a given force/stroke and coil former geometry, the magnetic field intensity developed by the coil H, is in the simplest case of a long solenoid given by;

$$H = IN \tag{2}$$

where I is the solenoid current and N is the number of turns. The inductance of the solenoid is given by;

$$N = \sqrt{\frac{L}{A_L}} \tag{3}$$

where L is inductance and A_L is a constant associated with the geometry and material. Ignoring drive resistance R_D, it can be shown that the time constant τ is given by;

$$\tau = \frac{H^2 A_L}{V^2} \tag{4}$$

where V is the designed operating voltage for the solenoid, indicating a reduction in time constant with higher operating voltage. It is unfortunate that to achieve faster switching speeds, higher operating voltages (often comparable to those now associated with piezoelectric multilayer actuators) are necessary. There are other techniques at the disposal of designers to facilitate faster effective electrical switching speeds, such as current dumping, but ultimately it is not always the electrical nature of the solenoid which limits its speed performance; it is the fundamental nature of force coupling within the device which is significant in determining mechanical speed.

1.2.2 Mechanical Speed.

The force acting on a piece of magnetic material is proportional to the total magnetic flux passing through it. Geometrically, the amount of flux which can permeate an object is linked to some function of its surface area (as well as other factors associated with the magnetic pole-pieces). Practical systems are limited as to the maximum attainable flux densities by the choice of materials. In general, as the dimensions of a device increase, its surface area (and hence the forces that can be developed) rises as a square law, but its mass rises according to a cubic relationship.

A departure from this general relationship can be achieved if the designed profile of a small solenoid can be extended in a third dimension. This results in a long thin device which for convenience can be wrapped around itself in the form of a coil or helix, possibly with a progressively changing radius (like a 'fusee'). Devices of this type [1] have found application in the automotive industry as prime movers for pneumatic servo systems.

1.2.3 Power.

The nature of the solenoid is such that to sustain a force generated by the magnetic field, the drive current must be maintained. This necessitates a continual power loss in the form of heat simply to hold position and do no external work. This is not the case with piezoelectric actuators which are by nature capacitative. With a piezoelectric device, a change in drive voltage produces a change in strain energy and external work can be done, but in the steady state a force can be maintained without any appreciable power [1] being dissipated.

---

[1] Very small leakage currents of several microAmp are typical in modern actuators, constituting a holding power of less than 1 mW.

1.2.4 A Typical Device.

To appreciate the significance of the factors mentioned above, it is necessary to examine certain features of the specification of an example solenoid. Taking a solenoid operating from a 24 V supply, with a self inductance of 50 mH, and a series resistance of 55 Ω, the electrical time constant of the device is less than 1 ms. This device is designed to operate over a displacement of 12 mm, but at this range, the mechanical response time of the device is greater than 10 ms. It could be used over a much shorter range with an decrease in response time.

Such a solenoid might be capable of developing a maximum force of 1.75 kgf for a zero field gap, falling to 0.35 kgf at 3 mm field gap. This could accelerate the magnetic core (of typical mass 8 g) from 3 mm 'out' to complete closure in just over 3 ms. The steady-state power requirement of this device is 10 W in the on-state. The work done over the operating stroke of 3 mm is 30 mJ.

1.3 DISCRETE MOTION DRIVES.

Since there is an on going need for ever-faster actuators, and the limit of solenoid technology has been approached for many years (and can not be significantly advanced because of the fundamental nature of the solenoid), the potential of piezoelectric actuation is attractive.

The availability of useful actuators with response times of less than 1 millisecond would permit the design of faster machines, in which cyclic or repeated motion could be coupled or clutched (such as in printing and textiles machinery). This clutching would occur at a point in the cycle where the relative velocity if the components was at or very close to zero, reducing the possibility or rate of wear.

Conceivably, clutching could be achieved either by a latching process, where the actuator causes a change in the physical location of another latching component, or by direct action of an actuator, where the actuator generates the necessary clutching force. Latching and direct acting processes have been well exploited already using solenoids. It will be seen that the use of piezoelectric actuators (and in particular multilayer stack type devices) makes possible the design of machines where clutching can be achieved by direct action in under 1 ms.

2 PIEZOELECTRICITY AND ITS APPLICATION IN ACTUATORS.

This thesis in centred on the application of piezoelectric multilayer actuators to high-speed clutching, therefore this chapter presents an introduction to the phenomenon of piezoelectricity in the context of its general application to sensors and actuators, with a particular bias towards actuators and motors.

In the context of actuation, it is also concerned with an assessment of the basic functionality and general characterisation of piezoelectric multilayer devices, and includes not only such topics as their basic electro-mechanical nature, but also practical considerations such as mounting techniques and electrical drive techniques.

2.1 THE PHENOMENON OF PIEZOELECTRICITY.

A piezoelectric material is one which develops an electrical charge when subjected to mechanical stress. Naturally occurring piezoelectric materials such as quartz were investigated in the 1880's, but piezoelectric ceramics and ferroelectricity were not discovered until the 1940's. In the 1950's, the strong, stable piezoelectric effects of lead zirconate titanate (PZT) were discovered [2]. Although other ceramics with improved properties have appeared recently, PZT is still the dominant piezoelectric ceramic, not least because its crystal structure permits a wide range of solid solutions with different additives, allowing ceramicists to tailor its properties to suit a diverse range of applications. PZT can be manufactured in many sizes and shapes; these include plates, sheets, blocks, discs, hemispheres, tubes and rings. More recently, it has become possible to include the electrode structure of such shapes as sintered material within the ceramic structure [3].

When some ceramics cool from the high temperatures used during manufacture, a random configuration of domains [2] forms. In this state the ceramic does not display

[2] Each domain is a region with a specific polar orientation.

any piezoelectric properties, but these can be acquired by a polarizing (also known as poling) process. Poling is achieved by applying a large d.c. electric field across the material whilst at temperatures usually in the range 100°C to 200°C. Over a short period of time, domains already aligned with the electric polarising field tend to grow at the expense of others. The temperature is then reduced and the electric field removed, leaving the new domain configuration in tact, and the material retains its polarisation. Materials behaving in this way are known as ferroelectric.

After the poling process, the material is non-isotropic and so the way it responds, when subjected to stress or an electric field, depends upon the relationship between the axis and direction of polarisation, and the magnitude of excitation [4].

2.2 APPLICATIONS OF DIRECT PIEZOELECTRICITY.

As shown in Figure 1, an early application of the direct piezoelectric effect was to convert the vibrations of a phonograph stylus into electrical signals.

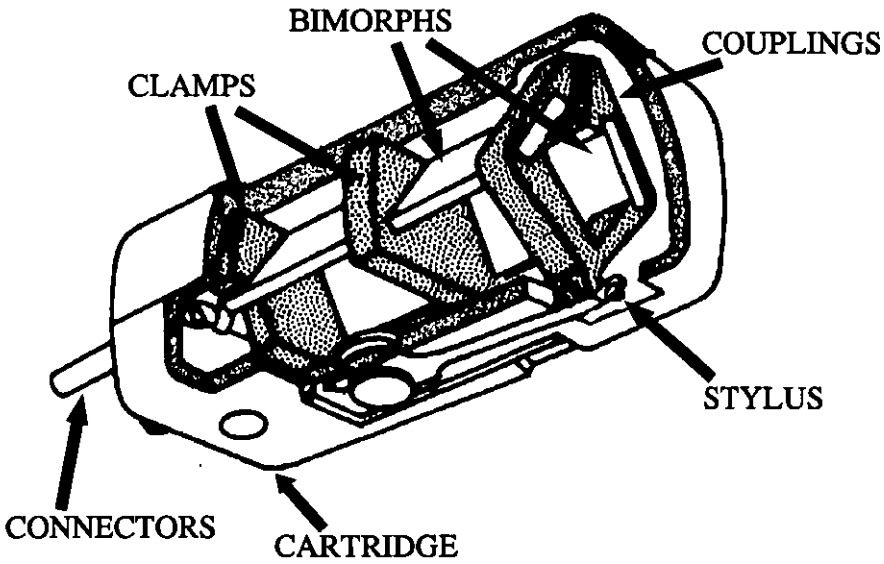

Figure 1: Stereo Phonograph 'Pick-up'.

In the example, voltages are generated by two beams which are mutually mounted at right angles. Orthogonal vibratory components are resolved and detected by each bimorph (as seen in Figure 2), resulting two signal channels, which are then electronically amplified.

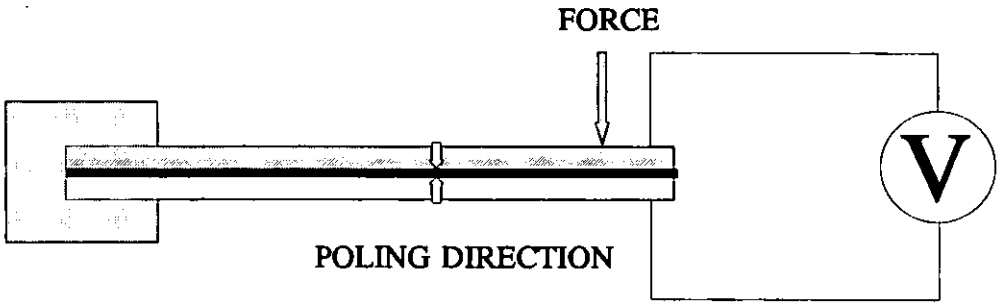

Figure 2: Series Connected Ceramic Pick-up Element.

A typical device would generate a voltage of 0.5V peak.

The piezoelectric effect is also used in sensors which generate an analogue voltage when exposed to pressure or acceleration, such as the accelerometer shown in Figure 3. In this device, vertical acceleration forces produce shear stresses in the ceramic element, causing a corresponding voltage to be generated.

High voltages can be generated when piezoelectric ceramics are compressed. Timed delivery of a 20 000 V pulse, for the ignition spark of petrol engine has been provided by cam-operated compression of a stack of piezoelectric ceramics [5]. Most domestic gas lighters operate by a similar principle.

2.3 THE CONVERSE PIEZOELECTRIC EFFECT.

When an electric field is applied to a piezoelectric material, it causes mechanical straining or movements; this effect is known as the converse or reverse piezoelectric

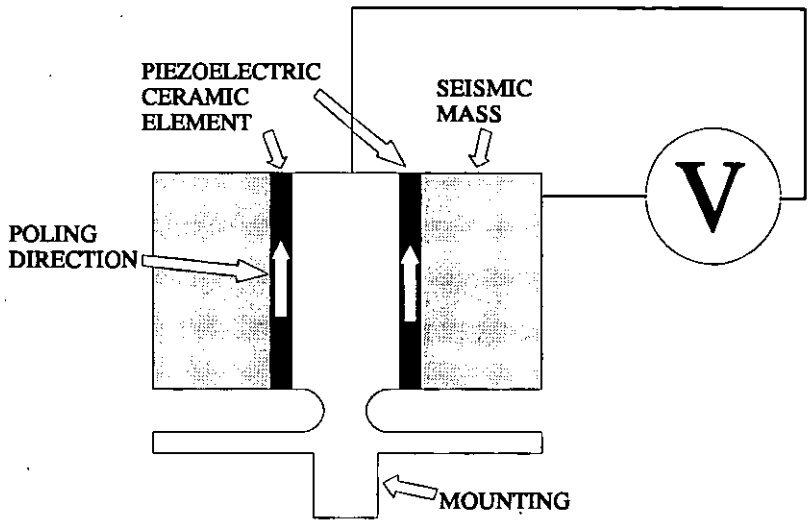

Figure 3: Cross-section of Tubular Ceramic Accelerometer Element.

effect, as shown in Figure 4.

Thus, piezoelectric materials have the ability to generate high frequency vibrations, as found in devices used for ultrasonic scanning, cleaning, welding, drilling and in sonar systems, acoustic transducers and non-destructive testing.

In recent years, research has lead to the development of actuators with various forms of ceramic components which together with mechanical amplifiers, can provide larger displacements. These advances have enabled piezoelectric actuators to be applied more widely.

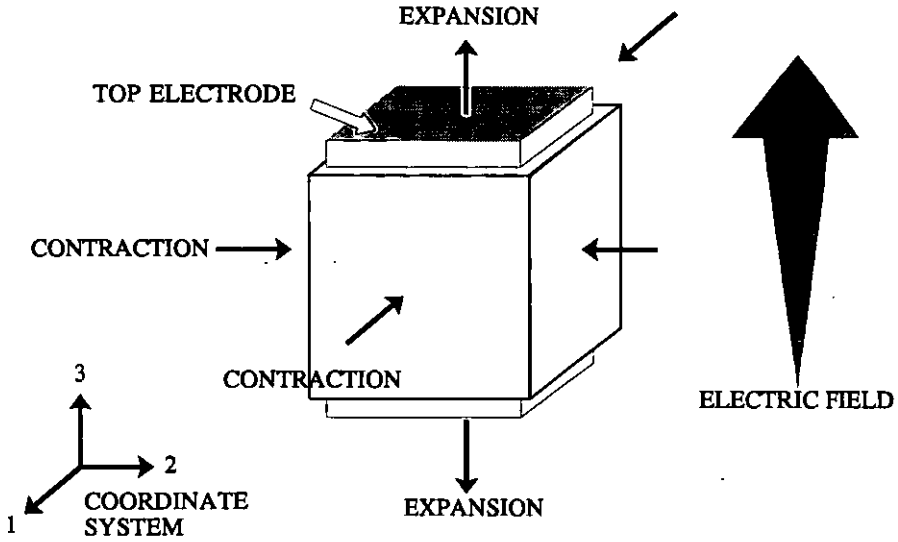

Figure 4: Electric Field Inducing Expansion of a Piezoelectric Material.

2.4 RECENT APPLICATIONS OF PIEZOELECTRIC ACTUATORS.

2.4.1 Optical Alignment Actuator.

Since Piezoelectric actuators can provide very small controllable movements, they are useful in the positioning of optical components; this is a major area of application. A device marketed by Burleigh Instruments Inc. is shown in Figure 5. The device uses inexpensively constructed tube sections as the prime movers and is capable of tilt in two axes and extension in a third orthogonal axis, and is thus ideal for optical alignment and interferometric applications.

Translators are often made from flat strips packaged in parallel, with alternate strips polarised complementary alignment. They are frequently long and thin and are only suitable for application in tension, thus the maximum stress that can be endured by the device is limited due to its ceramic composition.

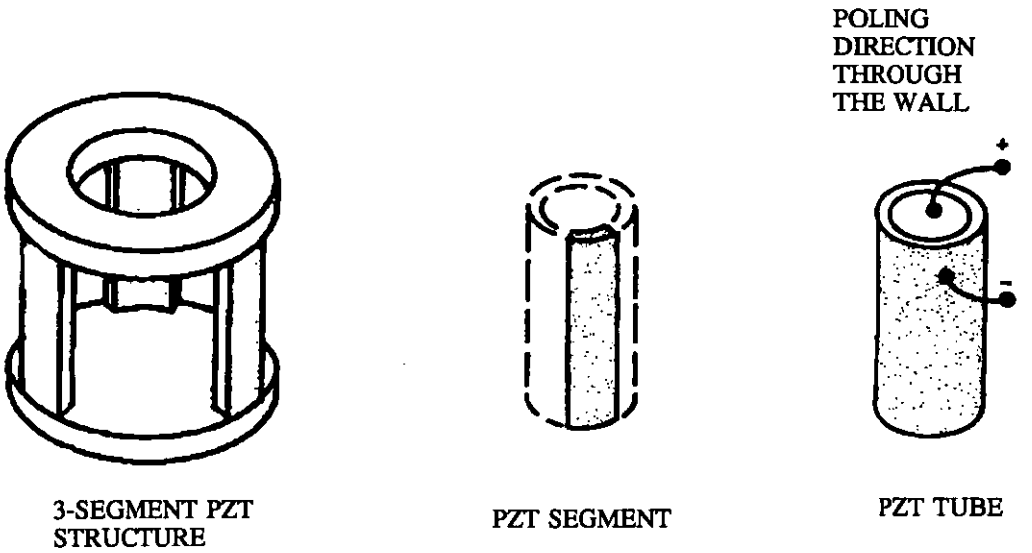

Figure 5: Optical Aligning and Translating Actuator.

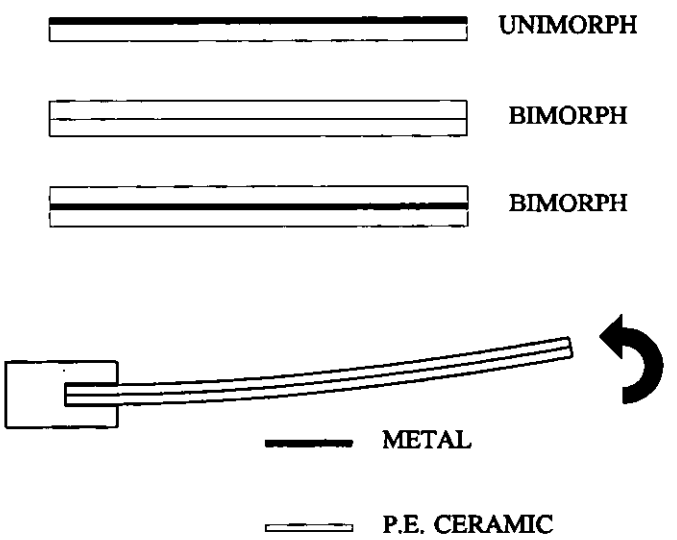

Figure 6: Bimorph and Unimorph Topologies.

2.4.2 Bimorphs and Unimorphs.

PZT strips can be made into bimorphs or unimorphs (in combination with metal strips) as shown in Figure 6. These operate by the simultaneous contraction of one strip with

the expansion of the other [3], resulting in bending. Output movements can be large, but forces small, so actuator applications are restricted accordingly to those where little force is required, such as in the first stage of servo or fluidic valves [6]. Discs clamped at their edges can be made to act as three-dimensional bimorphs, so that their centres rise to form a rounded cone.

2.4.3 Stacks.

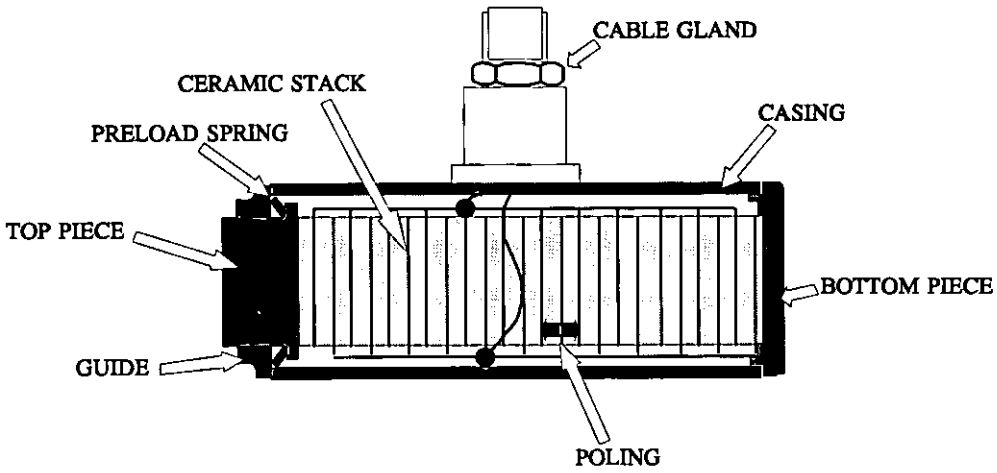

Figure 7: Stacked Ceramic Actuator.

Discs of piezoelectric ceramic material are often bonded together to form a stack, as shown in Figure 7. Each disc receives the full applied voltage, so the total displacement generated at the top piece with respect to the bottom piece depends on the number of discs and the displacement generated by each disc. As a general rule, the displacement which can be generated is proportional to the length of the actuator. Commercial units, which can be used for positioning and clamping, are usually

[3] Or a nominally fixed length of metal in the case of a unimorph.

supplied in a rigid casing of aluminium of stainless steel. The stacks are often axially preloaded.

In recent years however, the techniques employed for the manufacture of multilayer capacitors have been applied to the manufacture of piezoelectric ceramics 'stack' actuators, and the effect of this approach on the material specifications of the devices produced has been revolutionary [7]. Since the electrode structure, previous produced as discrete thin metal discs, is now sintered into the ceramic, no adhesives are required to bond the stack together. The result is a much stiffer device with the similar extension characteristics; a significant increase in the specific work ability of the new material.

2.4.4 A Piezoelectric Print Head.

The movements can be increased further by amplifying linkages such as that shown in Figure 8.

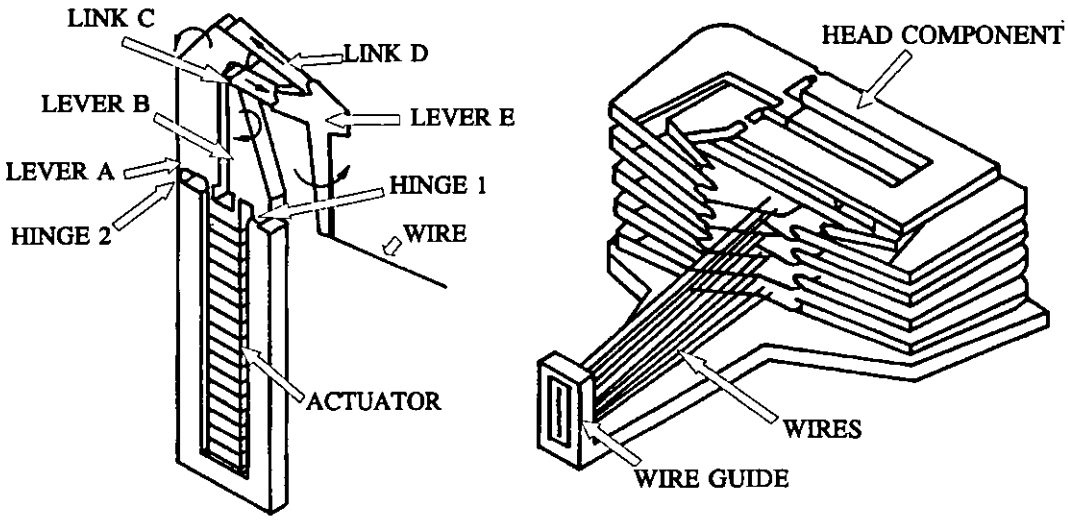

Figure 8: Piezoelectric Dot-matrix Printing Head (Single element).

When the actuator is electrically excited and the actuator expands, levers A and B pivot apart around hinges 1 and 2. Links C and D are pushed and pulled respectively causing lever E to rotate and the printing pin (wire) to be moved away from the assembly. The print wire strikes an inked ribbon which in turn presses against the paper. Since the assemblies are narrow, they can be stacked together as shown.

This printing head is claimed to be capable of a very much higher printing speed than a comparable electromagnetic one, since it generates little heat; a fact which allows the head to be shrouded to reduce printing noise [8].

2.4.5 A Rotary Wave Motor.

Rotating motors in various forms have been proposed, one by Matsushita Electrical Industrial Company of Japan for example, shown in Figure 9.

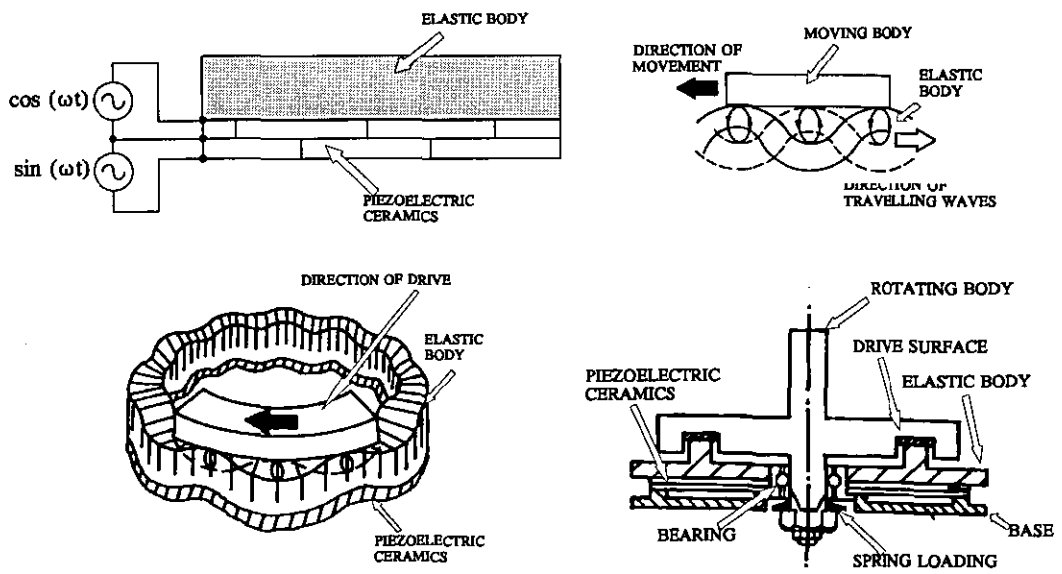

Figure 9: Piezoelectric Ceramic Powered Rotary Motor.

A piezoelectric ceramic driving element is constructed from a series of ceramic disc segments, bonded together in what can be described as a circular 'brick wall' two

elements deep. Adjacent elements are alternately polarised. When electrically excited using two sinusoids in quadrature [4], a vertical displacement 'wave' is set up un the ceramic wall, which rotates as the drive waveform progresses with time. The ceramic structure is bonded to an elastic body. Individual points on the opposite side (unbonded) of the elastic body describe an ellipse as a result of the mechanical distortion of the ceramic. Since the elastic body is held in compression against a rotor, the rotor experiences a displacement in step with the driving waveform.

A middle range motor has a diameter of 40 mm and is 12 mm high. When supplied with 30 V at 70 kHz it has a no-load speed of 800 r.p.m.. It can exert a torque of 0.06 Nm at half this speed. The advantages claimed for these motors are small size, light weight, low speed, high torque, good control and quick response [9]. Applications include auto-focus motors on cameras.

2.4.6 A Piezoelectric 'Inchworm' Drive.

The 'Inchworm' Motor manufactured by Burleigh Instruments Inc. is a linear actuator capable of large movements (100 mm is typical). It achieves this displacement by integrating the small incremental movements generated by an piezoelectric extender (item 2 in Figure 10), and clamping onto the central shaft at appropriate times. For motion to be achieved, six clamping phases are required and these are shown in the figure. These motors are capable of speeds from 4 nm s^{-1} to 2 mm s^{-1} and can exert forces in the order of 1 N [10,11].

2.5 CHARACTERISTICS OF PIEZOELECTRIC MATERIALS.

The breadth of application of piezoelectric ceramic actuators is considerable. This breadth is more clearly seen in the literature review in chapter 3. Ingenious amplifying

[4] The phase angle between the two sine waves is 90°.

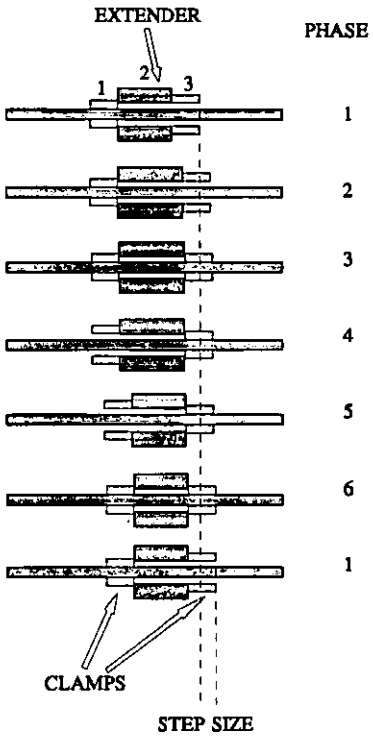

Figure 10: Operation of the 'Inchworm' Motor.

mechanisms have been designed to overcome the problems encountered when dealing with displacements of perhaps only 10 μm. But a more thorough appreciation of the design aspects of piezoelectric actuators is only possible with an understanding of the physical behaviour or characteristics of such devices. A detailed appraisal of these characteristics follows.

2.5.1 Compliance: S^E.

Mechanically, multilayer devices behave elastically (disregarding the effect known as creep, q.v. section 2.5.4) and therefore exhibit compliance. Since in piezoelectric materials there is a strong interaction between electrical and mechanical behaviour, this compliance depends on the electrical loading of the actuator . The most useful

parameter in this respect is the S^E compliance tensor, which universally relates stress to strain in the bulk material, for a *constant applied voltage* (usually zero) [5]. If the actuator is electrically unloaded and stress is applied, the direct piezoelectric effect causes an electric field to be developed, which can be considered to cause a strain in opposition to the applied stress. In practice however, since such actuators are often driven directly, the S^E tensor is relevant.

By virtue of their construction and application, many piezoelectric devices can be modelled uniaxially, and therefore most tensor elements are of no interest save those designated S_{33}^E and S_{31}^E, where the subscripts refer to the alignment of the applied stress with the poling direction of the piezoelectric material. Stacks and multilayers are usually constructed along the '33' direction where the desired extension is coaxial with the applied electric field (see Figure 4), while multimorphs and bimorphs exploit the properties along the '31' 'direction', where contraction is perpendicular to the applied electric field.

For soft piezoelectric materials, a typical S_{33}^E value might be 2×10^{-11} m^2/N, but for a hard piezoelectric material, a value of 1.5×10^{-11} m^2/N, would be typical. This apparently stiffer behaviour of hard materials is greatly offset by the ability of soft materials to develop at least twice as much extension or strain for a given applied field. This implies that soft piezoelectric materials are capable of higher specific work per cycle, than their hard counterparts.

2.5.2 Dynamic Operation.

Since piezoelectric actuators behave elastically, have mass and are lightly damped, they are capable of exhibiting mechanical resonance. A simple mass-spring model is often favoured when trying to predict resonant frequencies and response times of

[5] The tensor describing the behaviour of such materials when electrically open circuit is sometimes designated S^O.

multilayer actuators, and this method is adequate if approximate results will suffice. This model fails to predict those facets of behaviour which are intimately related to the coupling between the electrical and mechanical natures of the these devices. A more detailed study of this can be found in chapter 8.

However, by considering the system to be a simple second order system, response times can be estimated by modelling the piezoelectric actuator as a spring of stiffness k_p and mass m_p, with displacement restrained at one end, and an additional mass M at the other. The resonant frequency of such a structure is given by [12];

$$f_0 = \frac{1}{2\pi}\sqrt{\frac{k_p}{m_p + 2M}} \text{ Hz} \tag{5}$$

A simple, commonly used rule of thumb for the estimation of a minimum response time is;

$$t_{min} = \frac{1}{3f_0} \tag{6}$$

Applying this method to modern multilayer devices (which may be considered as homogeneous for this purpose) of length l, elastic modulus E and average density ρ, with no additional mass M = 0;

$$t_{min} = \frac{2\pi\, l}{3}\sqrt{\frac{\rho}{E}} \tag{7}$$

An alternate approach involving the phase velocity of axial longitudinal waves has been proposed, which by an argument involving wave propagation and reflection, arrives at a similar rule of thumb [13]. Since E and ρ do not vary widely from manufacturer to manufacturer a simple rule can be applied where the minimum response time is proportional the length by approximately $0.5\text{x}10^{-3}$ sm^{-1}. This is a very simplistic approach which is probably only accurate to within half an order of magnitude.

2.5.3 Hysteresis and Non-Linearity.

The expansion of piezoelectric material in response to a linear change in electric field is non-linear and hysteretic. The degree of these phenomena from ideal behaviour depends greatly on the type of material from which the actuator is made, that is, whether the piezoelectric material is either *hard* and *soft*.

It is a common mis-conception that hard and soft refer to the stiffness of the material, but in fact it is the hysteresis and non-linearity which vary greatly between these two categories. For example most hard-types have hysteresis and non-linearity figures of less than 1% to 2% of full range output, whereas 10% might be typical for a soft type. Soft piezoelectric devices are usually employed where more output displacement is required and these phenomena are not important. Figure 11 shows a typical extension-voltage characteristic for a soft piezoelectric material.

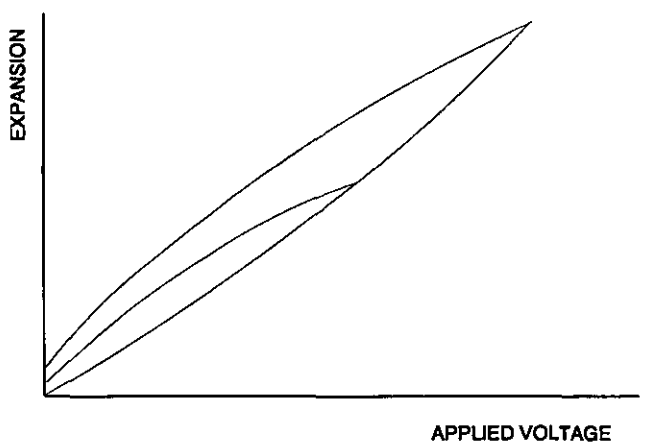

Figure 11: Typical Hysteresis Behaviour of a Soft Piezoelectric Actuator.

2.5.4 Creep.

When the voltage applied to an actuator changes, (for example as a step change, with which the phenomenon is the easiest to observe), after any ringing dies away the

device responds by following the trend of the drive waveform, but there is an additional creep or drift associated with that change. The behaviour is described by;

$$\Delta L(t) = \Delta L_{\tau}\left(1 + \gamma \log \frac{t}{\tau}\right) \qquad \textbf{(8)}$$

where ΔL_{τ} is the expansion after time τ (this is usually taken as 0.1 s), t is time, γ is a drift coefficient, the values of which commonly lie between 0.01 and 0.02.

2.5.5 The d_{33} Coefficient.

In the same way that a tensor is required to describe the linear approximation of the compliance behaviour of piezoelectric ceramics, the d tensor is required to describe the extension or contraction of the material in response to a general electric field. In essence it is the reverse piezoelectric sensitivity of the material. In multilayer (stack type) devices, excitation is always engineered in the '3' direction, which is also the direction of expansion, so the sensitivity is described by d_{33}. For bimorphs, where the useful extension is perpendicular to the electric field, the sensitivity is described by d_{31}. Typical values for soft PZT's at room temperature are;

$d_{33} = 600 \times 10^{-12}$ m/volt and $d_{31} = -275 \times 10^{-12}$ m/volt.

The negative sign for the later coefficient indicates contraction.

2.5.6 Temperature Response.

Two major temperature effects associated with these devices are;

1] The variation of the temperature coefficient of the d_{33} (or d_{31}) value.

2] Linear thermal expansion.

Figure 12 shows typical variation of the d_{33} value of a typical soft piezoelectric material with temperature. The shape of the curve shows that over the temperature

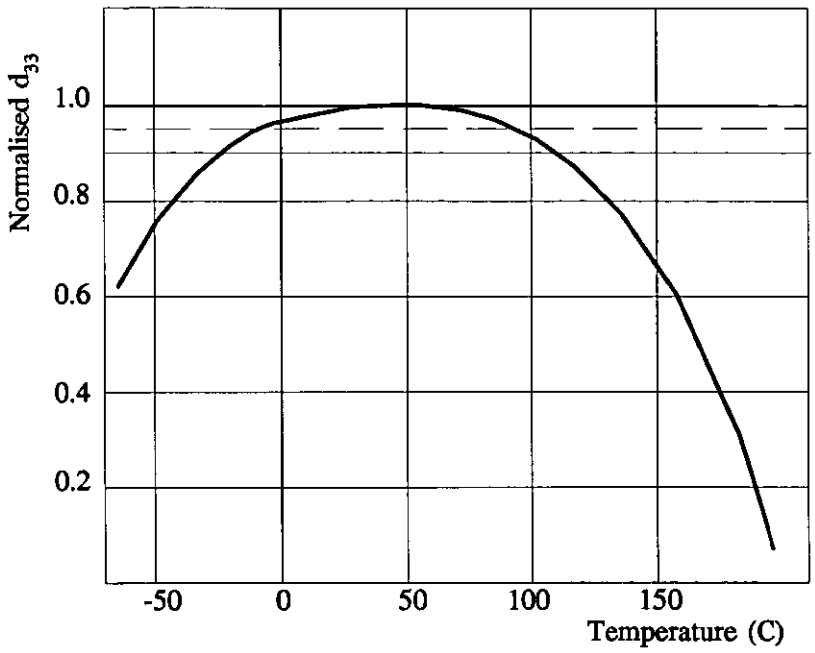

Figure 12: Temperature Dependency of the Piezo Effect for a Typical Material.

range of -10°C to +90 °C, the coefficient stays within a ±2.5% band of nominal. A ±5% band extends the temperature range to -25°C to +110°C. For cryogenic applications at 4 °K (-269 °C), the coefficient is approximately 30% of its room temperature value.

A critical effect of temperature is the variation of rest length with temperature. At room temperatures and above, this expansion with increasing temperature can be considered as approximately linear. Typical values of linear coefficient of expansion range from 3×10^{-6} °C $^{-1}$ to 8×10^{-6} °C $^{-1}$, and can depend slightly on mechanical pre-load. The design ramifications of this are discussed in more detail in chapter 4.

2.6 MECHANICAL LOADING.

The ability of a piezoelectric device to transfer energy into a load has been the subject of some confusion. This confusion sometimes arises from the inability to statically model a piezoelectric device succinctly. Experiment shows that the extension of a piezoelectric element under differing fixed loads is almost constant; in fact, the extension increases slightly with increasing loads. This represents a small deviation from Hookean behaviour, typically no more than 1% of the full range output.

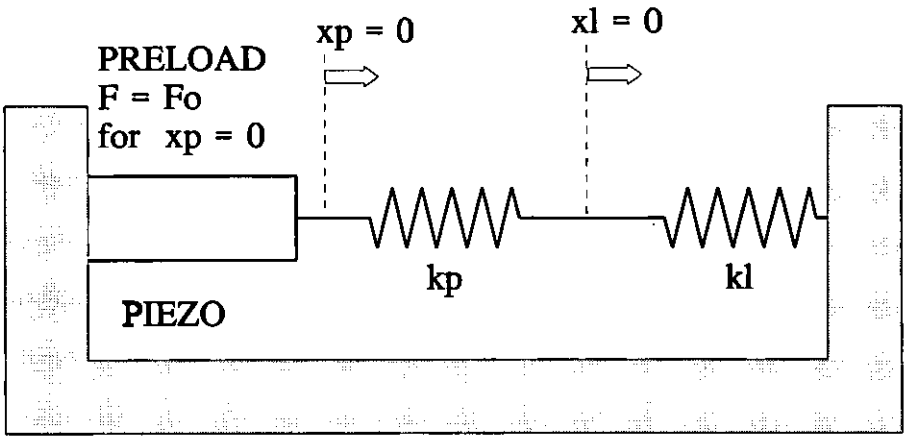

Figure 13: Non-Isodynamic Loading of a Multilayer Actuator.

Figure 13 shows a simple model of a force (F_o) pre-loaded [6] actuator coupled to a Hookean load of stiffness k_l. The model for the piezo, also Hookean, can be considered as an infinitely stiff displacer x_p coupled through the device stiffness k_p. The actual displacement of the actuator is given by x_l. Defining the compression of the piezo and load respectively as c_p and c_l, the force experienced by all components F is given by;

[6] F_0 is the compressive force experienced by the actuator when $x_p = 0$.

$$F = F_o + k_p c_p \tag{9}$$

and;

$$F = F_o + k_l c_l \tag{10}$$

This relates the compressions under any force condition as;

$$c_l = c_p \frac{k_p}{k_l} \tag{11}$$

And the actual movement is given by;

$$x_l = x_p \frac{k_p}{(k_p + k_l)} \tag{12}$$

The force in the system is therefore given by;

$$F = F_o + x_p \frac{k_p k_l}{(k_p + k_l)} \tag{13}$$

From this, we can see that the apparent stiffness *seen* by the infinitely stiff displacer is;

$$k_a = \frac{k_p k_l}{(k_p + k_l)} \tag{14}$$

The work done by the actuator moving from rest to x_{pmax} is;

$$E_p = \int_0^{x_{pmax}} F.dx_p = F_o x_{pmax} + \frac{k_a x_{pmax}^2}{2} \tag{15}$$

Similarly, the work transferred to the load is;

$$E_l = \int_0^{x_{lmax}} F.dx_{lmax} = F_o \frac{x_p k_p}{(k_p + k_l)} + \frac{k_l k_p^2 x_p^2}{2(k_p + k_l)^2} \tag{16}$$

Since;

$$x_1 = x_p \frac{k_p}{(k_p + k_1)} \tag{17}$$

The transfer coefficient can be expressed as;

$$C_e = \frac{E_1}{E_p} \tag{18}$$

Defining the stiffness ratio as;

$$\kappa = \frac{k_1}{k_p} \tag{19}$$

we can rewrite;

$$E_p = F_o x_{pmax} + \frac{\kappa}{2(1+\kappa)} k_p x_{pmax}^2 \tag{20}$$

and;

$$E_1 = F_o \frac{x_{pmax}}{(1+\kappa)} + \frac{\kappa}{2(1+\kappa)^2} k_p x_{pmax}^2 \tag{21}$$

To rationalise the effect of preloading on the transfer coefficient, we can define dynamic energy E_d and static energy E_s as;

$$E_s = F_o x_{pmax} \qquad E_d = \frac{k_p x_{pmax}^2}{2} \tag{22}$$

and a ratio of these, which we can call the preload ratio;

$$\gamma = \frac{E_s}{E_d} \tag{23}$$

Therefore;

$$E_p = \gamma E_d + \frac{\kappa}{(1+\kappa)} E_d \tag{24}$$

and;

$$E_l = \frac{\gamma E_d}{(1+\kappa)} + \frac{\kappa E_d}{(1+\kappa)^2} \tag{25}$$

The transfer coefficient can now be expressed succinctly as;

$$C_e = \frac{\kappa(1+\gamma) + \gamma}{\kappa^2(1+\gamma)+\kappa(1+2\gamma)+\gamma} \tag{26}$$

The above relations can be used to determine the optimum energy coupling into the load. Unfortunately, this is a maximum when the load stiffness is much greater than that of the piezo, and consequently the real movement is very small. However, many applications require a condition where the force displacement product into the load is maximised, specifically in amplifying structures. If we consider these systems as reversible, then all of the strain energy is recoverable over an operating cycle, and further, the static preload force does no net work. The isentropic energy coupling is therefore;

$$E_{li} = \frac{k_l x_{lmax}^2}{2} \tag{27}$$

Which in terms of the stiffness ratio is;

$$E_{li} = \frac{k_p x_{pmax}^2}{2} \frac{\kappa}{(1+\kappa)^2} \tag{28}$$

There will be a certain value of stiffness ratio where E_{li} is a maximum and can be determined by the relation;

$$\frac{\partial E_{li}}{\partial \kappa} = 0 \tag{29}$$

This solves for;

$$\kappa = 1 \tag{30}$$

This result means that maximum useful work is done into the load when the stiffnesses of the piezoelectric actuator and the load are equal. The preload force does not directly affect the recoverable energy put into the load, but is important in practice

because the free movement x_{pmax} is slightly affected by the preload [10]. Additionally, it if often necessary to preload the actuator to avoid tensile stress, for example, during retraction of the actuator if it is bonded into a host structure. The best operating point is a compromise between these criteria, and is often found to be approximately ⅓ of the force required to return an actuator to its rest length, when experiencing full electrical excitation [7].

The coupling coefficient is given by;

$$C = \frac{\kappa}{(1+\kappa)^2} \tag{31}$$

where;

$$E_{li} = C\,\frac{k_p x_{pmax}^2}{2} \tag{32}$$

and is plotted in Figure 14. It can be seen that the maximum coupling coefficient is 0.25, with reference to the stall energy of the piezo.

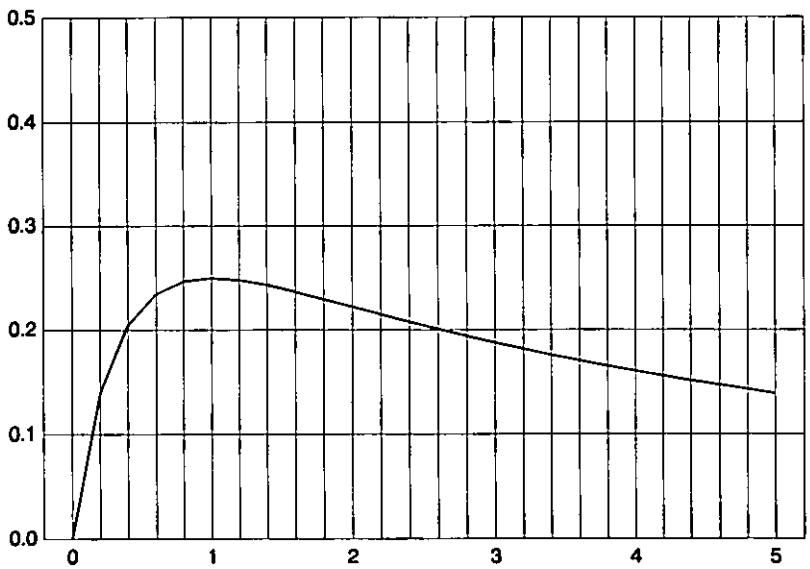

Figure 14: Coupling Efficiency versus κ.

[7] This is later referred to as 'stall force'.

2.7 ELECTRICAL DRIVE SYSTEMS.

Piezoelectric multilayer actuators behave electrically as capacitors in a simplistic sense. This view is almost sufficient in the design of the electrical drive circuits necessary to exploit their full potential as fast actuators. The only additional consideration required is of the behaviour of such devices in terms of the back e.m.f. they produce in response to applied stress. Statically, the behaviour of such devices can be modelled in terms of linear coefficients.

This thesis is principally concerned with high-speed actuation. This promotes a need to understand and develop electrical drive systems which can swiftly achieve a desired voltage and strain state within the piezoelectric actuator. For clutching applications we are interested principally in two-state systems.

2.7.1 Simple Drives.

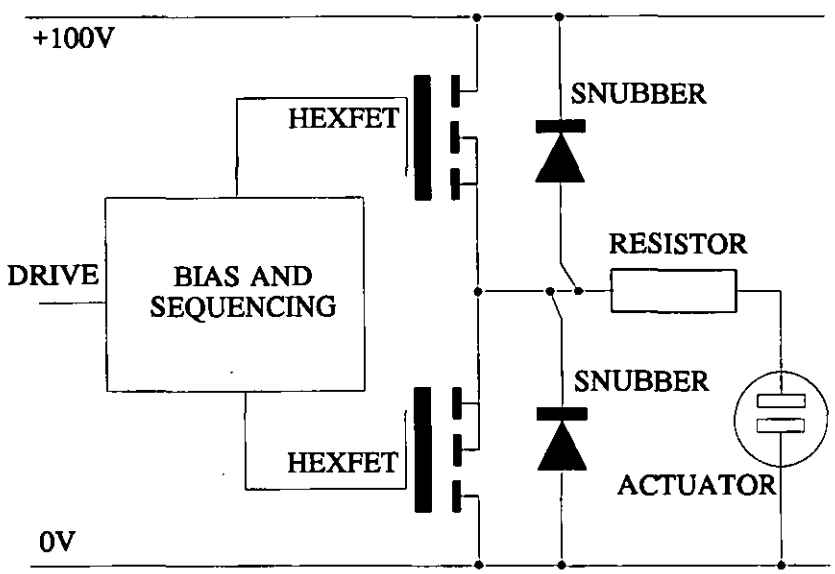

Figure 15: Circuit Diagram of a Simple Drive System.

The simplest way of achieving a two-state actuator drive is by using high-current solid-state switching devices such as field-effect transistors, such as the International Rectifier 'Hexfet' series of devices. Such a circuit is shown in Figure 15, which

includes a non-overlap and bias circuit to ensure correct phasing of the required drive pulses to the FET gates; avoiding the possibility of both FETs being on simultaneously. Additionally, snubbers (in this case catching diodes) prevent the FETs from experiencing under-voltage or over-voltage transients which can result from mechanical stress transients in the actuator. A resistor is necessary in series with the actuator, to limit the maximum inrush or outrush current which occurs when the actuator is required to change state. Mechanical interaction aside, the response would follow a classical first order lag, satisfying the equation;

$$V = V_0\left(1 - e^{\frac{-t}{RC}}\right) \tag{33}$$

Idealised Voltage and Current waveforms for a single step change of state are shown in Figure 16.

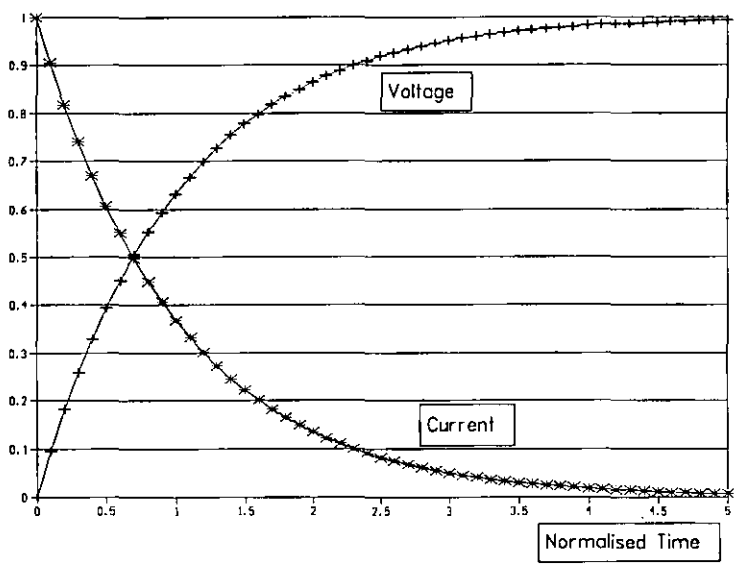

Figure 16: Voltage and Current Waveforms for the Simple Drive Circuit.

It will be noticed that this basic approach unavoidably involves a high peak inrush current given by;

$$\hat{i} = \frac{V_0}{R} \tag{34}$$

where V_0 is the supply voltage. The value of the peak current must be kept within limits if the device is not to be over current-stressed.

2.7.2 Digital Drives.

To achieve a rapid injection of charge, and therefore a rapid actuator response, involves a more sophisticated approach to avoid unacceptable peak electrical current stressing. Moreover, whilst high speed is achieved, the simple resistive technique results in the generation of a high level of mechanical ringing, containing harmonic components which are usually undesirable.

Assuming that the mechanical work done by the actuator is zero, from the point of view of current stress, the ideal circuit would have voltage and current waveforms as shown in Figure 17, and could be achieved using a high-speed constant current circuit. Such a requirement can be achieved with the circuit shown in Figure 18.

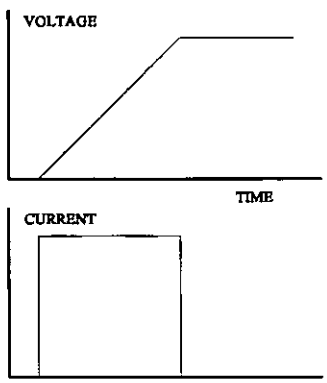

Figure 17: Ideal Voltage and Current Curves.

This is not purely a constant current drive, but acts as a current limiter based on the forward transconductance of the FET, when there is sufficient voltage across the circuit. Switch-on is 'softened' by the addition of a capacitor which slows the switch on of the FET. This also helps to reduce the harmonic content of the drive waveform and hence the mechanical transient. As the circuit approaches steady state, the voltage across the current limiter droops and the circuit ceases to function, allowing the final charge injection to occur solely though the bleed resistor. This effect also softens the

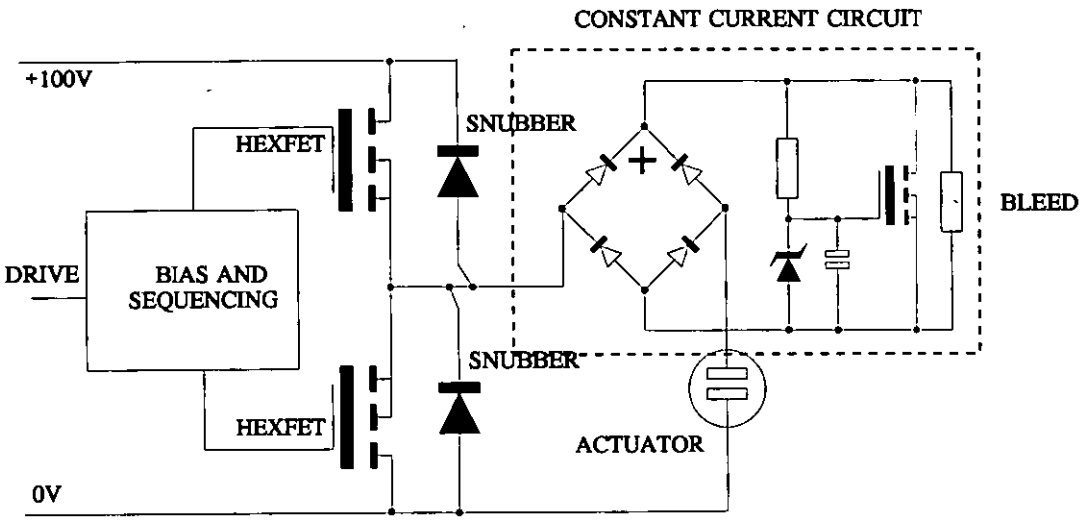

Figure 18: A Bi-directional Constant Current Circuit.

current profile.

The inclusion of an inductance in series with the simple drive circuit can be beneficial. This is covered in more detail in chapter 8, which deals with pulse response modelling in the context of establishing the feasibility of an simple impulse coupled actuator. In summary, the peak inrush current can be reduced by this method and help to reduce unnecessary peak mechanical stress for a given application, since in many systems, the mechanical response of the system being driven is much slower than the actuator itself.

2.7.3 Linear Drives.

At the commercial expense of providing a linear amplifier for every actuator, it is possible to drive piezoelectric ceramic actuators in a linear fashion. This approach opens up the two basic approaches of Active Damping, and Waveform Profiling.

1 ACTIVE DAMPING.

This technique involves a closed-loop servo system in which there is active control of the voltage applied to the actuator. Whether the actuator is assumed to be part of a larger mechanical system or not, is unimportant. In principle, the current through the device is a function of the applied voltage *and* the charge feeding back from the actuator in to the drive amplifier as a result of mechanical strain. This makes partial active damping possible. This technique has been successfully employed as active vibration control, and is one aspect of 'Intelligent Structures'.

2 WAVEFORM PROFILING.

By contrast with active damping, this is an open loop technique and although there are several variants, the principle is common to all. One technique [14], found in the literature survey (Chapter 3) is to use a D-A convertor to drive a 150V linear amplifier. The D-A convertor is clocked with data from a computer to provide a drive waveform designed to achieve optimum switching performance from the actuator. The wave shape is essentially constructed from the step response summed with a variant of the normal ringing response of the actuator.

An alternate method is to filter out of the step waveform any harmonic components which can cause the structure to ring. This technique is investigated in this thesis (Chapter 6)

Linear methods are undoubtedly appropriate where the transient response of the actuator / mechanism are primary, but add unnecessary complication to systems where other methods might suffice, e.g. passive mechanical damping.

2.8 MOUNTING CONSIDERATIONS

In all situations where a multilayer actuator in employed, the static stress state, and the way in which force is transferred from the actuator to its host are prime considerations. It is pointless for example, to employ a high-efficiency, high-stiffness device in an a displacement amplifying structure if the interface between device and structure is highly compliant, as in the case where layers of epoxy are used. In consideration of this, the method employed throughout this work was firstly to retain the actuator without adhesive by ensuring that the structure imparted a static pre-load force, so that the mounting faces of the structure were capable of gripping the actuator. Secondly, a small quantity of adhesive was added to the edges of the actuator, to encourage ingress to the interface by capillary action.

This has an additional advantage. It has been shown experimentally that slightly more useful work can be transduced per full actuation cycle if the device is operated with a pre-stress corresponding to approximately ⅓ of the stall stress achievable in full actuation. This is generally true for most piezoelectric materials [10]. This effect only yields an additional 2% to 3% of output displacement for a given drive voltage, but it can be exploited, especially since operating with an ambient negative (compressive) stress reduces the magnitude of any transient tensile stress which can occur due to during transient loading; a general condition which should be avoided with ceramic materials.

The dynamic loading of the actuator is more complex, since it is influenced broadly by the speed of response of the actuator in combination with the electrical drive, and the speed of response of the host structure. The combined system is further complicated by the possibility that during the retraction phase of actuation; separation from the host will occur if the piezo' is being driven too quickly. Whilst this might be attractive from the point of view of avoidance of tensile stressing in the ceramic, it could give rise to fretting between the actuator and host, and the destruction of any bonding layers between the two. These considerations suggest that for any actuator host combination, there is an ideal electro-mechanical time-constant value. This is

application specific, since there may, for example, be situations where the speed of response during the advance phase is more important than the retraction phase, and so it may be possible in certain designs to switch on quickly and return at a more slowly, thus avoiding the problem.

The use of an anaerobic fast cure adhesive such as those in the cyanoacrylate family are recommended by manufacturers of piezoelectric multilayer actuators as a permanent method of secure installation. The author favours the use of this technique after the application of ambient stressing of the structure, relying on capillary action to draw the adhesive in to any available voids. This avoids the creation of boundary layers of adhesive between structure and actuator.

2.9 DISCUSSION.

The phenomenon of piezoelectricity and the converse effect have been investigated and the physical and behavioural characteristics of piezoelectric actuators have been discussed. This chapter imparts a working knowledge of these devices, including methods of mechanical installation and electrical drive.

It has been shown there are many diverse applications for piezoelectric actuators in their various geometries that have been proposed and successfully implemented. The few examples shown in this chapter are probably the most well known, or at least exhibit more innovation than the many others which have been put forward over the last decade. However, a deeper assessment is required, to discover if any useful application techniques have been proposed, which might be employed for clutching or gripping purposes. This assessment is carried out in chapter 3. It is clear, however, that actuators based on piezoelectric ceramic technology, are capable of operation with very low response times.

3 HIGH SPEED ACTUATORS : A LITERATURE REVIEW.

A literature search was conducted during December 1989 and January 1990, using databases such as Compendex and Inspec, targeted on articles and papers appearing since 1985, concerned with 'actuators', 'clutches' or 'brakes', in combination with 'piezoelectric', 'magnetostrictive', 'high-speed' and 'rapid'. Many interesting applications of piezoelectric ceramics were found and, in common with a prior data search, most of these applications originated in Japan, with only a few from the U.S.A. and Europe.

Relevant material obtained can be broadly divided into these four basic categories;

1) Application techniques of electrical drive and/or performance enhancement
2) Characterisation and modelling of materials and devices
3) Specific actuator applications
4) General papers and reviews

Much of the material collected is not directly relevant but is interesting from the point of view of appreciating the breadth of application of piezoelectric and other novel actuation technologies. Only a small number of articles on giant magnetostrictive materials or devices were found.

3.1 TECHNIQUES.

A number of papers put forward a technique for reducing the settling time of piezoelectric actuators. For example, in an application where the actuator must respond and settle quickly to a step change in voltage, tailoring the shape of the exciting pulse can reduce the ringing of the actuator. Another suggested the use of filtering techniques [15].

One author has used inductive flyback techniques involving energy dumping to obtain fast response from piezoelectric actuators. This technique facilitates the injection of

a fast high energy pulse into the actuator [17, 43].

A technique was found (using a series capacitor) to dramatically reduce hysteresis and long term creep from the settling behaviour [18]. This article demonstrated a technique for improving the linearity of piezoelectric actuators.

Several applications were described where piezoelectric actuators are employed in closed loop positioning systems, using positional feedback transducers; thus eliminating the need for a good linearity performance from the actuator [19, 20, 21].

3.2 CHARACTERISATION AND MODELLING.

Much information is now available about the performance of piezoelectric materials. Since the upsurge of interest in these actuator materials in the mid 1980's, this information has provided an essential breadth of data for the designer. Much of this literature is written by materials specialists and includes;

> Studies in the electrostrictive properties of PMN stacked actuators [22] and monolithic bimorphous actuators [23], more fundamental characterisations of piezoelectric ceramic multi-morph actuators [24], finite element simulations of piezoelectric motors/actuators [25], time responsivity of piezoelectric actuators [26], equivalent circuit parameters for piezoelectric ceramic resonators [27]. Some material is available on the strength [28] and temperature [29] characteristics of piezoceramics

3.3 SPECIFIC APPLICATIONS.

A multitude of applications for piezoelectric ceramics as actuators was discovered during the data search. Whilst it is possible to group these applications according to actuator geometry, for example; Stacks, Unimorphs, Bimorphs, Tubes and so on, the

basic advantages or otherwise of particular geometries are well known, and therefore grouping in this way is not especially useful. Therefore, they are grouped according to the mode of operation of the actuator, specifically;

Linear Mode	-	Displacement/Force controllers
	-	Wave (ultrasonic) motors
Mixed Mode	-	Inchworms (rotary/translational)
	-	Inertial pulse caterpillars (unique)
Pulsed Mode	-	Impulse transfer devices
Digital Mode	-	Bi-stables
	-	Clutches (NONE) [8]

3.3.1 Displacement/Force Controllers.

This category contains many applications since micro-movement is the obvious application for piezo devices. The geometry and size of the device will be dictated by the required force/compliance and speed characteristics. Applications found included;

> High-speed electro-hydraulic servo-valves [30] used for pressure control, active damping techniques to reduce vibration [31], many optical applications (mostly active mirrors) where the piezoelectric actuator was used directly [32,33,34]. Since piezoelectric ceramic actuators can function at very low temperatures, there are many possibilities for application in cryogenics [35]. The scanning tunnelling microscope [36,37] is a common area of application as are micro positioning in video head positioning systems [38]

[8] This group is included to indicate the lack of applications in which piezoelectric actuators are used for clutching.

3.3.2 Wave Motors.

A diagram showing the operation of this type of device can be found on page 14 in Figure 9. A wave motor consists of a composite ring of piezoelectric annular segments bonded to an elastic ring. This constitutes the stator. The rotor is a ring of material in contact with the surface of the elastic ring.

The construction of this is devised so that when the piezoelectric elements are excited by a two phase sinusoidal signal pair, a travelling wave of displacement is generated around the circumference of the annuli. The construction of the rings ensures that points on the surface of the elastic ring, in contact with the rotor, describe an ellipse.

Thus, as the travelling wave rotates in one direction, the rotor is forced in the opposite direction. The whole process is usually driven at ultrasonic frequencies since this results in useful angular velocities and quiet operation. It's applications are wide ranging where moderate torque and good efficiency are required. In addition, the motors perform well at moderate torques at very low speeds.

3.3.3 Inchworms (Rotary/Translational)

The inchworm, also discussed in section 2.4.6 on page 15, was originally designed as a long range, high resolution, low speed linear actuator. It's operation requires three actuators, specifically, two as clamps, and one as a linear displacer. Although this device is well known, it is noteworthy that the inchworm principle is applicable to many different geometries. Variants of the standard technique involve replacing one or both of the piezoelectric active clamps with passive clamps. Other variants have been proposed such as a piezoelectric driven turntable with high positioning accuracy [39].

3.3.4 Inertial Pulse Caterpillars.

This title attempts to describe an operating principle succinctly, and is best understood by example. Consider two dissimilar masses, joined by a stiff piezo-actuator. The largest mass rests on, or is compliantly constrained against a level surface, effectively clamped by static friction. If the actuator is electrically driven from a parabolic waveform, the small mass will accelerate away from the other, provided the reactive force is not large enough to overcome static friction.

At some point, the drive waveform is forced to zero quickly. This results in a contraction of the actuator and a sudden attraction between the two masses. Since this is an impulse, the near instantaneous force will overcome static friction, and the large mass will skid, then come to rest. The cycle is then repeated.

Thus, the mechanism can creep across a surface. By changing the sense of the slope of the drive waveforms, the motion is reversible. Two actuators mounted orthogonally can make an XY translation table. This technique will work also for a system with viscous drag rather than static friction [40].

This technique has been applied in relatively few micro- positioning applications as yet, but the appearance of further applications is anticipated, due to the simplicity of the technique.

3.3.5 Impulse Transfer Devices.

This category includes any actuator which transfers its electro-mechanical energy (or a fraction thereof) into the kinetic energy of another body, usually one of low mass. This need not involve a collision as such, since the energy transfer can occur via an elastic medium already in intimate contact. One advantage of this technique is that the actuator as a whole can deliver an energy impulse at a long displacement range compared with the free movement of the actuator alone. Examples of this principle

include a Printing flight hammer [41] for dot matrix printers, and a device used in the ceramics industry for punching out thin layers in the Green sheet manufacturing process [42].

3.3.6 Bi-Stables.

These are devices which employ an actuator to be in one of two well defined states. Only one example of this type was found, specifically a piezoelectrically operated electrical relay [16].

3.3.7 Clutches or Brakes.

No literature was found where either piezoelectric ceramics or giant magnetostrictors had been utilised as a clutching or coupling element for the control of discrete motion mechanisms or otherwise, other than the inchworm type of device where the discrete movements were extremely small.

3.4 General Papers And Reviews.

The subject material contained in this section is either application non-specific, or concerned with the application of actuators in generic fields. Subjects covered / titles were ;

Piezoelectric actuators: powerful and fast [17, 43]
Piezoelectric actuator and its applications [44]
PZT printing applications, technologies, new devices [41]
Development of piezoelectric technology for applications in control of intelligent structures [45]
Piezoelectric materials for low hysteresis actuators [46]

State and future trend of solid element actuator [47]
Multilayer Piezoelectric Ceramic Actuators and Their Applications [8]
Recent applications of PMN-based electrostrictors [48]
Precise Positioning with Piezoelectric Translators [49]

3.5 DISCUSSION OF REVIEW FINDINGS.

The literature review has revealed a very wide range of applications for piezoelectric ceramic actuators. Interestingly, the absence of applications where these devices are used in clutching or gripping is significant. This is likely to be due to the fact that the key to using piezoelectric actuators in clutching or gripping applications (whether acting directly or as a latch), lies in the ability to design efficient mechanical displacement amplifiers, to transform the movement which can be generated by a piezoelectric ceramic actuator, to a usable range. This is presented in the following chapter.

The design of displacement amplifiers, let alone those of high-efficiency, has not been revealed in the data search. This indicates a necessary area of research, which if fruitful would facilitate the design of machines as proposed in the introduction. Indeed, in the literature covered by the category of 'Displacement/Force Controllers', the only reference that could be found which held any design oriented information was concerned with the design of flexure hinges (Paros & Weisbord) [50]. Inspection of the designs for devices such as the cryogenic translation stage [35] showed no evidence of designing optimisation for either speed or mechanical efficiency for the complete (structure) amplifier.

The literature review also revealed interesting devices based on the principle of impulse transfer. As will be shown later, the requirements for an actuator which can control or regulate discrete motion drives, can be met by a solid-state displacement amplifying linkage, but for other latching applications, the long displacement ranges potentially offered by impulse transfer are attractive. The impulse transfer process is

briefly studied in chapter 8 on page 169.

4 FEASIBILITY OF DIRECT PIEZOELECTRIC CLUTCHING.

Between April 1989 and December 1989 two notional designs were proposed by Murphy [9], with the intention of demonstrating the feasibility of using fast piezoelectric actuators for direct clutching. One design was for a three clutch linear drive assembly, and the other for a rotary drive assembly. The mechanisms themselves were simply test beds for the clutching elements and were of sound design.

It was originally hoped that by achieving rapid clutching with actuation times of much less than 1 ms, it would prove possible to clutch on to a reciprocating component at a relative velocity very close to zero, and as a consequence attain clutching with a low rate of wear. This objective remained unrealised until a review of all of the relevant design criteria had been undertaken and whilst a detailed design study of the proposed mechanisms is not discussed here, consideration of these systems has brought forth design criteria which ultimately proved essential factors in the final design of two successful piezoelectric discrete motion drive systems referred to here as the *discrete motion machine* and the *rotary micropositioner* [10].

4.1 DIRECT ACTION PIEZOELECTRIC CLUTCHING.

In the linear drive design referred to above, the actuator is positioned in such a way, so that it is able to grip a thin (50 μm thickness) steel strip. There are two reciprocating strips, each with their own clutch. Both clutches are mounted on a common assembly which is free to move linearly. The arrangement is so designed that motion of the free assembly is derived from the motions of the reciprocating strips, in combination with electrical control of the clutches. In turn the reciprocating strips derive their motion from a rotating input shaft. Refer to Figure 112 on page 189 which shows a schematic diagram of the final discrete motion machine. The design concept

[9]Prior work does not exist in any presentable form.

[10]Refer to chapter 9 for details of these applications.

of the original and final designs is identical.

In the original design, the clutching elements essentially comprise a stack type piezoelectric actuator, a retention spring and a housing for the stack which offers an adjustable compression plate. The system was based on Burleigh PZO-007-0 actuators, and as their part number suggests these only develop a free displacement of approximately 7 μm. As the design stands, there are several points which can be identified as reasons why it would fail.

i) CLEARANCE.

The clutching element is unsatisfactory because of the full throw movement of the actuator is only 7 μm (0.3 thou). The magnitude of the required clutching force will determine how much of this movement is lost to compression of the actuator in developing this force. This reduces the effective clearance available between the clutching face of the actuator and the thin metal strip when in the 'off' state. The required stress is calculable from the inertial load of the system, the speed of rotation and eccentricity of the input shaft [11]. Assuming that in a typical application, no more than 30% of the full range of movement is lost to compressive stress the remaining clearance is approximately 5 μm.

ii) THERMAL CONSIDERATIONS.

The coefficient of linear thermal expansion for a typical hard PZT material is typically between $3x10^{-6}$ and $5x10^{-6}$ °C $^{-1}$. If the actuation element is 15 mm in length, then the rest length of the actuator will vary with temperature by 45 nm°C $^{-1}$ (Note: this does not include contributions from non-ceramic actuator components such as end caps and bonding materials).

[11]This is shown in detail for the new discrete motion machine in the chapter on applications.

For reliable operation, free from thermally induced drift, the length of the actuator housing should be equal to the length of the actuator at any temperature. Any mismatch will leave a residual temperature coefficient describing clearance against temperature. As an example, to keep the thermal movement to within 1 μm over a 50 °C range of temperature, the linear coefficients of expansion (c.l.e.'s) must match to within 1.3 ppm°C $^{-1}$. This is difficult to achieve even assuming perfect thermal tracking of all critical components. If the temperature changes by 10°C, the linear coefficients of expansion must match to within 6.5 ppm°C $^{-1}$. (As will be seen later, this is possible by using a soft piezoelectric material with a c.l.e. of 5 ppm°C $^{-1}$, in combination with a titanium alloy which has typical c.l.e. values of 9 ppm°C $^{-1}$). The use of steel devices is only feasible if the temperature range is restricted.

In addition, the prime sources of heat will be actuator itself, from losses both mechanical and electrical, and from the clutching surfaces. Thus, it is reasonable to assume that whatever geometry the housing assumes, there will be a thermal diffusion process, with a peak temperature originating within, or at the boundary of the actuator, thus generating a thermal gradient. For this reason, any materials chosen must have a low intrinsic temperature coefficient (e.g. Titanium [12]). In view of the exacting matching requirements, great care would be needed in the design of the housing.

A second effect is the variation of d_{33} with temperature. This will manifest as a variability of clutching force with ambient temperature. A typical curve for soft piezoelectric material is shown in Figure 12 on page 20.

Neglecting any variability due to hysteresis and creep, designing a device for operation over the range 0 to 100 °C would require a tolerance on output displacement of ±3% of nominal. The figure exacerbates the drift problem because of the partitioning of total output displacement into the two zones of clearance and force development.

[12]Invar is an interesting possibility since its c.l.e. is almost zero at S.T.P. Its elastic modulus of 145 GPa is also attractive.

iii) DEBRIS.

Particulate contaminants in the size range of the order of 1 μm, would cause serious problems at the clutching interface if the operating clearance of the device was in the order of 5 μm, possibly causing wear, scratching and premature failure. If the device were to be operated in a sealed or clean environment, this might not be such a serious problem but the intention is to develop a device which is robust enough to be able to exist and operate in environments such as those occupied by textiles machinery. This factor alone is sufficient to compel the design process towards achieving much higher displacements.

iv) CLUTCHING STRIP.

The clutching strips in the original design were specified at 0.002" (50 μm) thickness. One benefit of clutching on to a thin component is the advantage that thickness variations of that component are likely to be proportional to the nominal thickness. It is not difficult to envisage that a strip of 50 μm thickness might have variations around this value of several microns. In practice, the variation would have to fall below ±1 μm or better for this design, and that tolerance is quite demanding.

Additionally, very large tensions would be required in the strip to prevent fouling between the strip and the inactive clutch, which again is undesirable.

v) MATERIALS OR DEVICES.

Examination of the contemporary state of the art regarding piezoelectric / electrostrictive materials indicates the availability of devices of superior performance to those originally specified. As an example, a stacked Lead Magnesium Niobate (PMN) electrostrictive actuator was constructed by Nakajima [22] (et al) in 1985, who claimed that displacements in excess of 2000 microstrain were achievable. (It is worth pointing out here that this was an experimental electrostrictor rather that a piezoelectric actuator, with poor temperature dependence of displacement.)

Multilayer devices manufactured by Tokin Corporation (of Japan) exhibit performance specifications far superior to those offered by Burleigh Instruments, in terms of device stiffness rather than output movement.

vi) DESIGN RECOMMENDATIONS.

In view of the problems associated with using a piezoelectric actuator to directly clutch on to a component, it is evident that a transforming mechanism is required to increase the effective clutching movement, possibly by an order of magnitude, at the expense of clutching force. This would reduce the significance of the effects of debris, strip thickness non-uniformity and clearance / adjustment problems, although careful attention to the actuator housing / mount would still be paramount for reasons associated with their differential thermal expansion. The level of amplification depends on factors such as the precision to which the target machine is manufactured, and the environment in which it is operated. However, clearances in the order of 50 μm are not difficult to achieve and therefore a displacement amplifier generating movements of approximately 100 μm are appropriate.

4.2 MECHANICAL AMPLIFIERS AND ACTUATOR REQUIREMENTS.

The previous discussion has made clear that there is a need for the generation of movements greater than those normally associated with piezoelectric multilayer actuators. Although there are devices available which can produce movements approaching 50 μm, they have a long / thin aspect ratio and are very expensive. As an example, a stack or multilayer device developing this displacement would have to be at least 60 mm in length. Also, a multilayer device of reasonable aspect ratio (< 5:1) would be capable of producing a 4500 N stall force, which is very large compared to the forces required in clutching small high-speed components. This represents a significant waste of energy.

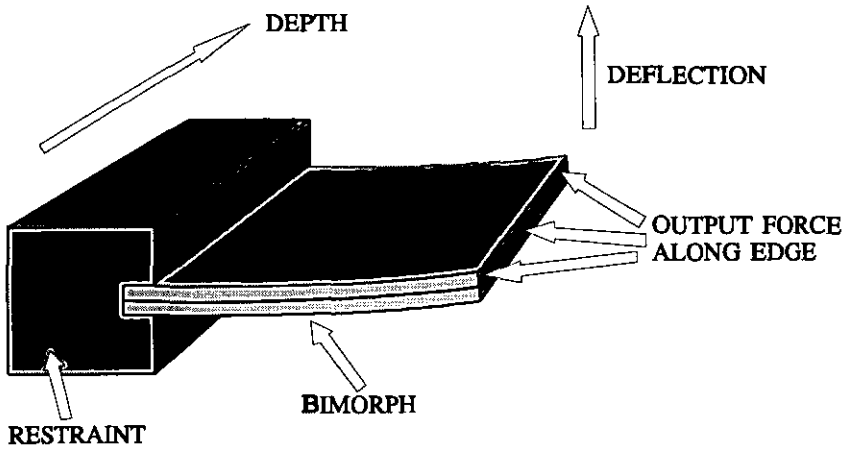

Figure 19: Bimorph Shape Required to Generate Larger Forces.

It is possible to consider piezoelectric bimorph or multimorph topologies for generating larger displacements. Some multimorphs are very similar to stacks in many ways, and no real technical advantage is gained by their use, and in fact for a given application a larger device (by volume) would be required. Some multimorphs and bimorphs can generate much larger movements than stacks, but to generate forces over say 10 N requires increasing the 'depth' of the actuator, as in Figure 19. It would be difficult to design this type of actuator into a compact device.

From this view point it becomes clear that a high performance mechanical amplifying linkage would be desirable, with which it would be possible to transform the movement generated by a piezoelectric ceramic stack or multilayer actuator, to a useable range of movement suitable for application in a working clutching mechanism. The remainder of this chapter details the findings of a preliminary design study which was intended to find transforming methods or mechanisms, based on an intelligent selection of candidates. It was assumed that a minimum clearance of 50 μm is required for use in a practical clutching mechanism.

4.3 AN APPRAISAL OF THE CLUTCHING FUNCTION.

Prior to designing a mechanical amplifier it is essential to understand the kinematics and allied processes likely to be involved in the operation of a good design. For this reason, several relevant topics are reviewed here.

i) Energy in Clutching.

In a perfect system, there might be materials for clutching surfaces of infinite stiffness or rigidity. If this were so, no work would need to be done in clutching since;

$$W = \int F.dx \qquad (35)$$

and no movement would take place. However, since all materials are compliant, the stiffness of the clutch materials and the host mechanism will determine the work done in achieving a given clutching force.

If the clutch is to couple a known load, it is possible to calculate the minimum clutching force required to guarantee no slip under dynamic or static load, based on the coefficients of dynamic and static friction between the clutching faces. In practice, this limitation will not come from the compliance of the surface against which clutching occurs, but rather from the output compliance of the clutching amplifier.

ii) Stiffness versus Coefficient of Friction.

In reality, appropriate materials must be chosen for the clutching faces such that the clutching movement is kept to a minimum. Therefore, the system must have the highest stiffness possible without violating other considerations.

Unfortunately, high stiffness and high coefficient of friction tend to be antagonistic characteristics, since for materials with similar bulk properties, rougher and hence more compliant surfaces tend to exhibit a higher coefficient of static friction.

iii) Energy of Translation.

The separation of the clutching faces in the de-clutched state is an important design aspect. This must be large enough to guarantee that variations in separation due to thermal, environmental and engineering tolerance effects, do not degrade or even prevent correct function. The larger the clearance the more robust the design, (e.g. against the effects of the ingress of particulate contamination).

A larger clearance will, however, increase the time required in traversing to and fro, or require more energy for the clutching face to reach it's target, since the mechanism will have to accelerate from rest prior to collision of the clutching faces. In practice, this energy will almost certainly appear thermally and acoustically, and therefore be lost. Unfortunately, stiffer mechanisms are generally more massive, and so enhanced stiffness will be paid for in the translational energy lost per cycle.

iv) Speed of Response.

The requirement for fast actuation needs to be re-stated, because the introduction of a linkage is certain to result in a response time (from de-clutched to fully clutched) which is less dependant on the responsivity of the driving piezoelectric device itself than the dynamics of the linkage. For a particular implementation, the greater the movement amplification, the longer the response time. A brief study has shown, however, that for the size and mass of mechanism likely to be involved and the movements traversed, response times in the order of tenth's of milliseconds are feasible.

4.4 CANDIDATES FOR DISPLACEMENT AMPLIFYING SYSTEMS.

During the literature survey, some interesting displacement amplification methods were found to have been employed in many of the applications for piezoelectric actuators.

Methods of amplification using leverage and exploiting flexure hinges were found recurrently. Significantly, methods of amplification using leverage and employing bearings, pins or other sliding surfaces were absent, and, the reason for this becomes clear on consideration of the forces which piezoelectric multilayer actuators can produce. Within such an actuator, direct stresses in the order of 30 to 40 MPa can be developed if expansion of the device is restrained, and typical 'stall' forces can approach 10^3 N in even modest devices. If an efficient amplifying linkage is to be designed, the pivots must be capable of withstanding the repeated application of such forces. Additionally, the pivots of such linkages must be free from backlash, either by pre-loading, or by intrinsic characteristic.

In the leverage methods described which follow, the bridge and the simple levers assume the use of flexural hinges. (In 'no-work' designs where only modest forces could be developed, these amplification methods could employ bearing surfaces in place of the hinges).

4.4.1 Simple Lever (Direct Output).

Probably the most obvious device for this application, is the simple lever. That is, an arm 'free' to pivot around one axis with the actuator and clutch being situated at different separations from the pivot, to obtain the required displacement amplification ratio. The term 'direct' refers to the direction of output movement with reference to the input movement. Displacement amplification can be inverting of non-inverting as shown in Figure 20.

In practice, because movements are so small, it would be inappropriate to use a pivot which relied on the rotation of bearing surfaces. A short, translationally stiff but torsionally compliant ligament would be an ideal solution. This pivoting technique is common in applications of piezoelectric ceramic devices, particularly stacks where large movements are required. Interestingly, during the literature surveys, no applications were found where the efficiency of the device was primary, i.e. most

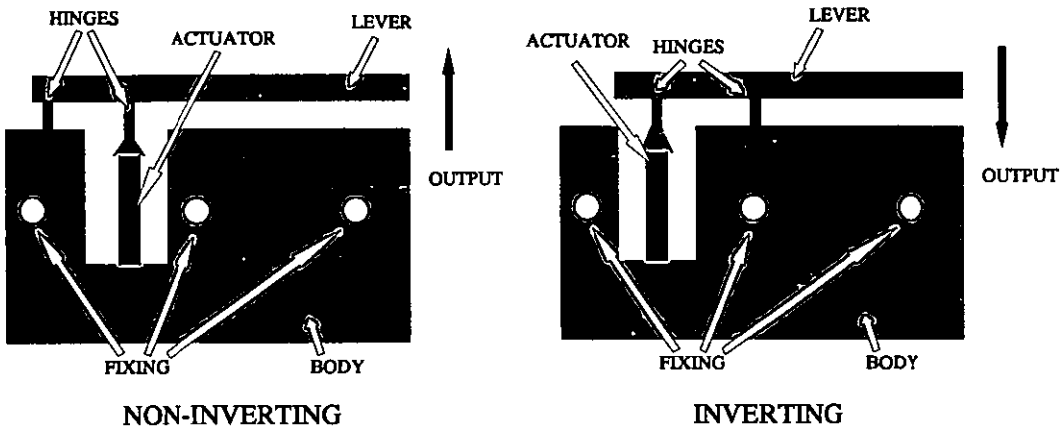

Figure 20: Simple Lever Displacement Amplifiers.

applications involved an output where no significant work need be done.

The design of such amplifying systems is covered in depth in a later section of this thesis [13]. At this point a simple idealised study of a displacement amplifier will illustrate the possible range of performance with the linear approach.

STUDY OF SIMPLE PIVOTS.

A brief simplistic study shows interesting results, based on using a NLA-5x5x18 actuator [14] and a simple pivot. For the sake of comparison with the bistable amplifier (see section 4.4.4), figures will be offered based on a clutching displacement of +275 μm.

(Note: In this configuration, a restoring force would be necessary to de-clutch, to avoid tensile loading of the actuator and ensure rapid withdrawal. This force might well be derived from the preload usually necessary for correct operation of a stack.)

[13]"Beam Designer Program" in chapter 6.

[14]Manufactured by Tokin Corp. of Japan.

For a linear amplifier, stall force falls off linearly with output position. It can be shown that the maximum force-displacement product of these terms occurs when the output displacement is exactly half of the free displacement, therefore this can be fixed at +550 μm, requiring a gain of 36.67 from an actuator delivering 15 μm of free displacement. Assuming perfect pivots, as in the example of the bistable device, this would give a zero displacement stall force of 23.3 N. The force at the half displacement point is exactly half this, i.e. 11.6 N. The force-displacement efficiency for this system is 25%.

4.4.2 Simple Lever (Transverse Output).

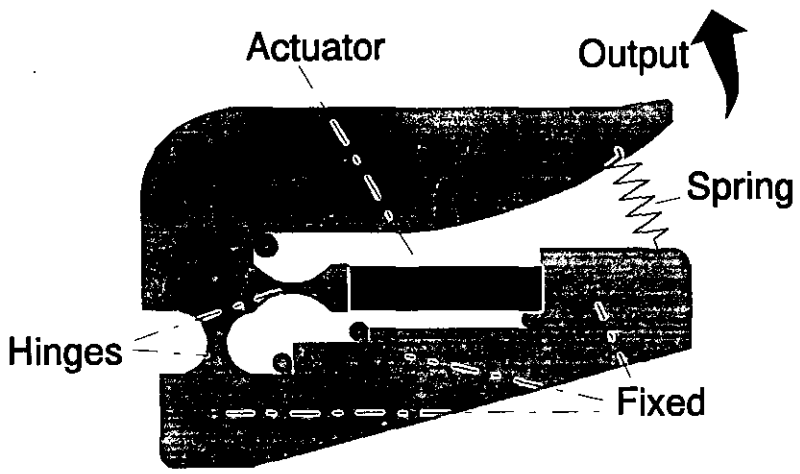

Figure 21: An Example of a Simple Lever Amplifier (Transverse).

Figure 21 shows a simple lever device which varies from its 'direct' counterpart in that the output movement is perpendicular to the input movement. Whilst this topology can lead to more compact designs, shear stressing of the hinge attached to the static part of the structure occurs when the output arm experiences a reaction. Unlike the direct output simple lever, the efficient design of this type of structure depends on low shear

compliance of the static hinge.

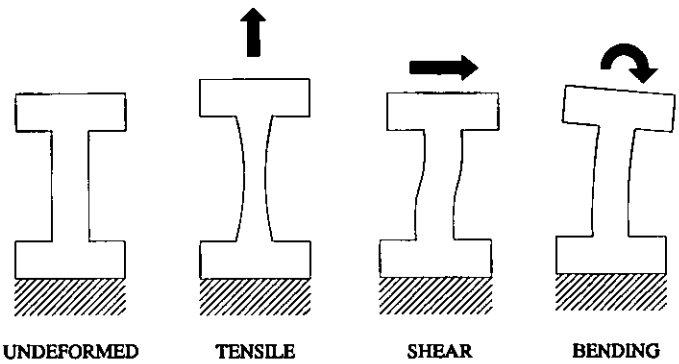

Figure 22: Static Modes of Deformation of a Flexural Hinge.

Figure 22 shows the way in which a flexural hinge deforms in response to tensile, shear and bending forces. The required behaviour for the direct amplifier is for low compliance to tensile forces, but high compliance to bending forces, whereas the transverse amplifier is burdened with the additional requirement of low shear compliance; making the design of efficient devices of this topology more difficult.

4.4.3 Compressive Flexural Bridge.

A Compressive Flexural Bridge is a mechanical system comprising an actuator, generating a large compressive force with small movement, acting in such a way as to deform the bridge against an end-stop, resulting in a large transverse movement at the centre of the bridge as in Figure 23.

If we define 'mechanical gain', as being the rate of change of transverse movement, with respect to axial movement, then this quantity varies strongly with axial position. The corollary is that the mechanical gain for small movements can be tuned or selected, by applying the appropriate pre-load or bridge angle.

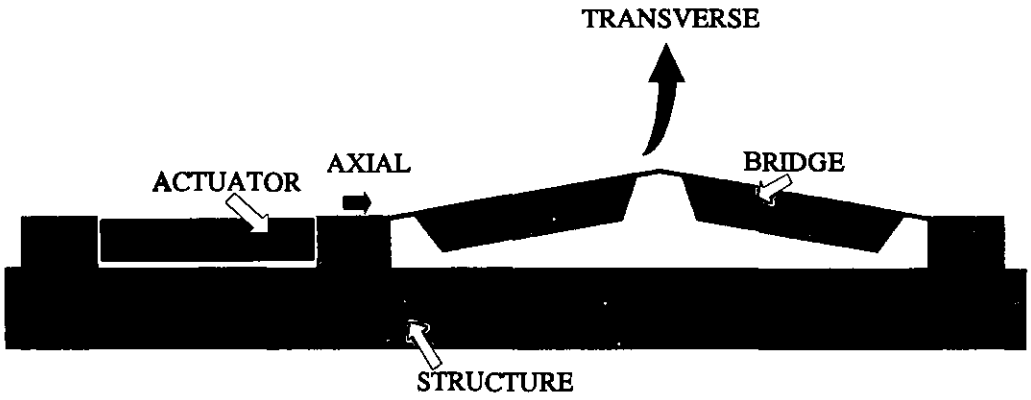

Figure 23: Basic Concept for the Flexural Bridge Amplifier.

Some typical figures will be of some interest. For a bridge with both arms equal to 10 mm. in length, a pre-bias of 50 μm will cause an initial transverse displacement of 707 μm (0.7mm). This gives the system a mechanical gain of approximately 7, yielding a 49 μm transverse movement for an input of 7 μm. At this operating point, the bridge slope is approximately 4 degrees. For perfect pivots, the relationship between drive force F_d and output force F_o is;

$$F_o = 2 F_d \sin(a) \qquad \textbf{(36)}$$

This gives $F_o = 0.14 F_d$, so for a 500 N driving force we could expect a 71 N output force if the output was restrained from moving, i.e. stalled. This might lead us to select a longer piezoelectric actuator, with longer movement (requiring lower mechanical gain), or a stack with broader elements giving more stall force, or an intermediate combination. Variations on this theme are possible. For example, a two element bridge could be replaced with a single leaf spring. Although the geometry changes from linear deformation to circular deformation, there are important advantages and disadvantages, specifically;

ADVANTAGES.

i) Inherent spring force keeps the system in compression, thus reducing hysteresis.

ii) Non-existence of centre pivot, i.e. a further contribution to the reduction of hysteresis.

iii) Tunability of gain by adjusting the preload displacement.

iv) Low Inertia

DISADVANTAGES.

i) Potential deformation of spring in one of several buckling modes.

ii) Potential reduction in clutching force due to deformation or bowing.

iii) Smaller bridge angles may result in higher direct compressive stresses when the output is stalled, making it difficult to produce a design which does not fatigue quickly, or in which the compressive strain energy losses become significant.

It is, however, possible to envisage a design of bridge which tempers the disadvantages and enhances the advantages of these two approaches. Such a design would therefore consist of a single beam of variable thickness along its length, the minimum thickness occurring at the centre of the beam, constituting a flexible hinge. This approach is later applied in combination with a flexural hinge (or simple beam) preamplifier, and constitutes the Strip Clutch Element, referred to in chapter 5.

4.4.4 Snap Action Toggle (Bi-Stable Device).

As a concept, this mechanism can be considered statically as one with a single degree of freedom, i.e. position, and can only occupy one of two discrete states. In any case, the distance between these two states will be commensurate with the actuating

distance required to give adequate operating clearance and sufficient clutching force.

The distinguishing feature of this generic device is that two distinct wells of potential energy exist at the extremes of movement within the allowed domain, and therefore, work must be done to overcome the potential barrier between these wells, should transition from one stable state to another be required. A simple model of this type of structure is shown in Figure 24.

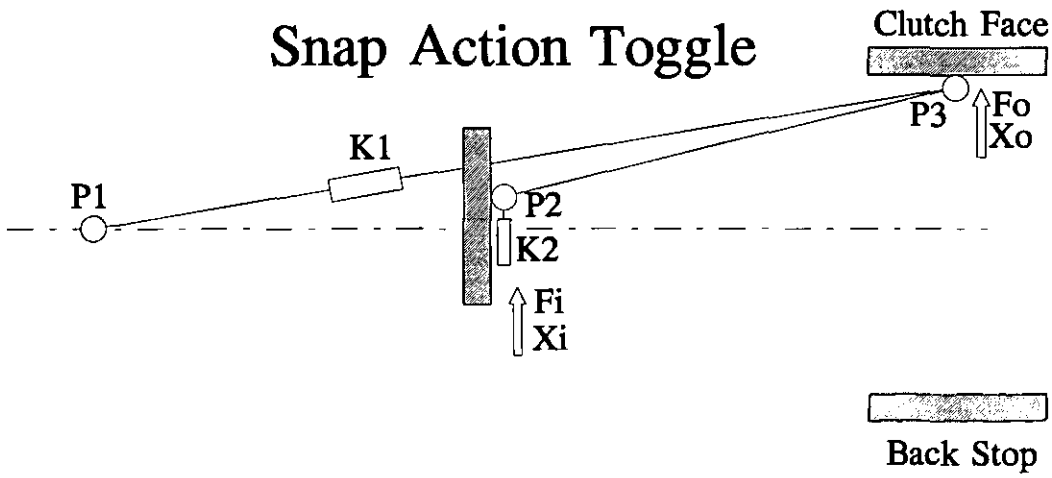

Figure 24: Operating Principle of a Snap Action Toggle.

The static characteristics of this structure can be seen in Figure 25. All graphs are plotted with the piezoelectric drive x_d as the independent variable. Graph A shows the input position x_i, graph B shows the corresponding input force F_i. Graph C shows the output position x_o (bi-state), and graph D shows the output force F_o. It is envisaged that the positions corresponding to the wells will be beyond the positions of clutch fully engaged and, fully disengaged. The piezoelectric actuator would be positioned and coupled in such a way as to be capable of overcoming the barrier bi-directionally. Inherent leverage (amplification) within the mechanism would be exploited.

In terms of force and displacement generated, this type of device is ideally suited to clutching. This is because (unlike a linear amplifier) the force generated and the output stiffness both attain a maximum much closer to the extremes of displacement.

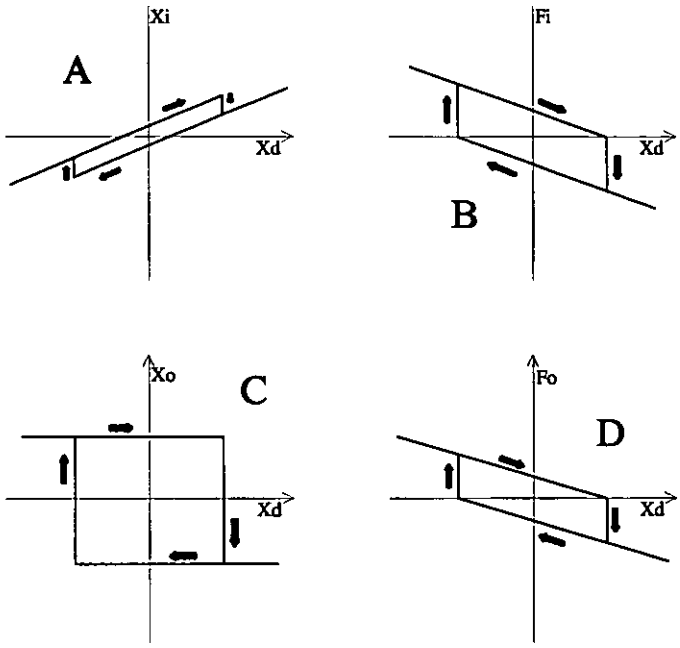

Figure 25: Force/Displacement Characteristics.

This type of device can be implemented in several ways, and structures can be envisaged which manifest the properties discussed. However, there is a variant of this class of device which not only exploits the bistability principle to achieve the large range with high force, but employs a dynamic approach. This is the subject of the following study.

STUDY OF A BI-STABLE, DYNAMICALLY-OPERATED MECHANISM.

The operating principle of a bistable device is shown in Figure 26. The piezoelectric actuator is at full extension in the quiescent state, and the pivots are considered to be perfect. When the actuator is caused to relax, tensile forces appear in the arms of the structure causing the mass to accelerate towards the central mean position. When the mass crosses the mean datum, the actuator is re-excited causing compressive forces in the arms. Simultaneously, the acquired momentum of the mass allows the structure to continue, as the forces increase accelerating the mass into the opposite stable state. The output force/displacement characteristics (under stall) of such a device are shown

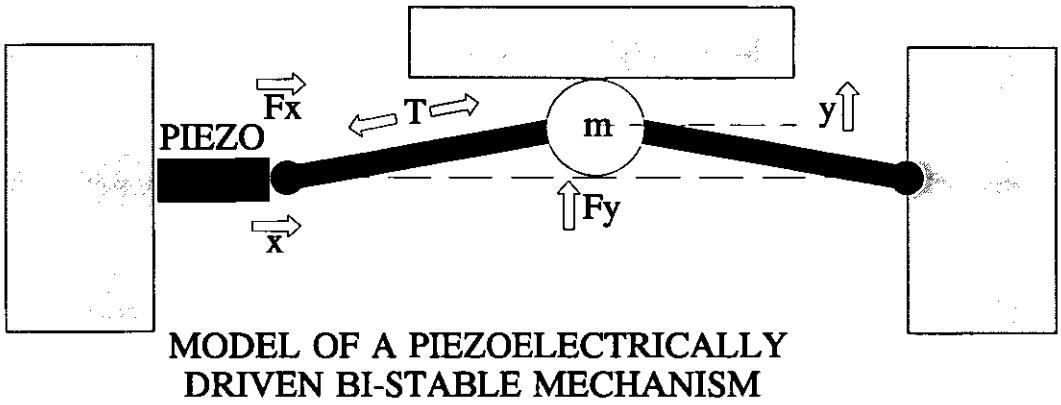

Figure 26: Model of a bistable mechanism.

in Figure 27. Interestingly, maximum force is possible when the output is displaced to approximately half of the relaxed displacement, in contrast to a linear amplifier, where the maximum force is developed at zero displacement, precisely where it is not required.

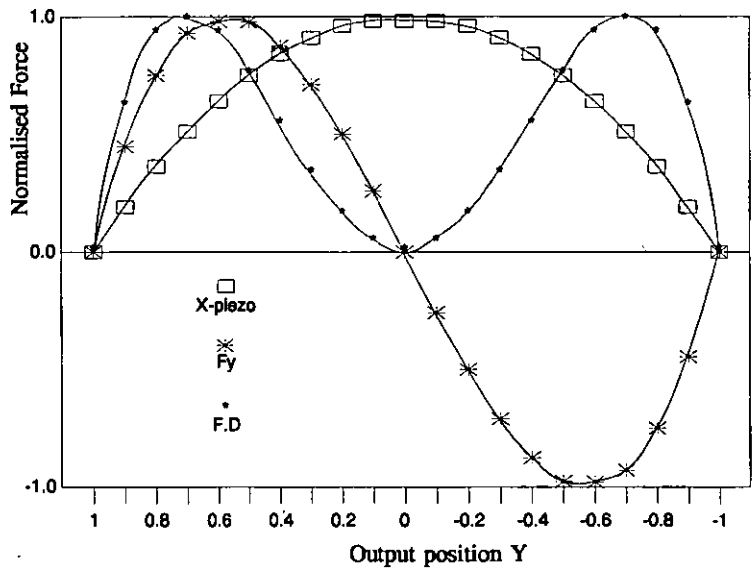

Figure 27: Static Internal and Output Force.

A simple time-dependent computer simulation of the forces and movements of a simple bistable device was undertaken. The device was modelled as a two pivot, two arm device as in Figure 26, with perfect pivots and infinitely stiff arms, and coerced into an operating zone forcing two stable positions, the two stable joint positions being separated by over 500 μm. Calculations were based on the Tokin NLA-5x5x18 actuator, generating 15μm of free displacement, with a stall force of 854 N. The arms were 20 mm in length and the central mass was 0.025 kg. The joint of the two arms was free to move between two positions or stops; both ±282 μm from the centre line of the two pivots.

It is not implied that this particular device is suggested for any particular real application, but it is offered as a demonstration of devices which fall into this category.

The modelling system employed was a host computer program called "Distime", a discrete time simulator running under MS-DOS and QuickBasic 4.5 [15]. The internal structure of the program can be studied in Appendix 3, however the model routine is listed here for clarity.

```
'
'       PC DISTIME
'
'       AUTHOR: J.K. THORNLEY
'

DEFSNG A-Z
initialise .025, .2, 3

'       piezo parameters

        emod = 4.1E+10
        piezo.area = .005 ^ 2
        piezo.length = .018
        piezo.stiffness = emod * piezo.area / piezo.length


'       dynamics parameters

        airviscosity = 0!
        boundviscosity = 500!
        boundstiffness = 1E+07
```

[15] Written by the author.

```
        mass = .025

'       collision / geometry parameters

        x0 = .000015
        s = .02
        yb.peak.force = SQR(s * x0 - x0 ^ 2 / 4)

        yboundary = yb.peak.force * .5

'       initial conditions

        y = yboundary
        x = 2 * (s - SQR(s * s - y * y))

DO
IF quitflag% THEN EXIT DO

    adjust "frequency", freq
    adjust "mass", mass

        trigger fire%, 1
        xd = x0 * (1 + fire%)
        IF zerocross(y) THEN
            reeset fire%
            tick 2
        END IF

        IF ABS(y) > ABS(yboundary) THEN
            stiffness = boundstiffness
        ELSE
            stiffness = 0
        END IF

        IF (y > yboundary AND vely > 0) OR (y < -yboundary AND
vely < 0) THEN
            damping = boundviscosity + airviscosity
        ELSE
            damping = airviscosity
        END IF

        IF y > 0 THEN
            penetration = y - yboundary
        ELSE
            penetration = y + yboundary
        END IF

        springforce = stiffness * penetration

        fx = (xd - x) * piezo.stiffness
        fy = 2 * fx * y / (s - x / 2)
        accy = (fy - damping * vely - springforce) / mass
        vely = vely + accy * delt
        y = y + vely * delt
        x = 2 * (s - SQR(s * s - y * y))

        IF springforce = 0 THEN tick 3

        plot 1000000! * xd, 20, "xd micro", "##.##"
        plot 1000000! * y, 500, "yo micro ", "####.#"
        plot springforce, 50, "force", "####.#"

LOOP
END
```

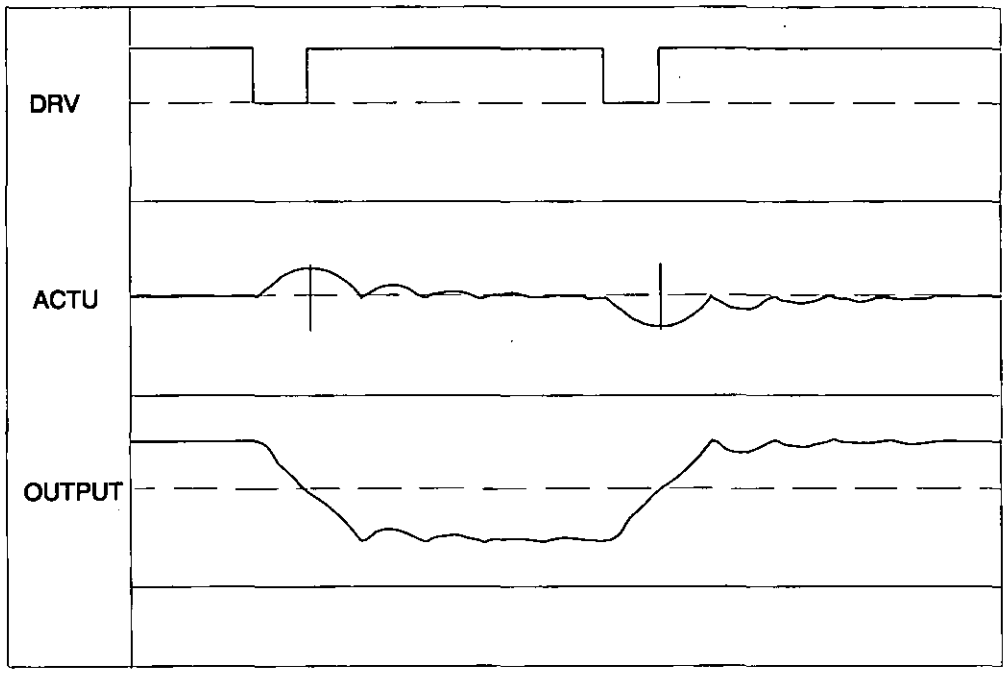

Figure 28: A Sample Output Trace from the Discrete Time Model.

A sample output from the simulation program is shown in Figure 28. The trace ' DRV ' represents the electrical drive to the actuator, ' ACTU ' is the input displacement, and ' OUTPUT ' is the resulting output displacement. The program also offered the time profiles of the drive and clutching forces (not shown). The data obtained from this model is shown in Table 1.

The force displacement efficiency for this system is given as;

$$\eta_{f.d} = \frac{F_o y_o}{F_i y_i} \tag{37}$$

and is equal to 37.8% in this instance.

Output Stall Force	17.6 N
Output Displacement	± 275 μm
Actuation time-zero crossing	1.85 ms
Actuation time-settling	4.09 ms
Input Stall Force	854 N
Input displacement	15 μm

TABLE 1: Results predicted by the Snap-Action Toggle Simulation.

LINEAR VERSUS BISTABLE.

There are advantages and disadvantages to utilising these general approaches. There exists as yet no real design for a bistable device based around a piezoelectric multilayer actuator (stack), but it is clear that this approach offers some promise, simply because of the apparent efficiency advantage over the linear approach. In fact, the efficiency figures do not allow for the fact that the bistable is an inherently bidirectional device, and thus it could be conceptually argued that the efficiency for the bistable should be doubled to make a fair comparison in some applications, giving an even greater advantage to the bistable system. In some applications where precise timing is not required, the bidirectionality of the device may reduce the complexity of the machine system.

The main difficulty associated with bistable type structures is likely to be a severe material property requirement for resistance to fatigue, should flexure hinges be used.

4.4.5 Hydraulic Amplifier.

The basic principles involved in hydraulic coupling (master/slave systems) are well known. Exploitation is usually made of the force magnifying properties of

piston/cylinder combinations in series, having dissimilar cross sections. Such an arrangement is shown in Figure 29. Ideally, work done against the master piston is usefully recovered at the slave. In an ideal system, where fluids and seals are incompressible, and therefore isentropic, and there is little mechanical friction, it is possible to envisage a fluid coupling where movement is efficiently amplified.

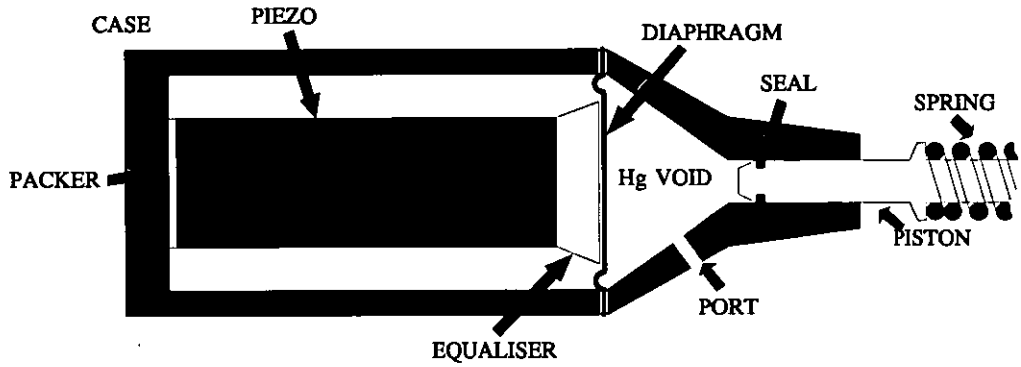

Figure 29: A Hydraulic Displacement Amplifier.

Calculations show that the pressures required to couple useful work from a piezoelectric actuator such as the NLA 5x5x18, are of the order of 10 MPa. For a 7.5mm diameter master cylinder, the swept volume of the actuator coupling face is 0.662×10^{-9} m ^{3}, or 66.2 μlitre. This volume is far too small to be useful at these pressures, since deformations of seals would result in major losses. If the design were made to operate with constant fluid pressure in static equilibrium, however, the deformation of seals would become nominally constant, and would therefore not affect significantly the no-load mechanical gain of the device. Additionally, since the primary movement is small (15 μm), the primary piston can be a flexible diaphragm, since the movement to diameter ratio is very low.

A hydraulic amplifier was accordingly designed and constructed as seen in the cross-section shown in Figure 30. Plate 1 on page 298 shows the component parts of this design and Plate 2 the assembled device [16].

[16]In practice, the disk-springs were replaced by a single coil spring for initial testing.

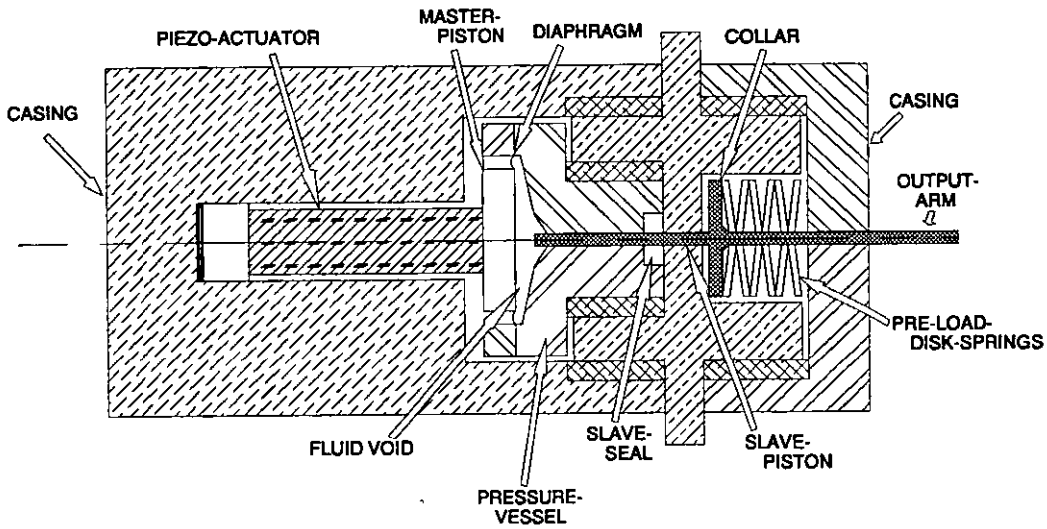

Figure 30: Hydraulic Amplifier (Cross-Section).

The seals in the device represent a major design problem. The primary (master) seal is designed around a diaphragm as shown in Figure 29. If pressure is constant, then the seal will bow out and remain under constant loading. In this seal the movements are small and can be accommodated by flexure of the diaphragm. The secondary piston is problematic as in theory the movement of the piston could be greater than 1 mm; representing a gain of x66. On the scale demanded by the size of available actuators, and the required diameter of the secondary (slave) piston, diaphragm seals could not be used because the ratio of movement to diameter is too high, and a sliding seal is necessary. Friction here, caused by the fluid pressure and tribology of the seal on the piston caused complete stalling and no measurable output was obtained from the prototype device.

Since a successful hydraulic amplification system has been developed for application in active vehicle suspension systems [51], the selection of a more modest gain or a different type of secondary seal may have resulted in a successful design.

4.5 MISCELLANEOUS DISPLACEMENT AMPLIFIER DESIGNS.

Whilst considering the available methods (above) of displacement amplification for piezoelectric ceramic actuators, several concepts for specific applications and device designs arose. Once the basic mechanisms had been defined, designing a solid-state displacement amplifier became a process of choosing appropriate amplifier topologies. Three of those designs are discussed here; the first two of which were modelled in perspex for the purposes of functional validation.

4.5.1 Piezoelectric Electronic Jacquard Actuator.

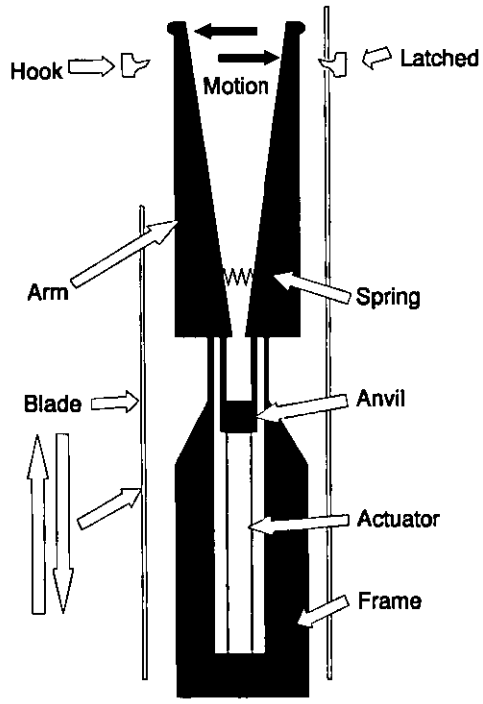

Figure 31: A Piezoelectric Electronic Jacquard.

The electronic jacquard is a device which controls the 'vertical' position of a group of threads in the loom of a weaving machine. To achieve this, existing technologies use a solenoid to pull or retract reciprocating blades onto hooks at appropriate times during the weaving cycle. The vertical motion of the thread is then controlled by the

motion of the blades.

Because of the size of typical devices, it is difficult or impractical to consider controlling individual threads with solenoid technology. However, it is possible to design a low-power piezoelectric replacement actuator only 2.5 mm thick (which makes the devices 'stackable' across the loom bed), to perform a similar function, either by using a pair of bimorphs, or by using a stack type actuator with a displacement amplifier. Such a device fitted with a Tokin NLA 2x3x18 actuator is shown in Figure 31. It is based on the simple lever (transverse output), and produces bilateral movement of lugs at the ends of swinging arms which are controlled by the extension of a single piezoelectric stack actuator (multilayer).

This device was modelled in perspex and its extension measured to be 0.4 mm at the end of each arm; sufficient to cause a blade in an existing jacquard design to be caught by one of the holding hooks. In practice, perspex would not be used if such a device were to be designed as a real application.

The advantages of such a solution include very low power and small size.

4.5.2 High-Gain Compound Amplifiers.

It is possible to design a high-gain displacement amplifiers comprising two distinct lever systems.

Such a design is shown in Figure 32. When extension of the actuator occurs, the first lever rotates causing the lever end to push against the flexural hinge of the second lever. This is a conceptual design and is not claimed to be efficient, for reasons which have already been discussed in section 4.4.2. This device was modelled in perspex and fitted with a Tokin NLA 5x5x18 actuator. An output displacement of approximately 1 mm was achieved.

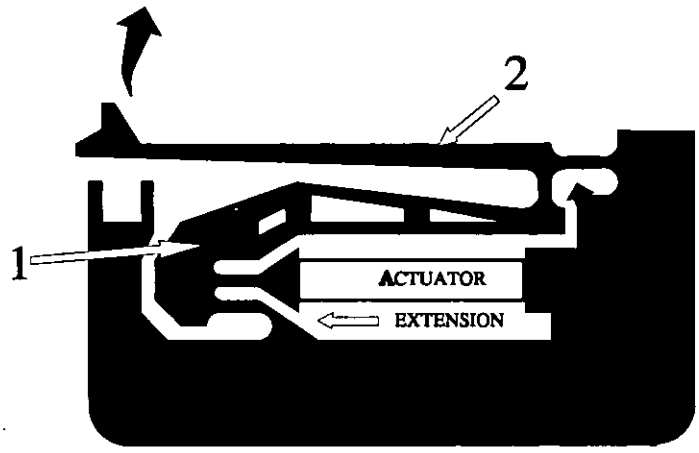

Figure 32: A Two-stage Displacement Amplifier.

A second two-stage device was designed using a pair simple levers of the direct type.

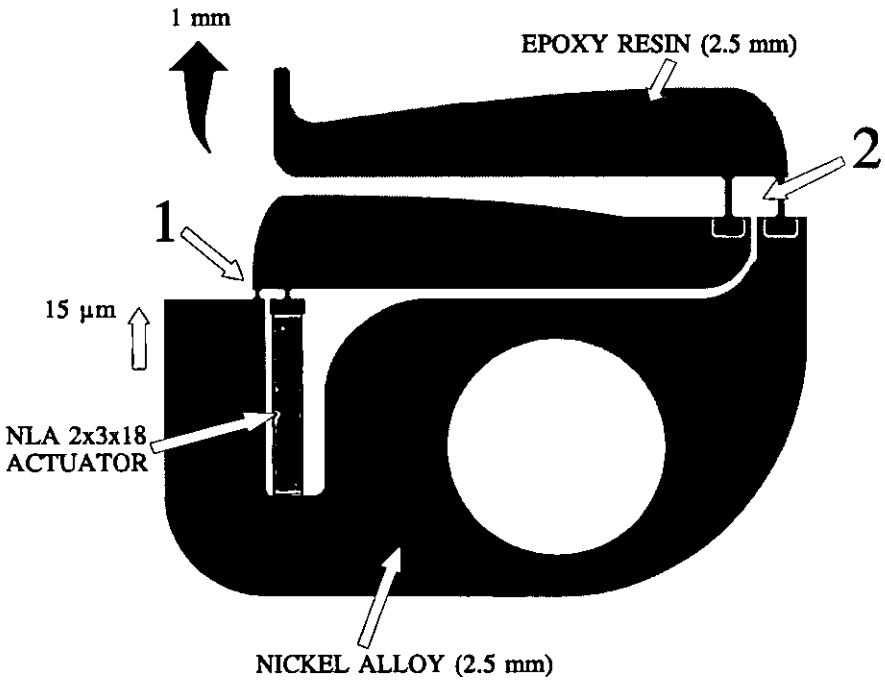

Figure 33: High-efficiency Two-stage Amplifier.

This device which could be made as a compound structure from two different materials (shown in Figure 33) transforms displacement from 15 μm to 1 mm. The

'Beam Designer' program, discussed later in chapter 6 on page 94, produced the data for the geometry of the hinge pairs and beam profiles, and predicted an overall device efficiency of nearly 60% with a safety factor of 0.2 for maximum stressing in both materials.

4.6 ACTUATOR REQUIREMENTS.

4.6.1 Selection of Actuator.

Whatever form an actuator/clutch assumes, providing the assembly behaves in a linear fashion, (i.e. non-toggle type behaviour) the required constraints of clutching force and clearance can be expressed as an energy or work function.

We could specify the clutching action to begin at 50% of the actuator's free full travel (X_{max}) at full electrical drive (this is not an unreasonable assumption). This would result in a developed force of precisely half that of the isometrically developed force (F_{max}). Thus the work function can be expressed as;

$$W = \frac{F_{max} X_{max}}{4} \tag{38}$$

If we consider one layer in a piezo stack, thickness t, area A, driven electrically to full strain ε_{max}, we have;

$$\epsilon_{max} = \frac{\delta t}{t} \tag{39}$$

For n layers the total extension is;

$$X_{max} = n.t.\epsilon_{max} \tag{40}$$

If we now consider the stack driven fully but isometrically, the stress is given by;

$$\sigma_{max} = E.\epsilon_{max} \tag{41}$$

where E is the Young's Modulus, and the total force developed is;

$$F_{max} = \sigma_{max}.A \tag{42}$$

Since the volume of the stack is;

$$V = nAt \tag{43}$$

it can be shown that;

$$W = \frac{VE\epsilon_{max}^{2}}{4} \tag{44}$$

Since E and ε_{max} are constant for a particular material, we can calculate the approximate volume of piezoelectric ceramic required. In an application where a 100 N clamping force is produced at a range or clearance of 50 μm, W = 1.25 mJ. Using materials currently used in actuators such as the Burleigh PZO-015, we can calculate an effective Young's Modulus of 5.66 GPa, (including internal actuator bonding effects) and a required volume of 1.73 x10 $^{-6}$ m ^{3}. (This is equivalent to a cube with 12 mm sides.) As a direct coupled actuator, this would imply an actuator length of 70 mm.

Using the Tokin NLA multilayer type actuator, the required device volume is only 1.76 x10 $^{-7}$ m ^{3}; approximately one tenth of the volume required with the stack. For a specific application, providing the minimum volume is adhered to, and allowing for losses in the amplifying linkage, the range and force criteria can be met.

A figure of merit can be adopted to assist in choosing the actuator most suitable for an application. Some examples are shown in Figure 34. Whilst this is probably one of the most useful approaches, the criterion must be tempered with other factors, such as hysteresis and speed of response.

Each group contains devices of similar construction but of differing size. Note that the devices in group 1 are constructed from a material with similar bulk composition, but are constructed as stacks, using adhesives, whereas the remainder are of multilayer construction. The low figures, produced by these older style stacks (Group 1) are

overshadowed by multi-layer piezoelectric devices (Groups 3,4 and 5), and still further by new generation electrostrictors (Group 2).

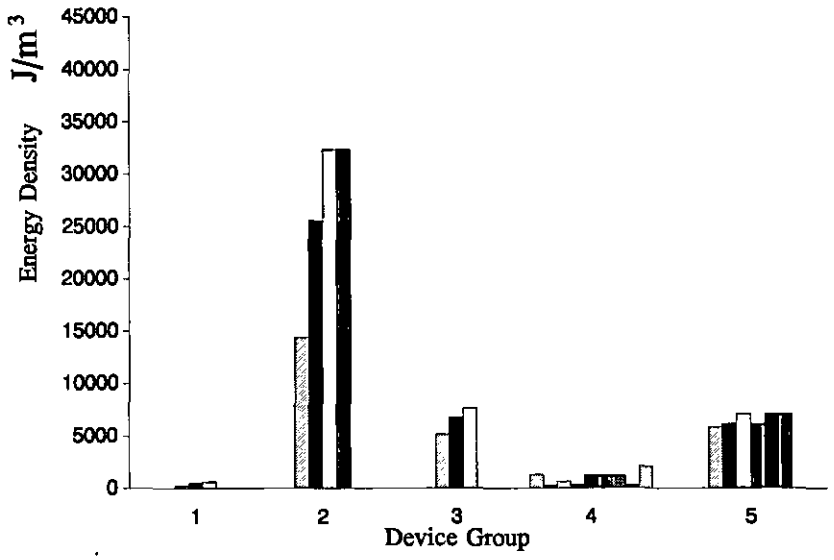

N.B.: Group 2 devices are electrostrictive.

Figure 34: Relative Energy Densities of Differing Piezoelectric Actuator Groups.

4.6.2 Specification.

Table 2 shows an initial specification for a family of piezoelectric ceramic actuators suitable for the type of application discussed. A target clutching force of between 25N and 100N has been assumed. The devices can be stacks or multilayer devices, probably but not necessarily of disks, generating compressive force into an external load. Due to the advancement of actuator technology over the last seven years, particularly in Japan, stacks manufactured with discrete interstitial electrodes can no longer be considered to be competitive, from cost or performance criteria.

Active Volume	$2x10^{-6}$ m^3
Electrical Capacitance	≤5.0 μF
Force Displacement product	0.02 Nm *
Minimum Full range motion	20 μm
Maximum Full range motion	100 μm
Minimum Full Isometric Force	200 N
Maximum Load	As appropriate
Hysteresis	< 5% FRO
Linearity	< 15% FRO
Drive Voltage for FRO	100 - 200V d.c.
Linear Collective Modulus	> 5 GPa

*e.g. F_{max} = 200N, X_{max} = 100 μm *or* F_{max} = 500N, X_{max} = 40 μm etc.

TABLE 2: Initial Specification for a Suitable Actuator.

4.7 OBSERVATIONS

Of the configurations considered, the three which offer themselves as candidates for potentially successful design, are the simple lever (direct), the compressive flexural bridge; (or a combination of both systems) and the hydraulic amplifier. A practical bistable device has not been designed although this has interesting advantages. The transverse simple lever topology can not produce structures which are as efficient as its direct counterpart. The bimorph and multimorph approaches do not generate force / stroke characteristics in a suitable combination.

The hydraulic displacement amplifier, whilst interesting, and no doubt promising as least as far as obtaining modest gains, is sophisticated compared to pivoting and flexure hinge based systems like the simple lever and flexural bridge. For the reason of simplicity, this avenue has not been explored thoroughly or in great detail, although

a somewhat ambitious design was made and tested with no success [17].

The flexural bridge and simple beam displacement amplifier are mechanically simple, robust and as will be seen, capable of high-speed (sub 1 ms) actuation, and in view of the lack of bibliography concerning design of efficient devices in these families, this was felt to be a fruitful line of research. The following chapter is concerned with the design and testing of a solid-state displacement amplifying linkage, which employs both the flexural bridge and the simple beam mechanisms. Further, it is clear that a detailed study of the design of these mechanisms is required, and this is presented in chapters 6 and 7.

The specifications for the piezoelectric ceramic actuator itself which will take the form of a stack or multilayer are detailed in the table above. There will be a family of solutions, (one of which will require no amplification) of various lengths, diameters, number of elements and ceramic doping etc. Each of these will vary the parameters of speed, inertia, clutching force, longevity, efficiency and simplicity of the final designs.

[17]The expected output movement was 1000 μm.

5 A PIEZOELECTRIC CLUTCHING ELEMENT.

5.1 OVERVIEW.

The necessity of understanding the behaviour of amplifying linkages, particularly those employing flexure hinges, was identified in chapter 4. It was intended early in the work, to develop such a linkage which could be employed in the discrete motion machine (section 9.1 on page 189). The mechanism described in this chapter is one design in a series of monolithically constructed devices designed around flexure hinges. It generates a 30 Newton stall force, with an unrestrained movement of over 110 μm, derived from a piezoelectric device which extends by only 15 μm in the no-load condition. Although the device can not be considered as highly efficient, it transforms the output movement up to a level which can be used directly with components produced to moderate degrees of surface finish and tolerance. The prototype device described is intended to rapidly clutch a thin metal strip. Performance data is presented including speed of response, electrical clutching energy and mechanical performance.

5.2 THE CLUTCHING APPLICATION.

The design of machine systems in the textiles manufacturing fields of knitting and weaving, often requires the fast selection and movement of *individual* threads. Practical implementations have often necessitated the undesirable compromise of working with groups of threads, to reduce the number of actuators required. Electronic jacquards often employ a solenoid to latch a reciprocating metal strip to achieve control over a group of warp threads within a loom. A reduction in size of the electronic jacquard could help to improve the feasibility of a 'one actuator per thread' design solution, and hence complete thread control with increased freedom of pattern production. The realisation of such an application might involve the use of a piezoelectric bimorph, whose deformation could steer the path of reciprocating components onto latches, or alternately, actively clutching a thin reciprocating strip

at critical moments in the weaving cycle.

This is just one potential application of a small high-speed device, and there are many others where a small low-power high-speed device would be advantageous. Solenoids have drive limitations in terms of speed and holding power, whereas piezoelectric actuators require almost no power to hold their position, and since they are voltage driven (as opposed to current) with modest electrical capacitance [18], they can be fully excited typically in less than 200 μs.

5.3 DEVICE DESIGN.

5.3.1 Overview.

Device simplicity was taken as an axiom. For this reason a flexure hinge approach was adopted, since a flexure device can be manufactured monolithically by either milling or electrical discharge machining (E.D.M.). The clutching application specification required a free movement of >100 μm and a stall force in excess of 20N. This constitutes an energy requirement of 2mJ. Manufacturers data suggested a compatible actuator would be the Tokin NLA-5x5x18, which produces a free extension of 15μm and a stall force of 854N. This would allow for losses of up to 75% in coupling efficiency.

As the work with the beam designer and flexural bridge designer programs will show in the following chapters, these two displacement amplifying topologies are feasible. It was decided to include both topologies in one design, and as the design emerged, it became apparent that a symmetrical layout for the amplifier was the simplest to manufacture, and resulted in a design where little material was required for the host portion of the structure.

[18] Typical values for multilayer devices fall in the range 1 to 10 μF.

5.3.2 Design Techniques.

Initial finite element modelling showed that the required gain (in excess of x 6) could be achieved with a single lever stage, but that a faster, slightly less efficient design was possible with a two stage system. This design is shown schematically in Figure 35, manufactured from 6.5 mm thick Titanium.

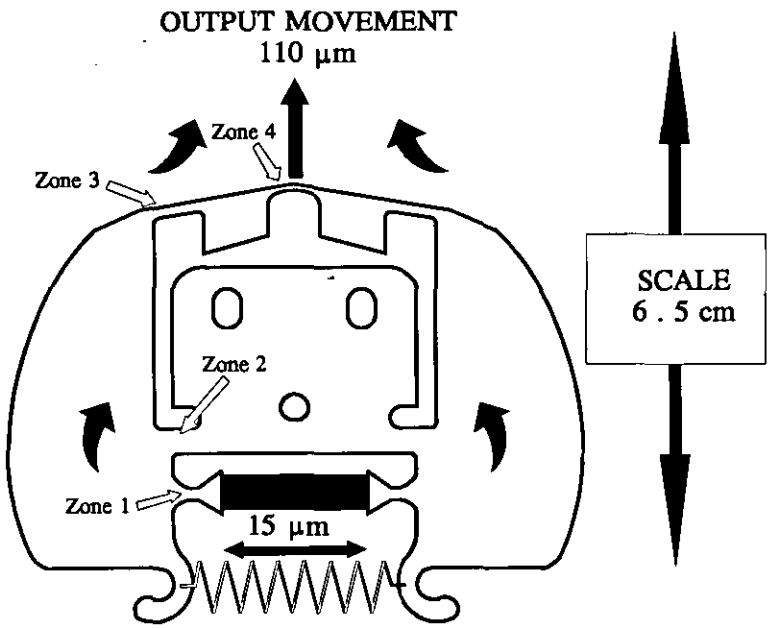

Figure 35 : Clutching Element Schematic.

Note the shape of the first stage levers at either side of the structure. These are of a generally elliptical shape as generated by the simple beam designer program (q.v.), although the sense of amplification is inverting. The first stage has a gain of approximately x 4 but this gain operates on an input displacement of only half of the free extension of the piezoelectric actuator, for reasons of symmetry. The movement generated by the first stage is experienced by the input to the flexural bridge at the top of the structure. The analysis of this part of the structure is detailed in chapter 7, and indeed is used as a *test-case* for the flexural bridge designer program. It can be appreciated that the compliance relationship, between the output of the beams and the input of the bridge, is critical in determining the overall efficiency of the structure.

5.3.3 Materials.

Ultimately, choice of material is application specific. However, one severe limitation exists when selecting a material which can efficiently amplify displacements; namely Elastic Modulus. However, Titanium was chosen in preference to others because it possesses several desirable mechanical properties. These are discussed below;

FATIGUE RESISTANCE.

The material must be able to strain to a high a level as possible with low probability of fatigue. This implies a high yield strength, and or U.T.S. A useful parameter can be defined ;

$$\varepsilon_w = \frac{n\sigma_{yield}}{E} \qquad \textbf{(45)}$$

which should be maximised as far as possible. Note that n is a safety factor associated with the structure.

HIGH ELASTIC MODULUS.

This should be maximised because increasing values of E imply a smaller geometry and hence greater speed of response (See following topic). From a static design view point, it is difficult to arrive at a high gain design with lower E values since this implies thicker hinges to achieve direct stress stiffness, which in turn increases torsional hinge stiffness, (according to a cubic relationship). This is undesirable since this factor increases the loading of the actuator and hence reduces its output displacement. Another significant factor is that the elastic modulus of the material determines the apparent rigidity of the host structure when the device is under partial or full stall. This factor is discussed in more detail in the chapter concerning the Simple Beam Designer. Since the Elastic Modulus of modern piezoelectric materials

is of the order of 40 GPa, materials of similar stiffness, e.g. Aluminium alloys, can not be employed in structures to offer a sufficient rigidity.

SPEED OF RESPONSE.

Simple modelling shows that for a given geometry, a structure's resonant frequency is related to E and density by;

$$f_{res} \propto \sqrt{\frac{E}{\rho}} \tag{46}$$

We can therefore write a speed factor for a material as;

$$t = \sqrt{\frac{\rho}{E}} \tag{47}$$

This factor requires minimisation.

SURFACE HARDNESS.

This importance of this factor depends on whether the structure itself will perform clutching directly. This is so in this case, and therefore materials such as aluminium alloys are unattractive in this respect. Materials such as titanium and various steels are more suitable for this application. However, this limitation can be overcome with the application of a hard surface coat by plating or deposition.

5.3.4 Design Method.

This design was developed using a combination of analytical beam modelling and intelligent tuning algorithms, with verification and refinements achieved through finite

element analysis. The design techniques used to produce this structure are complex and will be covered in another chapters 6 and 7. The salient points of the design are that;

1) Under no situation is there a stress level of more that 20% of the yield strength, in normal operation, complete stall or off-load conditions. This value is based on the inspection of typical cyclic fatigue characteristics such as those shown in Figure 45 on page 90, and leads to a long device life. This value is often used as a rule of thumb when designing structures which must endure an indefinite lifetime.

2) Each flexure hinge is optimised for high normal and shear stiffness, in combination with a low bending stiffness. This results in an optimised energy coupling factor for the whole structure.

5.3.5 Finite Element Analysis.

Figure 36 and Figure 37 show the F.E. mesh used for both static and dynamic analyses. The graphical output from the static analysis is voluminous and so the peak principal stresses realized in the four critical zones 1 - 4 (as shown in Figure 35) are tabulated below. The dynamic analysis identifies the resonant modes of oscillation and their respective frequencies for the structure.

5.3.5.1 Static Analysis.

The static principal stress levels in the structure are limited by design to within 20% of the material's yield strength. This gives a maximum stress level of 96 MPa for the Titanium alloy used, and maximum levels occur exclusively in the thin (0.3mm) flexural hinges (flexors) at the top of the structure.

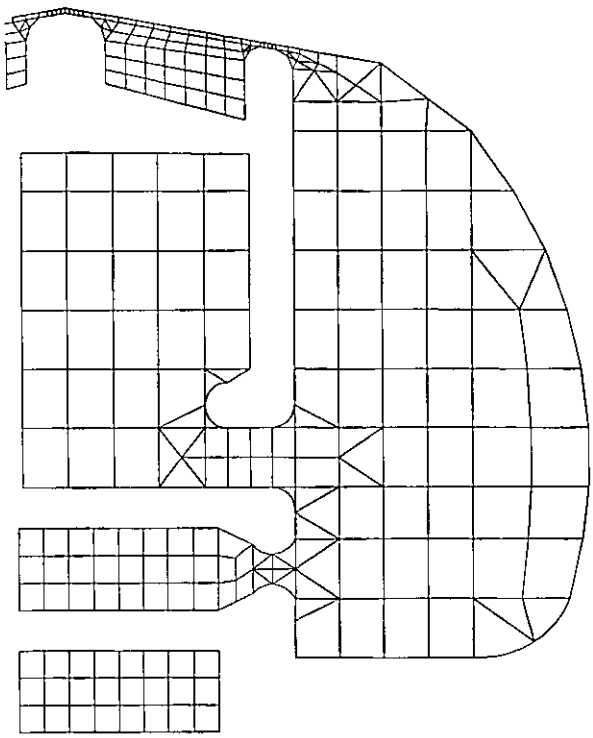

Figure 36 : Finite Element Mesh Half Structure Shown.

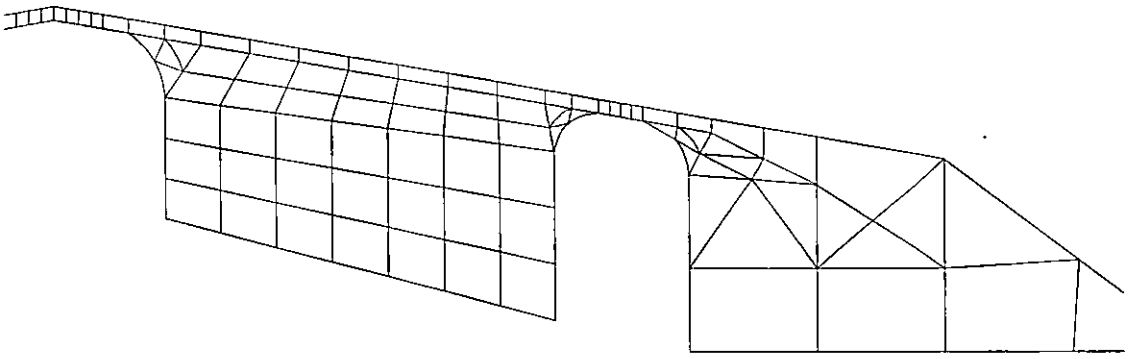

Figure 37: Finite Element Mesh Bridge Structure Detail.

The dynamic stresses in response to device switching are difficult to estimate, but it is unlikely that these will rise by a factor of 2 above those values in the above table. This can be justified by the approximation of considering the structure as a second order system. Applying a step to such a system, either in terms of stress or displacement can only result in a maximum transient response of double the magnitude [52].

ZONE	FREE	STALLED
1	18 MPa	10 MPa
2	38 MPa	34 MPa
3	94 MPa	16 MPa
4	93 MPa	10 MPa

TABLE 3: Maximum principal stresses within the structure.

5.3.5.2 Dynamic Analysis.

Figure 38 shows the results of dynamic analysis of the Titanium alloy strip-clutch element showing the first ten modes of oscillation, according to the results obtained from finite element analysis. They are shown in order of ascending frequency. The resonant modes are shown on the diagram.

5.3.6 Fabrication.

Conventional N.C. milling techniques were used to fabricate the device, however, electric discharge machining does offer certain advantages, and has been exploited with other prototypes. It has shown to be a more direct route requiring less sophisticated machine programming, and since the device flexes and generates certain zones where the stress is tensile, surface finish becomes an important factor in reducing the probability of induced fatigue. On a practical level, conventional milling with a Titanium alloy proved difficult, requiring many cutting passes to achieve the desired profile. The cutting tool diameter was limited to only 2.0 mm for some sections of the structure, thus limiting the depth of cut for each pass.

Since it was vital to make a good interference fit between the actuator and the structure, some post-milling work was required to produce plane perpendicular faces

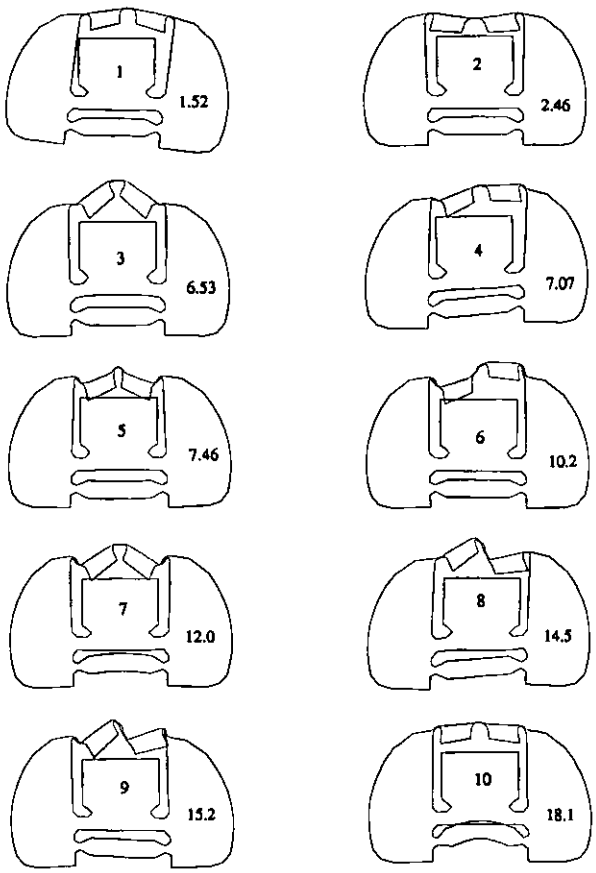

FREQUENCIES SHOWN ARE IN kHz.

Figure 38: First ten resonant modes of the Strip-Clutch.

to mate the actuator. Similar additional work was required on the clutching zone.

5.4 PERFORMANCE

5.4.1 Static.

Having an electro-mechanical nature, the performance of the device is more easily considered from potential energy conversion data. The manufacturer's data and

structure performance data are shown in Table 4.

PARAMETER	VALUE
Full operating Voltage	100 V
Electrical Capacitance	5 μF
Piezo Free Movement	15 μm
Piezo Stall Force	854 N
Output Free movement	110 μm
Output Stall Force	30 N

TABLE 4: Device and structure data for the Tokin NLA 5x5x18 / Strip Clutch.

The input electrical energy ($\frac{1}{2}CV^2$), is 25 mJ. The piezoelectric force-displacement product (F_{pstall} x_{pfree}) is 12.45 mJ, and the output force-displacement product (F_{ostall} x_{ofree}), is 3.3 mJ, giving a structural energy efficiency of 26.5%. Note that the electrical energy and the force-displacement product can not be directly compared without considering the energy transformation process; for linear structures such as this, the best coefficient for electrical to mechanical conversion would be 0.5 [10].

The mechanical compliance characteristics of the strip-clutch were determined experimentally by using a jig as shown diagrammatically in Figure 39. The jig facilitated monitoring of the position of the output section of the strip-clutch to within 0.5 μm, whilst it was loaded with external weights (weight cradle not shown). This was designed so that variation in test load did not influence readings taken by the LVDT. Figure 40 shows the output displacement of the structure against excitation voltage for a range of applied loads at the output. The bowing of the curves is attributable to non-linearity in the characteristics of the soft piezoelectric material. Note the series designated '0 kgf (REP)'; this refers to a repeat of the initial zero load series '0 kgf'. The difference in output displacement is typical of the creep behaviour of soft piezoelectric ceramics.

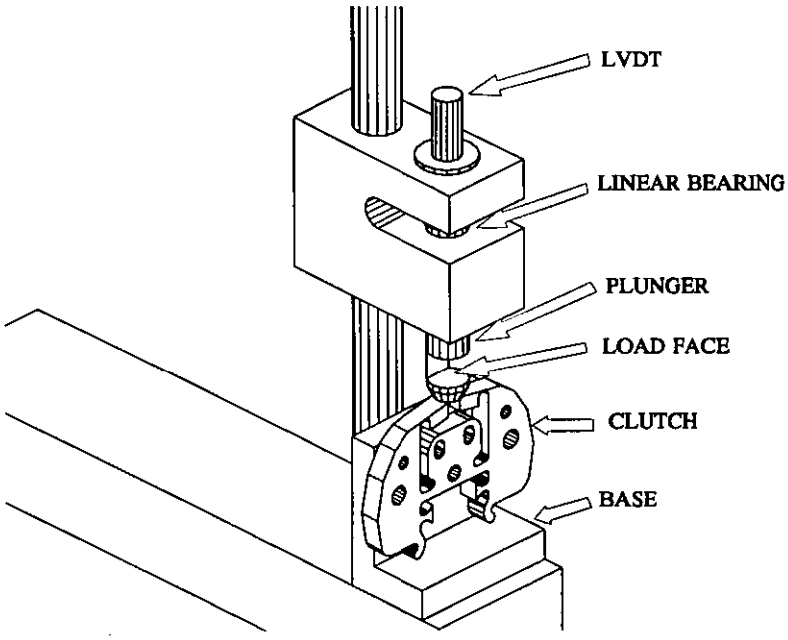

Figure 39: Static Compliance Test Jig.

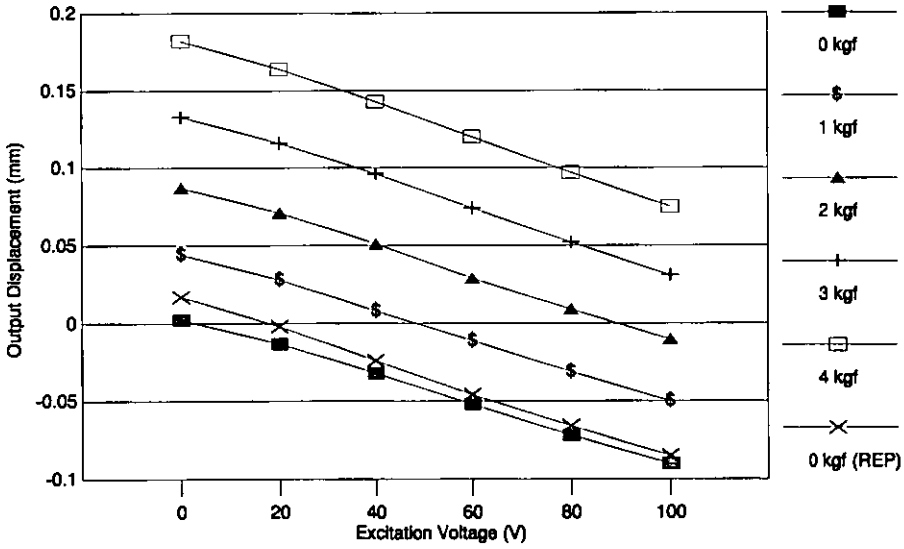

Figure 40: Displacement against excitation voltage.

5.4.2 Dynamic.

In order to test the accuracy of the dynamic response finite element predictions, a laser vibrometer was used to examine the velocity/time behaviour of the strip-clutch element in response to step changes in the electrical drive voltage. The basic layout is shown in Figure 41.

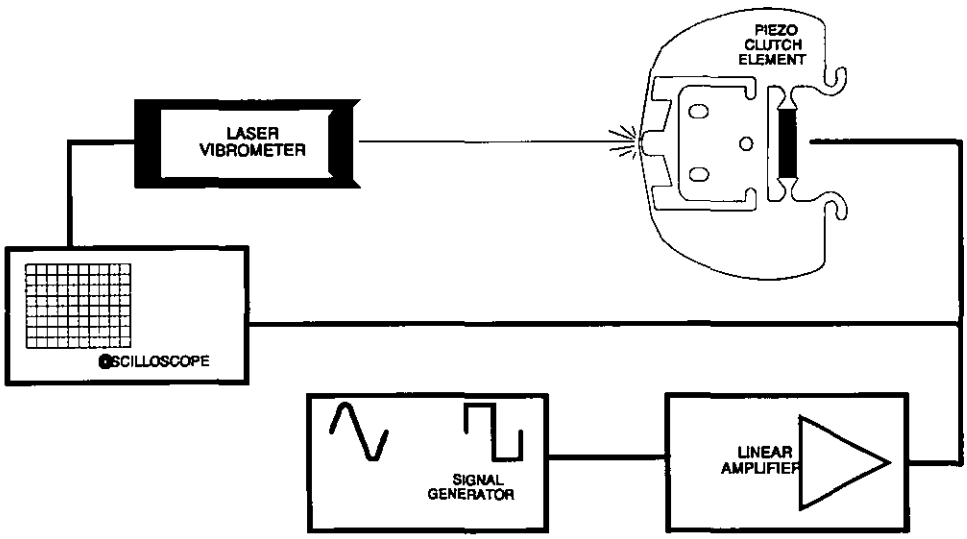

Figure 41 : Test-rig for the examination of the velocity/time profile of the Strip-Clutch.

The clutch element was excited by a 20 Volt square wave operating at approximately 1 Hz. The magnitude of the excitation waveform was kept to 20 V to avoid gross saturation of the vibrometer circuitry [19]. The response of the Strip-Clutch Element to this excitation is shown in Figure 42.

[19] The Vibrometer output voltage was limited to ±2V at a calibration of 6.32Vs/m.

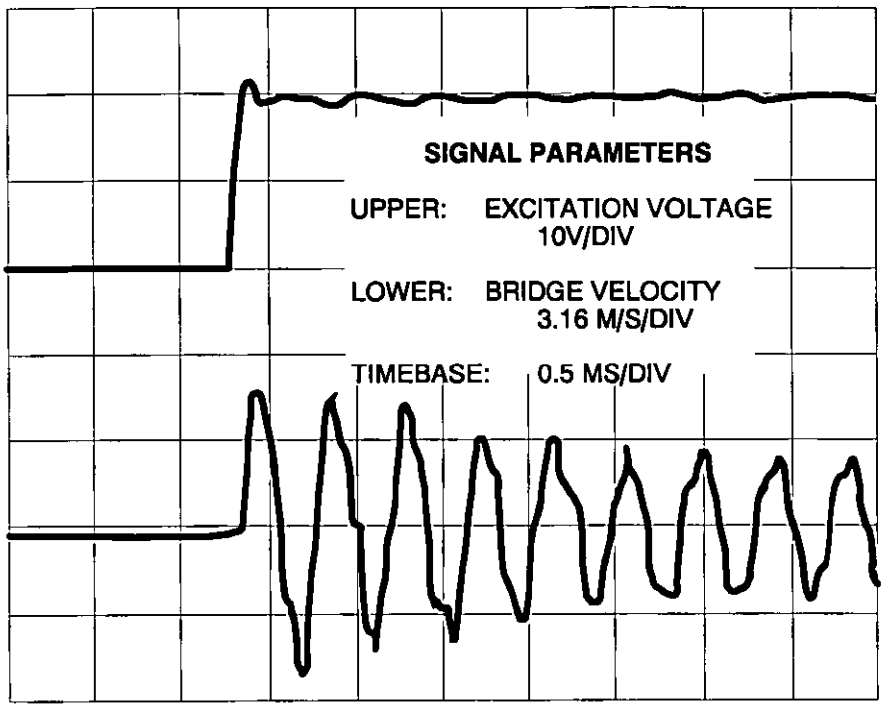

Figure 42: Dynamic response; Output Bridge Velocity for an undamped structure.

Interestingly, the natural frequency of vibration shown in the trace is approximately 2.5 kHz, which corresponds well to mode 2 in Figure 38. Since the device is normally excited symmetrically, mode 1 is unlikely to be a significant component, so the correspondence is valid. Although the device is not intended to be operated with the output bridge completely free, the free ringing characteristics suggest that bounce may be a problem in the clutching application. The device exhibits ringing which decays only after around 5 ms (off the trace). This is undesirable, especially considering that the device achieves first overshoot within 200 μs. Clearly, some technique of damping is required to reduce the effects of ringing, and ensure bounce free operation.

5.4.3 Device Damping.

Since the device is electro-mechanical, two basic approaches can be taken to achieve damping, and hence useful operation; electrical damping and mechanical damping.

On first inspection, the electrical approach would seem promising. This could be achieved by using energy dumping circuitry within the drive switching transistors. Other methods could be adopted such as filtration of the drive waveform, to remove stimulating Fourier components.

Electro-mechanical energy commutation is evident in the drive voltage waveform of Figure 42; this might afford the possibility of direct electrical damping. Whilst the approach is viable, the mechanical approach is far simpler to implement in the form of filling the internal void of the strip-clutch element with a suitable elasto-plastic compound. Compounds such as L.P.R. (manufactured by Morton Thiokol), which is a polysulphide rubber, lend themselves to this technique since they have a suitable complex elasticity modulus, giving practically un-impeded slow speed movement, whilst displaying useful dash-pot type properties at high frequencies.

This approach has been successfully applied. The voids in the device were filled with L.P.R., allowed to cure for 24 hours and subjected to the same dynamic tests as the undamped device. The results are shown in Figure 43, and the effect is dramatic. The free structure exhibits almost complete extinction of ringing energy within 1.2ms of actuation.

Tailoring of the compound's complex elasticity modulus, in combination with topographical changes should facilitate the production of a critically damped device. This technique is highly attractive because of its mechanical simplicity and the total absence of any complex energy dumping components in the electrical drive system.

5.5 FATIGUE STUDIES.

Since the strip-clutch has been designed for use in high-speed machines, certain applications will undoubtedly involve high repetition rates. This means that such devices might have to endure many operating cycles without failure, possibly in excess of 10^9 cycles. From this perspective, the importance of design for high longevity is

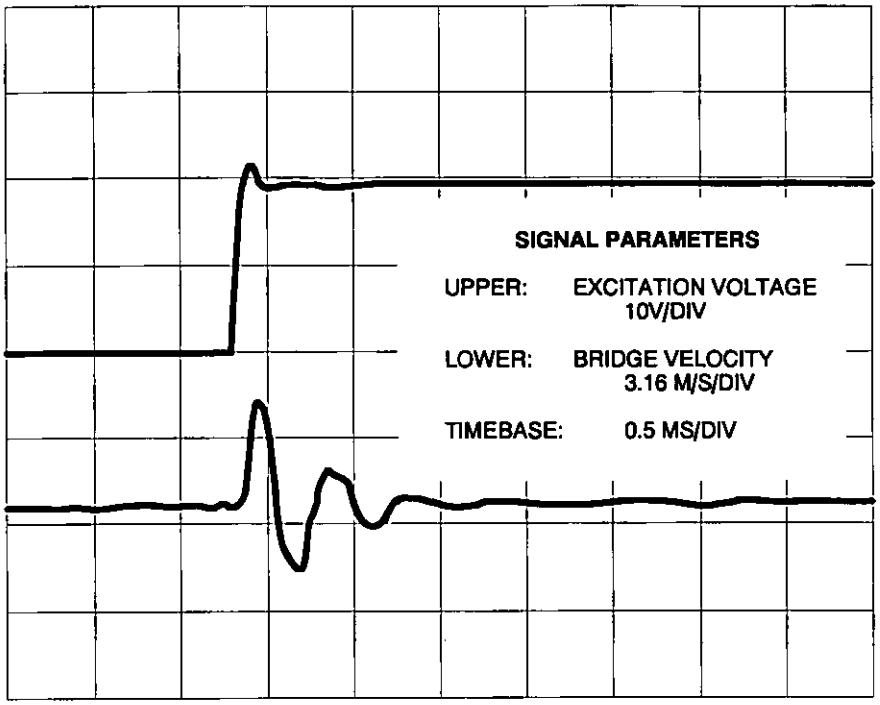

Figure 43: Output Bridge Velocity for a damped structure.

plain, thus necessitating a study of the fatigue characteristics of this particular device.

5.5.1 Loading.

The device was designed such that in no portion of the structure (as seen in Figure 35) would a stress of greater than 20% of yield be experienced under any static load condition. (Dynamic stressing is difficult to model, and in this case impossible to measure locally, a further impetus for the fatigue investigation.) As a consequence, it is important to understand the process of fatigue within the elastic limit of the material.

The two extreme loading conditions are where the output is free and when it is stalled, both at full electrical excitation. The static finite element analysis results are given in Table 5, and show the maximum principal stresses in certain zones of the structure. Clearly, the worst case stress occurs when the device is off-load, in zones 3 and 4, and will fall off with increasing load. Fully loaded (stalled), the structure experiences

ZONE	OFF-LOAD	STALLED
1	18 MPa	10 MPa
2	38 MPa	34 MPa
3	94 MPa	16 MPa
4	93 MPa	10 MPa

TABLE 5: Maximum principal stresses within the structure.

mostly direct stress, and in this mode in the critical areas, the stress is compressive. In practice, the clutch element would never completely experience the off-load condition (unless actuated in a non-typical condition, say for test purposes), but rather somewhere in between the two, depending on the clutching clearance and the stiffness of the clutch anvil.

If the device should fail after a number of cycles in the off-load case, it is likely that failure would take longer in a real application. For this reason, it was decided to perform an endurance test in the worst possible mode using the off-load condition.

5.5.2 Fatigue Under Repeated Stress.

During off-load operation of the device, bending stresses (which can be tensile or compressive) develop in zones 3 and 4 as a result of the forces required to distort the bridge structure. These forces also develop direct stress. However, the bending stresses are usually dominant.

When a material is subjected to repeated tensile stress (positive by convention) within the elastic range, the material fatigues. In general, the lower the peak tensile stress level experienced by the material, the greater the number of stress cycles that can be

endured before fracture occurs. The general form of this relationship is given by;

$$\sigma_{max} = \sigma_0 - k \,.\log n \quad , \qquad \sigma_{max} \ngeq \sigma_{end} \tag{48}$$

However, below the stress level known as the endurance limit, failure should never occur. This holds providing that structural defects are either not present or do not seed crack propagation. This relationship is best demonstrated graphically and is shown in Figure 44 for mild steel and a typical medium strength titanium alloy. An aluminium alloy is included to demonstrate the contrast in behaviour between materials which exhibit an endurance limit (at any given stress level), and those which apparently do not. The fact that materials such as steels and titanium alloys exhibit this endurance limit is useful, not only from the design viewpoint, but because it makes testing simple since the existence of an endurance limit implies a repetition value which if it can be exceeded under test, should assure non-failure of the component during typical operation.

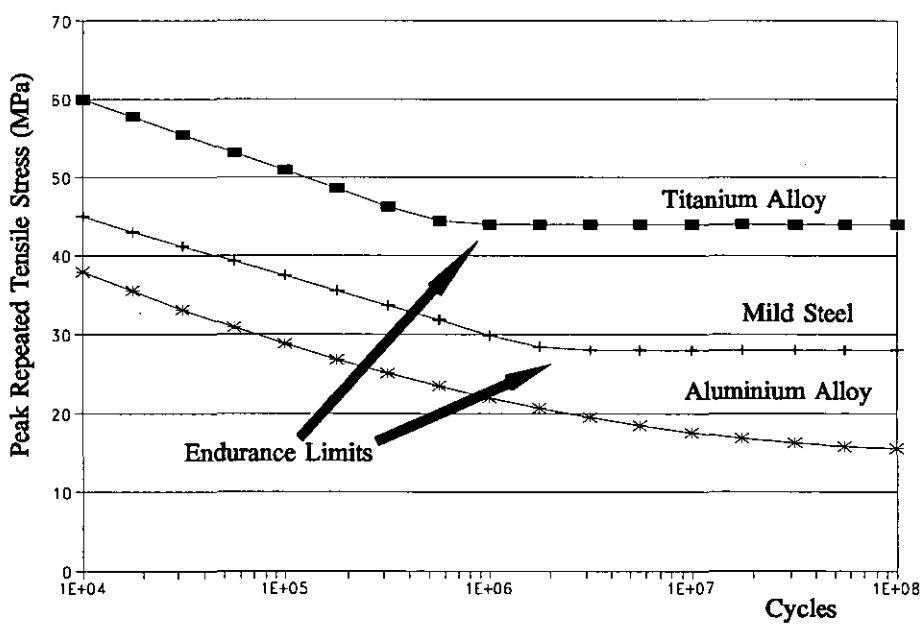

Figure 44: Endurance Limits For a Typical Titanium Alloy and Mild Steel.

Another common method for displaying the fatigue characteristics of a particular material is the Master Diagram. A typical example (for steels) is shown in Figure 45.

Alternating stress is plotted against mean stress, and for the specific loading of this test, where mean and alternating stresses are equal in magnitude, the load point on the graph lies on a line passing through the origin at 45° to the x-axis. The series of curves represents differing numbers of cycles to failure, in steps of powers of 10. The lowest curve represents the endurance stress, below which failure can not occur.

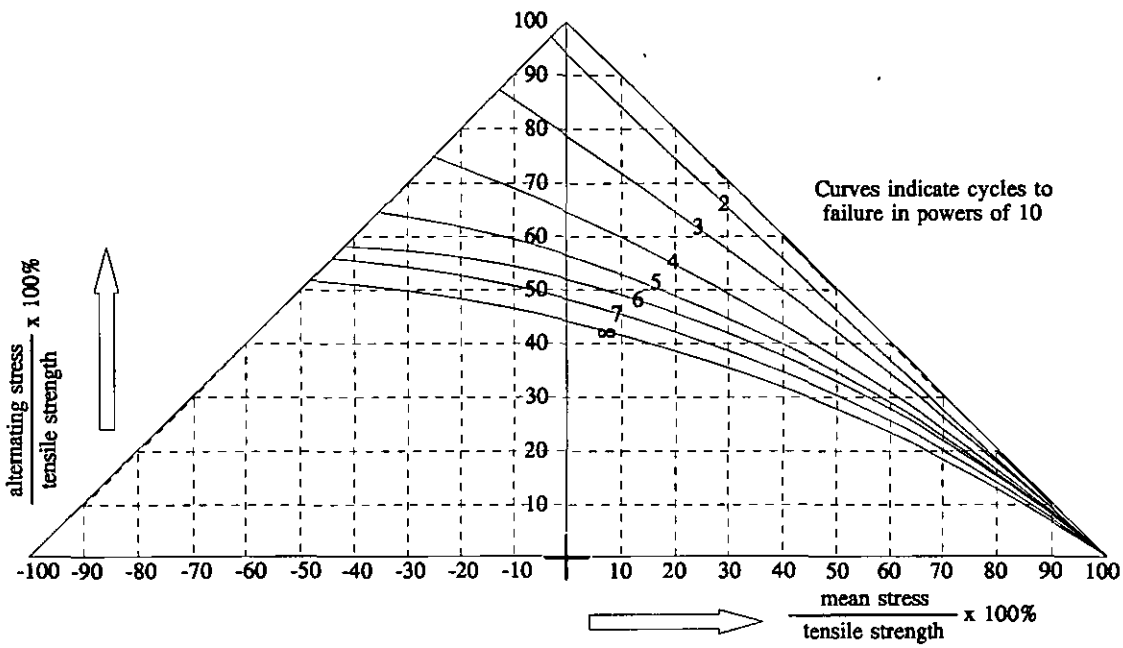

Figure 45: Generic Master Diagram for the Fatigue Life of Steels.

Data on endurance of engineering materials are usually available over the range of 10^5 to 10^8 cycles, and most data lie below the limit of 10^6 cycles [52]. The data are usually presented statistically, aiding in the prediction of number of cycles to fracture for a known peak stress level. However, the finite element method employed yields only static information, and so there is uncertainty in the true stress levels achieved, particularly in zones 3 and 4 of the structure. For this reason, the endurance test was designed to run over 10^8 cycles.

5.5.3 Endurance Test.

The test itself was simple in that a new strip-clutch was manufactured, assembled and secured to a mounting plate. A signal generator was connected to a custom built amplifier to drive the piezoelectric actuator with a 100 V square wave drive, running at 11.57 Hz., as shown in Figure 46. Additionally, the electrical supply was monitored by a programmable hours counter to facilitate reliable time logging in the result of an unanticipated power failure during the test. The set frequency resulted in 10^6 cycles per day.

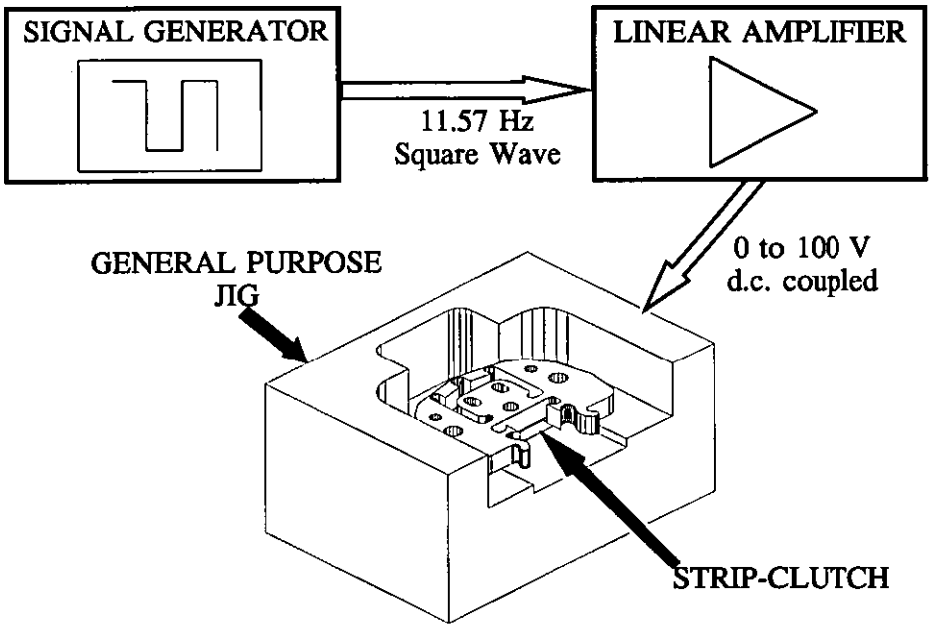

Figure 46: Schematic of the Endurance Test Experiment.

The state of the device was monitored both visually, and by scanning electron micrography for signs of fatigue cracks, particularly in the high stress zones in the upper flexure hinges, at approximately logarithmically progressing `milestones' throughout the test, as given in Table 6.

STAGE	CYCLES
1	10^4
2	3×10^4
3	10^5
4	3×10^5
5	10^6
6	3×10^6
7	10^7
8	3×10^7
9	10^8

TABLE 6: Fatigue Test.

5.5.4 Results.

The device endured 10^8 cycles. Whilst zones 3 and 4 were inspected closely using a scanning electron microscope (S.E.M.), no signs of fatigue cracking were evident. One of the micrographs obtained is shown in Plate 5, but of the several taken, none indicated any signs of cracking. Any cracking must therefore have been beyond the resolution of the S.E.M. at the surface of the structure, i.e. less than 1μm in length or width. In any event, since the device endured, this implies that any cracks would have fully developed by the end of the test.

5.6 DISCUSSION.

A piezoelectrically driven flexural amplifying structure, comprising levers and a bridge structure has been designed, constructed and tested. It has shown that structures so designed can perform well, both in terms of speed of response and with respect to the transformation ratio of electrical energy to useful work. The design in this chapter is

approximately 25% efficient as a *mechanical transformer*, but it will be shown in a later chapter that efficiencies much greater than this can be attained, for example with simple levers and single bridge structures manufactured from steels.

Whilst the design discussed is intended primarily for two state actuation, it is an inherently linear device, which extends its application to areas where a linearly controllable displacement with high stiffness is required, for example, in high precision gripping applications. The device has been incorporated into a machine designed to demonstrate its action, and this is detailed in chapter 9 (q.v. section 9.1 on page 189).

The transient response of such structures can be usefully controlled by the application of polymers (rubbers), the use of which is normally associated with areas such as automotive vibration control, and more complex electrical damping methods can sometimes be avoided.

It is possible to design structures possessing even higher gains, but with lower electro-mechanical efficiencies, and accordingly longer response times, whereupon their speed advantage is lost. It is believed that such structures offer great potential in replacing electromagnetic devices in a wide range of applications. They also offer the potential of great longevity, due to low design stressing and the absence of friction generating surfaces, as has been demonstrated.

6 THE DESIGN OF SIMPLE BEAM DISPLACEMENT AMPLIFIERS.

6.1 INTRODUCTION

The design of mechanical displacement amplifiers for piezoelectric ceramic multilayer-actuators involves devising structures which must be both robust, and yet efficient in terms of their output work potential when referred to the prime mover. These factors are generally antagonistic and therefore the design process involves compromise.

The input displacements generated by the prime mover are small, typically 15×10^{-6}m and the accompanying stall forces are large. One of the simplest mechanical solutions is therefore to use levers in combination with flexure hinges, since zero backlash and hysteresis are primary requirements, and flexure hinges offer these characteristics when used within their elastic limit.

This chapter describes an approach to the design of a simple mechanical amplifier or transformer, using beam bending formulae and intelligent algorithms in the form of a simple expert system. The technique assumes that a solution to a specific mechanical amplification problem exists in a generic design as described in the following section.

6.2 THE GENERIC SOLUTION.

The algorithms described in this chapter are implemented in QuickBasic Version 4.5. Full details of the program are included in appendix 2 as they are voluminous and not directly relevant to understanding the principle of solution seeking. Any high-level structured language would suffice, but QuickBasic offers a friendly and efficient environment.

The system seeks an efficient solution based on the following parameters or variables;

i) The material's modulus, billet thickness, yield stress and stress safety

factor.

ii) Input parameters of compliance and displacement.

iii) Output displacement required.

iv) Tuning factors associated with compliance matching between various structural zones, selected by the designer, but which ultimately affect the force displacement efficiency and actuation speed of the final design.

The structure is of uniform thickness b, and is idealised in accordance with Figure 47. In this type of device, it can be seen that as the actuator extends, the flexure hinges distort, principally in bending when the structure output is unloaded, and in direct stress when the output is stalled. In real systems, some combination of the two modes applies, but the design procedure assumes that these modes can be combined additively. When the structure is unloaded, the lever system rotates approximately about the geometric centre of what can be designated the static flexure hinge, i.e., the hinge which is not attached to the actuator.

The diagram shows linearly tapered beams, and their use is possible, but some justification can be made for using beams of elliptical shape, although this argument is not discussed here. The derivation of the compliances of both structure types are given for completeness, but the program was finally configured to assume elliptical beams.

6.3 DESIGN METHODOLOGY.

The structure is considered in two modes of deformation. Mode 1 corresponds to the structure being completely unloaded at the output, and mode 2 to the output being stalled or vertically constrained. In both modes the input is fully driven from an

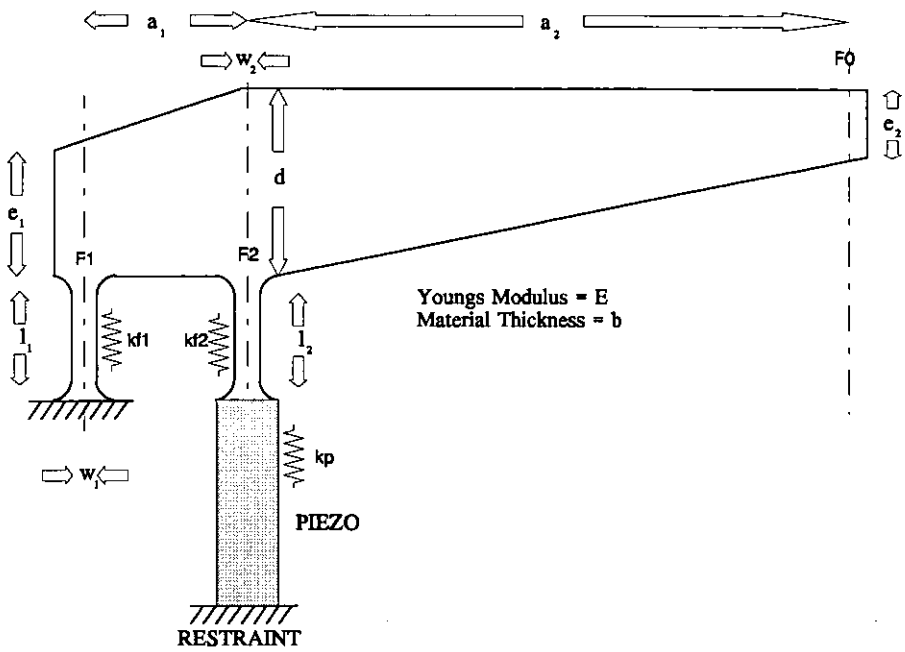

Figure 47: Idealised Amplifier.

external compliance, usually, but not necessarily an actuator.

The finite element analysis of structures of this type has shown that maximum stressing can always be found in the flexure hinges, as expected. For this reason, the solution algorithm does not check for stresses in the elliptical beam members.

6.3.1 Output Force / Displacement Characteristics.

The output characteristics required are entirely application specific, however it is possible to loosely define a working envelope. Firstly, the generic topology can not exist for gains of less than x1. Gains between 0 (zero) and 2 can be achieved with a slightly different topology where the direction of output movement is inverted with respect to that of the input. Gains greater than x2 are favoured, with no theoretical upper limit. For a particular actuator, the required output displacement determines the gain factor required.

The envelope for output force is intimately linked with displacement. A useful criterion for such structures is the force-displacement product.

6.3.2 Choice of Actuator.

It will be seen later that overall device efficiencies of between 50% and 85% are possible, with practical values between 60% and 70%. These figures can be used, in conjunction with the required output characteristics, to select a suitable actuator. As an example, an output displacement of 200 μm with a stall force of 30 N represents a force displacement product of 6×10^{-3} Nm. Assuming a conservative device efficiency of 50%, this represents an input force displacement product of 1.2×10^{-2} Nm. Using an actuator which develops a free movement of 15 μm, it must therefore be capable of developing a stall force of 800 N.

6.3.3 Choice of Material and Billet Thickness.

A determining factor for the thickness of material is that of actuator geometry. Billet thicknesses less than the actuator thickness are possible but not recommended, since under stall conditions, this will imply higher stress levels in the amplifying structure than those which will exist in the actuator; possibly in the order of 35 MPa. However, there are materials where this may be acceptable, such as high-strength steels.

Efficient structures favour thick billets with thin hinges, but extremes here are usually impractical. For reasons associated with stress loading and actuator/billet elastic modulus, values of billet thickness of approximately 120% of the actuator are practical and result in designs which have an acceptable (near) minimum overall thickness. Designs with thicker billets require two high-stiffness couplings between the actuator ends and the structure, which in some circumstances may be an acceptable design complication.

6.3.4 Solution of l_1, l_2, w_1, w_2.

Identification of these dimension labels can be seen in Figure 47 on page 95. The vertical (elliptical) beam compliances are considered to be zero. Whilst this is not strictly true, it is a valid approximation since these compliances will later be designed to be small enough for the approximation to hold. Moreover, it isolates the above parameters to facilitate a solution. In addition, substantial inefficiencies can occur through bending of the beams. It is therefore important to keep these compliances to a minimum.

In mode 2 (stall), the response of the structure will approximately be manifested as direct stress in both hinges. This stress can only be determined by knowing the input compliance of the structure in its currently modelled state. The input compliance in mode 2 will be given by;

$$s_i = \frac{\left(\frac{l_1}{w_1} + \frac{l_2}{w_2}\right)}{Eb} \qquad \textbf{(49)}$$

From consideration of coupling minimum energy into the structure, the perfect situation would be with the input compliance equal to zero. This is impossible, so a *tuning factor* is introduced which relates the input compliance s_i to the compliance of the actuator (or drive) s_d ;

$$k_{stall} = \frac{s_i}{s_d} \qquad \textbf{(50)}$$

which should be minimised as far as possible, to achieve an acceptable overall efficiency, without the geometry becoming unwieldy. This factor can be set from the main program. Typical values lie in the range 0.10 to 0.25. Should the resulting design be too inefficient, the design process can be repeated.

It can be seen that the aspect ratio of the hinges is determined for this relation, in;

$$r_{aspect} = \frac{s_i E b}{2} \tag{51}$$

and this can be chosen to satisfy the stall stress relation. To solve this, the stall force must be determined by;

$$f_{stall} = \frac{x_{i_{free}}}{(s_i + s_d)} \tag{52}$$

where x_{ifree} is the ideal free displacement of the actuator. Assuming that the widths of the hinges are equal, as are the lengths, then the widths become fixed by;

$$w_1 = w_2 = \frac{f_{stall}}{b\sigma_{max}} \tag{53}$$

where;

$$\sigma_{max} = n\sigma_{yield} \tag{54}$$

Therefore;

$$l_1 = r_{aspect} w_1 \qquad l_2 = l_1 \tag{55}$$

6.3.5 Solution of a_1, a_2.

The geometry a_1, l_1, l_2, w_1, w_2, b and Young's Modulus E, will determine the structural loading on the input drive in mode 1 (free). This loading must be minimised to optimise efficiency. The only remaining variable which can facilitate a solution to this is a_1. In addition, the selection of this variable must be tempered with the criterion of stress loading.

The relation between input displacement, input force, input compliance and maximum stress is complex and is determined by the solution of simultaneous equations of the third order. The algorithm for this procedure is given in Appendix 2.

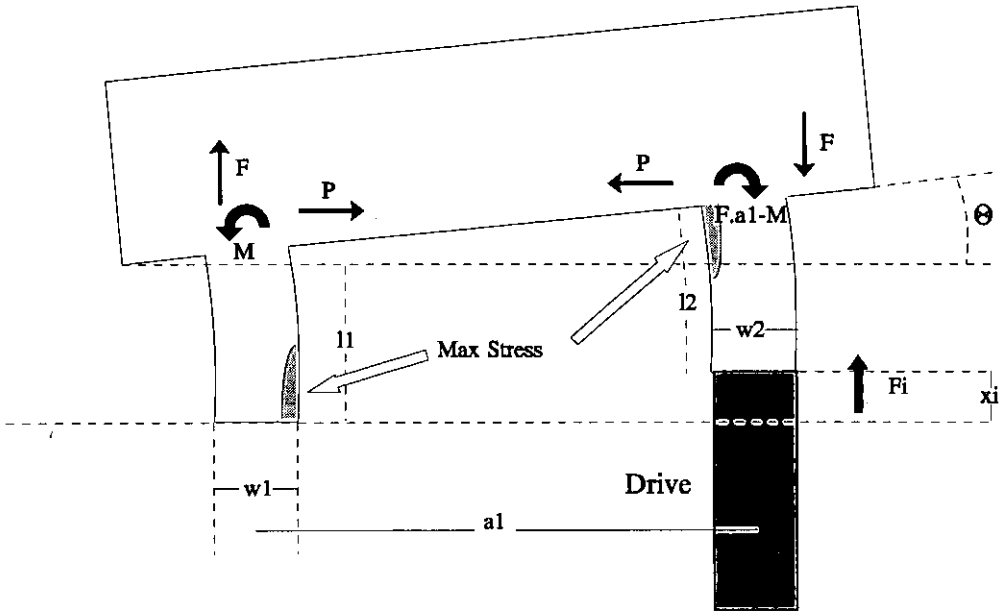

Figure 48: Geometry of flexors at full drive.

Figure 48 shows the idealised deformation of the flexors at full input drive, but with no output load (mode 1). Although this is simplified, we can calculate the maximum stresses due to bending, which will occur at the periphery of flexors, assuming that the stiffness of the host beam remains far greater than that of the flexors. We know that the extension of the drive component is given by;

$$X_{i_{true}} = X_{i_{free}} \frac{S_{hrot}}{(S_{hrot} + S_d)} \qquad \textbf{(56)}$$

where s_{hrot} is the input compliance of the structure due to rotation and distortion of the two hinges, and therefore;

$$\theta = \frac{x_{i_{true}}}{a_1} \tag{57}$$

where x_{itrue} is the real input displacement. If the beam is sufficiently stiff over the length a_1, we can assume that the top end of the flexors undergo the same angular deflection. Thus;

$$\theta = \frac{x_{i_{true}}}{a_1} = \frac{-Pl_1^2}{2EI_1} + \frac{Ml_1}{EI_1} = \frac{Pl_2^2}{2EI_2} + \frac{(Fa_1 - M)l_2}{EI_2} \tag{58}$$

By a similar argument, the lateral deflection of both flexors must be approximately equal. And so;

$$\frac{Pl_1^3}{3EI_1} - \frac{Ml_1^2}{2EI_1} = \frac{-Pl_2^3}{3EI_2} - \frac{(Fa_1 - M)l_2^2}{2EI_2} \tag{59}$$

These equations can be solved to find F and therefore the input compliance. The force is given by;

$$F = E\,\frac{x_{i_{true}}}{a_1}\left(\frac{\dfrac{I_1}{l_1(\delta - l_1)} + \dfrac{I_2}{l_2(\delta - l_2)}}{\dfrac{\varepsilon}{(\delta - l_1)} + \dfrac{(a_1 - \varepsilon)}{(\delta - l_2)}}\right) \tag{60}$$

where;

$$\delta = \frac{2\left(\dfrac{l_1^3}{I_1} + \dfrac{l_2^3}{I_2}\right)}{3\left(\dfrac{l_1^2}{I_1} + \dfrac{l_2^2}{I_2}\right)} \qquad \varepsilon = \frac{a_1}{\left(1 + \dfrac{l_1^2 I_2}{l_2^2 I_1}\right)} \tag{61}$$

Giving a solution for P as;

$$P = \frac{EI_1 x_{i_{true}} - Fa_1 l_1 \varepsilon}{a_1 l_1 (\delta - l_1)} \tag{62}$$

and;

$$M = \delta P + \varepsilon F \tag{63}$$

The input compliance (no load) is defined as;

$$s_{hrot} = \frac{x_{i_{true}}}{F} \tag{64}$$

The maximum stresses within the structure can be estimated by considering the individual contributions from direct force F, lateral force P and bending moment M. Within the two flexors at the points indicated in Figure 48, respectively these are;

$$\sigma_{F1} = \frac{F}{w_1 b} \qquad \sigma_{F2} = \frac{-F}{w_2 b} \tag{65}$$

$$\sigma_{P1} = \frac{-Pl_1 w_1}{2I_1} \qquad \sigma_{P2} = \frac{-Pl_2 w_2}{2I_2} \tag{66}$$

$$\sigma_{M1} = \frac{Mw_1}{2I_1} \qquad \sigma_{M2} = \frac{(M - Fa_1)w_2}{2I_2} \tag{67}$$

The peak stresses in each flexor are therefore;

$$\sigma_1 = \frac{F}{bw_1} - \frac{6Pl_1}{bw_1^2} + \frac{6M}{bw_1^2} \tag{68}$$

$$\sigma_2 = \frac{-F}{bw_2} - \frac{6Pl_2}{bw_2^2} + \frac{6(M - Fa_1)}{bw_2^2} \tag{69}$$

Finding a value for a_1 is achieved by testing the torsion algorithm for increasing values, and terminating when a value is found which results in a good matching

efficiency. This matching value is given by;

$$k_{rot} \leq \frac{s_{hrot}}{s_d} \tag{70}$$

This solution is then tested for stress safety by re-calculating the newly found input compliance;

$$f_{i_{rot}} = \frac{x_{i_{free}}}{(s_d + s_{i_{rot}})} \tag{71}$$

where f_{irot} is the vertical force due to compliance loading s_{irot}, i.e.;

$$x_{i_{true}} = f_{i_{rot}} s_{i_{rot}} \tag{72}$$

Re-running the torsion algorithm checks for the maximum stress obtained in mode 1, and increases a_1 if or until the stress value is acceptable.

The final value of a_1 and the input compliance is used to re-calculate the real input movement as before, and thence the value of a_2 necessary to generate the required output of the structure. The gain is given by;

$$g = \frac{x_o}{x_{i_{true}}} \tag{73}$$

and therefore;

$$a_2 = a_1(g - 1) \tag{74}$$

6.3.6 Solution of d, e_1, e_2.

The value of these dimensions determines the input compliance of the beam section of the structure. The geometry of the structure can therefore be adjusted to result in an acceptable value of beam input compliance. There is little point in choosing an

excessively small value, since values lower than those determined by the flexure hinge and drive combination will force the absorption of strain energy in the hinges, and the whole structure will become unnecessarily bulky. An unnecessarily high value will lead to a structure design which is not efficient. For this reason, an input compliance for the beam structure is sought, simply supported at both ends, and measured from the top of hinge 2. The value of this is set to;

$$s_{i_{beam}} = k_{beam}(s_d + s_1 + s_2) \qquad (75)$$

where k_{beam} is another tuning factor. The geometric solution for this is found iteratively, by firstly locking $e_1 = .99\ d$ and $e_2 = e_1$. The input compliance (at hinge 2) for the beam alone, simply supported at both ends is given by;

$$s_{i_{beam}} = s_{b1}\left(\frac{a_2}{a_1 + a_2}\right) + s_{b2}\left(\frac{a_1}{a_1 + a_2}\right) \qquad (76)$$

The dimension d is varied to satisfy this equation, and represents a value for d, beyond which geometries become unnecessarily bulky. It is effectively the sum of the compliances of individual members of the structure, reflected through appropriate pivotal centres. Each component therefore has a *weighting factor* associated with it, derived from geometrical values.

The individual components considered are;

i) Compliances due to linear extension/compression of the hinges (flexors) s_{f1} and s_{f2}.

ii) Compliance due to the bending of the two beam structures to the left and right of the axis of the piezo; s_{b1} and s_{b2}.

(Note that stiffness due to the bending of the hinges is ignored.)

From statics we know that;

$$f_o + f_2 = f_1 \tag{77}$$

and from taking moments about the output point;

$$f_2\ a_1 = f_1(a_2 + a_1) \tag{78}$$

If hinge 2 is in compression and the drive experiences the same force, by assuming rotation about hinge1 (static) we can say;

$$s_{of2} = \left(\frac{a_2 + a_1}{a_1}\right)^2 s_{f2} \tag{79}$$

where s_{of2} is the output compliance solely due to hinge 2 compressing. Similarly, by pivoting about hinge 2, we get the effective output compliance due to hinge 1 extension as;

$$s_{of1} = \left(\frac{a_2}{a_1}\right)^2 s_{f1} \tag{80}$$

The compliances of each hinge s_{f1} and s_{f2} are simply given by;

$$s_{f1} = \frac{l_1}{Ebw_1} \qquad s_{f2} = \frac{l_2}{Ebw_2} \tag{81}$$

The output compliance of the structure can now be calculated for the case when e_1 and e_2 are nearly d. This compliance is;

$$s_{o_{best}} = (s_1 + s_{b1})\left(\frac{a_2}{a_1}\right)^2 + (s_2 + s_d)\left(\frac{a_1 + a_2}{a_1}\right)^2 + s_{b2} \tag{82}$$

From this point, the e_1 and e_2 values are iteratively decreased to reduce mass, and the output compliance allowed to rise, again according to a criterion dependent on the beam tuning parameter, i.e.;

$$\frac{s_o}{s_{o_{beat}}} = 1 + k_{beam} \tag{83}$$

This parameter is adjustable from the program. A graphical illustration of this process is indicated in Figure 49.

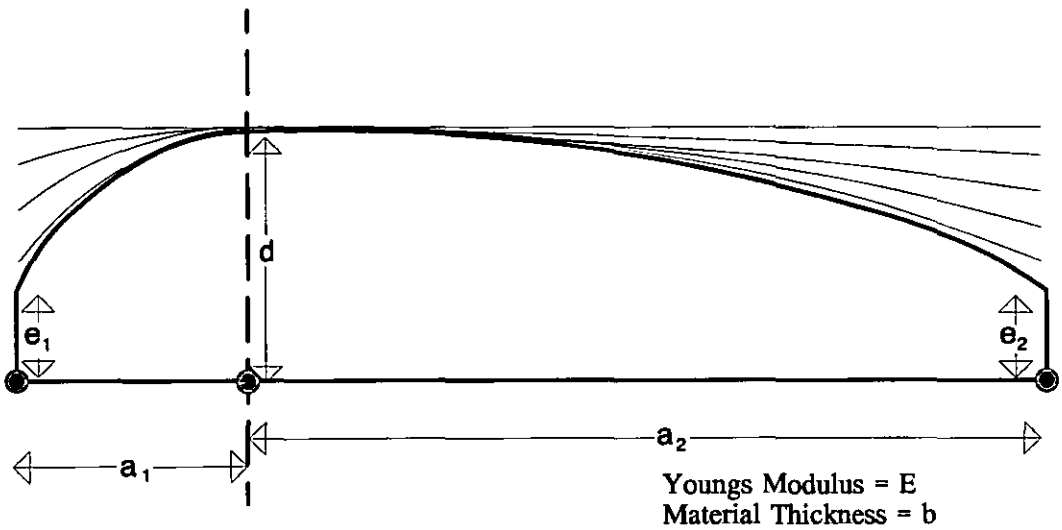

Figure 49: Solution of d and e values.

The overall force-displacement efficiency is defined as;

$$\eta_{fd} = \frac{x_{o_{free}} \; f_{o_{stall}}}{x_{i_{free}} \; f_{i_{stall}}} \tag{84}$$

6.4 MATERIAL AND TOPOLOGICAL LIMITATIONS.

The ability of a structure to amplify the output displacement from a prime mover efficiently is limited ultimately by the structure's material stiffness in relation to that

of the prime mover. Modern piezoelectric actuators present a problem in this respect since their elastic modulus can be greater than 40 GPa, i.e. nearly 60% as stiff as Aluminium or its alloys. This is advantageous from the point of view of energy density of the actuator, but can make the design of very efficient structures complex or impossible.

A main assumption made for the beam designer program is that the root or base of the static hinge is fixed. In practice, this point is not immobile, especially when the structure output is stalled and the static hinge is in tension. The degree of displacement of this hinge with respect to the movement of the actuator sets an upper limit to the overall efficiency of the structure, but advantageously reduces real stall stresses, from those predicted by the program.

The three main metallic groups of Steels, Titanium and Aluminium alloys are probably of most interest from the designer's view point and, whereas various alloys within a group can offer quite wide ranging ultimate strengths, the values for elastic constant do not vary significantly. The effect on device efficiency of the materials' elastic coefficients is briefly studied here.

6.5 Assessment of Maximum Attainable Efficiency.

To study the limiting effect of material choice, a simple Finite Element Mesh was constructed, representing a very large plate of thickness equal to that of the driving actuator. The plate, a half section of which is shown in Figure 50, represents a theoretically maximal stiffness load that can be obtained with a particular material, purely due to the very large relative extent of the plate with respect to the size of the actuator, and therefore allows the prediction of the maximum possible efficiency of a beam amplifier made from a particular material of given thickness.

Under extension of the piezoelectric actuator (half shown), the deformation of the actuator-plate boundary can be clearly seen in Figure 51. Although the shape of the

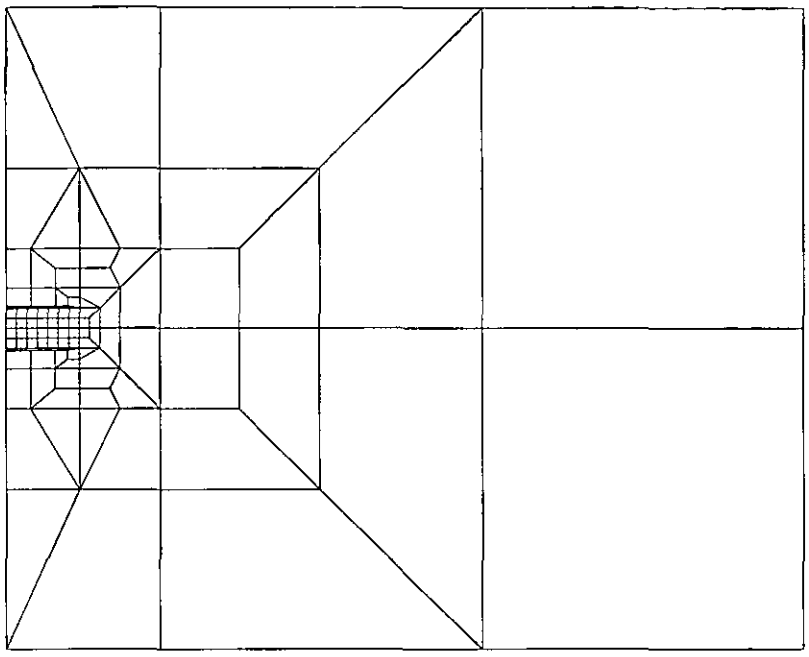

Figure 50: Finite Element Mesh for Actuator Stall-Loading Tests.

boundary is curved, an assessment of the loading effect of the plate on the actuator can be made by assuming that the boundary is approximately straight. The comparative loading effects of steel, titanium and aluminium are compared with free space. Unfortunately, as might be expected, the resistance offered by the plate is a function of the geometry of the actuator, or more generally, its aspect ratio. Since one particular actuator, the NLA 5x5x18 has been used extensively, this has been selected and used as an example.

Assuming a value of Young's Modulus for the actuator of $E_{piezo} = 41$ GPa, and values for Steel, Titanium and Aluminium of 210, 110 and 70 GPa respectively, the piezo-actuator was modelled by assuming a uniformly distributed load of 850 N across the output face. For the three materials, the distortion wave-fronts are shown in Figure 52.

The relative movements have been identically scaled. It is possible to make a crude assessment of what these deformations imply in terms of maximum potential device efficiency, by considering the relative stiffnesses of the three materials as follows. By considering the work done by the actuator at a point on the actuator/plate boundary

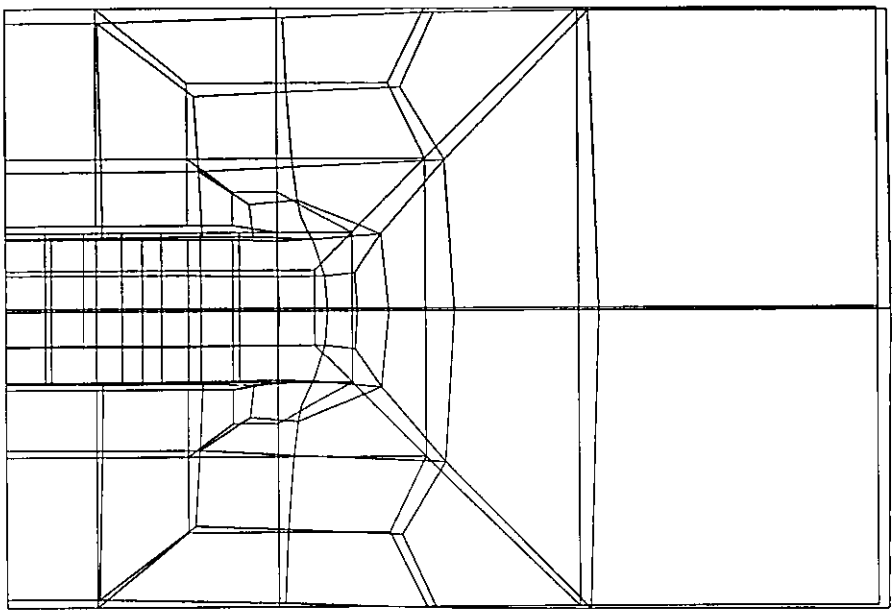

Figure 51: Local Deformations of the Half-Plate.

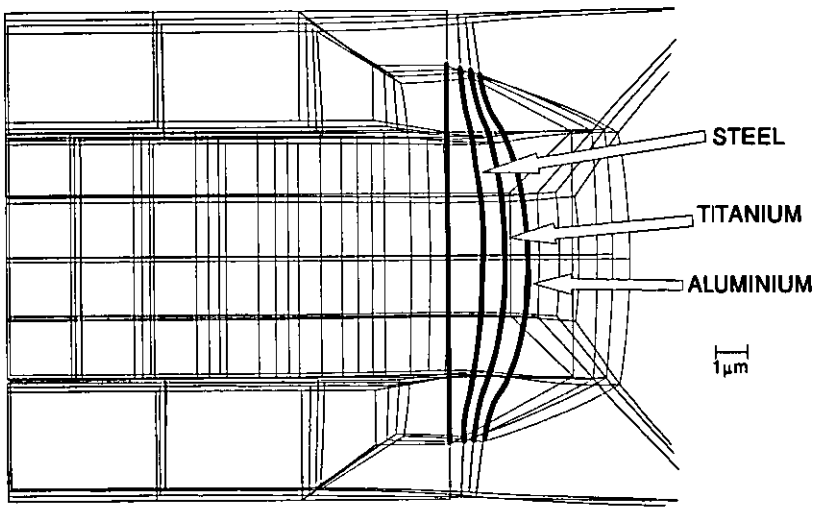

Figure 52: Distortion Wave-Fronts for 3 Materials with a Tokin NLA-5x5x10 Actuator.

(x_e), whilst the actuator is fully driven, the work done by the actuator is given by;

$$E_p = \int_0^{x_e} k_p \, (x_p - x) \, dx \tag{85}$$

where;

$$x_e = x_p \left(\frac{k_p}{k_p + k_s} \right) \tag{86}$$

This is maximised when the stiffness of the structure is zero and therefore the efficiency is zero, giving;

$$E_{p0} = \frac{k_p \, x_p^2}{2} \tag{87}$$

Therefore, the structural limitation of efficiency is approximately given by;

$$\eta_s = \left(\frac{k_s}{k_s + k_p} \right)^2 \tag{88}$$

Relating this equation to the wave-front distortions in the Finite Element Models, it can be shown that;

$$\eta_s = \left(1 - \frac{x_e}{x_p} \right)^2 \tag{89}$$

For Steel, Titanium and Aluminium respectively, the efficiency limits are 81%, 71% and 49%. This directly implies that for simple monolithic designs (with no reinforcing) using a plate thickness equal to that of the actuator, these values are un-surpassable.

It is disappointing to note that a material such as Titanium with its qualities of resistance to cyclic fatigue and corrosion, can only permit a force displacement efficiency of 71%, due to host structure stiffness limitations. The use of a thicker billet would no doubt increase this figure, but probably not more than approximately 5%.

At this point, the assumptions made pertaining to a plane stress state in the structure would break down, resulting in inaccuracies in modelling.

Steel is nearly twice as stiff as Titanium but only facilitates a 10% potential improvement in force-displacement efficiency. It is almost twice as dense however, which for a device of similar proportions, would result in a slower response time.

6.6 REAL STRUCTURES

In practice, it is difficult to design a structure where the maximum theoretically possible stiffness can be provided for the base of the static hinge. It is more likely that a practical structure will only be capable of offering support along one side of the actuator. For this reason, it is necessary to understand the stiffness behaviour of plates in response to quasi-point loading. This system can be modelled as a plane stress problem.

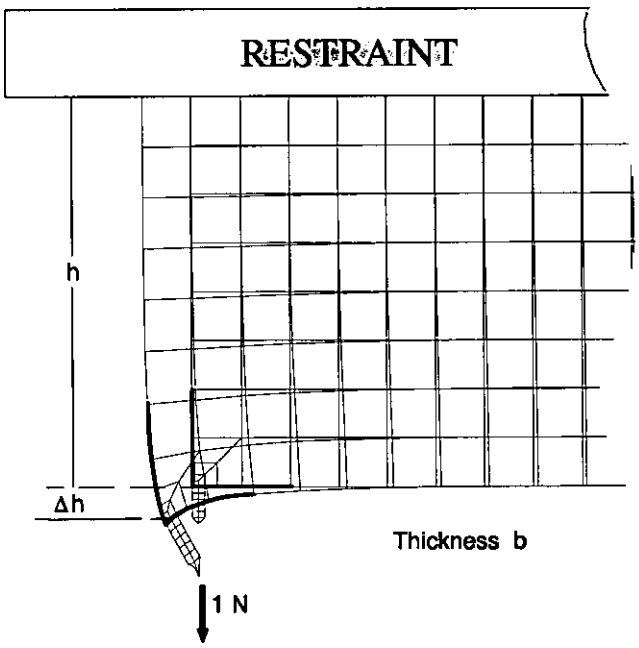

Figure 53: Finite Element Mesh for Edge Loading.

Finite element techniques are useful for this study, and a suitable mesh shown in Figure 53 shows the magnified response of the mesh to a unit vertical load on a thin ligament (bottom left hand corner), for a particular height of material. The material was modelled as 5 mm thick Titanium, but results for other materials and thicknesses can be inferred from the following results. The position of the restraint line was altered to evaluate the effect of height (h) on compliance (Δh).

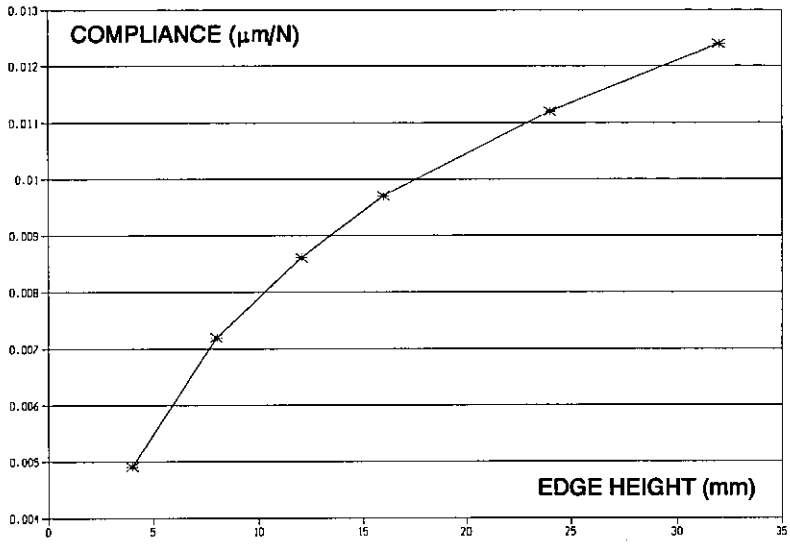

Figure 54: Graph showing Vertical Compliance of Hinge Anchor.

The results of this investigation are shown in Figure 54, and curve fitting reveals a well behaved cubic relationship between the compliance and height of material in;

$$s = \sqrt[3]{\alpha + \beta h} \qquad \textbf{(90)}$$

where $\alpha = -1.31766 \times 10^{-7}$ and $\beta = 6.39768 \times 10^{-8}$. Analytical methods can be used to arrive at a similar result, however the use of a Finite Element approach is probably more reliable in that it requires no simplifying assumptions for the model.

The performance of other systems can be inferred from this model. If the vertical force is considered to act along a line (preserving plane stress symmetry), then data for other

thicknesses of material can be linearly scaled, as can elastic materials of differing Young's Modulus. Empirically then, the equation describing the vertical edge compliance is given by;

$$s = \frac{\gamma}{Eb} \sqrt[3]{\alpha + \beta h} \qquad \textbf{(91)}$$

where $\gamma = 55 \times 10^{11}$, E is the Young's Modulus in MPa, b is thickness and h is the edge height (both in millimetres).

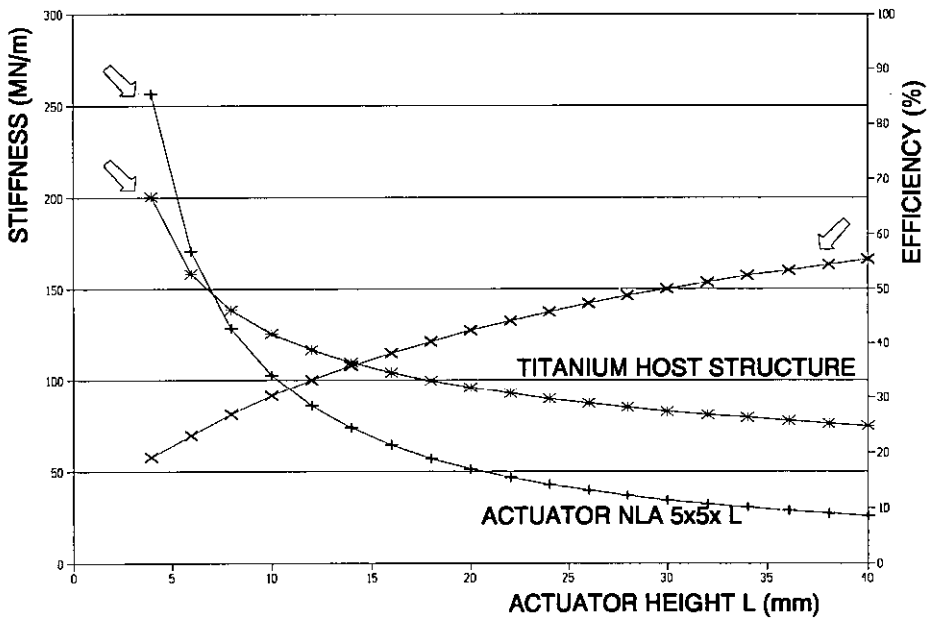

Figure 55: Actuator and Structure Stiffness with Actuator Length.

Choosing long actuators is advantageous since less gain is required for the amplifying structure, but an additional consideration of equal significance is the variation of stiffness with length for the actuator, and the corresponding host structure. Figure 55 shows a direct comparison of structure stiffness with that of a hypothetical actuator with a 5 mm x 5 mm cross section, for a range of actuator heights (lengths). Additionally, in accordance with Eqn (88), the maximum possible efficiency for this type of structure is given. By comparison with the real device in Example 2, an actuator length of 18 mm corresponds to a maximum efficiency of just over 40%, and

this agrees well with experiment. This shows a real advantage in employing long actuators, since the ratio of actuator stiffness to host stiffness falls off rapidly with increasing actuator length. This inevitably infers that a wider piece of material is required to ensure that the maximum host stiffness is achieved. As might be expected by invoking Saint Venant's Theorem, it is unnecessary to design-in a width of material which is much in excess of the actuator length, and since this is a plane stress problem, this must imply an aspect ratio of width to height beyond which no additional stiffness is obtained. This is demonstrated graphically in Figure 56.

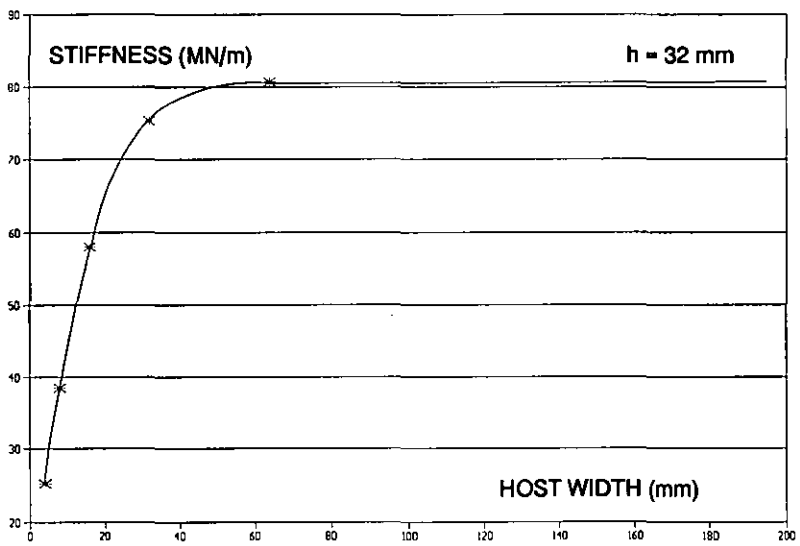

Figure 56: Effect of Host Width on Hinge Anchor Stiffness.

Since this effect is ratiometric between height and width, a general rule may be proposed; that the lateral width of the host structure at the base of the static hinge need be no longer than twice the actuator length.

6.7 TEST CASES.

The program was used to solve for two example specifications, both of which can be considered as typical in respect of achievable output displacement. These are;

i) NLA 5x5x18 actuator to give an output with 0.2mm displacement.

ii) NLA 2x3x18 actuator giving an output with 0.1mm displacement.

It must be stated that the program can not produce a unique solution for a particular problem since there are many degrees of freedom to solve. Additionally, many design parameters exist which the program calculates but does not solve for, such as device mass. See section 6.7.1 for an example.

6.7.1 Example 1: 0.1 mm Output.

As an example the program was used to find a solution to the problem of generating a high force output with 100μm displacement, from a Tokin Corp. NLA 2x3x18 Actuator employing a single stage amplifier.

A piece of 2.5mm thick SAE 4340 steel was chosen as the billet from which the device could be manufactured. A typical family of solutions is shown in Figure 57. The program control parameter of device efficiency was used to generate this group, and as can be seen, devices approaching 80% efficient can be designed, but with the penalty of increasing device mass. Generally, the resonant frequency and hence speed of response of such a family of devices, can be related to the function;

$$f(m) \propto \frac{1}{\sqrt{m}} \qquad \textbf{(92)}$$

and this relationship is shown in Figure 58.

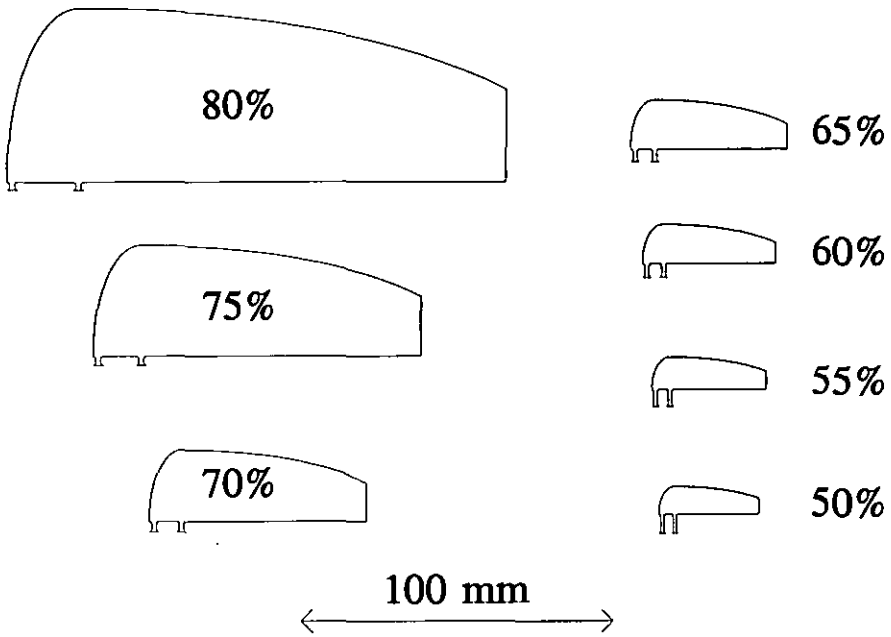

Figure 57: Family of solutions for the 100 μm amplifier (Example 1).

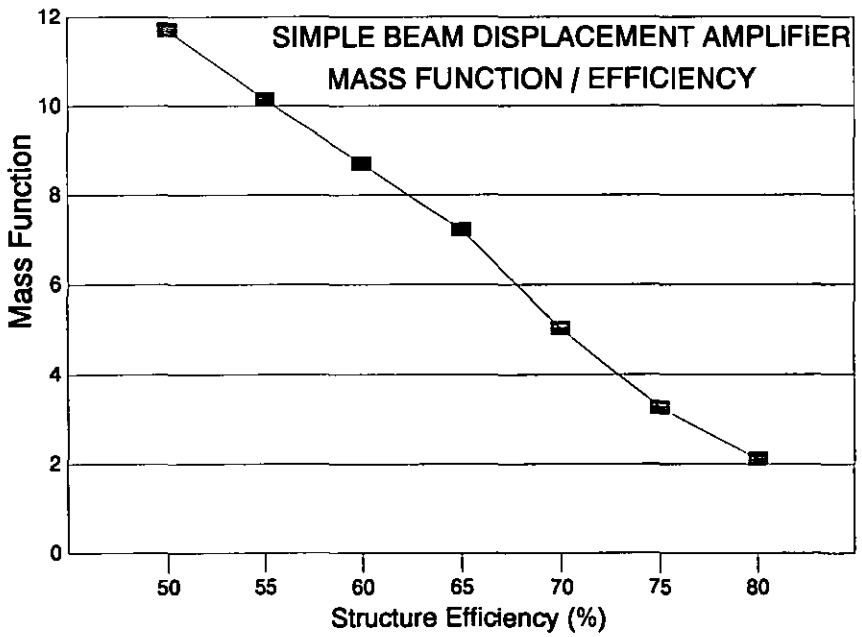

Figure 58: Relationship of mass function against efficiency for the 100 μm amplifier.

DIMENSION	VALUE(mm)
a_1	5.36
a_2	31.90
l_1	4.07
l_2	4.07
w_1	0.92
w_2	0.92
d	9.07
e_1	0.89
e_2	4.85
b	2.50

TABLE 7: Geometry produced by the Beam Designer Program for Example 1.

A compromise between response speed and efficiency would normally be resolved by considering the particular factors in a real design problem. For the purpose of this design study, the 70% efficient device was chosen. A screen-dump of the program, running the example is shown in Figure 59. The geometrical data generated by the beam designer program is shown in Table 7.

These values were used to construct a finite element mesh using PIGS 4.2, via the DXF output option of the beam designer. The results obtained from the F.E. analysis are shown in Table 8, along with the values predicted by the beam designer program, and the data taken from measurements performed on the real device. A set of devices was manufactured by the wire E.D.M. process, based on the DXF file produced by the program. Two views of the manufactured monoliths can be seen in Figure 60. The assembled actuator was subjected to load and excitation testing, allowing a direct comparison of real data with both F.E.A. and the beam designer. The static test rig used was basically similar to that used in the examination of the strip-clutch element; see Figure 39 on page 82. Graphical data of the static performance of this device are shown in Figure 61, displaying the output displacement against drive voltage to two

SAE 4340
x1.0

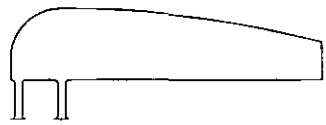

GEOMETRY STATUS

MATERIAL THICKNESS (B)..	0.002500	HINGE SEPARATION (A1)...	0.005355
OUTPUT BEAM LENGTH (A2).	0.031917	ANCHOR HINGE LENGTH (L1)	0.004065
INPUT HINGE LENGTH (L2).	0.004065	ANCHOR HINGE WIDTH (W1).	0.000916
INPUT HINGE WIDTH (W2)..	0.000916	MAX BEAM WIDTH (D).....	0.009074
MIN BEAM WIDTH 1 (E1)...	0.000893	MIN BEAM WIDTH 2 (E2)...	0.004854

PERFORMANCE STATUS

EFFICIENCY.....	0.696048	FREE STRESS [MPA].....	67.151070
STALL STRESS [MPA].....	87.331757	OUTPUT FORCE.....	20.867588
OUTPUT MOVEMENT.....	0.000100	MASS [GRAM].....	5.811242

PARAMETRICS STATUS

MATCH.FACTOR.STALL.....	0.100000	MATCH.FACTOR.ROTATE.....	0.100000
MATCH.FACTOR.BEAM.....	0.100000	SAFETY.FACTOR.....	0.150000
YIELD.STRESS.....	469.000000E+06	YOUNGS MODULUS.....	210.000003E+09

Figure 59: Screen Dump of the Beam Designer Program; Example 1.

PARAMETER	PREDICTED	F.E.A.	ACTUAL
Output Movement	100 μm	92 μm	101μm
Output Stall Force	20.8 N	18.6 N	18.2 N
Max Stall Stress	87 MPa	72 MPa	-----
Max Free Stress	67 MPa	59 MPa	-----
Efficiency	69 %	57 %	61%

TABLE 8: Comparison of Modelling Performance with F.E.A. and the Manufactured Device for Example 1.

mechanical constant force loads. The hysteresis of the device is in the order of 10% of full range movement. Figure 62 shows the deviation of full range output (SPAN) and zero positions for increasing mechanical load.

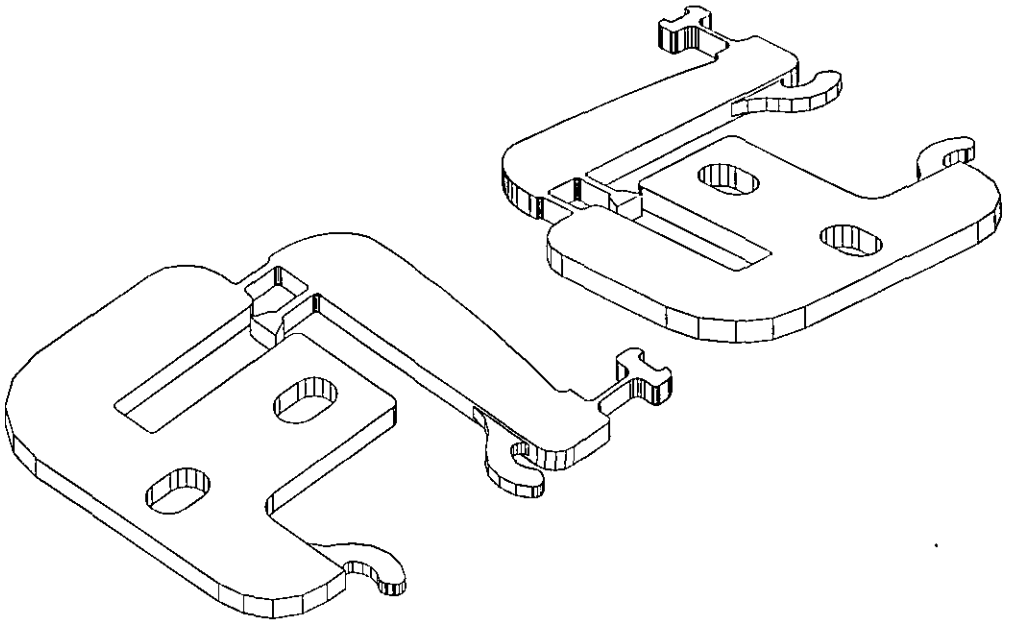

Figure 60: Two views of the 100 μm Amplifier Monolith.

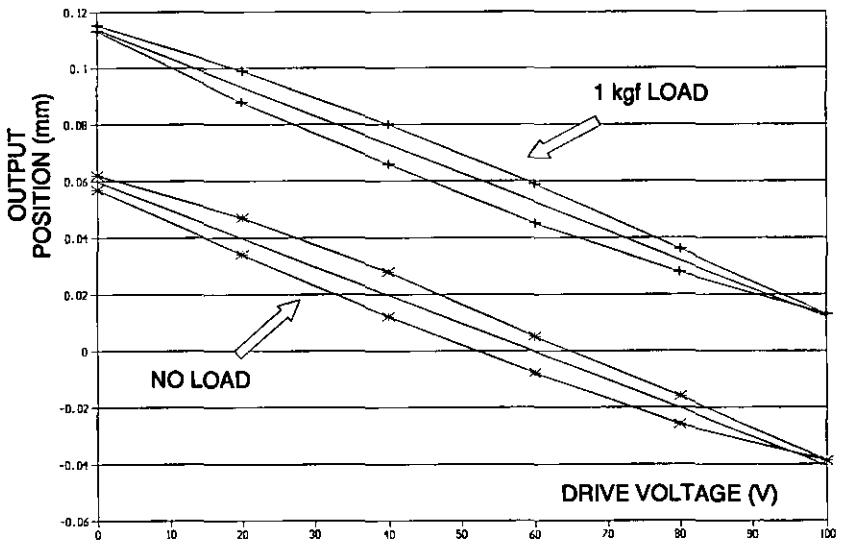

Figure 61: Output Displacement (mm) against Drive Voltage.

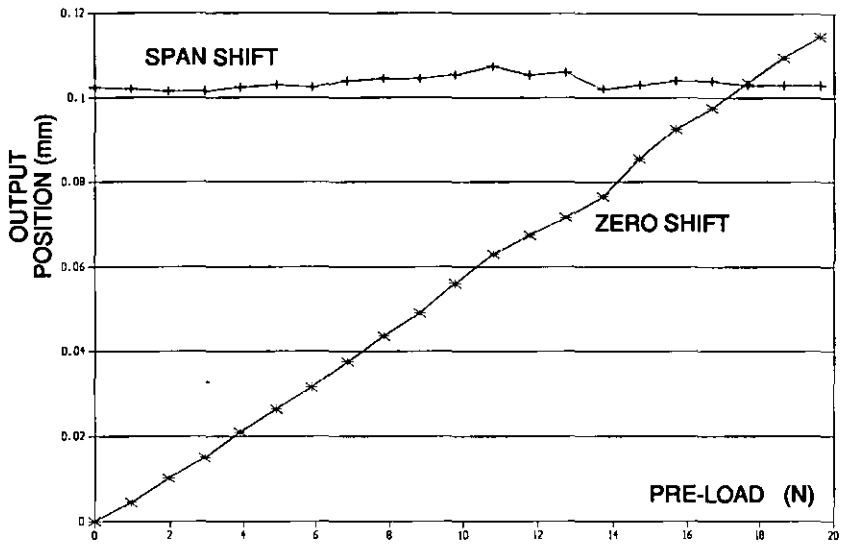

Figure 62: Deviation of Span and Zero for Increasing Static Load.

With reference to Table 8, most parameters fall within a 12 % band of those generated by F.E. analysis. The stress values obtained by the beam designer program were all conservative by this standard, i.e. the actual stresses predicted by the F.E. technique were slightly lower than those predicted by the program. The discrepancies produced are believed to be mostly due to inadequacies in the modelling which fail to take account of *local* distortions and stresses generated in the beams by the hinges, for example, within the hinge fillets. The `beam designer' modelling also fails to account for distortions of the host structure at the `static' end of the actuator. Most seriously, the FEA prediction of output displacement is poor by comparison with the `beam designer'.

The stiffness of the host structure in the area between the anchor zone of the static hinge and the base of the actuator is assumed to be large enough to be negligible in comparison to the direct stiffness of the flexure hinges. Clearly, if this assumption is violated, the accuracy of the 'beam designer' is compromised. This factor is highlighted in Example 2.

6.7.2 Example 2: 0.2 mm Output.

The amplification of a displacement of 15 μm to 200 μm represents a gain of approximately x13.3. Experimentation with the designer program had shown that to achieve higher efficiencies of around 70%, the aspect ratio of the flexure hinges tended to have to be reduced, to achieve high direct stiffness in order to reduce high strain energies in these components. This raises several problems. At some point, the thin beam assumption used to calculate structural rotational stiffness, breaks down and in addition, the modelling of rigid restraints assumed at the boundaries of these beams must also break down. The anchor point of the static hinge anchor can no longer be assumed to be immovable, resulting not only in a significant reduction in efficiency, but also a reduction in the maximum stresses attained in the hinges in both modes of static deformation.

To examine these assumptions, it was decided to target the designer towards a solution which might significantly compromise them, and so a required efficiency of 70% was demanded. Additionally, since the theoretical limit for a titanium structure with the NLA 5x5x18 actuator is less than 70% for a full plate support, and much less for a single edge of this length, this requirement would explore the stability of the program in failure when compelled to produce *impossible* structures.

A Tokin NLA 5x5x18 actuator was selected as the prime mover. As an additional design feature, a two-element pre-load shear spring was included in the monolithic construction to simplify assembly. The shear spring was designed to develop a 25 N biasing force with a mean end deflection of 2 mm. Referred through the amplifying structure, this develops a 300 N pre-load within the actuator. In terms of bending stress in the shear spring, this average load represents 75% of yield stress for titanium, and the cyclic stress present is less than 4% of the yield stress. The static stress level might seem unduly high, but the cyclic stress component is low enough to theoretically guarantee a cyclic fatigue life in excess of 10^9 cycles.

```
TITANIUM
x1.0

                                GEOMETRY STATUS

MATERIAL THICKNESS (B)..   0.006500     HINGE SEPARATION (A1)...   0.003764
OUTPUT BEAM LENGTH (A2).   0.048765     ANCHOR HINGE LENGTH (L1)   0.000849
INPUT HINGE LENGTH (L2).   0.000849     ANCHOR HINGE WIDTH (W1).   0.000644
INPUT HINGE WIDTH (W2)..   0.000644     MAX BEAM WIDTH (D)......   0.012628
MIN BEAM WIDTH 1 (E1)...   0.001243     MIN BEAM WIDTH 2 (E2)...   0.007111

                              PERFORMANCE STATUS

EFFICIENCY..............   0.696367     FREE STRESS [MPA]....... 167.890732
STALL STRESS [MPA]......  203.108582     OUTPUT FORCE............  44.393387
OUTPUT MOVEMENT.........   0.000200     MASS [GRAM].............  16.949249

                               PARAMETRICS STATUS

MATCH.FACTOR.STALL......   0.100000     MATCH.FACTOR.ROTATE.....   0.100000
MATCH.FACTOR.BEAM.......   0.100000     SAFETY.FACTOR...........   0.150000
YIELD.STRESS............ 480.000000E+06 YOUNGS MODULUS.......... 109.999997E+09
```

Figure 63: Screen Dump of the Beam Designer Program; Example 2.

A screen dump of the beam designer program running Example 2 can be seen in Figure 63, with the resulting geometrical data shown in Table 9. The design of the remainder of the host structure can be seen in the perspective view of the device in Figure 64.

The device was manufactured from a Titanium Alloy with a quoted yield strength of 480 MPa.

6.7.2.1 Static Performance.

The static performance of the device was determined by the use of a L.V.D.T. resolving to 0.5×10^{-6}m, in combination with a suitably designed jig which could accommodate a range of pre-load weights. The data gathered during this experiment

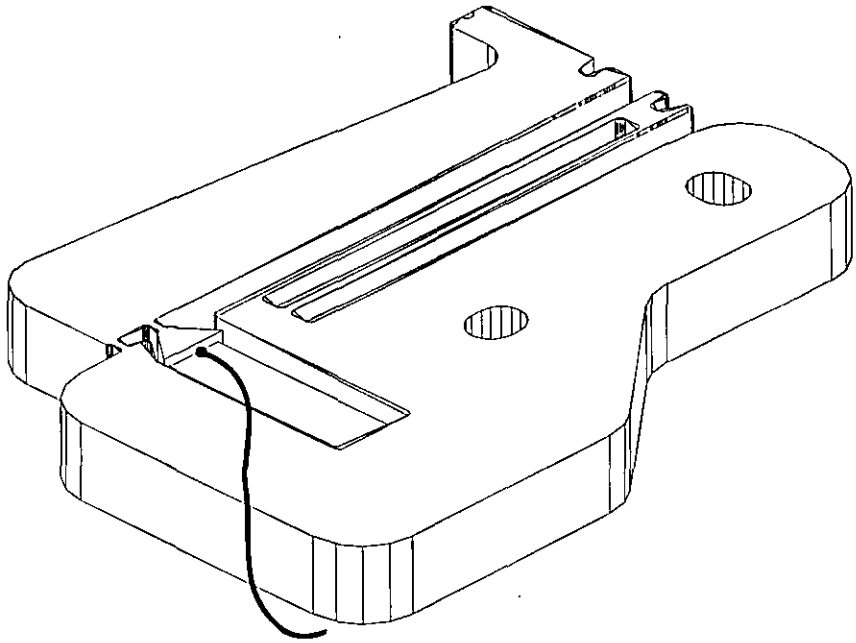

Figure 64: Perspective View of the 200 μm Amplifier.

DIMENSION	VALUE(mm)
a_1	3.76
a_2	48.77
l_1	0.85
l_2	0.85
w_1	0.65
w_2	0.65
d	12.63
e_1	1.24
e_2	7.11
b	6.50

TABLE 9: Geometry produced by the Beam Designer Program for Example 2.

is shown in Figure 65, and shows the output position against excitation voltage for differing values of mechanical loading.

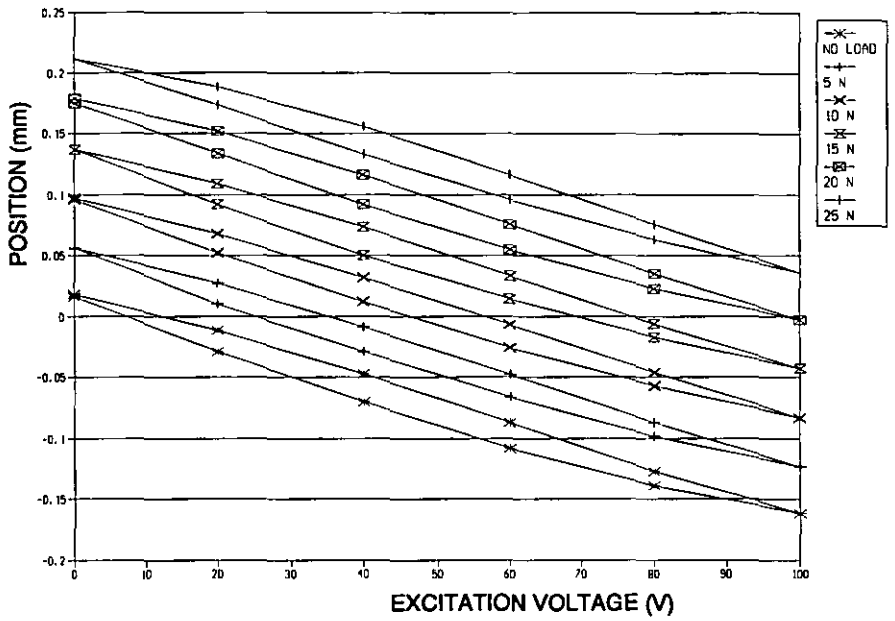

Figure 65: Results of the Static Tests for Example 2.

In this way, it was possible to determine the output compliance and the free movement of the structure. In order to check these results against a theoretical basis, a finite element mesh was constructed in order to predict stress, compliance and displacement data. The mesh used is shown in Figure 66. The structure was restrained encastre around the mounting holes.

This mesh was used for the static data and for the dynamic analysis which follows. The static data is shown in Table 10, along with the data predicted by the Finite Element Mesh and the Beam Designer Program.

The efficiency figures are disappointing, but not surprising since one intention of the exercise was to push the designer program past the point where its intrinsic assumptions fail.

As can be seen in Figure 67, even when the device is unloaded at the output, there is a discernable movement of the static hinge anchor point.
In stall mode, as seen in Figure 68, the situation is even worse where the anchor point

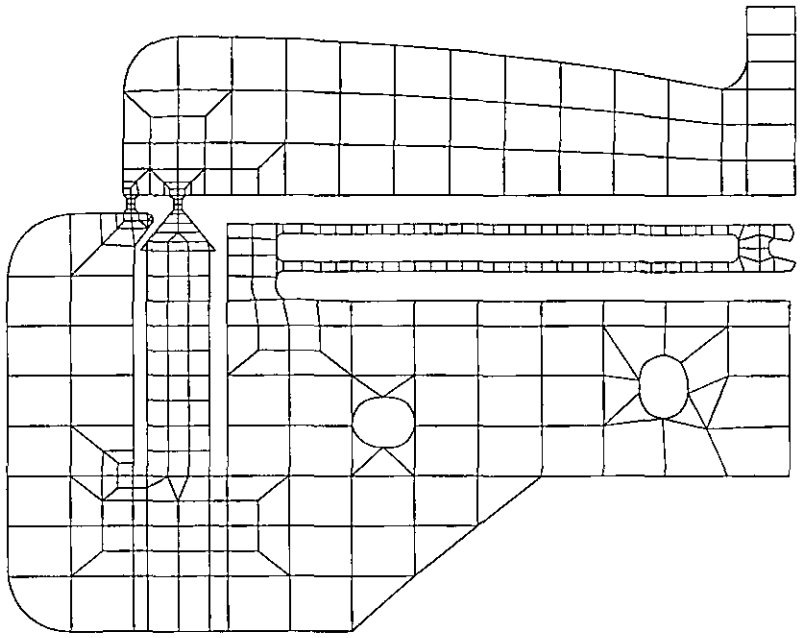

Figure 66: Finite Element Mesh used to model Example 2.

PARAMETER	PREDICTED	F.E.A.	ACTUAL
Output Movement	200 μm	197 μm	203μm
Output Stall Force	44.4 N	23.1 N	26.2 N
Max Stall Stress	203 MPa	83 MPa	-----
Max Free Stress	168 MPa	85 MPa	-----
Efficiency	69 %	36.5 %	42%

TABLE 10: Comparison of Modelling Performance with F.E.A. and the Manufactured Device for Example 2.

has displaced nearly 5 μm in the stall condition. To isolate the effect of the host structure, the finite element program was re-run, but with idealised restraints at the base of the actuator and static hinge. The result of this analysis are tabulated in Table 11.

It is evident that remodelling the Finite Element Mesh, to substantially eliminate the effects of the host structure, shows a better degree of agreement with the beam

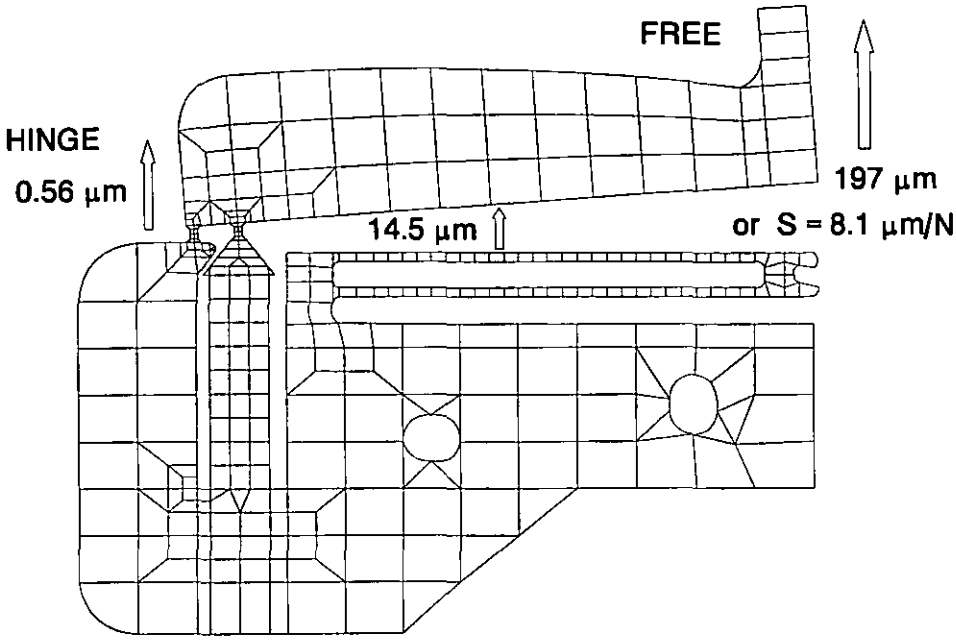

Figure 67: Finite Element Mesh showing Free Extension.

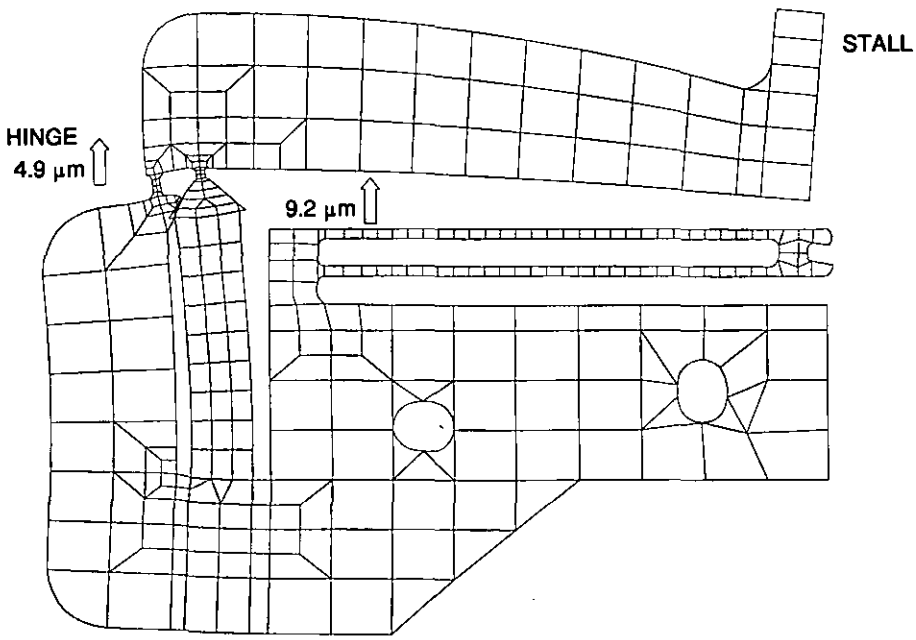

Figure 68: Finite Element Mesh showing Stalled Extension.

designer program. It is also evident that a useful enhancement to the designer program would be the inclusion of mathematics to model the effect of the host structure. This would be an advantage since the program at present is giving very conservative

PARAMETER	PREDICTED	IDEAL F.E.A.
Output Movement	200 μm	201 μm
Output Stall Force	44.4 N	35.6 N
Max Stall Stress	203 MPa	122 MPa
Max Free Stress	168 MPa	104 MPa
Efficiency	69 %	55.6 %

TABLE 11: Comparison of Modelling Performance with Idealised F.E.A. and the Manufactured Device for Example 2.

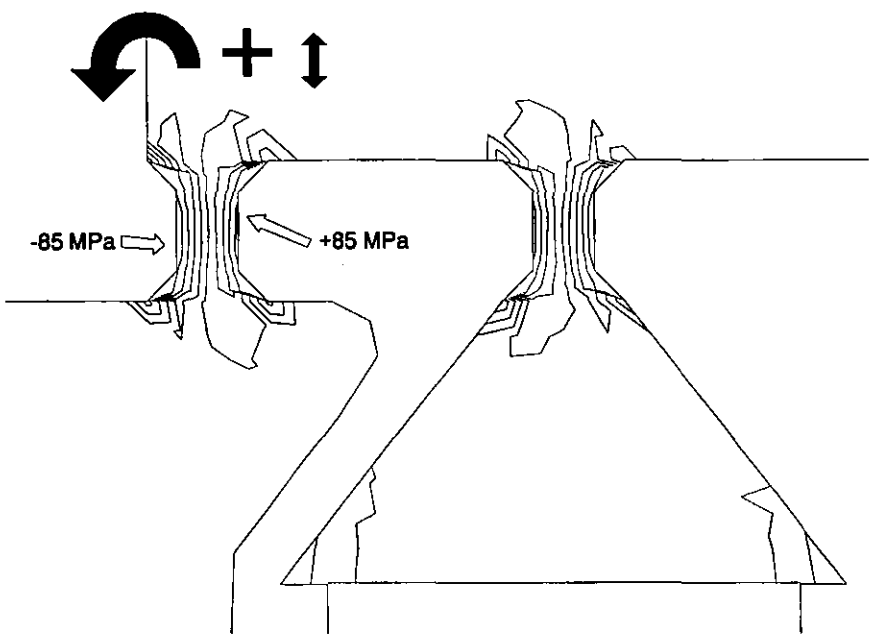

Figure 69: Diagram showing Stress Levels during Free Extension.

estimates of stress levels, and more precision here would result in less "*over-design*". The stress levels shown in Table 10 can be seen in Figure 69 and Figure 70.

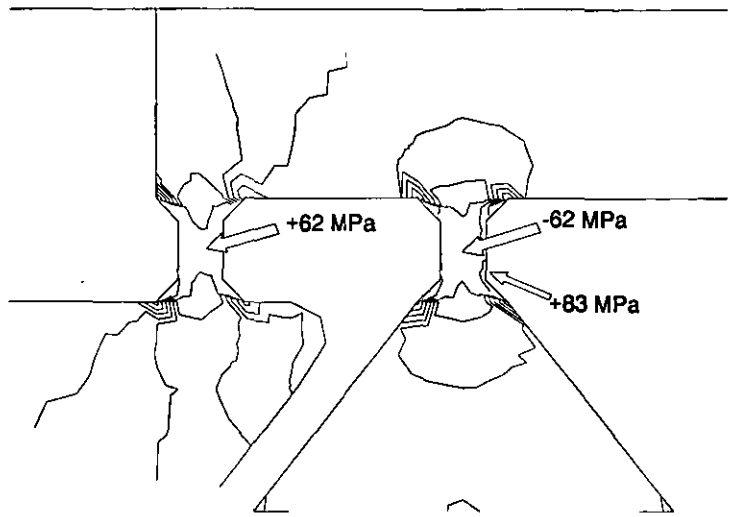

Figure 70: Diagram showing Stress Levels during Stalled Extension.

6.7.2.2 Dynamic Performance.

The finite element mesh was used in a dynamic model to ascertain the resonant modes and frequencies of oscillation. These first seven modes are shown in Figure 71, along with the frequency at which each mode occurs. Interestingly, the first (lowest frequency) mode occurs at only 553 Hz and corresponds to the natural frequency of the shear spring. In practice, this does not occur since the model is inaccurate where the restraint and couplings of the spring are concerned, specifically, in the real device the spring is held in tension with the output arm.

The second mode is the one which corresponds to the expected operational static mode, and this occurs at 700 Hz. Many other spring modes exist as expected with such a structure but one more important mode exists associated with lateral translation of the output arm, and from laser vibrometry, this might be detectable as can be seen later.

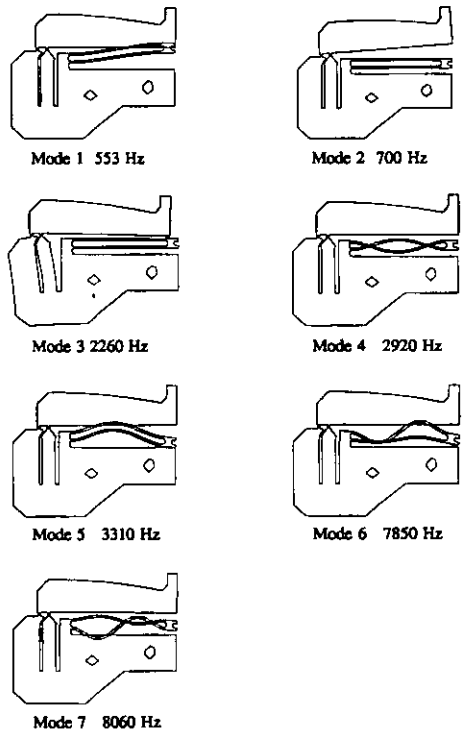

Figure 71: Modes and Frequencies of Vibration for Example 2.

Two basic methods were chosen to examine the dynamic performance of the actuator. Firstly, to determine response time and damping, the time domain behaviour was studied using an experimental setup as illustrated in Figure 72. Later, other methods were used to establish the frequency domain characteristics of the device.

The purpose of the test rig was to record the dynamic response of the actuator to a step change in drive voltage, in order to ascertain the speed of response and the damping characteristics. Included in the rig was a high-performance low-pass filter; the purpose of which was to remove certain Fourier components of the drive waveform. The laser vibrometer produced a velocity signal, calibrated to $6.32 Vsm^{-1}$,

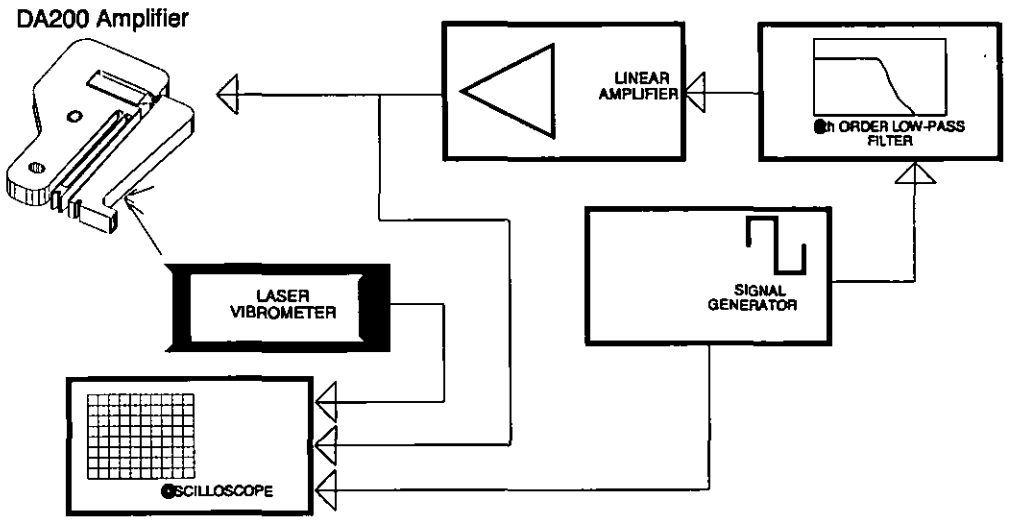

Figure 72: Schematic of the Test Rig used for Determination of Time Domain Response.

but produced a signal with a high noise floor [20], as will be seen from the resulting traces. The basic response of the device is shown in Figure 73.

As can be seen, the structure is only very lightly damped, with a resonant frequency very close to 700 Hz, and in a clutching application would probably be almost useless due to this resonant behaviour. The resonant frequency is determined largely by the stiffness of the actuator and the moment of inertia of the output beam about the static hinge.

To see the response of the structure in the frequency domain, a slightly different experimental set up was used involving a broad-band noise generator and a spectrum analyzer, essentially as illustrated in Figure 74.

[20] Partially due to a faulty instrument.

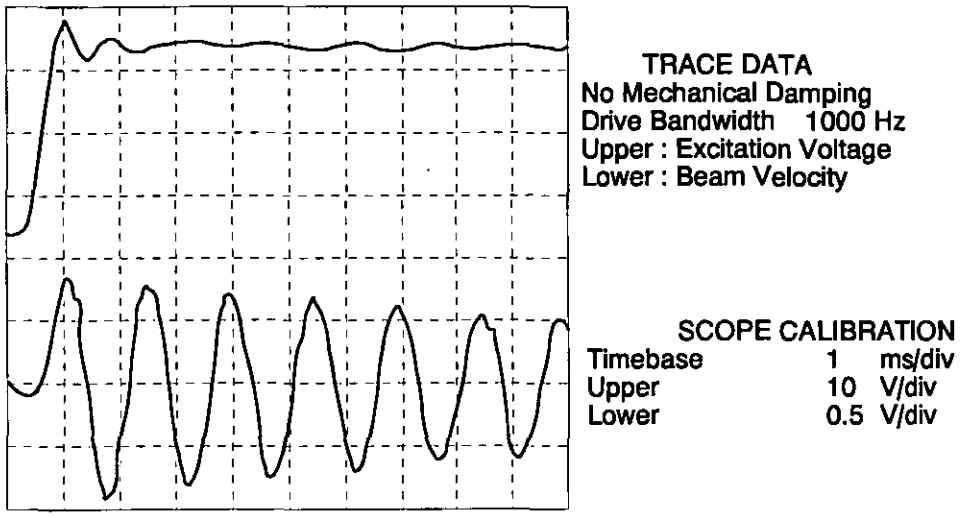

Figure 73: The Time-Domain Response of the actuator, with No Additional Mechanical Damping.

The undamped structure's frequency response is shown in Figure 75, and the resonant peak at 700 Hz., is approximately 20 dB above its response at frequencies below 100 Hz. This type of representation clearly illustrates the device's un-usability it its 'raw' form.

6.7.2.3 Mechanical Damping.

There are two basic methods that can be adopted to reduce ringing in this type of resonant structure. One method is purely mechanical, the other is electrical, of which there are several variations. The effect of introducing a damping (polysulphide rubber) compound into the void between the host structure and the amplifying arm can be seen in Figure 76. Interestingly, mode 3 of the dynamic finite element analysis seems to be present in the form of two very sharp peaks, one of which occurs at approximately 2.4 kHz.

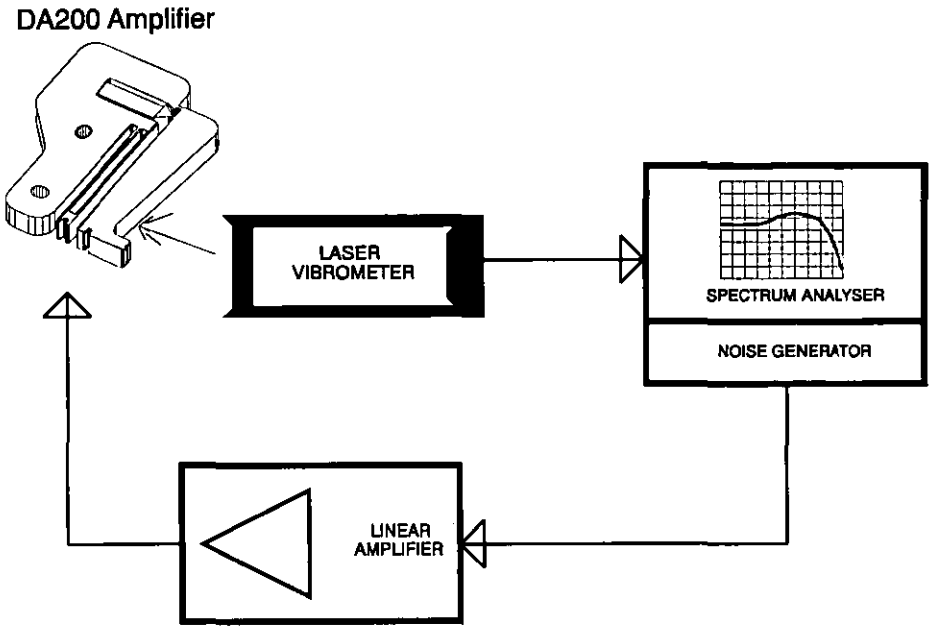

Figure 74: Test Rig used for Frequency Domain Analysis.

Although the precise effect of this is difficult to quantify, it can be seen that effective damping was easy to achieve on an ad hoc basis. The alteration to the frequency domain characteristics can be seen in Figure 77.

The result is interesting because the high-Q peak has not only been reduced in magnitude, but shifted in frequency to just over 1 kHz. This is accounted for by the added dynamic stiffness of the damping material. It is not suggested that this damping condition is ideal, but it is a viable, simple and mechanically robust technique for the avoidance of long settling times with ringing behaviour. The results of adding more damping are unclear in the time domain, but can be seen more clearly in the spectrum of Figure 78.

The goal of the beam designer is to produce a boundary of a working device. No attempt is made at mass optimisation. This process is one which usually involves

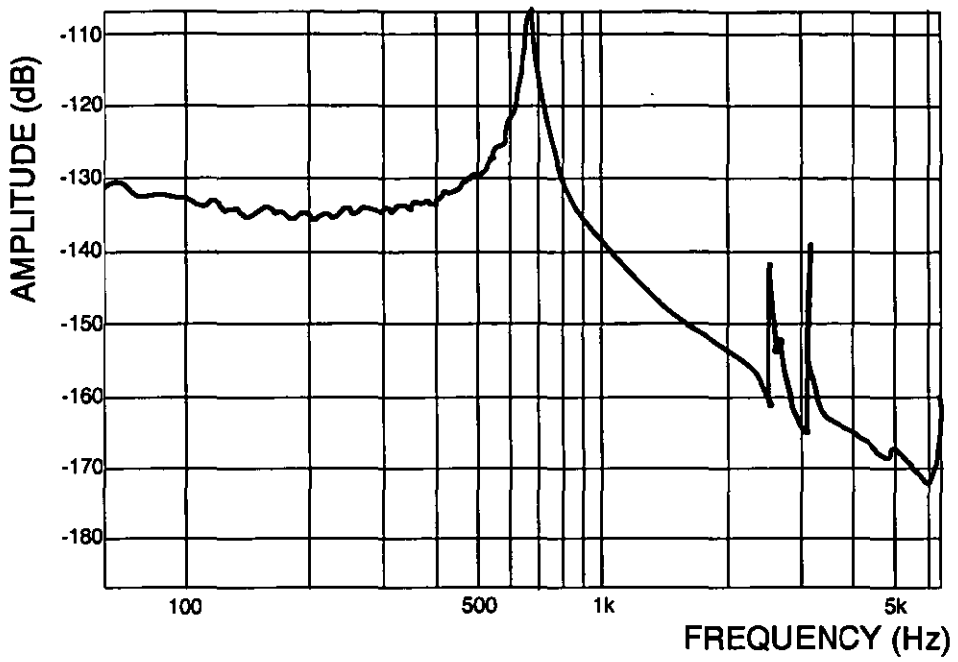

Figure 75: Frequency Domain Plot for the Undamped Structure.

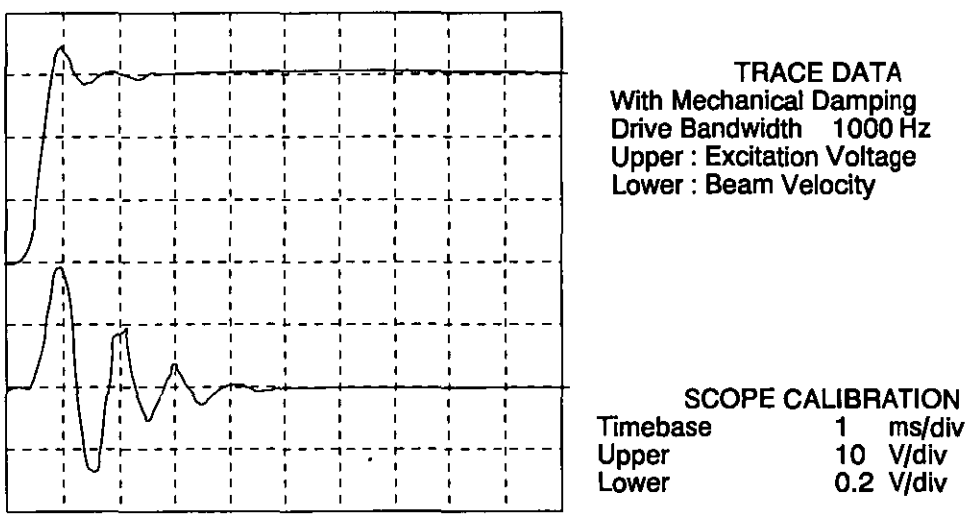

Figure 76: Time Domain Response of a Mechanically Damped Amplifier.

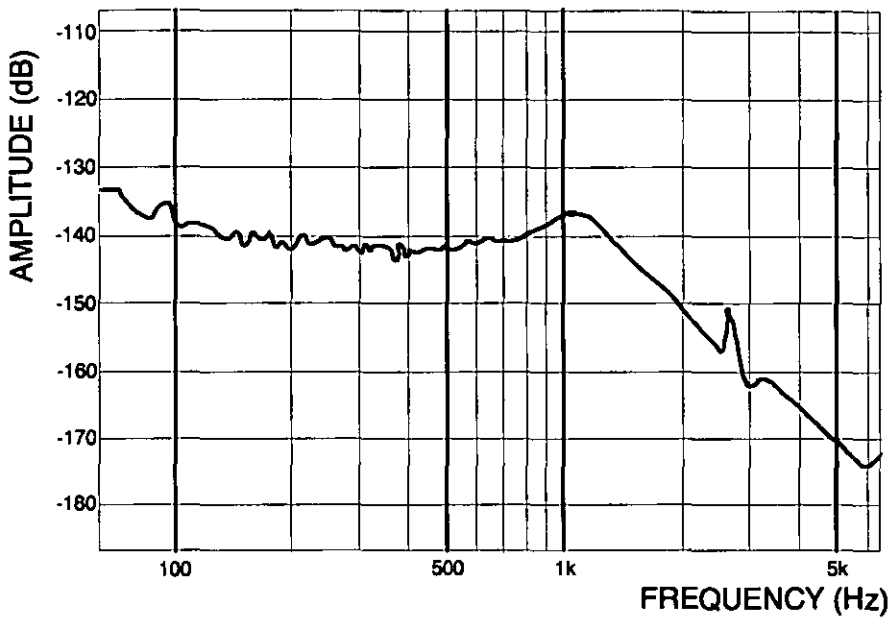

Figure 77: Frequency Domain Response of a Mechanically Damped Amplifier.

Figure 78: The Effect of adding more Damping.

Finite Element packages with a high degree of sophistication and is beyond the scope of a program of relative simplicity. As previously stated, the terms which dominate the resonant frequency of the device are piezoelectric actuator stiffness and moment of inertia of the amplifying arm about the static hinge. Little can be done about the

actuator, but some optimisation can be performed on the arm.This task was performed manually in an attempt to indicate the magnitude of improvements in speed that might be possible.

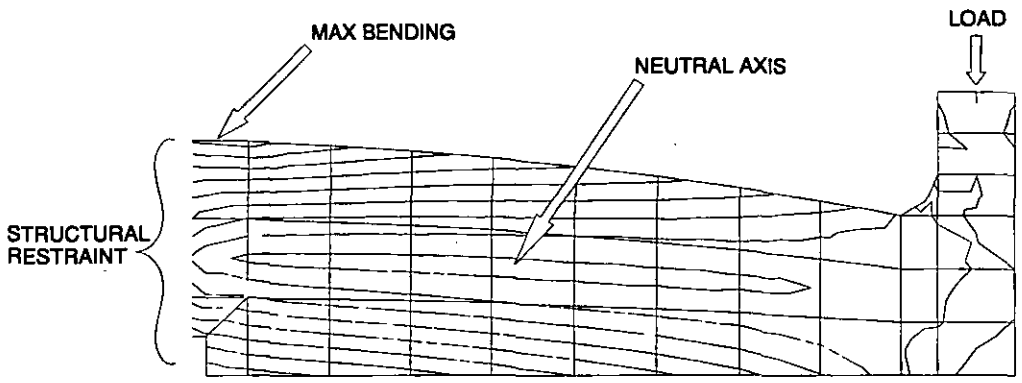

Figure 79: The Neutral Axis of the Amplifier Output Beam (Ex.2).

Inspection of a Finite Element Stress Plot as shown in Figure 79, indicated the neutral axis during stall loading. The precise loading is irrelevant but the axis position shows where material could be removed with minimum effect on the static performance of the device. On an experimental basis, material was removed from the F.E. model in the fashion shown in Figure 80; this included the thinning down of the output post.

Care was exercised to ensure that the output compliance was kept to within 1% of its original value, in other words a minimal change.

Dynamically, the shift in the undamped resonant frequency is significant but not vast, and it is questionable whether the speed increase is worth the additional machining cost, although this type of design choice is too application specific to be meaningfully discussed here. The Frequency Domain Plot is shown in Figure 81.

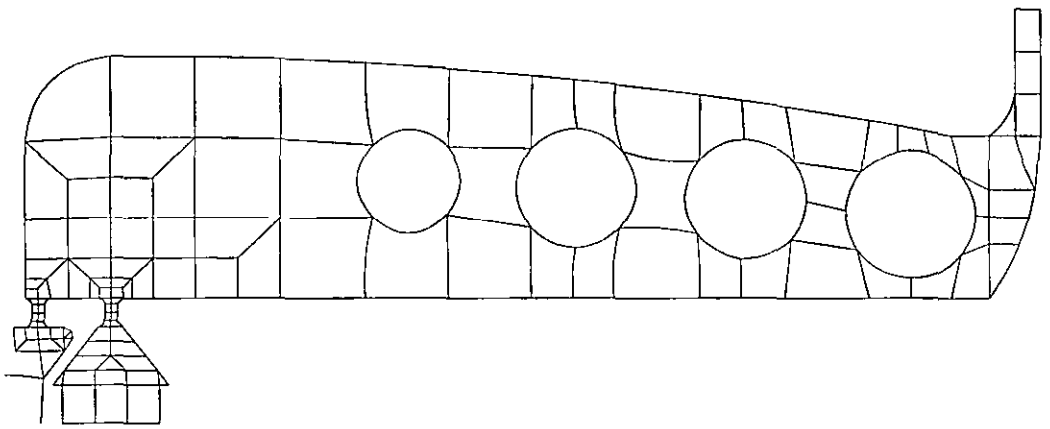

Figure 80: Removal of Material from the Output Beam (Ex.2).

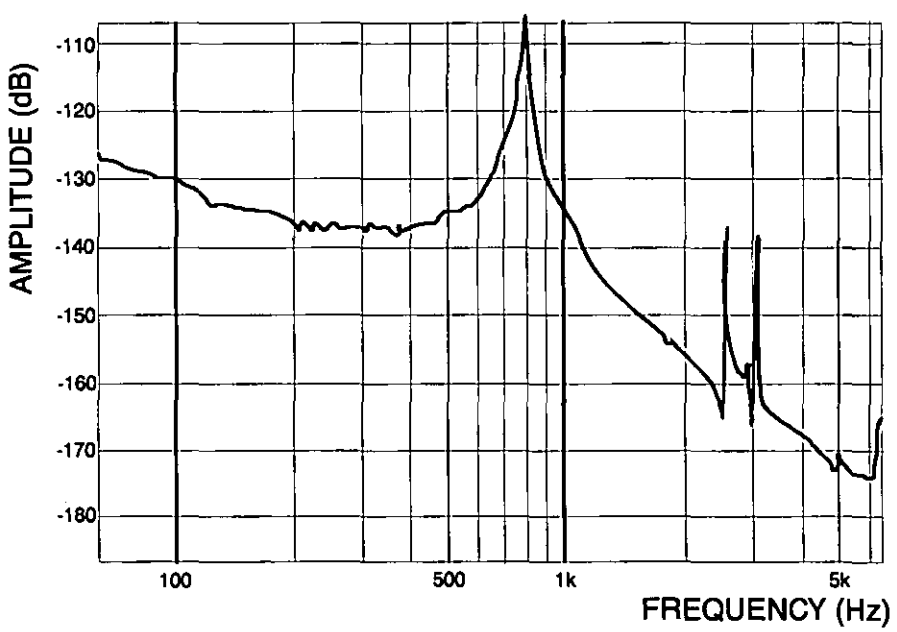

Figure 81: Shift of Resonant Frequency due to Optimisation.

6.7.2.4 Electrical Response Control.

The optimisation of speed of response of electro-mechanical systems is a vast subject beyond the scope of this thesis. Criteria such as tracking error and perturbation error, might be primary considerations in a given control system, and in this application it may be possible to apply these techniques. However, the original goal was to design a device capable of rapid switching with transition times in the order of 1 ms or better, and it is the ringing behaviour which is the sole limitation of application. Rather than using a closed loop control method, it is more appropriate to find a passive solution.

The reason why the ringing behaviour is so pronounced in the example is that the mechanical Q is very high and the driving waveform (edge) contains components in the frequency spectrum at the resonant frequency of the structure. It therefore requires only a small harmonic component to cause ringing. To illustrate this, the setup as shown in Figure 72 was used, where the frequency components of the driving waveform which stimulate the structure to ring, could be effectively removed from the drive signal.

Figure 82, shows the velocity response of the actuator whilst undamped; the same conditions which prevailed in Figure 73, but with a longer time base. Adjusting the pass-band of the low-pass filter to 360 Hz, (just below resonance) results in a dramatic reduction in oscillatory behaviour, as can be seen in Figure 83.

The same response can be seen in Figure 84, and at this time base it is interesting to note the propagation delay of the edge through the filter (the scope was triggered from the waveform generator and a 1.2 ms delay is evident). A further 1.2 ms elapses before the actuator arm velocity is zero again, and the rise time is approximately 1 ms (10% - 90%). Further reductions in ringing can be achieved by reducing the bandwidth only slightly more to 260 Hz and this result is shown in Figure 85.

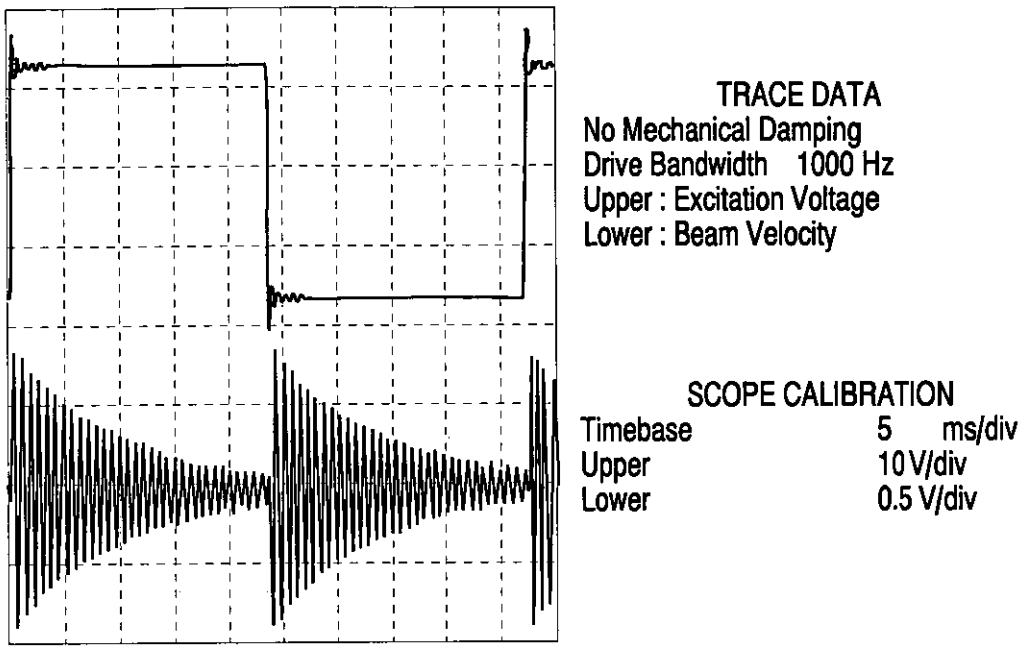

Figure 82: The Time-Domain Response of the actuator, with No Additional Mechanical Damping.

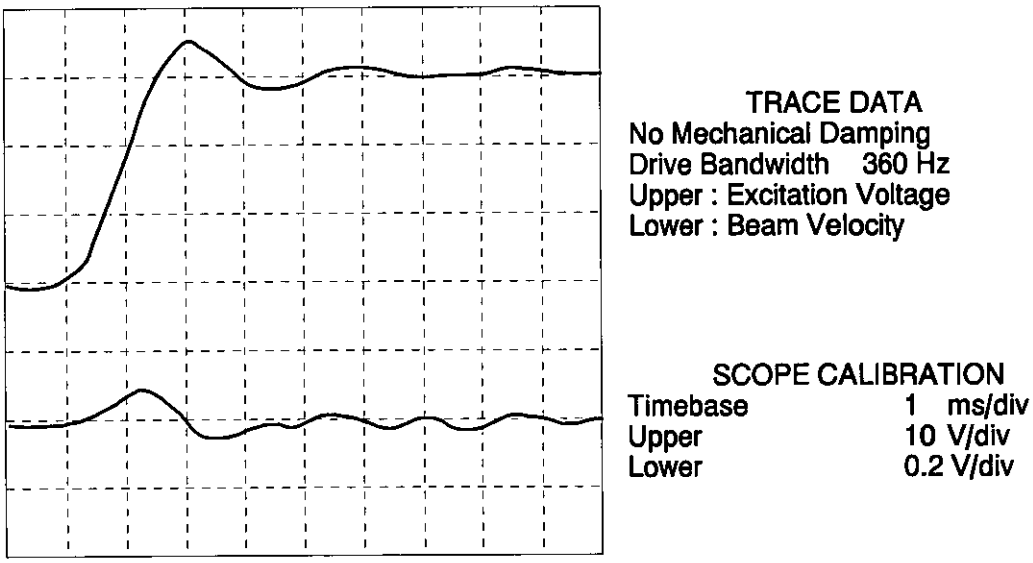

Figure 84: Response to a 360 Hz bandwidth limited drive.

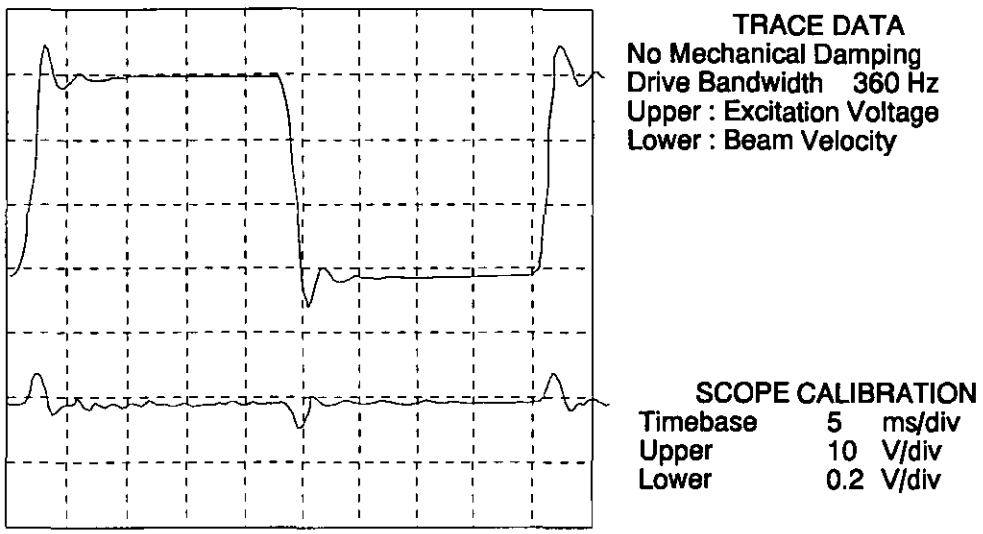

Figure 83: Response to a 360 Hz bandwidth limited drive.

Subjectively, in this case, all oscillatory behaviour has vanished approximately 7 ms after actuation.

In the above examples, the effects of electrical control and mechanical control have been independently demonstrated, but in practice a combination of techniques might be used, as in the case shown in Figure 86 where there is a 600 Hz bandwidth limit in combination with mechanical damping as before. A rise time of 1 ms is typical with extinction of oscillation after approximately 4.5 ms. This makes possible the use of such a device at surprisingly high repetition rates as shown in Figure 87, which is being switched at 200 Hz.

6.8 OBSERVATIONS

From the data resulting from tests on Example 1 and in more detail on Example 2, it is clear that the beam designer program performs moderately well within the

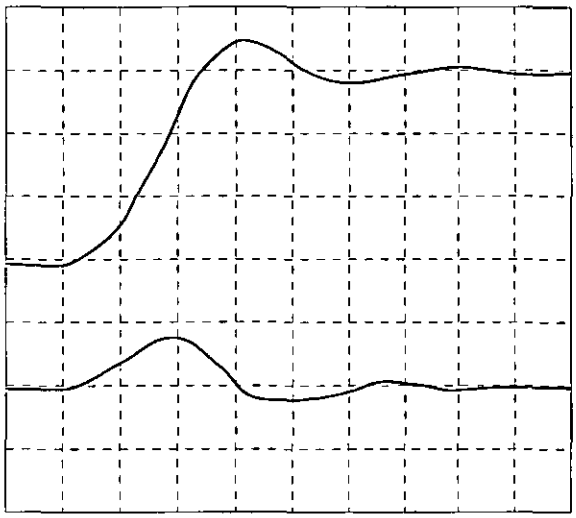

TRACE DATA
No Mechanical Damping
Drive Bandwidth 260 Hz
Upper : Excitation Voltage
Lower : Beam Velocity

SCOPE CALIBRATION

Timebase	1	ms/div
Upper	10	V/div
Lower	0.2	V/div

Figure 85: Response to a 260 Hz bandwidth limited drive.

assumptions and constraints on which it is based. It is clear that for higher efficiency devices, the assumption about the host structure's rigidity is not valid and will inevitable lead to errors in device efficiency but not output displacement, and the stresses predicted will be artificially high. Example 1 in section 6.7.1, illustrates that although the program produces results of moderate accuracy, it is conservative in its stress calculations and is therefore likely to produce designs which are more resistant to cyclic fatigue than expected. The program appears to be a useable tool for the rapid turn-around of simple beam designs. Section 9.2 covering the application of simple beam amplifiers to a rotary micropositioner details the employment of devices designed by the program.

The devices produced indicate that mechanical amplification (transformation) by the lever method, involving the use of flexure hinges, is viable, and can produce devices which are moderately efficient; in the region of 45% to 75%, depending on selection of host material. The speed of response of this class of device is typically in the region of 1 ms, even for devices with output displacements as high as 0.2mm.

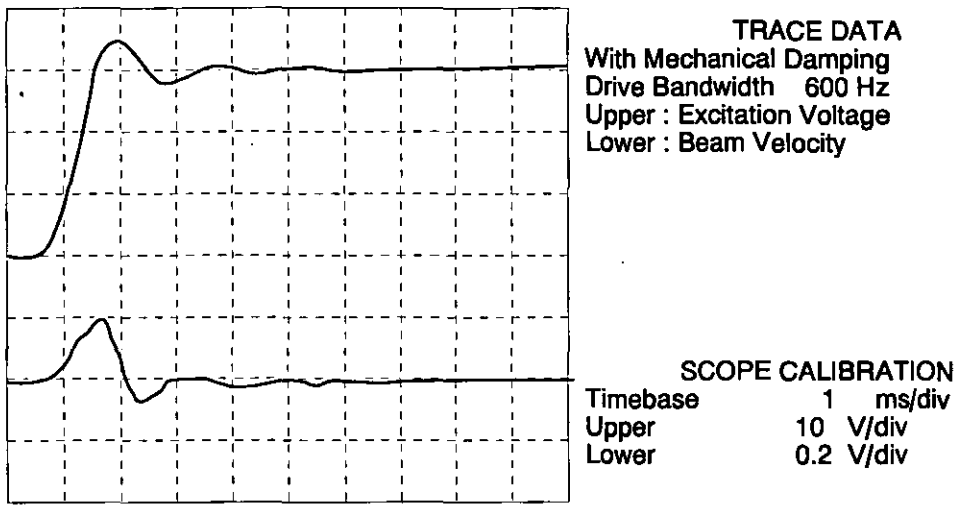

Figure 86: A Combination of Electrical and Mechanical Control.

Combinations of mechanical damping and electronic wave shaping can result in actuator transition behaviour which is conducive to operation of such devices at relatively high repetition rates. The low-power dissipation of such devices makes them attractive in high-speed mechanical switching applications, such as clutching, and in particular where high-speed and low holding power are primary.

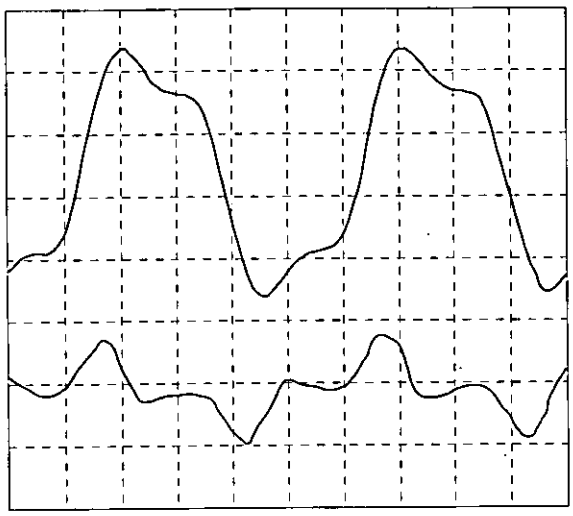

TRACE DATA
With Mechanical Damping
Drive Bandwidth 600 Hz
at 200 Hz repetition
Upper : Excitation Voltage
Lower : Beam Velocity

SCOPE CALIBRATION
Timebase1 ms/div
Upper 10V/div
Lower 0.2V/div

Figure 87: Operation at a Repetition Rate of 200 Hz.

7 THE DESIGN OF FLEXURAL BRIDGE DISPLACEMENT AMPLIFIERS.

7.1 INTRODUCTION

The flexural bridge structure has been identified as a generically useful topology as a mechanical displacement amplifier. Modelling of the structure, as employed in the strip-clutch displacement amplifying mechanism, is worthy of study since it can be employed in many applications, with or without a lever pre-amplifying structure.

In contrast to the simple beam amplifier, it produces output with motion in a direction perpendicular to the direction of input, and in this way offers added flexibility for the designer. This chapter covers a semi-analytical approach to the design of such structures and compares the results with modelling based on a Finite Element approach.

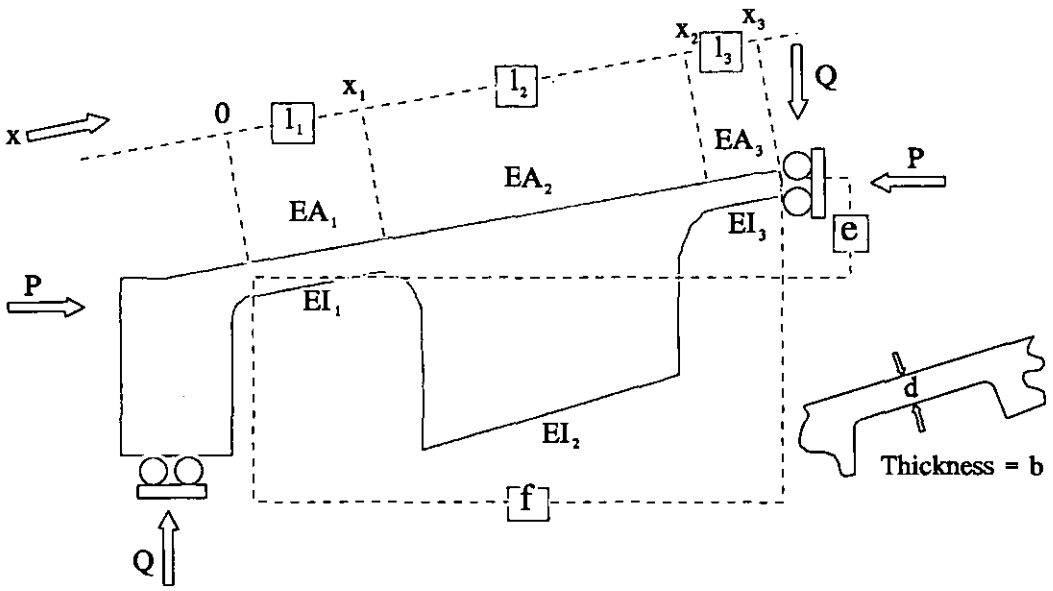

Figure 88: Semi-symmetrical Model of the Flexural Bridge Structure.

7.2 SEMI-ANALYTICAL MODEL.

Figure 88 shows half of a typical bridge structure and is annotated in accordance with the analysis in para 7.2.1. The device would always comprise a symmetrical arrangement with two half-bridges as shown, however, the device could be operated from a single ended input or from both sides. In the former case, the output does not displace vertically but displays a slight horizontal skew, which in many applications may be unimportant. In the strip-clutch, this effect would be problematic. The model represents only half the structure where both sides of the bridge are subjected to symmetrical drive characteristics, and in this case, the output displacement predicted by modelling will be valid, providing the requirement for symmetrical drive is remembered. The output compliance for the full bridge will be half of that predicted by the model.

The model can also be applied to systems which are asymmetrically driven, for example if the input to one half bridge is completely constrained. In this case the line of symmetry of the whole structure translates, so for the purpose of modelling, the input compliance must be doubled for the model and the idealised input displacement halved.

7.2.1 Analytical Solution.

In the case of the strip-clutch, the input to the structure manifests as rotation about a flexure hinge (not shown), however, the input displacement is small enough with respect to the radius of rotation, to consider the input movement as linear, rather than a combination of linear and rotary. Since the input end of the bridge is constrained by the preceding structure, input rotation is restrained. The output of the bridge is similarly restrained due to symmetry.

The model is most easily solved by the application of an energy method. Originally, an attempt was made to use a method involving Castigliano's theorem. This method

is only adequate in the simple cases where the output of the bridge is free (i.e., with Q = 0) or the input is free (P = 0, and this has no real application) or in the special case where the resultant of P & Q is coaxial with the centroids of the beams; this only occurs then the input or output are stalled, see Eqn.(96) . As will be shown later, although a more sophisticated method is required for the general solution of such structures, where the output loading is not contained in the previous set of special cases, this complex model is not necessary for the implementation of a designer program.

A further simplification for the analytical model is that all the centroids are coaxial, which in the case of the flexure bridge of the strip clutch is not valid. Additionally, the simple analytical model does not account for the progressive small scale alteration of the geometry, when varying loads are applied.

The structure can be partitioned into zones (1 to 3) in the general case, each having length (l), area (A) and second moment of area (I) as shown. Energy due to bending is usually dominant is such structures, but in this case, when the output is vertically constrained or stalled, direct stress is dominant, and therefore both bending strain and direct strain energies are considered for each zone.

The bending energy for the structure is given by;

$$U_b = \frac{1}{2EI}\int_{x_a}^{x_b} M^2 dx \qquad \textbf{(93)}$$

where;

$$M = \frac{(Pe - Qf)}{2}\left(1 - \frac{2x}{l}\right) \qquad \textbf{(94)}$$

Similarly, the direct energy component is given by;

$$U_d = \frac{1}{2EA}\int_{x_a}^{x_b} W^2 dx \qquad \textbf{(95)}$$

where;

$$W^2 = P^2 + Q^2 \tag{96}$$

Integrating over the three zones,

$$U_b = \frac{\Omega}{8E}(P^2e^2 + Q^2f^2 - 2PQfe) \tag{97}$$

where;

$$\begin{aligned}\Omega = & \frac{x_1}{I_1} + \frac{(x_2 - x_1)}{I_2} + \frac{(x_3 - x_2)}{I_3} \\ & - \frac{2}{l}\left(\frac{x_1^2}{I_1} + \frac{(x_2^2 - x_1^2)}{I_2} + \frac{(x_3^2 - x_2^2)}{I_3}\right) \\ & + \frac{4}{3l^2}\left(\frac{x_1^3}{I_1} + \frac{(x_2^3 - x_1^3)}{I_2} + \frac{(x_3^3 - x_2^3)}{I_3}\right)\end{aligned} \tag{98}$$

The direct energy is given by;

$$U_d = \frac{\Gamma(P^2 + Q^2)}{2E} \tag{99}$$

where;

$$\Gamma = \frac{x_1}{A_1} + \frac{(x_2 - x_1)}{A_2} + \frac{(x_3 - x_2)}{A_3} \tag{100}$$

Thus the total energy is given by;

$$U = U_b + U_d = \frac{1}{8E}(\Omega(P^2e^2 + Q^2f^2 - 2PQfe) + 4\Gamma(P^2 + Q^2)) \tag{101}$$

Applying Castigliano's theorem, the input displacement for a force P is given by;

$$\delta_i = \frac{\partial U}{\partial P} = \frac{2P(e^2\Omega + 4\Gamma) - Qfe\Omega}{8E} \tag{102}$$

and if the output is free and therefore Q = 0; then the input compliance is given by;

$$s_i = \frac{e^2\Omega + 4\Gamma}{4E} \tag{103}$$

For the case when the input is laterally unconstrained and therefore P = 0, the output movement is given by;

$$\delta_o = \frac{\partial U}{\partial Q} = \frac{Q(f^2\Omega + 4\Gamma) - Pfe\Omega}{4E} \tag{104}$$

and the output compliance is given by;

$$s_o = \frac{f^2\Omega + 4\Gamma}{4E} \tag{105}$$

In the case where the output is stalled, the relation;

$$Q \approx \frac{Pe}{f} \tag{106}$$

allows a solution for the input energy;

$$U = \frac{\Gamma P^2}{2E}\left(1 + \frac{e^2}{f^2}\right) \tag{107}$$

and hence the stalled input compliance;

$$s_{is} = \frac{\Gamma}{E}\left(1 + \frac{e^2}{f^2}\right) \tag{108}$$

Finally, with the input stalled, the output compliance can be shown to be;

$$s_{os} = \frac{\Gamma}{E}\left(1 + \frac{f^2}{e^2}\right) \tag{109}$$

Note that due to symmetry, the output compliances (both free and stalled) will be precisely half the respective compliances for the full bridge.

In a real system, the input to the bridge can be modelled as an infinitely stiff ideal displacement δ_d, coupled through a compliance s_d. An equally valid view, and hence

interchangeable, is the model of a force F_d coupled through the same compliance. Since the structure has finite input compliance s_i, the input drive is effectively loaded, and consequently reduced to a real value of;

$$\delta_r = \frac{\delta_d s_i}{(s_d + s_i)} \tag{110}$$

Therefore, the real gain of the half-bridge is given by;

$$g_r = \frac{s_i}{(s_d + s_i)} \frac{f}{e} \tag{111}$$

STRESS.

Stress levels in the structure will be due to direct stress induced by P and Q, and bending stress induced by the couple (Pe - Qf). In zone 2, the width (d) will be an order of magnitude greater than the widths in zones 1 and 3, and therefore the effects of direct stress and particularly bending stress can be disregarded.

In a uniform beam of thickness d, experiencing a pure bending moment M, the principal stress is given by;

$$\sigma_b = \pm \frac{My}{I_z} \tag{112}$$

where the second moment of area is given by;

$$I_z = \frac{bd^3}{12} \tag{113}$$

and y is the distance from the neutral axis, i.e.;

$$y = \frac{d}{2} \tag{114}$$

Under a direct force W, the principal stress is given by;

$$\sigma_d = -\frac{W}{A} = -\frac{W}{bd} \tag{115}$$

In the general case, for all zones;

$$\sigma_{b+d} = -\frac{\sqrt{P^2+Q^2}}{bd} \pm \frac{3(Pe-Qf)}{bd^2} \tag{116}$$

Note that the direct component will always be negative (compressive) statically, whereas the bending component is bilateral.

Therefore, in stall (see Eqn.(106));

$$\sigma_{stall} = \frac{P_{stall}}{bd}\sqrt{\left(1+\frac{e^2}{f^2}\right)} \tag{117}$$

and when the output is free;

$$\sigma_{free} = \frac{P_{free}(d+3e)}{bd^2} \tag{118}$$

Therefore the value of P must be evaluated for an ideal input displacement δ_i, or force F_d for both free and stalled cases. In the free case;

$$\delta_{r_{free}} = \frac{\delta_i\, s_i}{(s_d+s_i)} \tag{119}$$

And in the stalled case;

$$\delta_{r_{stall}} = \frac{\delta_i\, s_{is}}{(s_d+s_{is})} \tag{120}$$

Therefore for each case;

$$P_{free} = \frac{(\delta_i-\delta_{r_{free}})}{s_d} \qquad P_{stall} = \frac{(\delta_i-\delta_{r_{stall}})}{s_d} \tag{121}$$

7.2.2 Testing the Semi-Analytical Model.

In order to test the accuracy of this modelling method, a finite element model of an idealised half-bridge structure was constructed. As an interesting study the dimensions of the strip-clutch bridge section were used, although the neutral axes of the three zones were modelled as coaxial rather than skewed. These are shown in Table 12.

DIMENSION	ZONE 1 (mm)	ZONE 2 (mm)	ZONE 3 (mm)
Length (l)	1.5	10.0	1.5
Width (d)	0.3	4.7	0.3
Thickness (b)	6.5	6.5	6.5

TABLE 12: Test Data for the Bridge Modelling Algorithms.

It should be noted that this idealised approach does not allow for the inclusion of filletting, which modifies the levels of real stresses and the distribution of strain energy, and therefore introduces some error. The Young's Modulus for the structure was taken as 1.1×10^{11} Pa (for Titanium), the material from which the strip-clutch is made. Values were taken for e = 2.2 mm and f = 12.5, which corresponds to an incline angle of 10° and an unloaded theoretical gain of x 5.68.

To simplify testing by comparison with a finite element model, four cases were tested using the above geometry without any consideration of the input drive. These are;

Test 1 Input compliance, output free
Test 2 Input compliance, output stalled
Test 3 Output compliance, input free
Test 4 Output compliance, input stalled

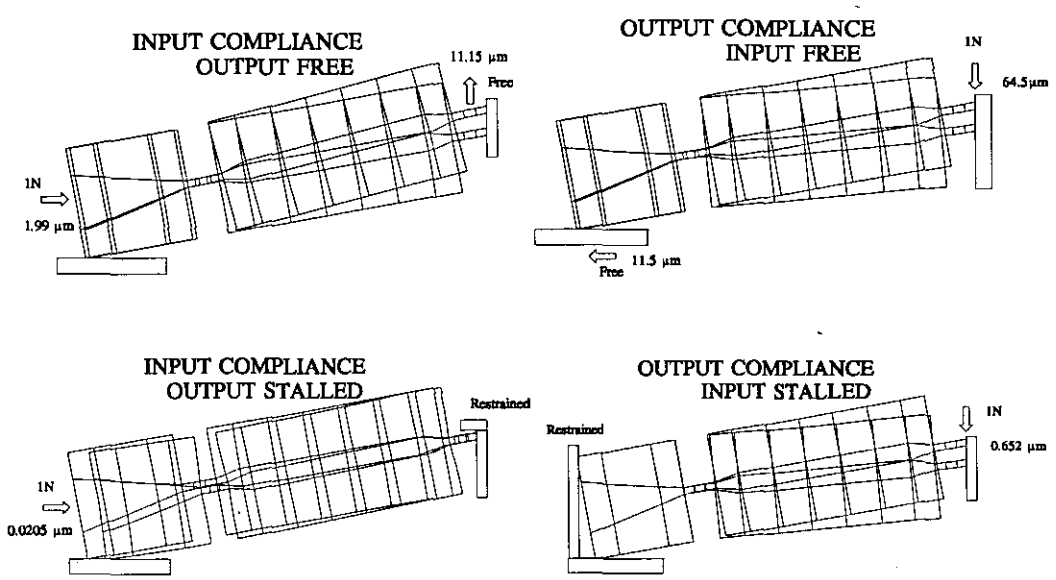

Figure 89: Finite Element Model Response to the 4 Test Cases.

The results of the finite element analysis are shown in Figure 89, which detail the input and output compliances in the test cases. These can be compared with the predictions for compliance made by the analytical method as seen in Table 13.

COMPLIANCES (μm/N)	ANALYTIC	F.E.A.	ERROR (%)
s_{ifree}	1.89	1.99	5
$s_{istalled}$	0.0175	0.0205	15
s_{ofree}	60.2	64.5	7
$s_{ostalled}$	0.563	0.652	14

TABLE 13: Comparison of Analytic with F.E.A. Predictions for Bridge Compliances.

The errors are quite acceptable for the free cases (5-7%) but become more significant for the stalled cases at approximately (15%) and this, upon inspection of the local distortions of the bridge structure in Figure 89, can be attributed to stress distribution in the middle member.

7.3 ITERATIVE SOLUTION.

In the general case, assumptions about the relationships for P and Q can not be made, since in practice, the output will generally not be presented with an infinitely stiff load. The stalled condition for $P \propto Q$ will not hold. Additionally, in the `stall' condition, the value of P will be large and consequently the direct energy component will be more significant. This results in shortening of the dimension l which strongly affects the geometry of f and e. This behaviour results in complex interactions between direct and bending energy. For these reasons, an iterative approach is desirable. In this case, the law on conservation of energy of a closed system is exploited; specifically, the work done by the prime mover is equal to the work done by the output plus the energy stored in the structure.

7.3.1 Basic Algorithm.

The algorithmic approach chosen was one where the structure was assumed to be driven by an elastic drive x_d, through stiffness k_d. The real input displacement x_i and the real output displacement y_o can be determined if the output force Q is specified, but an inherent assumption made is that the output characteristics are also perfectly elastic and that under all circumstances;

$$Q = 0 \quad \text{for} \quad y_o = 0 \qquad \textbf{(122)}$$

This assumption can be modified if required to incorporate a gapped output (or dead zone), with only a very simple modification to the algorithm.

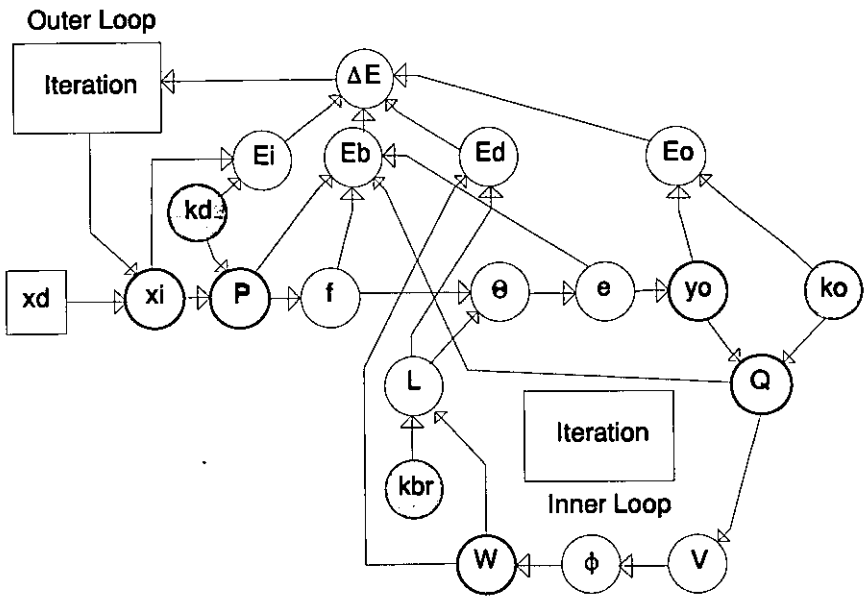

Figure 90: Iteration Parameter Network for the Half-Bridge Structure.

The algorithm is most easily understood by study of the Iteration Parameter Network shown in Figure 90. A detailed description of the parameters given in Table 14. The operation of the algorithm is as follows;

1 Set x_d and Q.

2 Choose an initial value of x_i.

3 Calculate P and therefore the compressive coaxial force W. Note; this calculation is iterative since W interacts with Θ and l, and therefore f and e.

4 Calculation of e gives output displacement y_o.

5 Calculate an energy error term ΔE.

6 Iterate by altering x_i until $\Delta E = 0$.

7.3.2 Iteration Algorithms.

Inspection of Figure 90 reveals a nested iterative structure, the heart of which is the algorithm which determines the input / output displacement geometry for given values

PARAMETER	UNITS	DESCRIPTION
x_d	m	Unloaded Drive Displacement
x_i	m	Loaded Drive Displacement
y_o	m	Output Displacement
P	N	Actuator Force
Q	N	Output Force
V	N	Resultant of P & Q
W	N	x-Component of V
k_d	Nm^{-1}	Drive Stiffness
k_o	Nm^{-1}	Output Load Stiffness
k_{br}	Nm^{-1}	Direct Bridge Stiffness
L	m	Length of Bridge
e	m	Geometric
f	m	Geometric
Θ	rad	Geometric
Φ	rad	Geometric
E_i	J	Work Done by Drive
E_o	J	Work Output of Structure
E_b	J	Bridge Bending Energy
E_d	J	Bridge Direct Energy
ΔE	J	Balance Energy

TABLE 14: Description of Parameters for Figure 90.

of x_i and P; the inner loop. The variables x_i, P and x_d can not be uniquely satisfied without recourse to the energy method. The algorithm for solving the geometry for a trial solution of x_i is as follows, for the initial determination of P and f with a first guess for l.

Hooke's Law gives;

$$P = k_d (x_d - x_i) \tag{123}$$

where;

$$f = f_0 - x_i \quad \text{with} \quad l = l_0 \tag{124}$$

The inner loop iteration sequence begins with the evaluation of e by Pythagoras;

$$e = \sqrt{l^2 - f^2} \tag{125}$$

Trigonometry gives;

$$\theta = \tan^{-1}\left(\frac{e}{f}\right) \tag{126}$$

and ;

$$y_o = e - e_0 \tag{127}$$

Assuming the output stiffness is Hookean;

$$Q = k_o (y_o - y_{gap}) \ \forall (y \geq y_{gap}) \tag{128}$$

Vector addition gives the magnitude of the resulting direct bridge load;

$$V = \sqrt{P^2 + Q^2} \tag{129}$$

and the angle of action of V is given by;

$$\phi = \tan^{-1}\left(\frac{Q}{P}\right) \tag{130}$$

Therefore, the magnitude of the force acting along the bridge is;

$$W = V \cos(\phi - \theta) \tag{131}$$

This direct force affects the length of the bridge according to;

$$l_{predict} = l_0 - \frac{W}{k_{br}} \tag{132}$$

where k_{br} is the geometry dependent longitudinal stiffness of the bridge. This generates an error term which is used to evaluate iterative convergence;

$$l_{err} = l_{predict} - l \tag{133}$$

At this point, the algorithm can terminate if l_{err} is small enough. Typically the algorithm can satisfactorily resolve values less than 10^{-14} m and so a maximum value of 10^{-13} was chosen. Until successful, iteration continues setting;

$$l \rightarrow l + \frac{l_{err}}{2} \tag{134}$$

The procedure above only finds a valid geometrical solution, with a resulting value for Q. At this point, the energy balance of the structure can be determined as;

$$\Delta E = E_i - E_b - E_d - E_o \tag{135}$$

where;

$$E_i = k_d \frac{x_i^2}{2} \quad ; \quad E_o = k_o \frac{(y_o - y_{gap})^2}{2} \tag{136}$$

and;

$$E_b = \frac{\Omega (Pe - Qf)^2}{8E} \quad \text{with} \quad E_d = \frac{\Gamma w^2}{2E} \tag{137}$$

where the geometric functions Ω and Γ are defined in equations (98) and (100) respectively. A typical energy balance (ΔE) curve if shown in Figure 91, and it can be seen from the shape of the curve that a simple basic iteration technique is unlikely to work, due to a high degree of slope variability. To enhance convergence stability, the technique employed was to take the trial value of x_i and an adjacent value

$x_i+\Delta x_i$ and evaluate ΔE for both values to obtain slope information. This results in a more stable and reliable convergence. Moreover, the value of Δx_i is dynamically updated as the interval between successive trials in reduced. This technique is particularly good at dealing with near-zero slopes close to the solution.

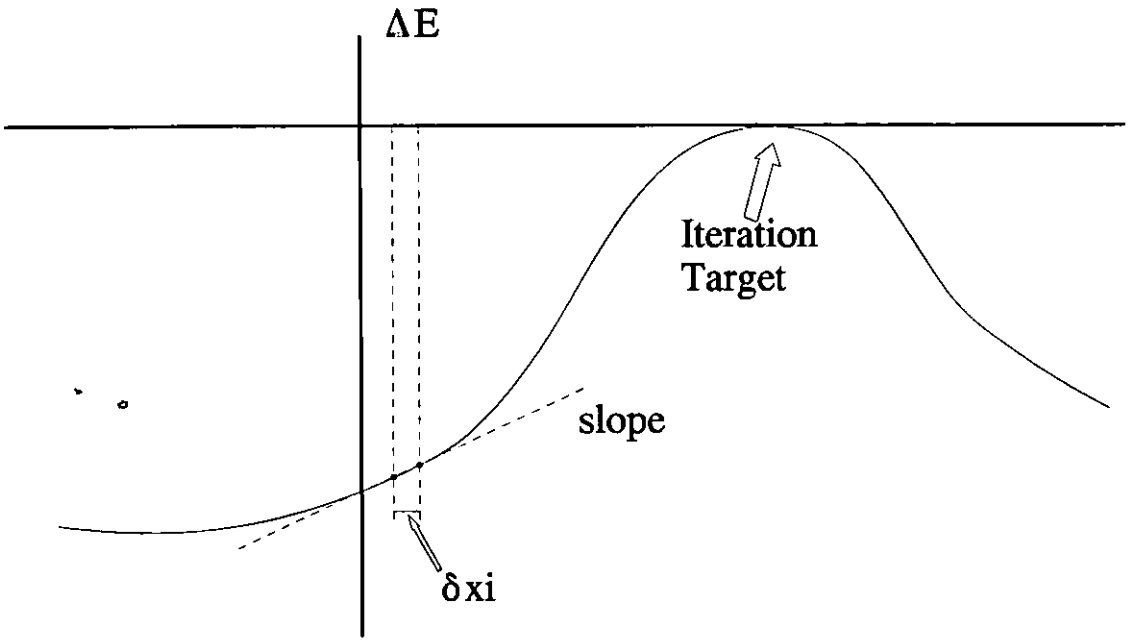

Figure 91: Nature of the ΔE Curve.

7.4 THE DESIGNER PROGRAM

Although the iterative technique appears attractive from the point of view of its ability to solve for any case for P & Q, it is numerically intensive and this is a deterrent against the inclusion of this method as the core algorithm of any designer program since the main program itself will be highly iterative. Additionally, as has been seen from the comparison of the F.E.A. results with the simpler analytical method, it appears difficult to derive compliance data in stalled modes to a high degree of accuracy, and the iterative technique would be unable to achieve a greater accuracy since the fundamental assumptions concerning uniform stress loading apply to both

methods. For these reasons, a method has been adopted which uses the faster analytic (non-iterative) technique to design and optimise the basic structure.

7.4.1 Method.

The width of the device b can be chosen in accordance with application specific criteria such as whether the device is directly driven from a piezoelectric actuator of given width, or if not, from an existing structure. In the former case a width b value of slightly greater than that of the actuator will be desirable. The materials criteria are discussed in some detail in the chapter on the 'Simple Beam Designer Program' and are not re-iterated here.

The force loading of the structure exhibits rotational symmetry about the centre of the middle member and for this reason the geometry of the two thin flexures is identically maintained. To deviate from this is pointless (whilst perfectly possible) since the overall geometry offers many permutations to arrive at a design specification. Therefore;

$$d_1 = d_3 \quad (= d_{13}) \qquad\qquad l_1 = l_3 \quad (= l_{13}) \tag{138}$$

To simplify computation further, the length parameters l_1, l_2 and l_3 are rewritten as;

$$l_{1,3} = r\, l \qquad\qquad l_2 = (1 - 2r)\, l \tag{139}$$

where r is a tuning parameter, and similarly the relationship;

$$d_2 = w\, d_{1,3} \tag{140}$$

is used. At the core of the designer program is an algorithm which assumes certain data, specifically; the free input displacement x_d, the input drive compliance s_d and the output displacement required of the structure y_o. The input compliances with the output free (mode 1) and the output completely stalled (mode 2) are calculated *dynamically* throughout the program based on the geometry of the present approximation to the solution. Additionally, the core algorithm assumes a particular

length l, and sets the parameter w set to a very high value of 1000. Both these parameters are tuned out later.

The algorithm iteratively attempts to find a value of r which satisfies the relationship;

$$\sigma_f = \sigma_s = n\sigma_y \tag{141}$$

where n is a static safety factor (typically 0.2), σ_y is the yield stress, σ_s is the maximum stalled stress and σ_f is the maximum free stress, by using the relationships;

$$\sigma_s = \frac{x_d}{(s_d + s_{is})\ b\ d_{13} \cos\theta} \tag{142}$$

and;

$$\sigma_f = \frac{x_d\ (d + 3e)}{(s_d + s_{if})\ b\ d_{13}^2} \tag{143}$$

as derived from equations (117) and (118). This is achieved by firstly choosing a value for θ which satisfies the relationship;

$$\tan\theta = \frac{x_d}{y_o}\frac{s_{if}}{(s_d + s_{if})} \tag{144}$$

and then finding a hinge thickness (d_{13}) which satisfies eqn.(142). At this point, if d_{13} should result in being not greater than a lower limit d_{min}, d_{13} is coerced to this value. The purpose of this is to allow the program user to specify a minimum practical machinable hinge thickness.

Once a working value for the hinge thickness has been established, the algorithm iteratively finds a value for r which satisfies the free stress equation, Eqn (143). The aspect ratio of the hinges is also checked to ensure that they are neither too short or long but fall in a range determined by two limiting parameters. If the aspect ratio criterion has to be violated to satisfy the free stress equation, and the user wishes, the program alters the length l until this can be satisfied.

Two operational modes are possible for the determination of l. In one mode, the program chooses the best value for length it can find according to the rules, but this can be suppressed in the other mode. This is useful if designing a bridge to fit into an existing structure of known geometry. At this point a complete geometry has been found except for an acceptable value for w. The user can specify what drop in efficiency can be tolerated in the design, as this is one of the effects of reducing this parameter. The correct value of w is found by iteratively reducing its value until the change in structural efficiency is achieved. The efficiency is defined as;

$$\eta = \frac{Q_{stalled}\, y_o}{k_d x_d^2} \tag{145}$$

A complete listing of the program can be found in Appendix 4.

7.4.2 Program Performance.

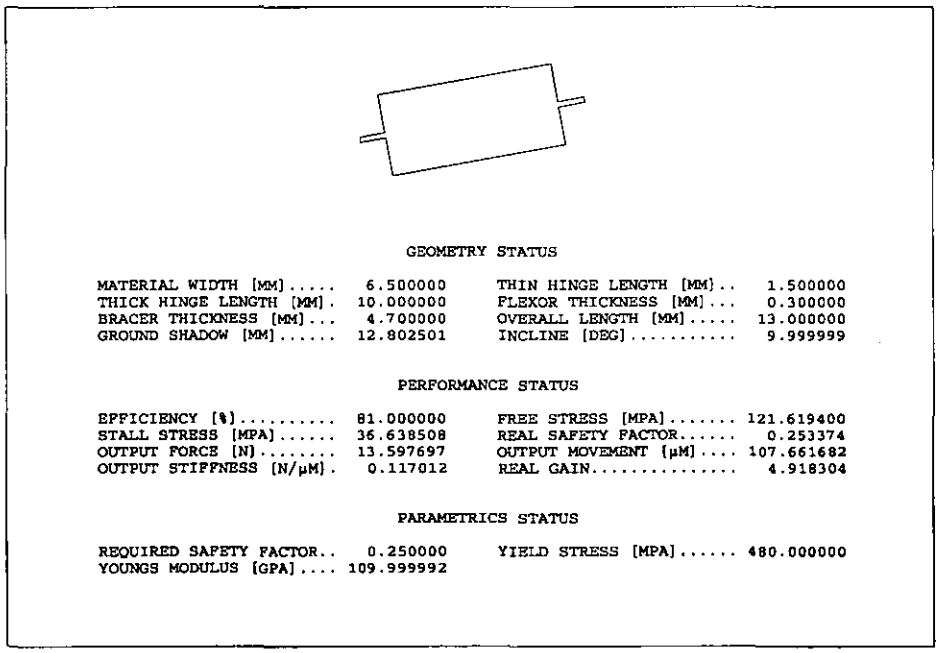

GEOMETRY STATUS

MATERIAL WIDTH [MM].....	6.500000	THIN HINGE LENGTH [MM]..	1.500000
THICK HINGE LENGTH [MM].	10.000000	FLEXOR THICKNESS [MM]...	0.300000
BRACER THICKNESS [MM]...	4.700000	OVERALL LENGTH [MM].....	13.000000
GROUND SHADOW [MM].....	12.802501	INCLINE [DEG].....	9.999999

PERFORMANCE STATUS

EFFICIENCY [%].....	81.000000	FREE STRESS [MPA].....	121.619400
STALL STRESS [MPA].....	36.638508	REAL SAFETY FACTOR.....	0.253374
OUTPUT FORCE [N].....	13.597697	OUTPUT MOVEMENT [μM]....	107.661682
OUTPUT STIFFNESS [N/μM].	0.117012	REAL GAIN.....	4.918304

PARAMETRICS STATUS

REQUIRED SAFETY FACTOR..	0.250000	YIELD STRESS [MPA].....	480.000000
YOUNGS MODULUS [GPA]....	109.999992		

Figure 92: Screen-shot from the Flexure Bridge Designer Program.

Figure 92 shows a typical screen display of the program whilst running an analysis of the geometry of the Strip-Clutch (q.v. section 5 on page 73). The drive data was obtained by partitioning the Finite Element model of the strip clutch and removing the bridge section as shown in Figure 93, and applying appropriate load cases.

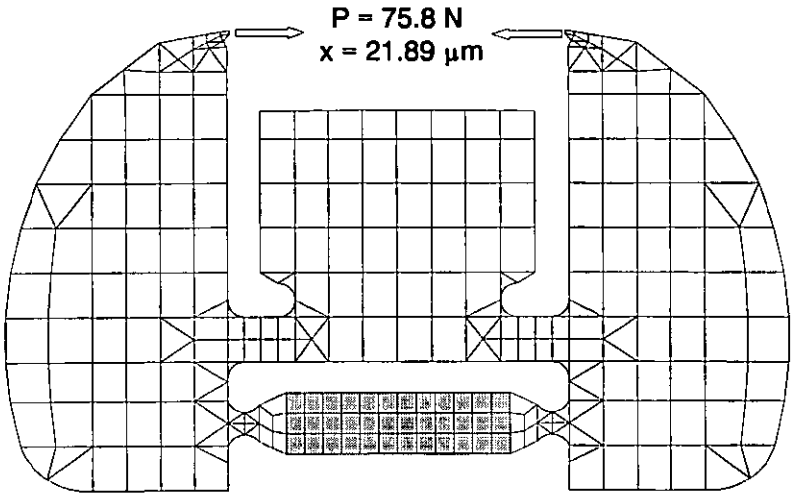

Figure 93: Finite Element Mesh Used to Evaluate Input Parameters.

It is interesting to note that although the detailed geometry was arrived at by trial and error; this has resulted in a sub-structure with a surprisingly good efficiency of 81% (see Figure 92). Table 3 in Chapter 5 shows the principal stress levels attained in the complete strip-clutch, and zones 3 & 4 correspond to the hinges on the bridge. As the modelling method assumes plane stress, the stress levels predicted by the model can be assumed to be in excess of the true values. In the free mode, F.E.A. gives 96 MPa compared with 121 MPa for the program. In stalled mode, the error is much greater as expected, although extremely conservative with the F.E.A. giving 16 MPa and the program 36 MPa. The predictions of output stall force are a little conservative, with the program predicting 27 N (2x 13.5) and F.E.A. estimation and measurement both giving 30 N. Prediction of output displacement is extremely accurate to within 2.5 μm.

Assuming a minimum possible hinge thickness of 0.3 mm, using the program to design the structure rather than simply analyze it, with the overall length constrained

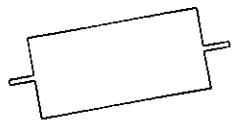

GEOMETRY STATUS

MATERIAL WIDTH [MM].....	6.500000	THIN HINGE LENGTH [MM]..	2.036505
THICK HINGE LENGTH [MM].	8.926991	FLEXOR THICKNESS [MM]...	0.300000
BRACER THICKNESS [MM]...	4.015616	OVERALL LENGTH [MM].....	13.000000
GROUND SHADOW [MM].....	12.800260	INCLINE [DEG].....	10.056721

PERFORMANCE STATUS

EFFICIENCY [%].....	82.000000	FREE STRESS [MPA].....	100.095825
STALL STRESS [MPA].....	36.015102	REAL SAFETY FACTOR.....	0.208533
OUTPUT FORCE [N].....	12.455047	OUTPUT MOVEMENT [μM]....	110.014244
OUTPUT STIFFNESS [N/μM].	0.113213	REAL GAIN.....	5.025776

PARAMETRICS STATUS

REQUIRED SAFETY FACTOR..	0.200000	YIELD STRESS [MPA].....	480.000000
YOUNGS MODULUS [GPA]....	109.999992		

Figure 94: The Program's Design Solution for the 110 μm Amplifier.

to 13 mm, (as would be dictated by the existing structure) the result is a device which is 82% efficient. The program display is shown in Figure 94. It is interesting to note that a lower stressing is obtained by lengthening the hinges to just over 2 mm. Relinquishing the constraint of minimum hinge thickness would have resulted in a 92% efficiency according to the program (not shown).

One of the characteristics of flexure type displacement amplifiers is that sometimes the best possible theoretical solution is at odds with other design criteria such as hinge thickness. In this event a minimum value is set and this can result in a less than optimum stressing [21].

[21] Dissimilar values of stress for each mode.

7.4.3 A Test Case.

It is possible to use this amplifier topology directly with piezoelectric actuators. Although the application of the designer program has shown acceptable correlation with data obtained from the strip-clutch device, it was desired to test the program on an alternate application. As a design example, a NLA 2x3x18 actuator was chosen and used in the general topological solution shown in Figure 95.

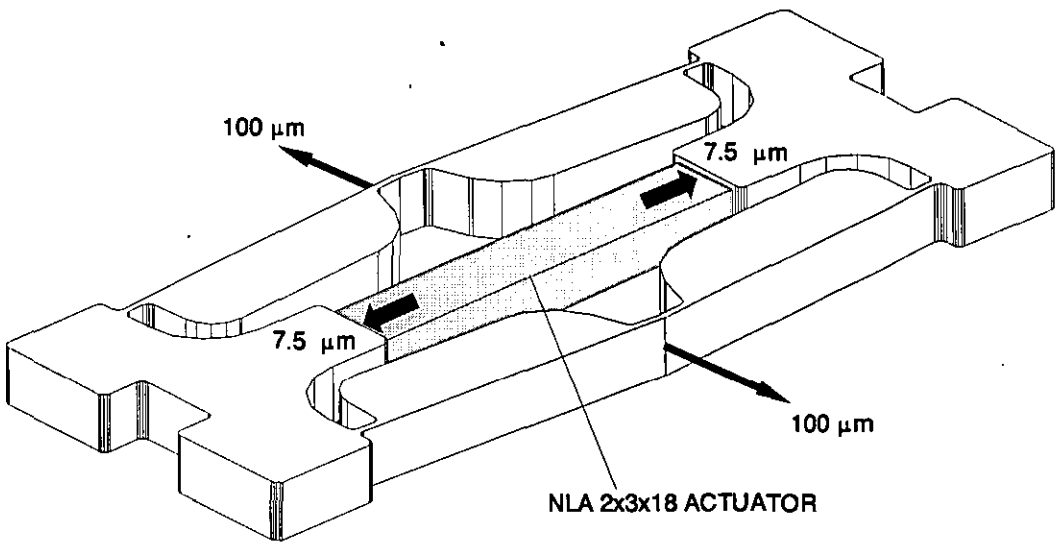

Figure 95: Perspective View of the 100 μm Bilateral Flexure Amplifier.

The pre-load spring assembly is omitted from Figure 95 for clarity, but the arrangement for the assembly can be seen in Plate 7. The device is designed to produce twin (bilateral) output displacements each of 100 μm with a stalled output force of approximately 8 N, derived from an actuator developing only 15 μm of free movement with a stall force of 200 N. Because of device symmetry, each arm of the structure could be considered as being actuated with a 7.5 μm displacement with a stall force of 100 N (half that of the actuator as a whole) for modelling purposes, since this satisfies the condition of total device potential energy (force displacement

product).

The program was run in the first instance with total freedom on the length of the bridge arm, but later constrained to approximately 15 mm since the program initially attempted to find solutions of greater length, which were felt to be less practical. The result is a design which is not as efficient nor as well matched in terms of stall / free stressing, but of an eminently more practical size when taking the actuator dimensions into consideration.

The design of the device is such that the actuator is housed inside the structure. To achieve a compressive pre-load in the actuator, small compression springs (not shown) are mounted inside the central bridge cavities and symmetrically react against the body of the piezoelectric actuator. This places the flexure structures in slight tension.

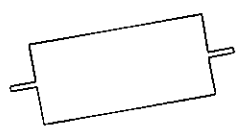

GEOMETRY STATUS

MATERIAL WIDTH [MM].....	2.500000	THIN HINGE LENGTH [MM]..	1.335665
THICK HINGE LENGTH [MM].	12.328672	FLEXOR THICKNESS [MM]...	0.300000
BRACER THICKNESS [MM]...	3.752190	OVERALL LENGTH [MM].....	15.000003
GROUND SHADOW [MM].....	14.963421	INCLINE [DEG].....	4.002327

PERFORMANCE STATUS

EFFICIENCY [%].....	58.000000	FREE STRESS [MPA].....	103.984291
STALL STRESS [MPA].....	84.950630	REAL SAFETY FACTOR.....	0.216634
OUTPUT FORCE [N].....	4.457846	OUTPUT MOVEMENT [μM]....	100.081581
OUTPUT STIFFNESS [N/μM].	0.044542	REAL GAIN.....	13.344212

PARAMETRICS STATUS

REQUIRED SAFETY FACTOR..	0.250000	YIELD STRESS [MPA].....	480.000000
YOUNGS MODULUS [GPA]....	109.999992		

Figure 96: The Constrained Design Solution for the 100 μm Bilateral Amplifier.

As can be seen in the perspective view, the centroids of the flexure hinges and the main arms are non-coaxial. In practice, since the central arm is so torsionally stiff compared to the flexure hinges, this feature can be neglected in the modelling.

7.4.3.1 Finite Element Modelling.

To simplify modelling a model of the idealised structure was used; based on a boundary generated by the program itself. This is shown in Figure 97.

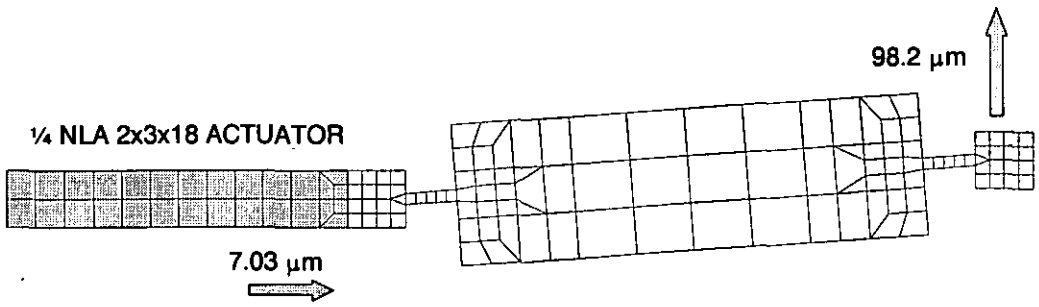

Figure 97: Finite Element Mesh used for Verification.

Also shown in this figure are the output displacement and the effects of structural loading on the extension of the piezoelectric actuator. The static results of the F.E.A. are compared with program predictions in Table 15.

PARAMETER	PREDICTED	F.E.A.	% ERROR
Output Movement	100 μm	98.2 μm	1.8
Output Stall Force	4.45 N	4.01 N	9.9
Max Stall Stress	84.9 MPa	81.9 MPa	3.4
Max Free Stress	103.9 MPa	89.3 MPa	14%
Efficiency	58 %	52.5 %	5.5%

TABLE 15: Comparison of Modelling Performance with F.E.A. for the Bilateral Amplifier.

Agreement between the F.E. model and the program predictions is quite good with most parameters falling within a 10% band except for the free stress estimate which

is conservative.

7.4.3.2 Real Device Performance.

The program is capable of producing a DXF object file, so this was imported into a CAD package and used as the basis for the design as shown in Figure 95. For practical reasons, the design was basically altered in two ways. Firstly, the centroids of the arms and hinges were altered so that the exterior facets of the device were flush. Secondly, the stress bias of the amplifier was reversed to accommodate the actuator between the two arm assemblies. This has consequences as far as stress loading is concerned, particularly in the free extension mode where the tensile loading combines with bending. However, since the bending term is dominant, the overall effect is small and so can be neglected.

The device was manufactured from 2.5 mm thick Titanium (certified U.T.S. >500 MPa) using E.D.M., enabling manufacture of six devices simultaneously.

Measurements carried out on the completed device gave an output displacement of 166 μm for a drive of 100V. It was found by direct measurement however, that under these conditions the actuators were only developing an unloaded displacement of approximately 13 μm, and so the peak drive voltage was elevated to 115 Volts to compensate [22] during further tests. As a result, the total output displacement increased to 184 μm (±92 μm bilaterally). It is believed that this shortfall in free displacement of the actuators was due to the unavoidable additional compliance of the output springs. The total output compliance was measured to be 51 μm/N, compared with the designer program prediction of 44.9 μm/N; a value more consistent with the F.E.A. method at 48.9 μm/N.

[22] This practice could not be recommended in normal circumstances.

A closer inspection of the DXF file used to manufacture a prototype, revealed that due to a programming oversight, the designer program had failed to allow for filletting of the flexure hinges, resulting in an unwanted fore-shortening from 1.3 mm to approximately 0.7 mm. Use of the analysis section of the program to re-check the effect of this, showed a reduction in expected output displacement to ±95 μm.

The fundamental resonant frequency of the free structure was found to be 2.3 kHz, indicating a best free response time of 150 μs, by eqn (6) in chapter 2, but in practice this might be difficult to achieve, and in a clutching application a value approaching double this might be more realistic.

7.5 OBSERVATIONS

Although there are errors in output compliance of the order of 11%, for a simple analytical design approach, the program performs usefully when gains as high as x 13 are required. For the lower gain required in the strip clutch example, accuracy is much better. It has not been possible to directly compare the stress levels occurring within the real device, with those assumed by either F.E.A. or the designer program, however agreement between the F.E.A. and the designer program does promote some confidence in the technique.

Since agreement between the F.E. model and the program for the value of output displacement is quite good (within 2%), it is possible that the poorer performance when comparing data with the real device is due to altering the specific geometry of the design, i.e. shifting the relative positions if the hinge and arm centroids. There may be other factors, but this must remain a subject for investigation for further work.

It is not the purpose of the designer program to offer highly accurate modelling of a given structure, but rather to embody a set of simple design rules to allow the semi-automatic design of such structures by computation. Its accuracy in assessment of stress will always be conservative by virtue of the rigid body assumptions made at the

outset, and therefore must succeed in producing fatigue robust designs *providing* the appropriate safety factor is chosen.

8 PULSE RESPONSE MODELLING.

8.1 INTRODUCTION

As previously discussed, high-speed clutching can be achieved by direct action of a piezoelectric actuator, possibly including an amplifier, or by latching where the actuator is required to alter the physical location of some other latching component. It is possible that for latching applications, the displacements required for the actuator would be larger than for the direct case. It is quite feasible to extend the achievable displacement range by coupling linear amplifiers (such as the simple beam and flexural bridge) together in series, however it is clear that the more gain required, the more massive the amplifying structure must become, and hence slower in response. Additionally, the efficiencies of two 'chained' amplifiers are multiplicative, although it could be argued that for indirect clutching, this is a secondary consideration. Further, to achieve larger displacements approaching 1 mm from a 15 μm displacer using a two stage amplifier, the use of two quite dissimilar materials is necessary, for example a steel first stage followed by an epoxy or carbon fibre second stage. Any attempt to avoid this results in extreme values for the hinge aspect ratios, which can result in a physical tendency to buckle at one extreme, or at either extreme a breakdown of the model theory.

Certain applications require a uni-directional actuation, otherwise known as 'one-shot', and a few applications cited in the bibliography involve the use of piezoelectric actuators in a mode where a component is subjected to short but rapid acceleration by the actuator.

The application of soft piezoelectric multilayer actuators in step or pulse mode operation, rather than in a low frequency linear mode, requires a detailed understanding of the nature of the electromechanical interactions involved. In terms of theory or modelling, many superficially relevant publications are either highly theoretical, and are of little value when it becomes necessary to predict dynamic performance variables such as output displacement and output force for a specific

application, or far too simplistic to be useful when applied to real systems. These variables are critically dependent, not only on the static and dynamic loading characteristics of the device, but on the electrical driving technique employed.

To summarise, during the transient response phase of a step actuation cycle, there is a continuous energy transformation which occurs at very high speed, between electrically stored energy and the development of mechanical stress and strain. This occurs dynamically along the actuator.

Additionally, the literature review conducted at the start of the project revealed applications where a portion of the electrical energy coupled into a piezoelectric actuator, was transformed into the kinetic energy of some other component; specifically the `Printing flight hammer' and the `Green sheet puncher' (q.v.). This principle of energy conversion makes possible the development of actuation systems with relatively long actuation displacements, although it does present difficulties if output work is required. Therefore, this approach lends itself primarily to latching applications where the actuator is not primarily required to do work.

It is important to understand the electro-mechanics of these systems. This chapter concerns the development of a purpose written uniaxial finite element model which deals with the dynamic response of a semi-restrained piezoelectric multilayer actuator, electrically coupled to a drive amplifier through a resistance and inductance. It explores the possibilities of designing an actuator system based on the principle of kinetic energy transfer. In the absence of experimental data, the model is partially verified against simple analytical mechanical models.

8.2 DISCRETE TIME MODELLING.

When a piezoelectric actuator experiences a change in applied potential difference, each slice or element experiences an effectively simultaneous increase in coupling force between its neighbours, since all elements are electrically connected in parallel.

For most of these elements at the instant of electrical change, the `hookean' forces experienced are equal and opposite, except in regions where axial symmetry does not apply, specifically at the free end. For this reason, electrical excitation results in the propagation of displacement and stress waves returning from the free end of the actuator.

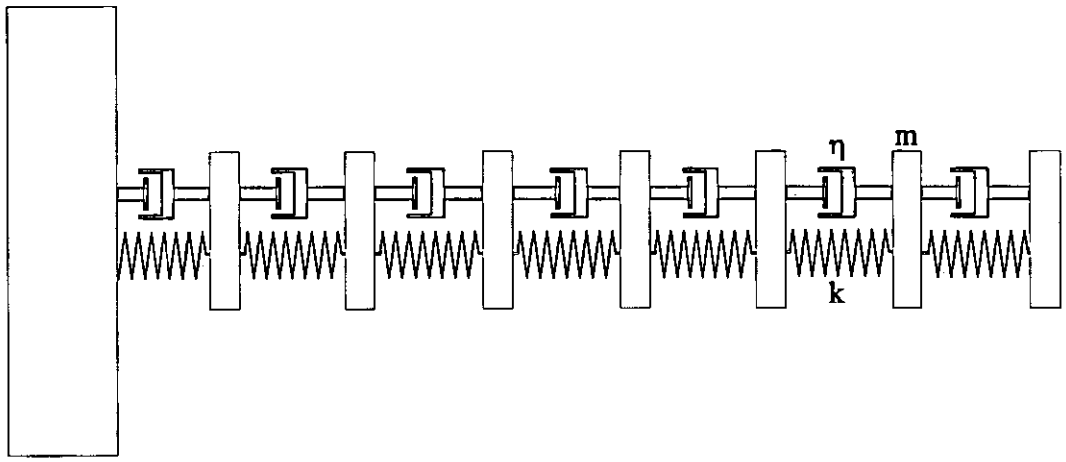

Figure 98: Uniaxial Finite Element Model of a Piezoelectric Multilayer Actuator.

Figure 98 shows a diagram detailing the construction of the model with no external loading. This is a simple model of a multi-element uniaxial structure with second order components of elemental mass m_e, elemental stiffness k_e and elemental damping η_e. Hysteretic behaviour is not modelled since the phenomenon is not fully understood, nor easy to implement in a model of any kind, but is replaced by linear damping for simplicity and model stability. A light damping value, and the time increment between array calculations was arrived at heuristically.

Modelling of the reverse piezoelectric effect is achieved by dynamically altering the rest length l_e of the spring elements according to equation (146);

$$F = k_e \, \delta l_e \tag{146}$$

where δl_e is the instantaneous extension of the element and k_e is the elemental stiffness. The extension is dynamically altered according to the effective voltage applied to the device V_{ce}, which in practice is influenced by a second order low pass filter, the characteristics of which are determined by the electrical drive resistance r_s, the series inductance l_s, and the elemental piezoelectric capacitances c_e.

The strain induced by the applied potential is given by;

$$\varepsilon = \varepsilon_{d33} V_{ce} \tag{147}$$

where ε_{d33} is a coefficient of strain per applied voltage, which for the Tokin NLA 5x5x18 device is 8.33'x10 $^{-6}$. Since each element is strained, the value of δl_e is modified according to;

$$\delta l_e = \varepsilon \, l_e \tag{148}$$

The mechanical interactions of the piezoelectric elements are subtle, but can be considered to be coupled to the electrical circuit by assuming that each element generates a voltage V_{be} in response to any developed direct stress σ_e, according to the relation;

$$V_{be} = \gamma_{d_{33}} \, \sigma_e \tag{149}$$

where the coefficient γ can be related to the value of d_{33}. See Figure 99.

The model is complicated by the effect of the elemental capacitances being mutually coupled in parallel. In reality, the electrical nature of this coupling would be principally resistive via the internal electrodes, although the resistances involved would be very small compared with the drive resistance of the circuit, and so can be ignored. For this reason, there is a phenomenon where stress can longitudinally propagate at much higher speeds along the active axis of the device, than those expected by considering the structure as purely mechanical, and hence limited by the phase velocity of longitudinal stress waves. Since the coupling resistances can be

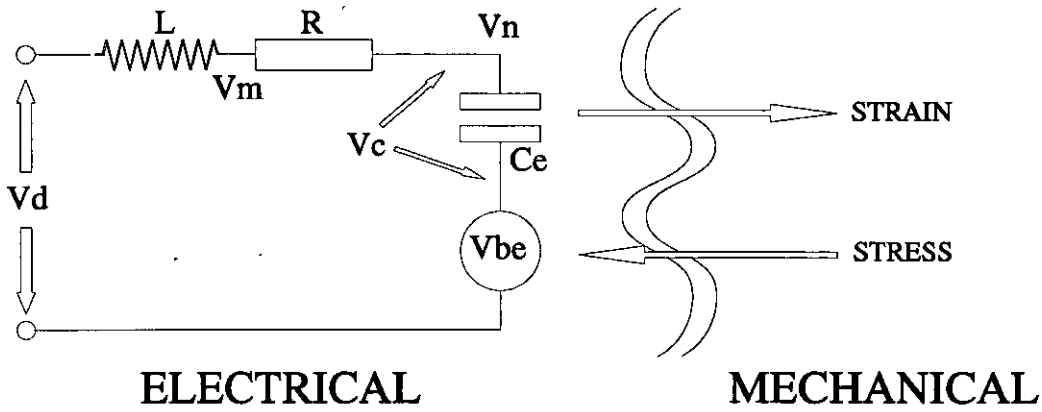

Figure 99: Model of the Electromechanical Interaction of an idealised Piezoelectric Element.

disregarded, the model can be assembled simply and the electrical node at V_n considered to be common to all elements.

The dynamics of each element are considered by calculating the elastic and viscous forces of the element and the adjacent element using positional and velocity data.

Within the program, a target mass was simulated by introducing a 'phantom' element at the free end, of mass m_t which was only capable of sustaining a compressive spring force through a stiffness of k_e (the elemental stiffness), in accordance with a program variable `*contact%*. (For contact to be maintained, the elemental spring force must be positive.) When the spring force falls below zero (tension), contact is lost and where appropriate the phantom element continues inertially, its velocity being relatively slowly reduced by the action of an external restoring force, in practice generated by a spring.

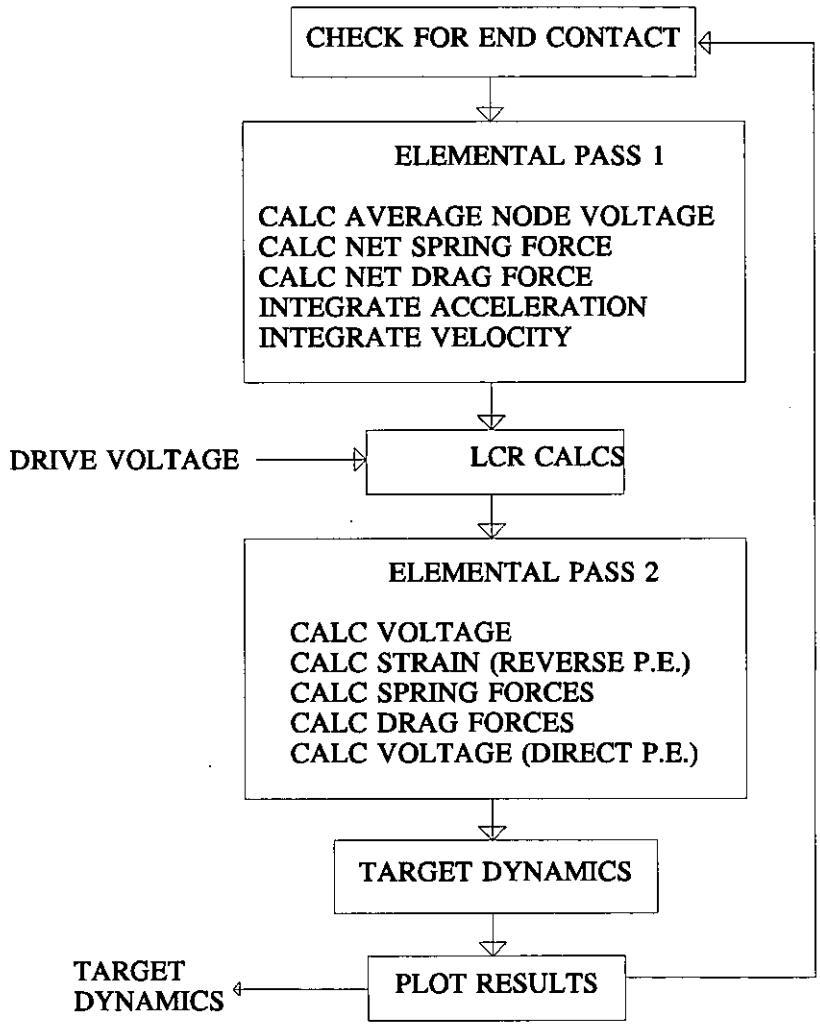

Figure 100: Flow chart for the "Distime" Impulse Response Model.

The structure of the model algorithm is shown in Figure 99 and the main program loop is listed below.

```
INITIALISE

DEFSNG A-Z
   elements% = 25
   elplus% = elements% + 1
   DIM SHARED a.e(elplus%), v.e(elplus%), x.e(elplus%)
   DIM SHARED d.e(elplus%), l.e(elplus%)
   DIM SHARED vc.e(elements%), vb.e(elements%)
   DIM SHARED fk.e(elplus%), fd.e(elplus%)

   REM electrical parameters
   vd.max = 100
   l.s = .0000002#
   r.s = 20

initialise .0001, .01, 6
      i.peak = 0

      REM external target data
      m.t = .0025

      REM piezo statics and dynamics constants
      k.p = 5.694E+07
      l.p = .018
      d.p = 2400
      n.p = 1
      x.max = .000015
      f.max = x.max * k.p
      area.p = .005 * .005
      vol.p = area.p * l.p
      mass.p = d.p * vol.p

      REM piezo electrical constants
      c.p = 1.73E-06 * vol.p / (.005 * .005 * .018)

      REM elemental conversions
      m.e = mass.p / elements%
      k.e = k.p * elements%
      n.e = n.p * elements%
      l.eo = l.p / elements%
      c.e = c.p / elements%

      REM lead wire data
      wire.strands = 50
      wire.rho = 1.7E-08: ' resistivity
      wire.shc = 385: ' specific heat capacity
      wire.dia = .00005: ' wire diameter
      wire.area = wire.strands * pi * wire.dia ^ 2 / 4
      wire.density = 8930
      t.const = wire.rho / wire.density / wire.area ^ 2 / wire.shc
      t.amb = 273 + 25
      t.melt = 1356


      REM electromechanical convertersions
      couple = .5
      vc2d = x.max / elements% / vd.max
      f2vb = couple * vd.max / f.max

      REM temporal initialise
      FOR j% = 1 TO elements%
       a.e(j%) = 0: v.e(j%) = 0: x.e(j%) = j% * l.eo
      NEXT j%
      vn = 0: vm = 0
      REM compensate for end face
      fk.e(elplus%) = 0
      fd.e(elplus%) = 0
```

```
        f.restore = 0: REM spring return force
        contact% = true%
        temp = 0

        acc.t = 0
        v.t = 0
        x.t = 0

        DO
         IF quitflag% THEN EXIT DO

         vd = -vd.max * (time > .0000005)
         adjust "inductance", l.s
         adjust "resistance", r.s

CHECK FOR END CONTACT

         IF contact% THEN
           f.end = k.e * (x.e(elements%) - l.p - x.t)
           REM flash
         ELSE
           f.end = 0
         END IF

ELEMENTAL PASS #1


         REM first pass
         vb.av = 0
         FOR j% = 1 TO elements%
           vb.av = vb.av + vb.e(j%) : REM AVERAGE NODE VOLTAGE
           f.spring = fk.e(j%) - fk.e(j% + 1) : REM NET SPRING FORCE
           f.drag = fd.e(j%) - fd.e(j% + 1) : NET DRAG FORCE
           IF j% = elements% THEN : REM LAST ELEMENT ONLY
              acc = (f.spring + f.drag - f.end - f.restore) / m.e
           ELSE
              acc = (f.spring + f.drag) / m.e
           END IF

           v.e(j%) = v.e(j%) + acc * delt : REM INTEGRATE ACCELERATION
           x.e(j%) = x.e(j%) + v.e(j%) * delt :  REM INTEGRATE VELOCITY
         NEXT j%
         vb.av = vb.av / elements% : NODE VOLTAGE AVERAGE
         contact% = (f.end >= 0 AND x.t <= (x.e(elements%) - l.p))

         REM external electricals : LCR CALCULATIONS
         i = integ(vd - vm, time) / l.s
         REM IF temp + t.amb > t.melt THEN i = 0: ' wires melted
         sit = integrate(i, time, 0, 0, (time < .0000005)) / c.p
         vn = sit + vb.av
         vm = vn + i * r.s

         IF i > i.peak THEN i.peak = i : REM LOG LARGEST CURRENT EVER

ELEMENTAL PASS #2

         REM second pass
         FOR j% = 1 TO elements%
           vc.e(j%) = vn - vb.e(j%) : CALC INDIVIDUAL VOLTAGE
           l.e(j%) = l.eo + vc.e(j%) * vc2d: ' DESIRED REST LENGTH
           sep.e = x.e(j%) - x.e(j% - 1): ' SEPARATION
           fk.e(j%) = k.e * (l.e(j%) - sep.e): ' SPRING FORCE
           fd.e(j%) = n.e * (v.e(j% - 1) - v.e(j%)): ' DRAG FORCE
           vb.e(j%) = f2vb * fk.e(j%) : ' DIRECT PIEZO EFFECT
         NEXT j%

         REM TARGET DYNAMICS
```

```
        acc.t = (f.end - f.restore) / m.t
        v.t = v.t + acc.t * delt
        x.t = x.t + v.t * delt

      face.disp = x.e(elements%) - l.p
      face.vel = v.e(elements%)

      REM thermal calcs

      t.partial = integ(i ^ 2, time)
      temp = t.partial * t.const
      x.end = (x.e(elements% - 1) - l.p * (elements% - 1) /
elements%)

      plot vn, 1.5 * vd.max, "vn", "###.#"
      plot i, 20, "current", "+###.#"
      plot 1000000! * face.disp, 20, "xface " + micron$, "+##.#"
      plot 1000000! * x.end, 20, "end face", ""
      plot v.t, 5, "vt m/s", "+#.###"
      plot i.peak, 10, "ipeak", ""
     LOOP
END
```

8.3 MODEL APPLICATION.

There are several independent variables to be considered, specifically target mass m_t, series resistance r_s and series inductance l_s. It can be assumed that the applied step voltage (d.c.) to the device will be +100 V, in accordance with manufacturer's recommendations, and that the device capacitance c_p is fixed. Further, the switching speed of the semi-conductor drivers is assumed to be negligible and switch saturation is not considered separately, but is included in r_s.

On first inspection it would seem logical for r_s to be minimised to reduce the time taken for full extension of the actuator to be realised. If this value were reduced to 1Ω for example, with a near zero series inductance, the maximum inrush current could theoretically be 100 A, which is clearly undesirable with regard to current stressing of the internal electrodes, and particularly, the device leads and drive system. Alternately, if r_s is too high, the actuator response will be too slow for any appreciable acceleration forces to develop, resulting in a poor transfer of energy (kinetic) into the target. The inclusion of a series inductance is beneficial in that it facilitates a limit on the maximum rate of change of current in the circuit, and therefore a maximum dynamic current level. A typical set of traces produced by the

model are shown in Figure 101.

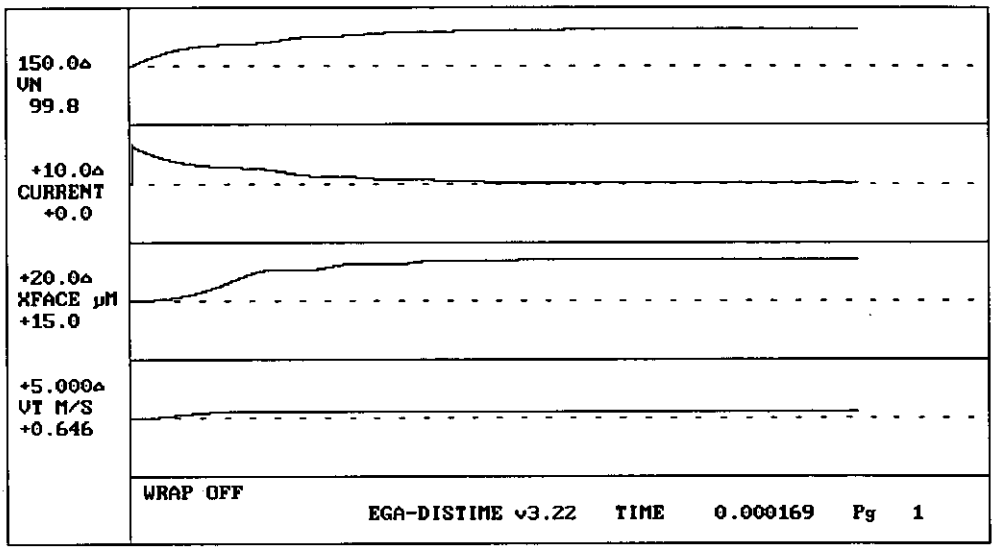

Figure 101: A Typical Set of Traces produced by the 'Distime' Impulse Model.

Whilst it is possible to study the behaviour of the model without consideration of a real application, the establishment of an objective specification is useful. Since fast actuation is seen as one of the principle advantages of employing piezoelectric actuators, an actuation time of 1 ms or less is an appropriate target since this value is faster than most solenoid type actuators available. An actuation range of 2 mm at this speed would be optimistic for a linear amplifying device (as discussed elsewhere in this thesis), but to achieve this by piezoelectric means would be of value.

The mass of the target is as yet an undefined parameter in this model. Series resistance and inductance are two further variables. To enable a sensible choice of actuator and target mass independently of the electrical drive parameters, a simple theoretical model was used to estimate the maximum possible departure velocities, based on the maximum work possible from each actuator. It can be shown that for an actuator of length l, area A and an elastic modulus E, generating a free displacement x_d, the maximum possible energy transfer into a free mass is;

$$E_{max} = \frac{EAx_d^2}{2l} \tag{150}$$

and since all actuators in a given family can develop an equal maximum strain (ε_{max}) across the device range, the maximum possible target velocity is given by;

$$v_{max} = \varepsilon_{max}\sqrt{\frac{EAl}{m}} \tag{151}$$

Note that the product 'Al' is the device volume. The results of this analysis are shown in Figure 102, and it can be seen that only the actuators with larger cross sectional areas are sufficiently energetic to produce velocities of 2 ms^{-1} or greater for the range of masses tried. The NLA 5x5x18 was chosen as the device on which to base further modelling since this appears capable of achieving this velocity with target masses up to approximately 3.1 g.

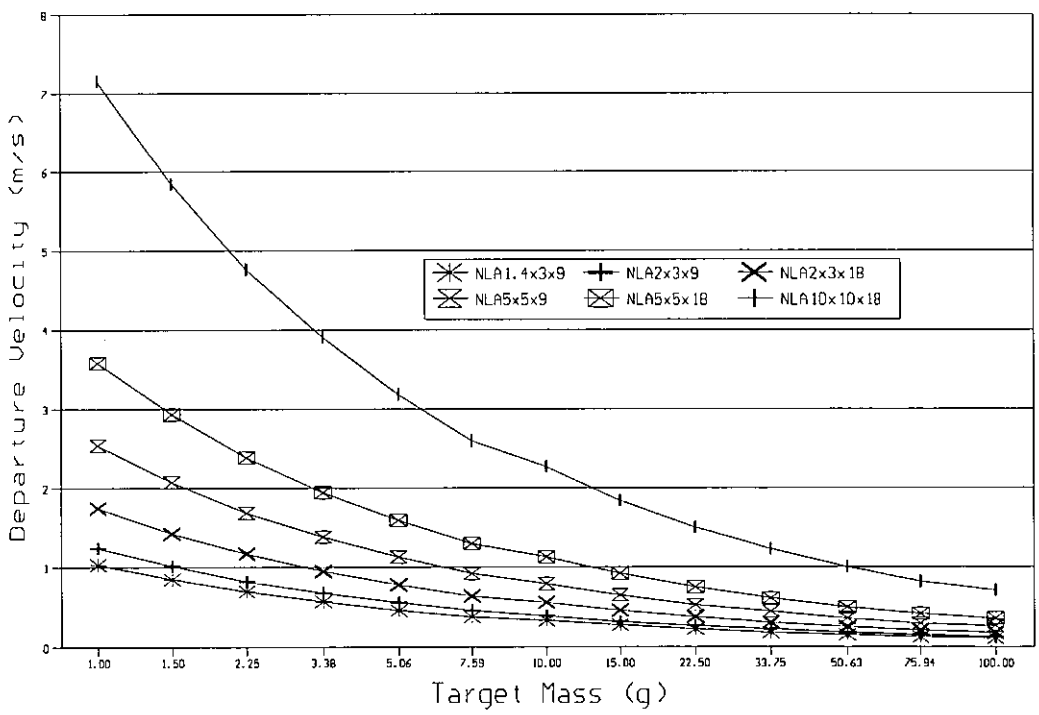

Figure 102: Maximum Theoretical Departure Velocities.

It must be remembered that the higher target velocities (lower masses) can not be achieved in practice with the mechanical system as described, due to simple mechanical laws. Considering two particles undergoing elastic collision, it is not

possible for a previously stationary particle to depart from a collision with a velocity of greater than twice the velocity of the incoming particle. For this reason it is difficult to see how the target mass can achieve higher velocities than those appearing at the end face of the piezoelectric actuator. This limit can be surpassed by matching the energy transfer process by means of an intermediate component (such as a reverse 'horn' where a strain pulse travels down a waveguide of decreasing cross section, finally developing an intense strain pulse at the output termination of the horn), as shown in Figure 103.

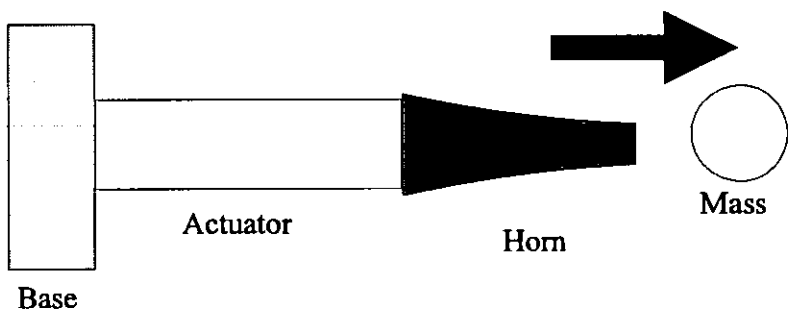

Figure 103: The use of a Matching Component for Impulse Transfer.

To model analytically the maximum velocity achievable, encompassing the electro-mechanical interaction of the actuator is highly complex. It can be approximated more simply by considering the piezoelectric actuator as a simple second order system undergoing a displacement perturbation at one end.

Considering the model in Figure 104, and assuming that the mass of the actuator (m_a) and the target (m_t) are combined into an effective mass (m_e) as ;

$$m_e = m_t + \frac{m_a}{2} \qquad \textbf{(152)}$$

during the acceleration phase of contact, the equation of state of the system under the influence of a step drive (zero electrical delays) is given by;

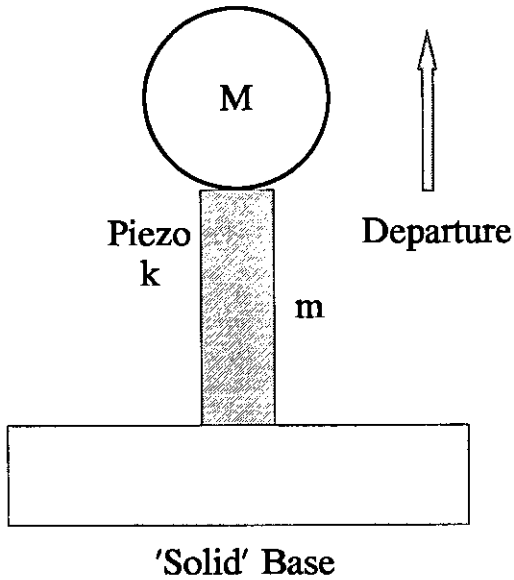

Figure 104: Simple Velocity Limit Model for the Impulse Actuator.

$$m_e \frac{d^2y}{dt^2} + \eta \frac{dy}{dt} + ky = kx\ H(t) \qquad \textbf{(153)}$$

where H(t) is the unit step function, x is the steady state change in actuator length, y is the displacement of the actuator, k is the actuator stiffness and η is a damping term. This solves for the step function H(0) as;

$$y = x\ (1 - e^{-\alpha t} \cos\omega t) \qquad \textbf{(154)}$$

where;

$$\alpha = \frac{\eta}{2m} \qquad \omega = \sqrt{\frac{k}{m} - \frac{\eta^2}{4m^2}} \qquad \textbf{(155)}$$

and therefore the velocity is;

$$v_y = x\ e^{-\alpha t}\ (\alpha \cos\omega t + \omega \sin\omega t) \qquad \textbf{(156)}$$

It can be shown that this has a maximum value when;

$$t = \frac{1}{\omega}\tan^{-1}\left(\frac{\omega^2-\alpha^2}{2\omega\alpha}\right) \tag{157}$$

Typically, the damping term will be less significant than the harmonic term. Oscillatory solutions to Eqn. (153), can only exist for damping values in the range;

$$0 \le \eta \le 2\sqrt{mk} \tag{158}$$

which guarantees solutions for velocity over a limited range. The velocity behaviour of this system is illustrated in Figure 105.

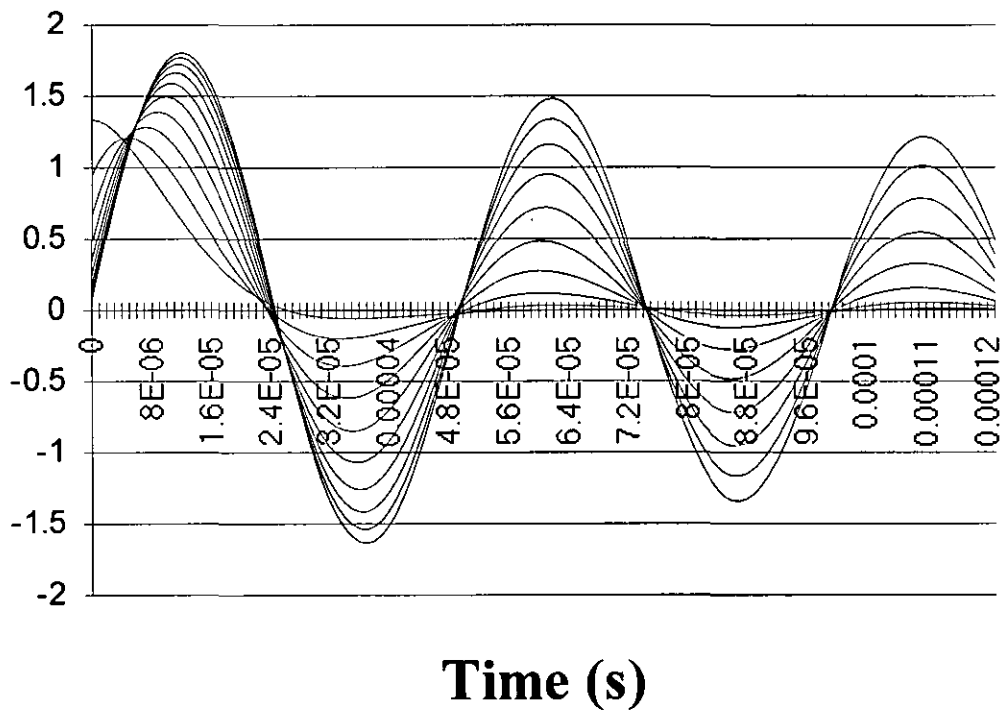

Figure 105: Impulse Response Predicted by Simple Analytical Second Order Model.

The maximum velocities obtained for various values of damping ratios are shown in Figure 106, where damping ratio is defined as;

$$X = \frac{\eta}{2\sqrt{mk}} \tag{159}$$

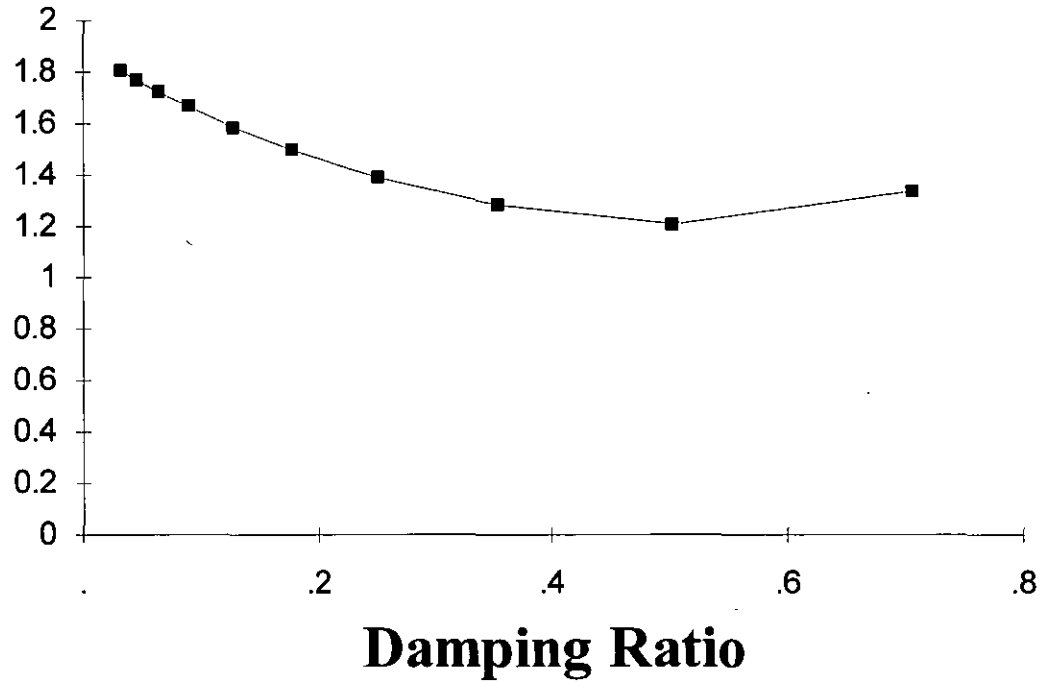

Figure 106: Maximum End Face Velocities for the NLA 5x5x18 Actuator (Analytical).

As can be seen, the maximum velocity attained for the same actuator with a 2.5 g mass is approximately 1.8 ms^{-1}, which agrees very well with the data in Figure 107.

Using the NLA 5x5x18 actuator specification in the finite element model, various masses and series resistance combinations were tried. The approach adopted, was one where the series inductance was initially kept to a minimum practical value and had little apparent effect on the mechanical and current surge characteristics; $l_s = 0.1$ μH was found to be satisfactory. Additionally, the only way to simulate a step drive function was to drive the actuator through a very low value of resistance and inductance. Variation of the inductance around the nominal value had no measurable effect on any of the departure velocities of the target mass. The results of these variations in mass and series resistance are shown in Figure 107.

As might be expected, the results show a general trend of increasing velocity with decreasing drive resistance and decreasing mass. It is interesting to note that with

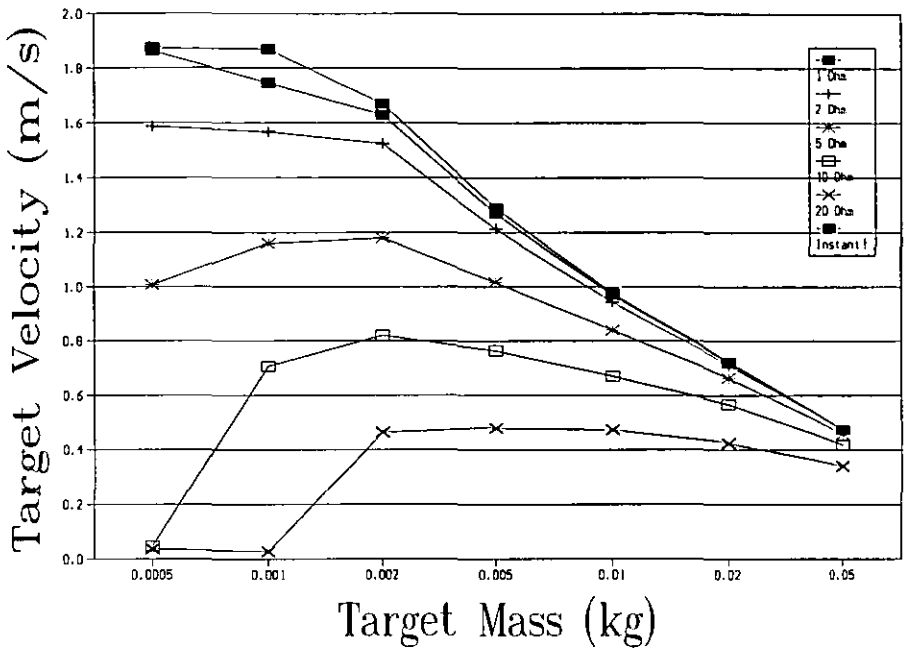

Figure 107: Departure Velocities Predicted by the 'Distime' Model for Differing Values of Series Resistance .

masses above approximately 5 g, the trend resembles that of Figure 102, but below this value, the limitation caused by the finite end face velocity becomes dominant. Additionally, with lower masses and larger resistances, 'kissing' occurs between the actuator and the target, and contact between the two is intermittent. The model only takes the first sustainable contact between the mass and the actuator into account, so these values may be artificially low, particularly in the cases with a 20 Ω series resistance and masses below 2g.. It is clear however, that a velocity of 2 ms^{-1} is almost achievable according to the model, and so far this is in approximate agreement with predictions made by the simplistic energy method as described by Eqn. (151). This adds some weight to the reliability of the model in the absence of any experimental data, however the effect of having a negligible value of series inductance is unclear from the data presented so far.

All of the model tests so far have been with the series inductance set to a low enough value to ensure no effect. Selecting a target mass of 2.5 g, a series resistance in the

range of 0.1 Ω to 10 Ω and a series inductance in the range of 0.1 μH to 100 μH, and evaluating the performance of the device reveals the possibility of tuning the response by altering the series inductance and resistance, whilst reducing the peak current. The peak currents for differing departure velocities are shown in Figure 108.

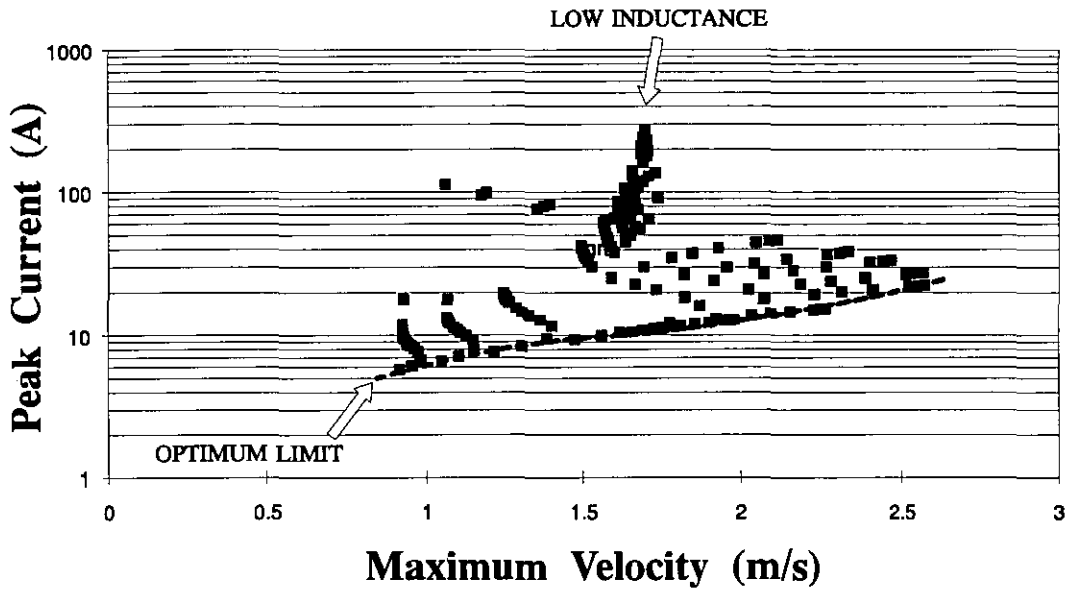

Figure 108: Scatter Graph of Peak Currents against Maximum Velocity.

One of the interesting features of this scatter graph is that the highest energy coupling or greatest velocity is not achieved with the highest peak (inrush) current. The asymptote drawn on the graph delimits the minimum inrush current for any particular velocity. At the end of the curve, are velocities in excess of 2.5 ms^{-1}, which clearly indicates that selection of the component values in the drive system is vital if best performance is required. For completeness, the entire set of velocity data produced by the model are shown in Figure 109.

The pseudo-3D representation is useful in that the response peak is easily identified. Peak response occurs for the lowest resistance value of 0.1 Ω, but for a series inductance of 22.5 μH, achieving a velocity in excess of 2.5 ms^{-1}. The shape of the curves in Figure 109 indicates a variable 'Q' resonant electromechanical system as would be expected. Since the electrical values were selected on the basis of a

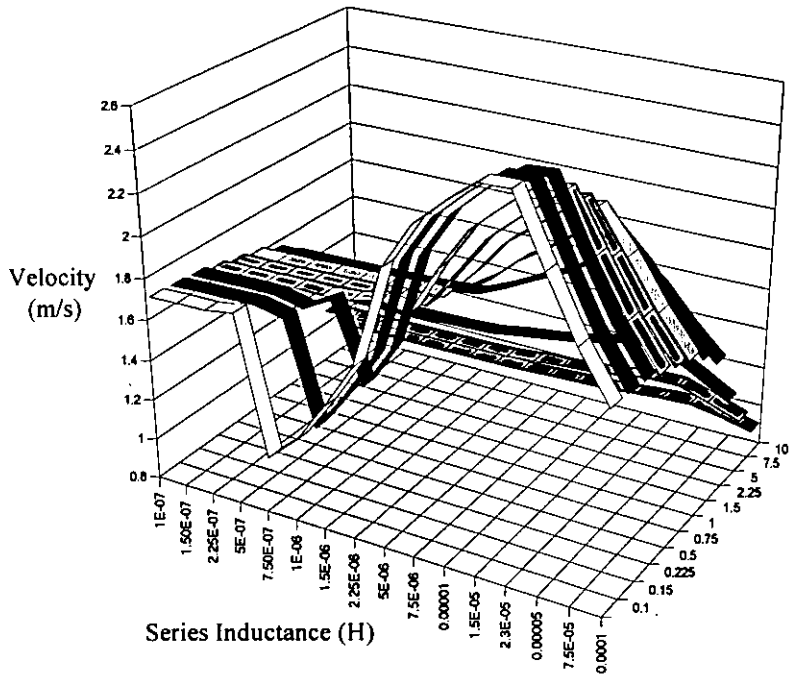

Figure 109: Graph showing the Dependence of Velocity on Series Resistance and Inductance.

convenient logarithmic progression within the model, the precise peak in performance was determined by successive bisection from which the best inductance was found to be 19 μH. The effect of series resistance for this value of inductance is shown in Figure 110.

The most interesting (and unexpected) result is that shown in Figure 111, showing the almost linear relationship between velocity and peak inrush current.

To achieve a velocity of 2 ms^{-1} would demand an inrush current of approximately 17 A, using a series resistance of 1.5 Ω

8.4 OBSERVATIONS

The model presented predicts departure velocities for ballistic masses. The predictions it makes have not been experimentally verified, however, agreement with simple second order mechanical theory does support their validity. In view of the over

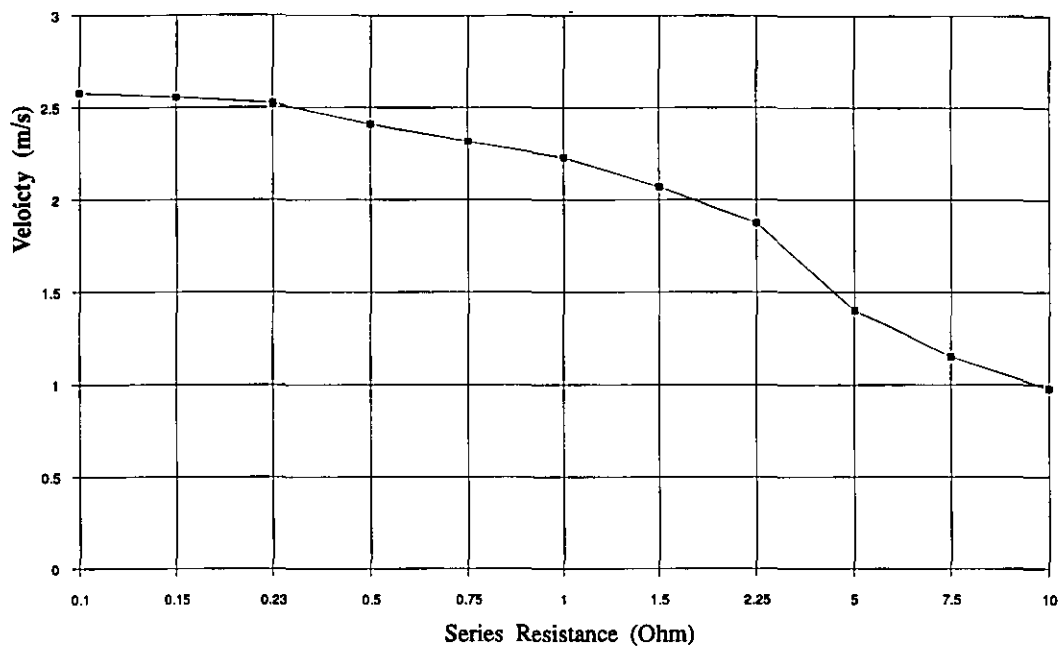

Figure 110: Relationship between Velocity and Series Resistance for Inductance of 22.5 μH.

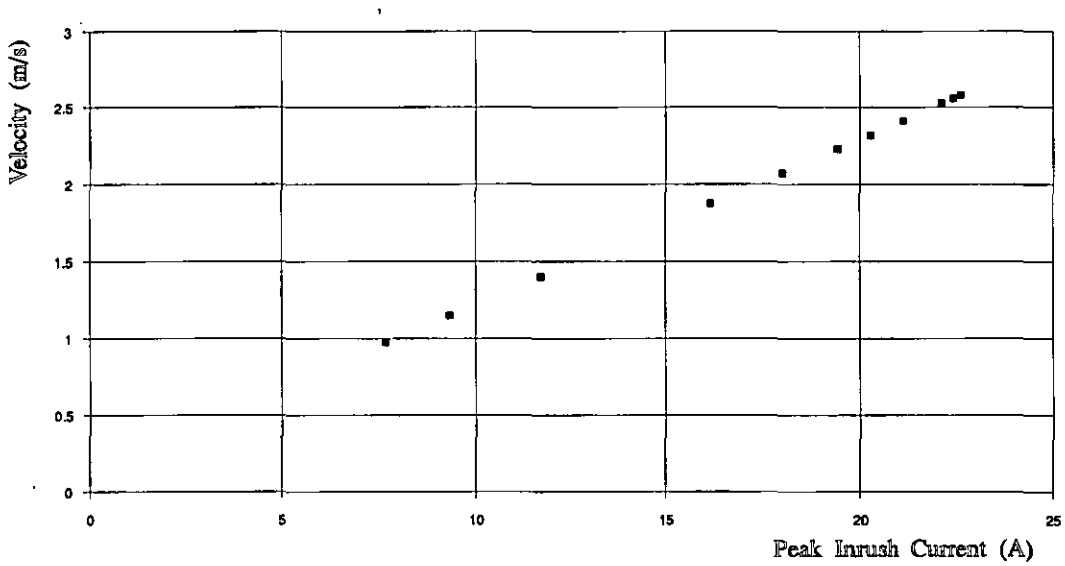

Figure 111: Relationship between Velocity and Peak Inrush Current.

simplification of the analytical model, i.e., the disregard for the electromechanical interaction during the expansion phase of actuation, some credibility can be given to the result obtained by the uniaxial F.E. model.

Further, as might have been expected, the selection of an appropriate series inductor and hence the alteration of the electrical resonant frequency of the system, can facilitate an improved energy match into the target, relative to that which can be expected by simply stimulating the device with a step waveform. There is also a significant improvement in peak inrush current. For a practical system, it is unfortunate that there is a requirement for large current pulses, although a typical peak value of 17 A is sustained for only a few microseconds. In practice, this may be tolerated quite well by the actuator, but places a demand on the drive electronics for high current capability and low on-state resistance drive transistors (FET's etc.).

The finite element model adds credibility to the assertion that a very simple type of impulse type actuator producing similar velocities is feasible without the matching component. In the context of this thesis, this work supports another method of achieving high-speed actuation, with displacements in the range of 1 to 2 mm and response times of approximately 1 ms. This approach could lead to the development of a fast latching actuator, suitable for high-speed clutching.

9 APPLICATIONS.

Chapters 6 and 7 describe how designs for simple beam and flexural bridge displacement amplifiers can be achieved. This chapter describes two machines which exemplify discrete motion control using piezoelectric actuators with these types of amplifying structures. The first is a linear discrete motion controller in which a small carriage derives linear step motion from a rotating shaft, using displacement-amplifying piezoelectric clutches. The clutch elements used are those described in chapter 5. The second machine can be described as a rotary micropositioner which controls the angular position of a test specimen by the use of a piezoelectric pusher and amplifying clutching devices as described in chapter 6.

9.1 A PIEZOELECTRICALLY CONTROLLED DISCRETE-MOTION MACHINE.

The successful development of a piezoelectrically driven strip-clutching element has facilitated the design of a discrete motion machine, which derives its quantised linear motion from a rotary shaft, coupled through a cycloidal cam. The concept of this machine, detailed in this section, was originally the parent of the strip clutch actuator; the device necessary to make this concept possible. Part of this chapter details much of the design work that was necessary to take the concept of this machine to a working prototype and make a basic evaluation.

9.1.1 Basic Design.

Figure 112 shows a schematic layout of the basic machine. A pair of thin metal strips, held in tension between two rockers, are forced to reciprocate in a manner dictated by the profile of the rotating slot cam. This is achieved by driving the input shaft from a 200W d.c. variable speed motor. The slot cam is profiled to generate reciprocation with two 40° dwell zones at the extremes of displacement, with a cycloidal profile in the transition zones. The lower strip passes through the clutch gap of the upper piezo-

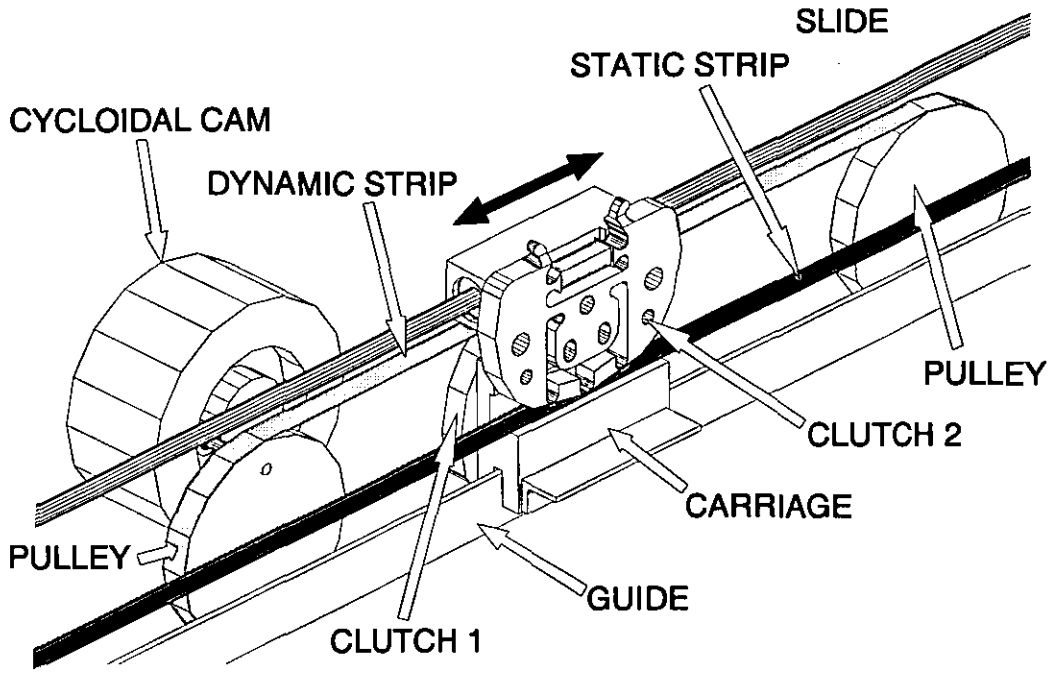

Figure 112: Mechanical Layout for the Discrete Motion Machine.

clutch and is responsible for the motion of the output shaft when engaged. The lower clutch is responsible for holding the output shaft stationary when the moving strip is not travelling in the desired output direction. The cam is interchangeable to facilitate alternate strokes.

9.1.2 Design Considerations.

9.1.2.1 Clutch Face.

One major consideration associated with clutching in this application, is the kinematics of the clutch and the strip, and particularly the way in which the strip is compressed against the anvil by the actuator. In practice, it is impossible to machine two faces to perfect parallelism to ensure an even pressure distribution, thus avoiding point stressing. Additionally, there is curvature in the design of the output section of the clutching element, so to accommodate this and to compensate for mis-alignments

elsewhere, two degrees of freedom have been introduced within the anvil. The nature of these freedoms is shown in Figure 113.

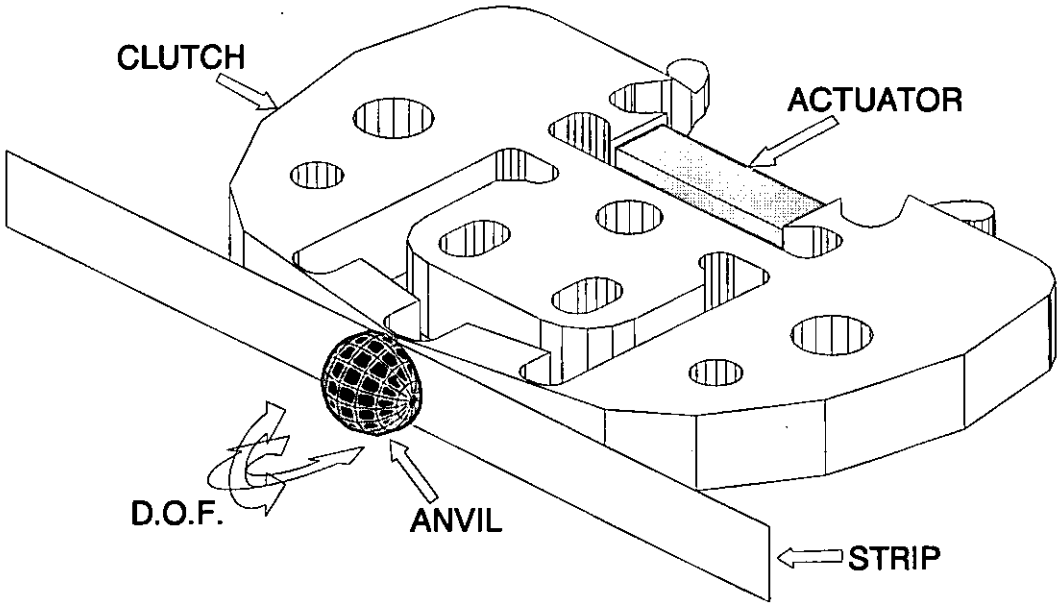

Figure 113: View of the Clutch and Anvil Arrangement.

9.1.2.2 Clutching Energy Loss.

To derive an oscillating linear motion (which is derived from constant rotary motion) of a component must inevitably involve some type of time varying coupling or clutching. This can occur by transfer processes such as impulse, ratchetting or direct friction. In this application, integration into linear motion is achieved by generating reciprocating motion in a mechanical component along one axis, and clutching on to this component at appropriate times.

The ideal time for clutching to occur is at a time when the relative velocity of the clutching elements is equal to or very nearly zero. This equality only occurs instantaneously as shown in Figure 114, and therefore the speed and repeatability of response of the clutching actuator are primary, for the reason that when two bodies

with initially differing velocities are forced together, energy is dissipated. The energy is dissipated through a complex process involving strain energy, heat, vibration (including acoustic noise) and therefore wear.

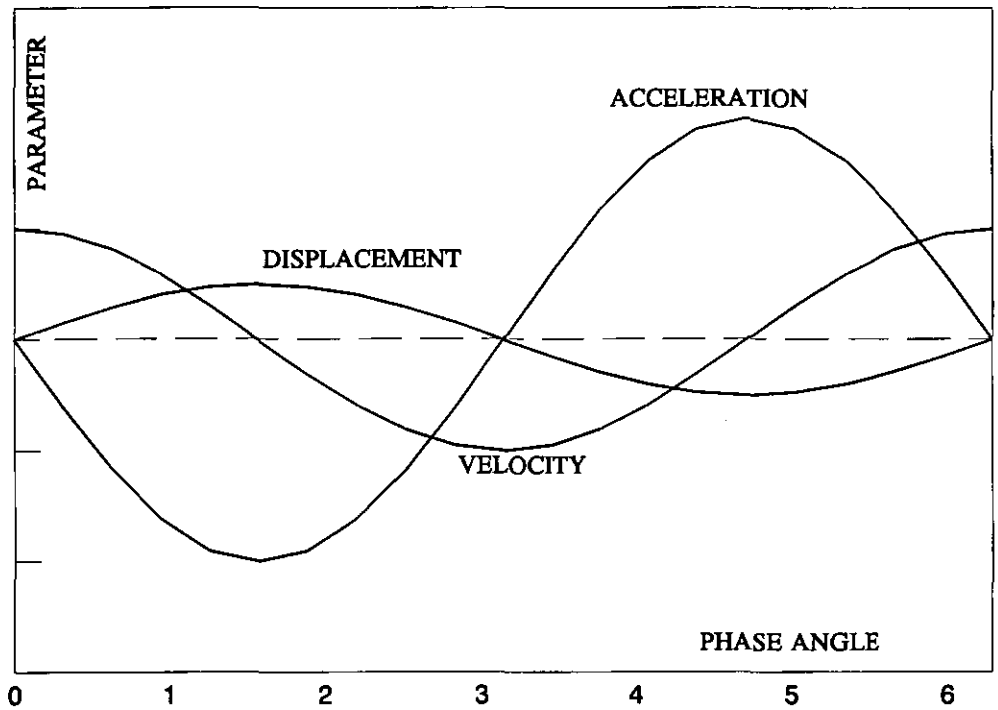

Figure 114: Displacement, Velocity and Acceleration experienced by a component undergoing Simple Harmonic Motion.

The amount of energy that can be lost in the collision process can be simply estimated in the following way. Figure 115 shows a simple model which can be used to evaluate clutching loss, by relating the work done by a large translating mass grabbing a small initially static mass m, through a viscous damper η.

Assuming the collision begins at t = 0, the equation of motion is given by;

$$m\,\dot{v} + \eta(v - v_a) = 0 \qquad \textbf{(160)}$$

which solves for v as;

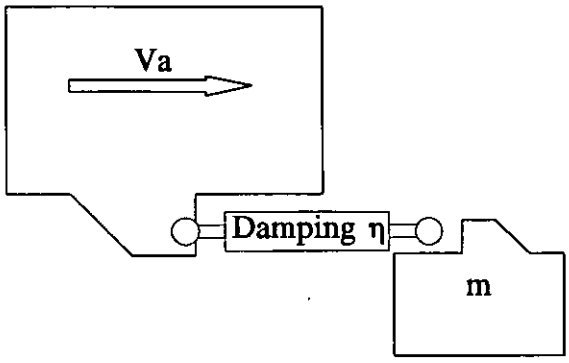

Figure 115: In-elastic collision model.

$$v = v_a\left(1 - e^{-\frac{\eta}{m}t}\right) \tag{161}$$

The force exerted by the large mass is given by;

$$f = m\,\dot{v} = \eta v_a\, e^{-\frac{\eta}{m}t} \tag{162}$$

Now the kinetic energy acquired by mass m is given by;

$$E_k = \int_0^\infty f\,dx = \int_0^\infty f\,v\,dt \tag{163}$$

Which solves as expected;

$$E_k = \frac{mV_a^2}{2} \tag{164}$$

But the work done by the large mass is given by;

$$E_{WD} = \int_0^\infty f v_a\,dt = m v_a^2 \tag{165}$$

Thus implying that the work done by the large mass is precisely *twice* that of the kinetic energy acquired by the small mass. This result emphasises a desirable feature of clutching at near-zero relative velocity.

In a real system, this is seldom possible. However, the machine described here has been designed using a cam with two 40° dwell zones, so that providing clutching occurs within these zones, zero clutching velocity is guaranteed and wear is only possible by shearing under excessive translational loading (see section 9.1.2.3), fretting or trapping particles.

In a system where the clutching speed is instantaneously zero, and reciprocation can be approximated to being harmonic, the following analysis can be applied.

Consider a reciprocating component oscillating at angular frequency ω, with amplitude a. The clutch will be actuated so that collision will occur when the velocity is zero, but there will be uncertainty in clutching time Δt. The rate of change of velocity with time will be given by;

$$\left|\frac{dv}{dt}\right| = a\omega^2 \qquad \textbf{(166)}$$

and therefore the lateral collision velocity will be approximately;

$$v_c = a\omega^2\Delta t \qquad \textbf{(167)}$$

Therefore the kinetic energy dissipated during the collision will be given by;

$$E_c = \frac{mv_c^2}{2} = \frac{ma^2\omega^4(\Delta t)^2}{2} \qquad \textbf{(168)}$$

Although this is a simplistic approach, it gives an indication of the relative importance of the parameters associated in clutching, when attempting to minimise clutching energy loss and therefore factors such as wear and acoustic emission.

9.1.2.3 Inertial Loading.

The maximum sustainable inertial load for the clutch can be determined from the clutch force f_c, the coefficient of static friction μ, cam angular frequency ω_0 and the cam rise / fall amplitude 2a, and for a simple harmonic cam is given by;

$$m_{max} = \frac{\mu f_c}{2a\omega_0^2} \tag{169}$$

since the maximum acceleration of the cam is given by;

$$\left|\frac{d^2x}{dt^2}\right| = a\omega_0^2 \tag{170}$$

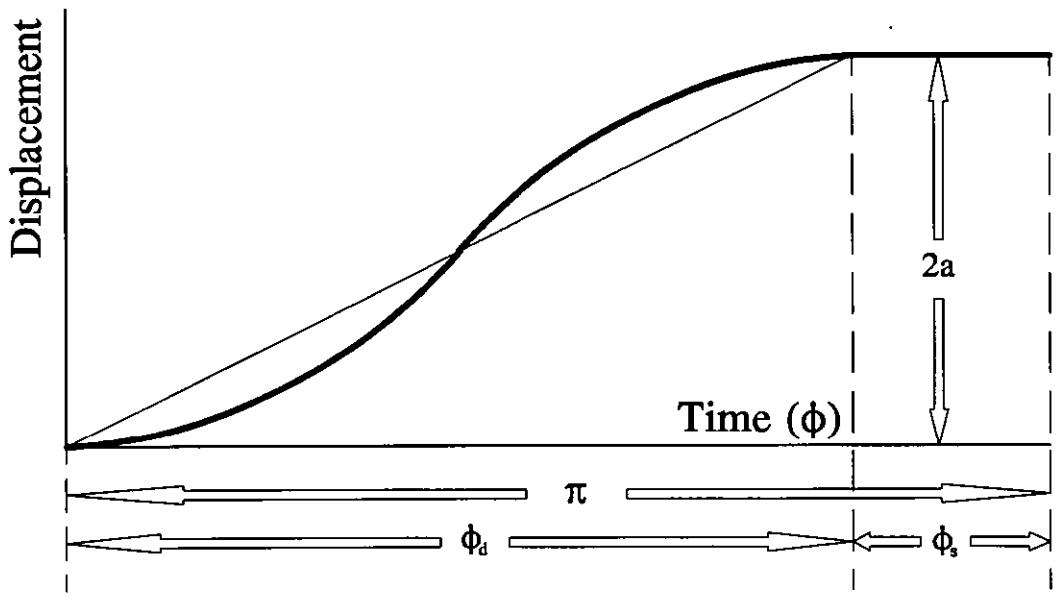

Figure 116: Lift profile for a cycloidal cam with dwell.

For a cycloidal cam with dwell, with a characteristic lift profile as shown in Figure 116, the situation is complicated by the existence of a dwell angle d° which occurs twice per cam revolution. Additionally, the harmonic component of the displacement is altered, since a harmonic term is subtracted from an otherwise linear ramp up, as given by;

$$x = \frac{2at}{t_c} - \frac{a}{\pi}\sin(\omega_c t) \tag{171}$$

where;

$$\omega_c = \omega_0 \left[1 + \frac{d}{(180 - d)}\right] \tag{172}$$

The maximum acceleration is therefore given by;

$$\left|\frac{d^2x}{dt^2}\right| = \frac{a\omega_c^2}{\pi} = \frac{4a\omega_0^2}{\pi}\left[1 + \frac{d}{(180 - d)}\right]^2 \tag{173}$$

Notice that in the limit of $d \rightarrow 0$, equations (170) and (173) are unequal.

9.1.2.4 Inertial Load Limit.

The mass of the clutch assembly, comprising the two strip-clutches, the carriage and the output arm, totals 0.149 kg. The clutches are designed to be used in an alignment where 0.5 (k) of the free movement is the operational clearance of the device, and therefore a 15N clutch force can be expected as a maximum. Using a coefficient of static friction $\mu = 0.35$, the maximum slew force sustainable by the carriage is therefore 5.25N. Algebraically;

$$F_{max} = F_c k \mu \tag{174}$$

Equating expressions (173) and (174);

$$\frac{F_c k \mu}{m} = \ddot{x}_{max} = \frac{4a\omega_0^2}{\pi}\left[1 + \frac{d}{(180 - d)}\right]^2 \tag{175}$$

therefore, the maximum angular frequency before the onset of clutch slippage will be given by;

$$\omega_0 = \left(1 - \frac{d}{180}\right)\sqrt{\frac{\pi \mu F_c k}{4ma}} \tag{176}$$

For an amplitude of $2a = 0.001$ (metre), this equates approximately to 186 rad s^{-1}, or 1770 rev/min. In practice, this value may not be achieved, since misalignments in the mechanism cause friction between the clutch assembly and the bearings and strips,

thus reducing the maximum operating speed.

Measurements taken of the machine showed that as the operating speed was increased, slippage began to occur at a rotational speed of approximately 1200 rev/min.

9.1.2.5 Actuators And Sensors.

The actuators used in this design are the strip-clutch fabricated from a 6.5 mm thick Titanium billet, housing a Tokin NLA 5x5x18 actuator, the details of which can be found in chapter 5.

The machine function relies on driving the piezo clutches synchronously with the rotation of the input shaft. To achieve this, a dual output optical stator was constructed to detect both dwell phases of the cam. This uses TTL logic compatible slotted opto-switches, which are triggered when a small tag passes through the opto-switches at the centre of the 40° dwell zone. End-stop detection was achieved using similar opto-switches, to prevent linear over-travel and possible damage to the mechanism.

9.1.2.6 Electronics.

Figure 117 shows a system diagram of the electronic system used to control the machine. The system contains PSU elements for the D.C. motor, the piezoelectric clutches and the logic (T.T.L.). Pivotal to the design is the Intel 5C060 Erasable-programmable logic device (E.P.L.D.) which governs the correct phasing of the static and dynamic clutch drive signals. It also copes with end-stop detection and directional input control. The clutch phase signals drive amplifier boards.

Figure 118 shows the basic timing diagram for the system. A 1 kHz clock causes a state change on a rising edge (positive delta). Signals A, B and C are synthesised with flip-flops, and the two signals F and E are used where appropriate to generate the

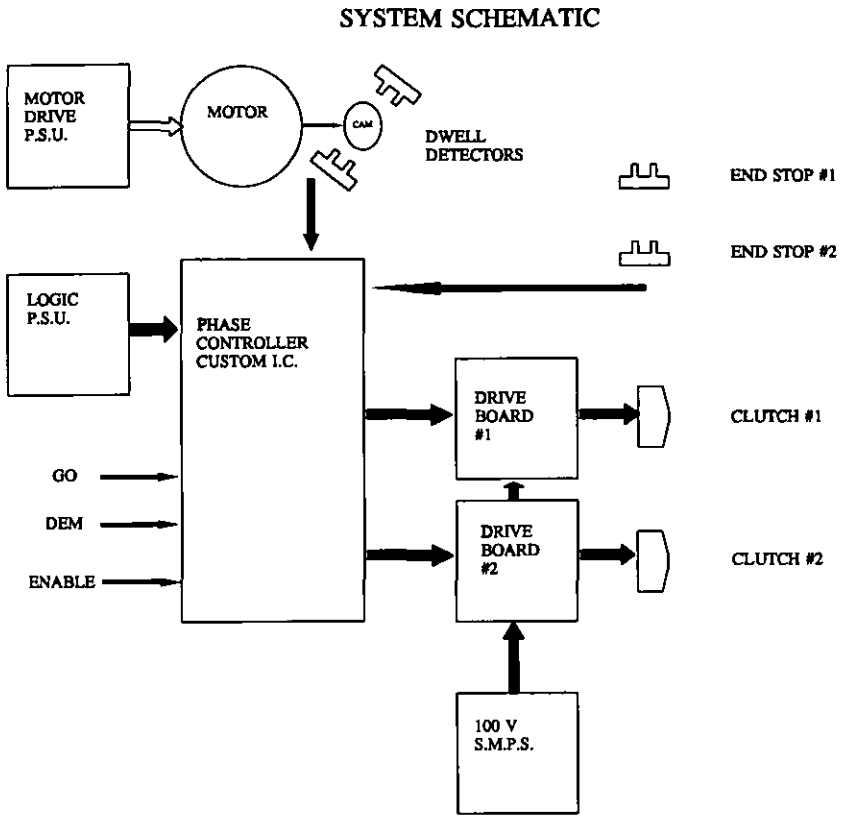

Figure 117: System Diagram for the Discrete Motion Machine.

static and dynamic clutch signals. The signals are interlocked with DEM and GO, along with end-stop detection (not shown). The 1 kHz clock results in a constant overlapping of the static and dynamic signals, designed to guarantee a 2 ms change over period during a cam dwell of 40 degrees at each change of direction. This ensures that at no time is the clutching assembly free, and is therefore under complete control even with inertial loads.

Figure 119 shows the logic structure used to generate the EPLD. Using the Intel IPLSII software, this design was programmed in, producing the ADF file below, and ultimately a JEDEC file, used to program the final EPLD.

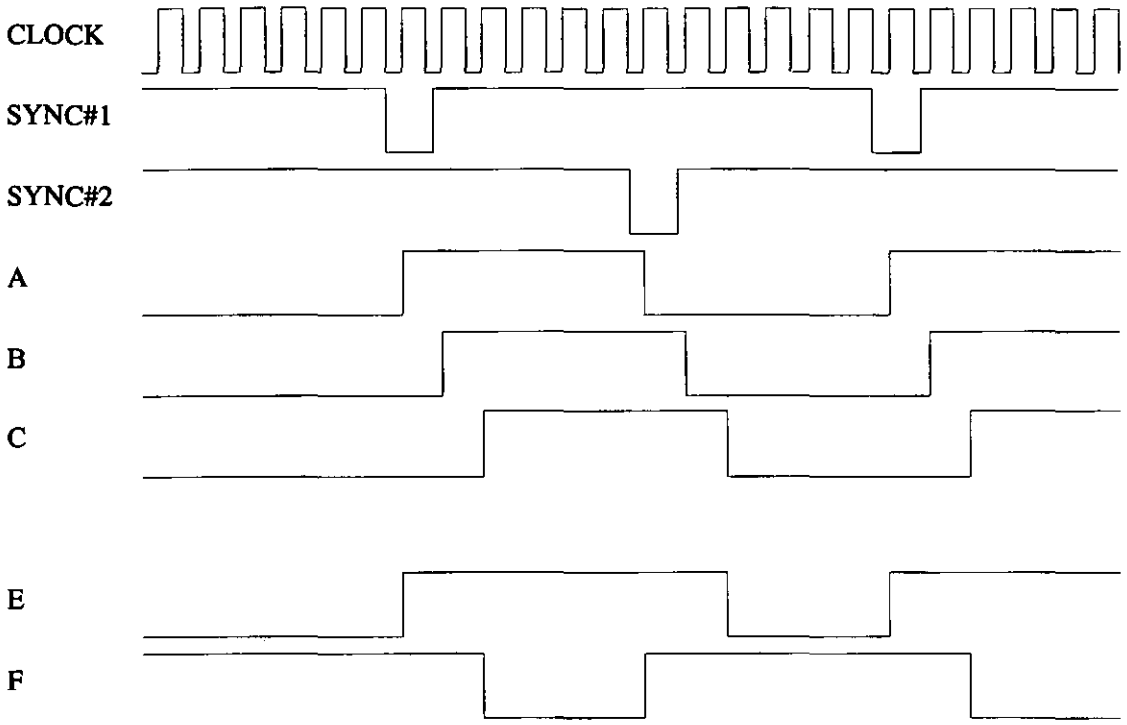

Figure 118: System timing diagram for the EPLD.

```
5C060
Twin Piezoelectric Clutcher: Sync Generator
LB Version 1.5, Baseline 4.0i 7/7/87
OPTIONS: TURBO=OFF
PART: 5C060
INPUTS:
clock@1,enable@2,go@10,rtes@11,ltes@14,atr@17,atl@18,
dem@23,syncin@13
OUTPUTS: syncout@9,static@7,dynamic@8
NETWORK:
syncout = CONF (n2,VCC)
static = CONF (sa,aen)
dynamic = CONF (da,aen)
aen = INP (enable)
da = OR (a1,a4)
a1 = AND (ltsync,f)
a4 = AND (e,rtsync)
e = OR (n3,n1)
rtsync = NORF (rt,clk2,GND,GND)
rt = AND (ago,ademb,artes)
clk2 = INP (syncin)
ago = INP (go)
ademb = NOT (adem)
artes = INP (rtes)
adem = INP (dem)
n3 = NORF (n2,clk1,GND,GND)
n1 = NOSF (al2,clk1,ar2,GND,GND)
al2 = NOT (al1)
clk1 = INP (clock)
ar2 = NOT (ar1)
ar1 = INP (atr)
al1 = INP (atl)
n2 = NORF (n1,clk1,GND,GND)
```

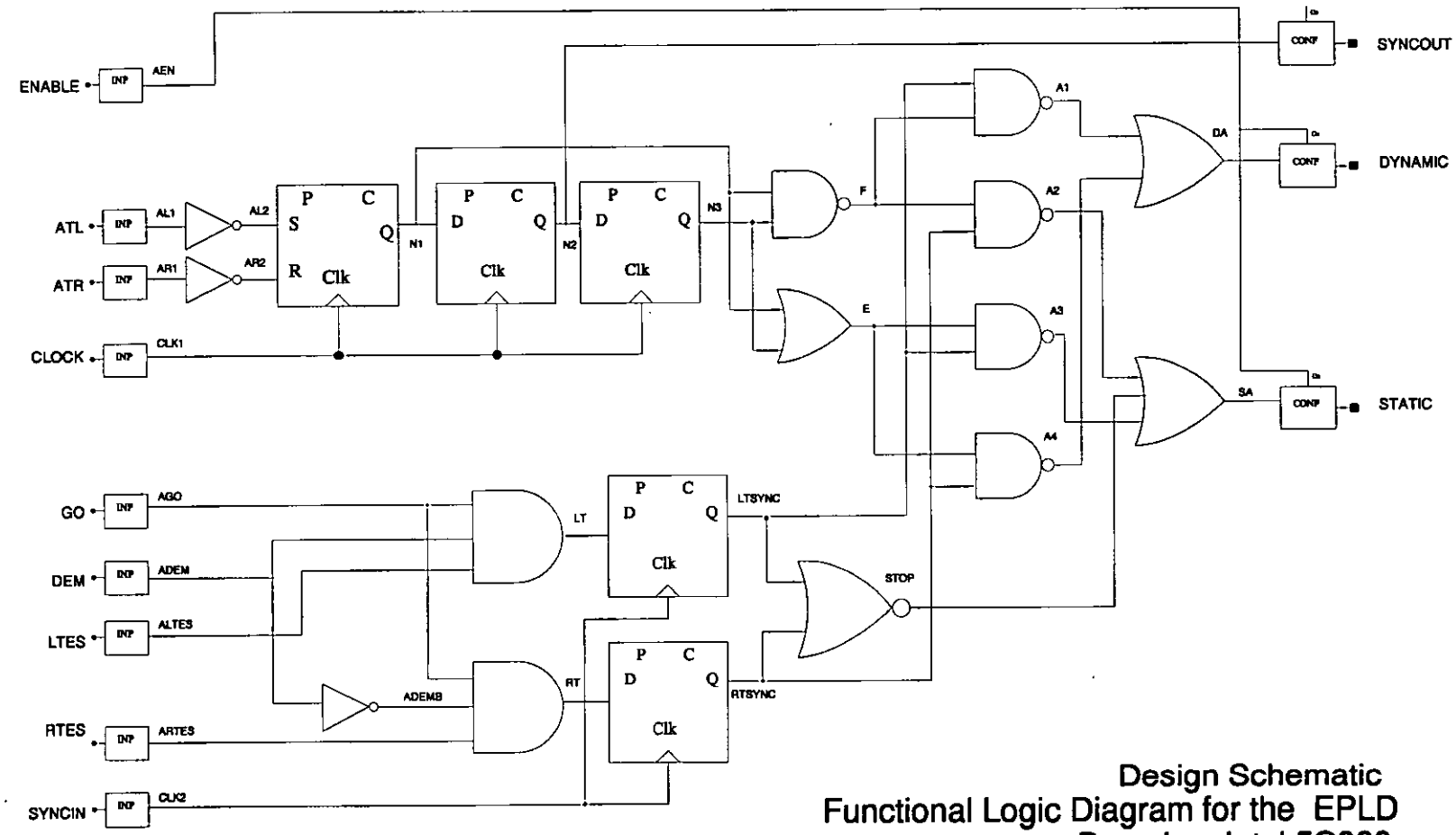

Design Schematic
Functional Logic Diagram for the EPLD
Based on Intel 5C060

Figure 119: The EPLD equivalent circuit.

```
ltsync = NORF (lt,clk2,GND,GND)
f = NAND (n3,n1)
lt = AND (ago,adem,altes)
altes = INP (ltes)
sa = OR (a2,a3,stop)
a2 = AND (f,rtsync)
a3 = AND (e,ltsync)
stop = NOR (ltsync,rtsync)
END$
```

Pin number assignments are as follows;

```
                 5C060
              - - - - -
      clock -| 1    24|- Vcc
     enable -| 2    23|- dem
   RESERVED -| 3    22|- Gnd
   RESERVED -| 4    21|- Gnd
   RESERVED -| 5    20|- Gnd
        Gnd -| 6    19|- Gnd
     static -| 7    18|- atl
    dynamic -| 8    17|- atr
    syncout -| 9    16|- RESERVED
         go -|10    15|- RESERVED
       rtes -|11    14|- ltes
        GND -|12    13|- syncin
              - - - - -
```

The circuit diagram for the phase controller board is shown in Figure 120, followed by the circuit diagram for the piezoelectric driver board, Figure 121.

9.1.3 Evaluation & Observations.

The purpose of the design, construction and evaluation of this machine was to test the postulate that piezo-electric actuators can be used to regulate discrete-motion drives, and to create a technology demonstrator. It has succeeded in both respects and functionally the machine performed as expected. The control system was subjected to all Boolean command combinations and no error conditions were generated by the sensor / electronics system either combinationally or sequentially.

It is not possible to be precise about the longevity of the machine as a whole, since the objective of the design was the demonstration of a principle rather than a `test to destruction'. Indeed, as a machine component, the cam/bearing assembly was felt to be most at risk from early failure.

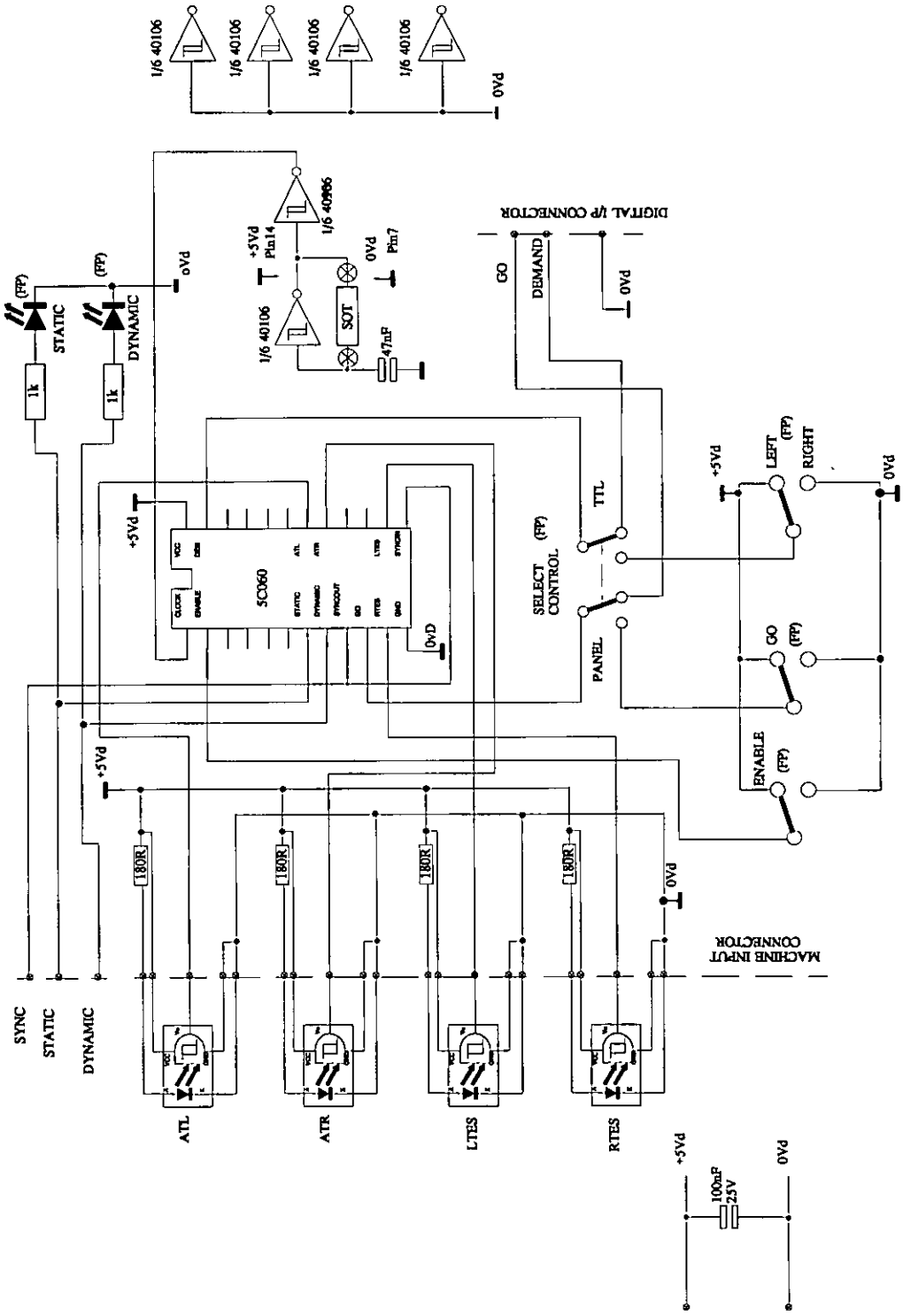

Figure 120: Circuit Diagram of the Control Board containing the EPLD.

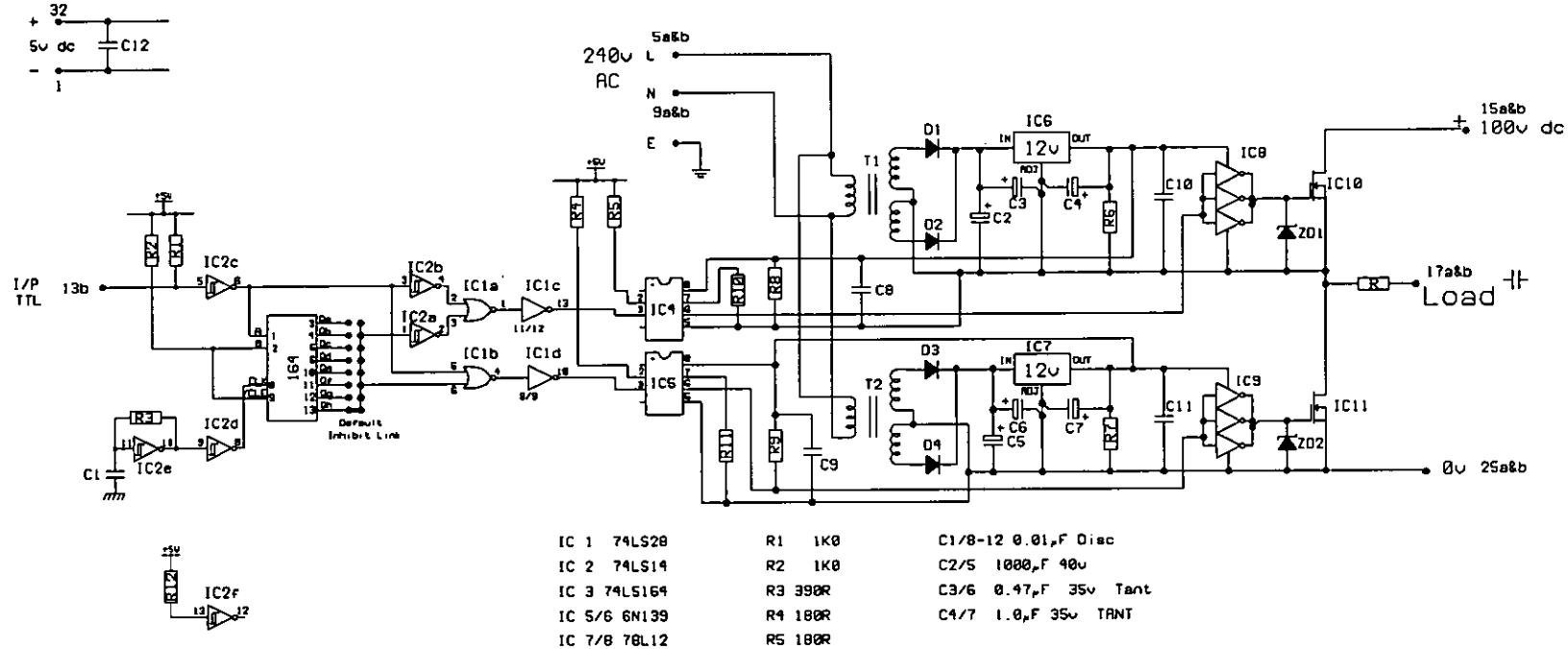

Figure 121: Piezoelectric Driver Board Circuit Diagram.

Some problems were experienced with the strips tearing away from their anchor points, largely due to the addition of tensile pre-load and impulse forces. The agreement between the theoretical speed limit due to inertial loading, and the value measured was not accurate. However, the theoretical value relies on an accurate knowledge of the coefficient of friction (μ) and the clearance constant (k), both of which were estimated. Therefore, an accurate correlation can not be expected.

It is unfortunate that the design's speed limitation was due to inertial load limiting of the two clutches and carriage, rather than the inherent speed of an individual clutching element. In this sense, the machine failed to demonstrate the true potential of piezoelectric clutching. Logically, an enhancement of operating speed could be achieved by designing a system with no large reciprocating components, where the piezoelectric clutching elements are static, but offer a bearing surface for other, smaller clutching components.

9.2 A ROTARY MICRO-POSITIONING INDEXER.

This section describes and evaluates the design and performance of one application of piezoelectric actuation and clutching, using a type of simple beam mechanical displacement amplifier as described in chapter 6. The control electronics is dealt with in sufficient detail to allow an appreciation of the overall system, however, the mechanical components specifically designed for clutching and extension are discussed more thoroughly.

The machine described in this section was developed for a surface metrology application in which maps of the surface microgeometric deviations of cylindrical test pieces are produced by repeated axial tracing of the test piece (using a stylus instrument), followed by a minute incremental test piece rotation. This procedure enables a 'raster scan' of the specimen surface to be built up. It is important for this application that the rotational increment is both repeatable and finely adjustable and that the mechanism is backlash free, with adequate positional stiffness to maintain the position of the specimen precisely during measurement. Additionally, the real time position of the rotor must be known.

The system described here is of closed loop architecture, with the ability to move or return to a prescribed angular position with repeatability of within 0.001°. The system requirements above demand two essential components. Firstly, a shaft encoder with a high angular resolution and secondly, a motor system capable of the required resolution and stiffness. Both these requirements are met. Figure 122 shows a basic layout of the system.

9.2.1 Prior Art.

The original clutching and extension assembly was developed in 1988/1989 by Dr. T. King and Mr. K. Allen of this University. Figure 123 shows the layout of the mechanical assembly. This system used actuators manufactured by Burleigh

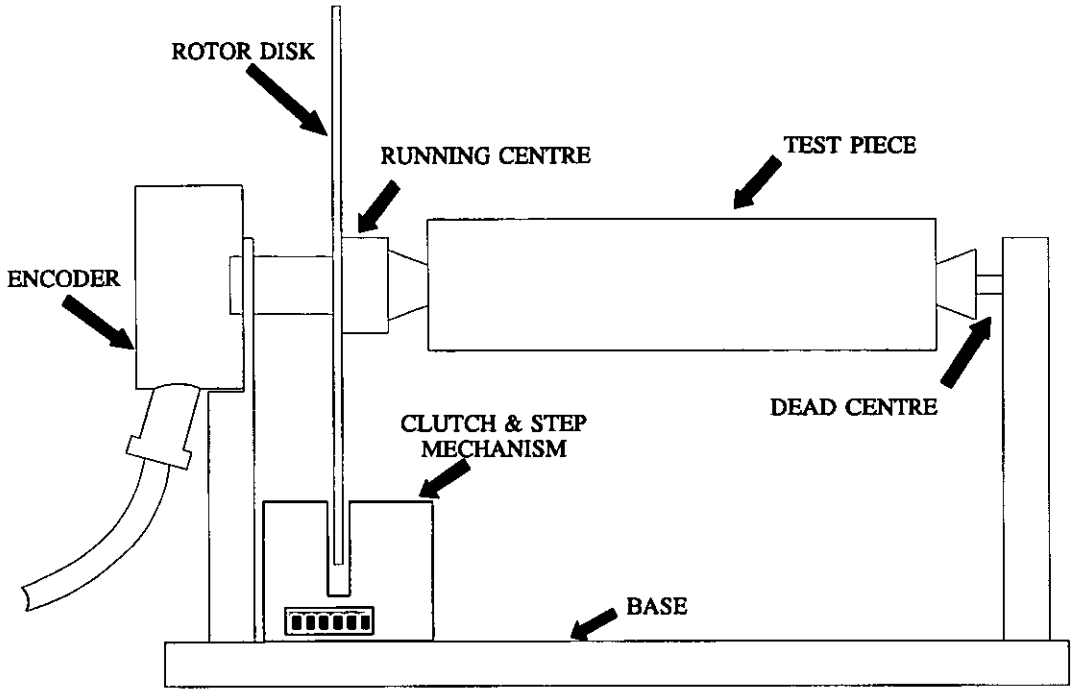

Figure 122: Basic Design of the Rotary Micropositioner.

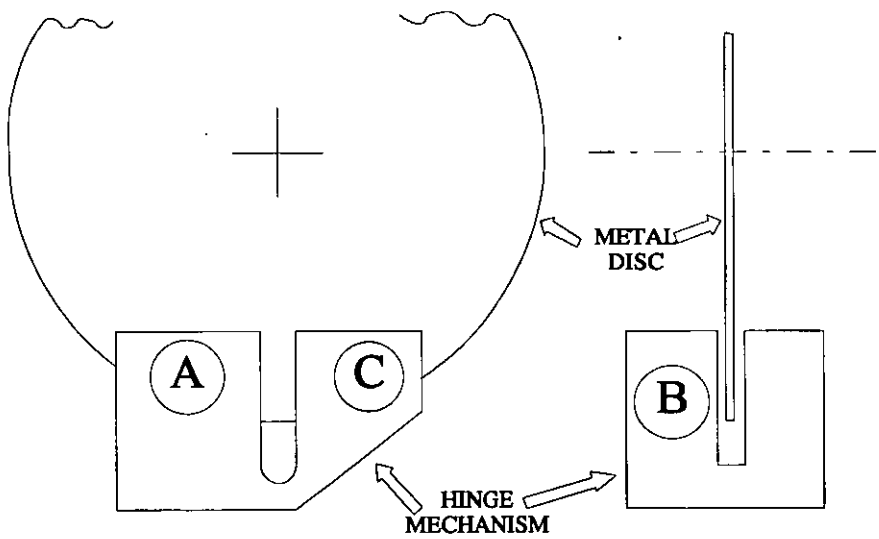

Figure 123: Diagram showing the original clutch and extension assembly.

Instruments, each capable of developing a free movement of approximately 15 μm. The extending and clamping mechanism is also shown in the two views of Figure 124. Two of the actuators are intended to clutch directly on to the metal disc (rotor), and the third intended to extend the centres of clutching on demand, by exploiting the intrinsic lever action of the structure.

This original design for the clutching and extension assembly was found to give unpredictable performance. Stepping behaviour in response to control commands to step clockwise as opposed the anti-clockwise was asymmetric, and in practice extreme difficulty was experienced in attempting to set the clutching clearance between the actuators and the rotor, due to the very small operating clearance necessary for this type of direct actuation. It was therefore difficult to achieve any repeatable results.

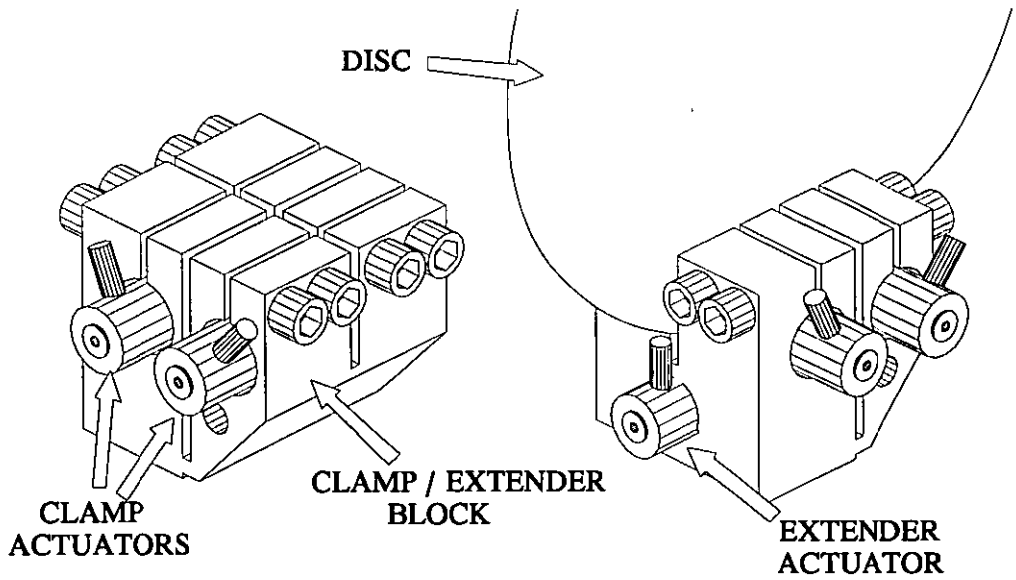

Figure 124: Two Views of the Original Extending and Clamping Mechanism.

9.2.2 Basic Design.

The basic principle by which rotation is produced is analogous to that of the linear 'Inchworm' actuator. In the Inchworm design two clamping collars are alternately clamped to a shaft whilst an extending element between them can vary their separation along the shaft axis. By controlling the sequence of actuation of the clamping and extending elements the device can be 'walked' along the shaft, rather like the caterpillar from which it takes its name. The operation of our rotary device might perhaps be likened to feeding the steering wheel from hand to hand when steering a car. (The cross section of the basic machine is shown in Figure 122.) The rotor disc

is located on the same axis of rotation as the component under investigation, and the motion of the disc is governed by the extension and contraction of three special piezoelectric actuator devices. Two of these devices are clamps with a free range of 0.1 mm, the third actuator develops a displacement of 15 μm, tangential to the disk. Despite a very slight arcuate misalignment, sequential stepping and clamping produces discrete rotary motion of the disk. The stepping sequence is shown in Figure 125. Since the radial position of the clamps and extender is at 6.5 cm from the centre, the angular step size on the prototype is approximately 50 seconds of arc. The use of a thin stainless steel rotor disc allows the clamping mechanisms to be 'single acting' since the disc is easily deflected laterally by the moving clamping surfaces to take up the running clearance between it and fixed clamping surfaces on the opposite side of the disc.

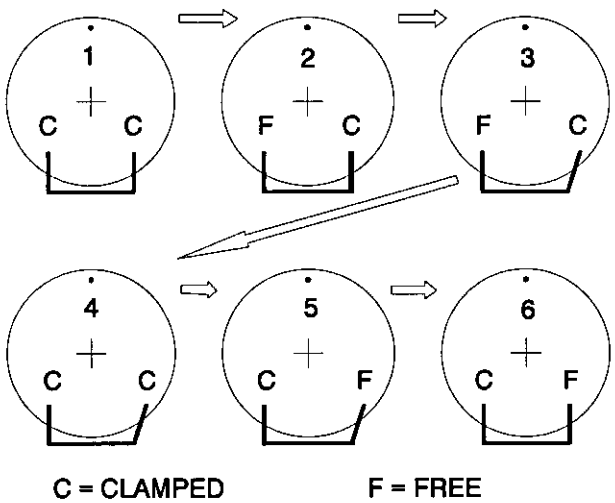

Figure 125: Sequencing of the Clamps and Extender.

The design described here follows from the earlier prototype which used pre-packaged piezo pushers (Burleigh PZO-015-0) without mechanical amplification. In the previous version, which was of generally similar configuration, the piezo devices used as clamping elements acted directly on the rotor disc. Although this configuration was capable of generating considerable clamping forces, setting up the clamp clearances to give satisfactory operation was difficult due to the very small displacements available (15 μm). This made it impossible to achieve reliable sustained operation of

the device once a small amount of wear and surface damage had taken place on the rotor disc. The second generation device therefore incorporates mechanical amplification of the clamp displacements to overcome these problems.

9.2.3 Revised Mechanical Design.

As shown in Figure 122, the test piece is supported at both ends by precision bearings, and directly coupled through to a shaft encoder. The encoder is a Dynamics Research Corporation model 35-11-B1F-9000, and is capable of resolving angular position to within 0.001°, with appropriate decoding circuitry.

The radius of the rotor disk at the clutching points is 65 mm, therefore the resolution of the shaft encoder corresponds to a rotation of 1.13 μm at the radius at which clutching is performed. The stepping actuator chosen in the redesign was a Tokin NLA 2x3x18, generating a displacement step of 15 μm. The resolvable increment corresponds to 7.5% of the actuator's full voltage (100 V) displacement, which also corresponds with the typical creep and hysteresis for this type of soft piezoelectric actuator. The actuator and encoder are therefore well matched for resolution.

The simple beam amplifier was designed to replace the clutching components in the original design is shown in Figure 126. It was manufactured from EN24 of thickness 2.5 mm. The pre-load spring is not shown, but the operating principle of the device can be seen to be that of a simple lever system which exploits the characteristics of flexure hinges. The design was arrived at through the use of the beam designer program, described in chapter 6, however, Figure 127 shows the textual output from the program. As can be seen, the device is capable of developing a 20 N stall force at full drive. Clutching force has been traded off against clearance; necessary for a system which can be built to more generous machining and alignment tolerances, and speed of response of the clutching elements.

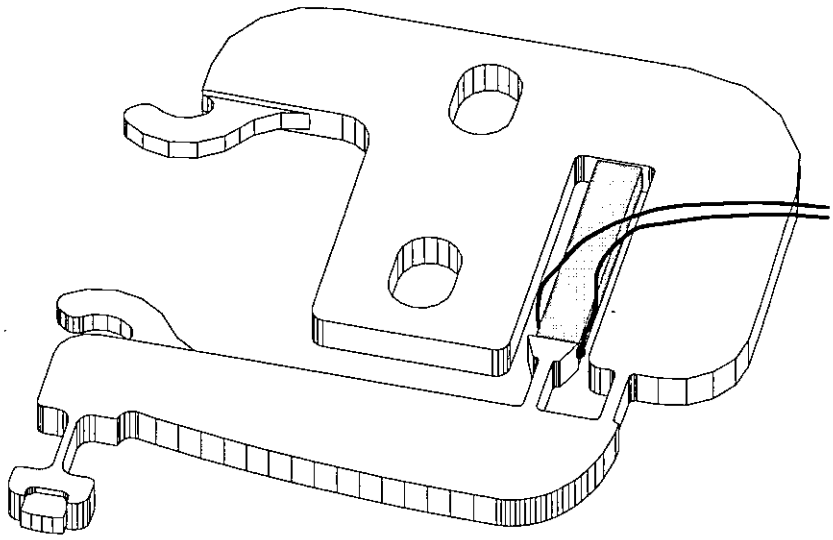

Figure 126: One of the Clamping Amplifiers.

```
                              GEOMETRY STATUS

MATERIAL THICKNESS (B)..    0.002540     HINGE SEPARATION (A1)...    0.005355
OUTPUT BEAM LENGTH (A2).    0.031917     ANCHOR HINGE LENGTH (L1)    0.004065
INPUT HINGE LENGTH (L2).    0.004065     ANCHOR HINGE WIDTH (W1).    0.000916
INPUT HINGE WIDTH (W2)..    0.000916     MAX BEAM WIDTH (D)......    0.009074
MIN BEAM WIDTH 1 (E1)...    0.000893     MIN BEAM WIDTH 2 (E2)...    0.004854

                            PERFORMANCE STATUS

EFFICIENCY..............    0.697789     FREE STRESS [MPA].......   67.106537
STALL STRESS [MPA]......   85.956459     OUTPUT FORCE............   20.933662
OUTPUT MOVEMENT.........    0.000100     MASS [GRAM].............    5.904222

                             PARAMETRICS STATUS

MATCH.FACTOR.STALL......    0.100000     MATCH.FACTOR.ROTATE.....    0.100000
MATCH.FACTOR.BEAM.......    0.100000     SAFETY.FACTOR...........    0.150000
YIELD.STRESS........... 469.000000E+06 YOUNGS MODULUS.......... 210.000003E+09
```

Figure 127: Textual Output from the Beam Designer Program.

The extender mechanism houses the same type of piezoelectric device as the clamps, but requiring no displacement magnification, the mechanism simply provides a gripping surface which is very stiff in the direction of the clamping force, but compliant in the direction of the extending actuator. The design of this flexural mechanism is shown in Figure 129. Both the clamps and the extender mechanisms were manufactured using a Wire E.D.M. process.

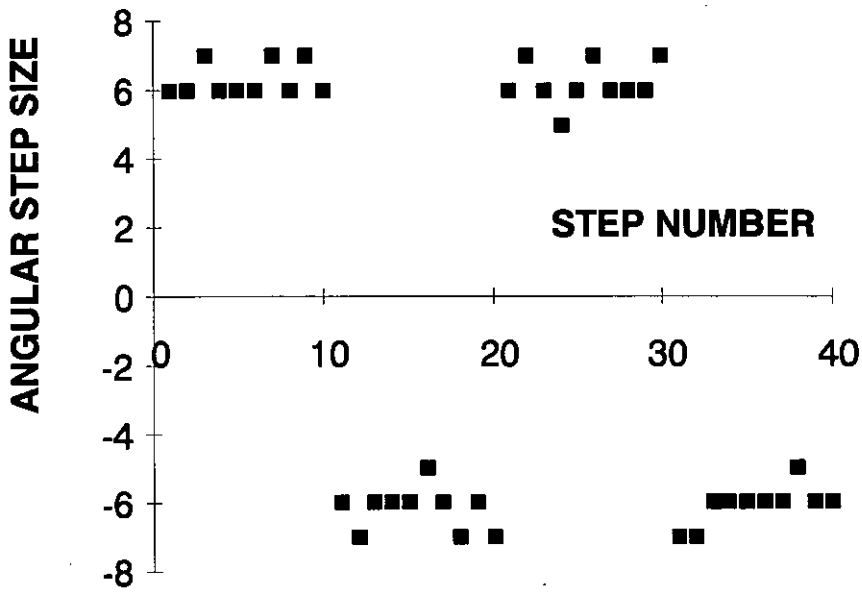

Figure 128: Step Size Variation.

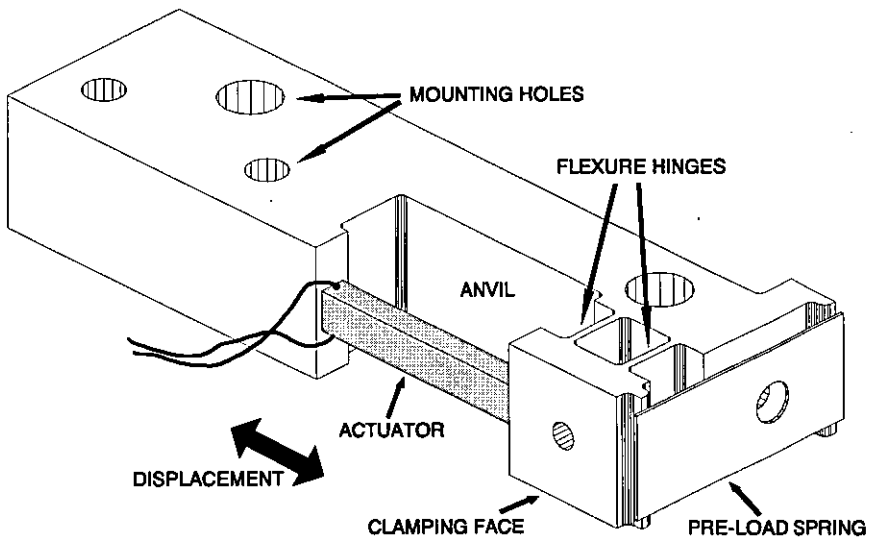

Figure 129: Perspective View of the Extender Mechanism.

9.2.4 Electrical Design.

The overall prototype system can be seen in Figure 131. The system is controlled by an IBM compatible personal computer, containing an I/O board with 3 output lines plus several interface lines for the shaft encoder electronics. The design of this board can be seen in the circuit diagram in Figure 130. The system is therefore under software control and can execute any control sequence according to the operators intent.

Control of the two clamp and one extender actuators is achieved via the piezoelectric drive boards, which are of the same type as those used by the previous application. Because of the variable moment of inertia presented by the mechanism and the mounted test piece, the speed of operation of the extender can not be fully exploited. Devices such as the actuator assembly used, can respond (but not necessarily settle) in less than 0.15 ms. In this application, the clamping force of approximately 10 N would be insufficient to guarantee the avoidance of shearing against the disk, and so the extender drive is intentionally slowed down by a simple resistor [23] to result in a drive rise time of approximately 2 ms (10%-90%). Since there are six phases of operation (see Figure 125), and clamping phases take approximately 1 ms each, this imposes a theoretical maximum cycle frequency of 125 Hz; much slower that an inch-worm for example.

The signals to the piezo drive boards are derived from the interface card, specifically Port A, bits 5-7 of the 8255, and the correct sequencing for this is generated by software. The 8255 also manages the HCTL 2000, which is a 12-bit counter with filtered quadrature detection, thus monitoring relative changes in shaft rotation angle. The 74LS245 is a tri-state 8-bit bi-directional buffer and simply manages i/o to the 8255. Address decoding for the board is derived from address lines A2..A9, via the GAL 16V8, with the base address chosen prior to programming (0300H). This chip generates the READ, WRITE and CS55 lines. The HCTL 2000 requires a relatively

[23]This results is a first order lag since the actuator is capacitative.

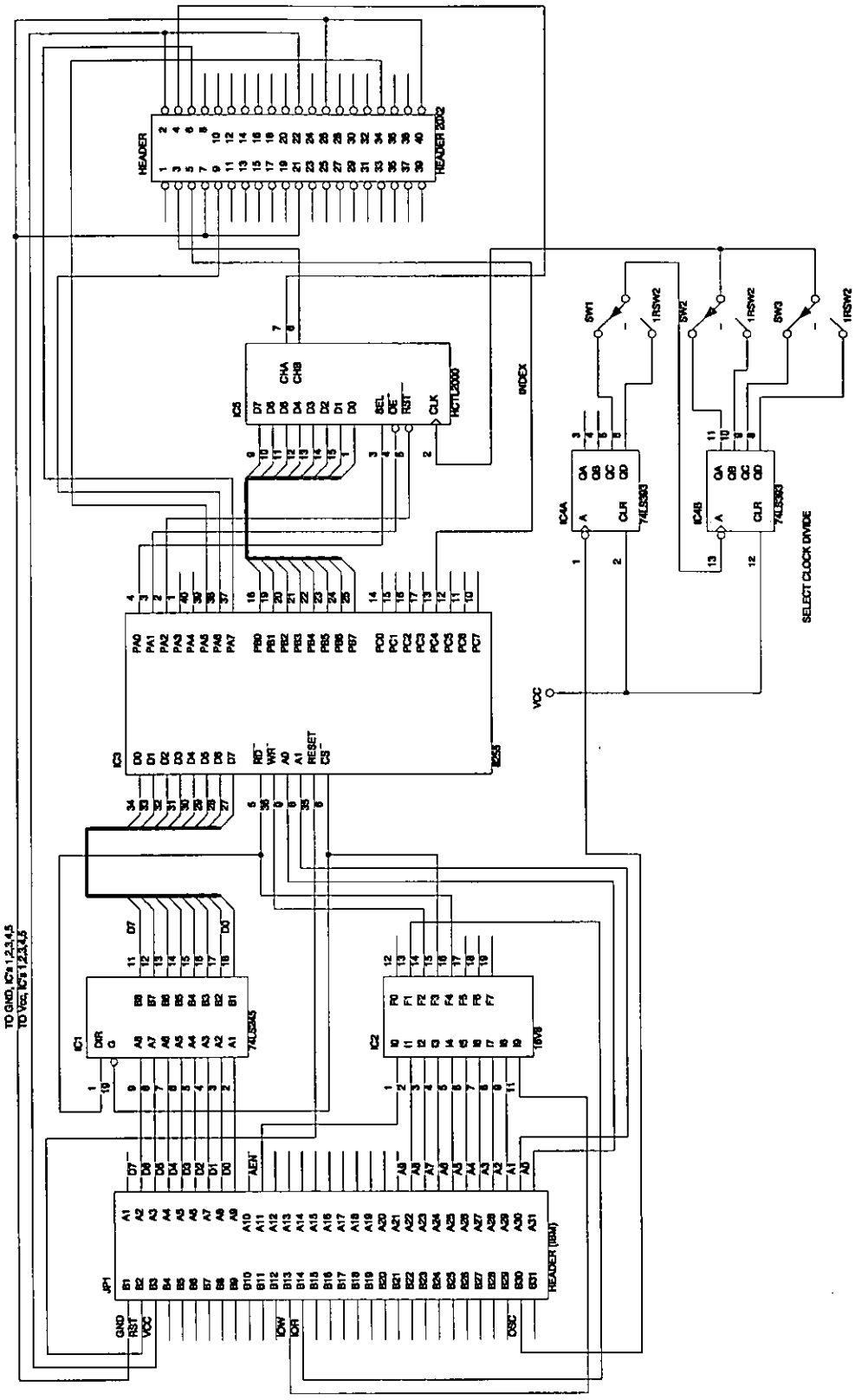

Figure 130: Circuit Diagram of the IBM PC Interface Board.

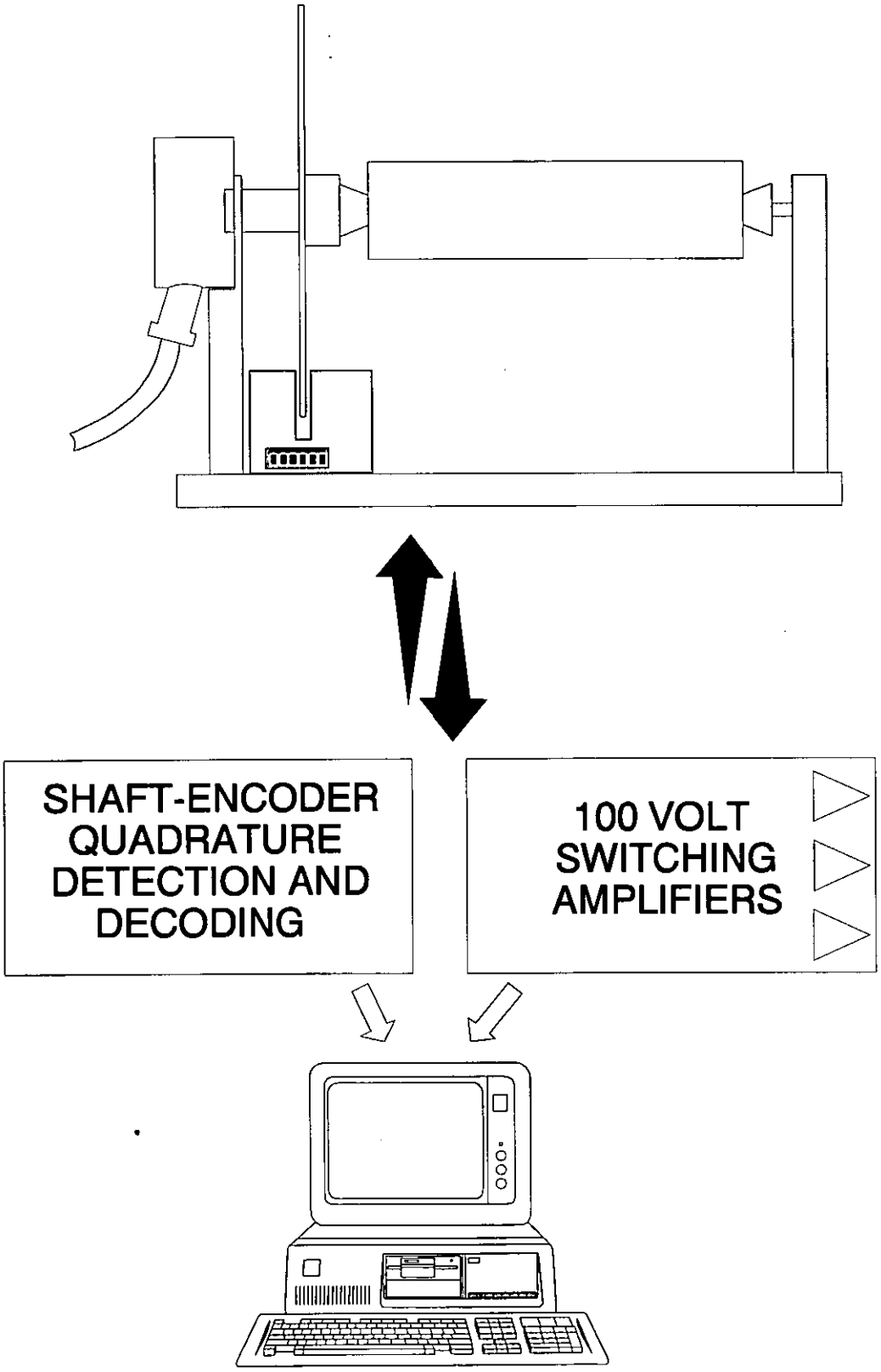

Figure 131: Schematic of the Rotary Micropositioner Control System.

low clock speed, and this is derived by selecting appropriate outputs from the 74LS393, a dual 4-bit binary counter.

9.2.5 Performance.

The purpose of the prototype was to establish the feasibility of the control of angular position in this way. There are many factors which could influence the possibility of a design such as this being successful from the point of view of component wear or failure. The long term performance has not been investigated at this time, but its repeatability has been established.

Since the system is intended to be operated in a closed loop architecture, repeatability over many steps is unimportant, from the control performance and stability view point. Stiction, deviations from overall linearity, or any variations from repeatability at the step-size level are problematic, but as Figure 128 shows, this does not appear to be a problem. This figure shows step to step variation in the angular variation for 30 successive increments, with two changes in direction. Scatter within ±1 count has been achieved and is acceptable. (This corresponds to a rotational uncertainty of ±25 seconds of arc. The device has been successfully operated up to a 'complete-cycle' frequency of 30 Hz resulting in an angular frequency of approximately 500×10^{-6} rad/s. It can sustain a static torque of 0.3 Nm, with no slippage.

9.2.6 Evaluation and Observations.

Functionally, this device is comparable with a rotary inch-worm. It is slow however, and in its present form can rotate at only 1½ minutes of arc per second. In the no-slip condition, the angular stiffness of the system is extremely high and this lends itself to rotary positioning in surface metrology where variability in torque loading could result in shifting of the point of interest.

The prototype has established the feasibility of using displacement amplifiers in this configuration for high-speed clamping or clutching. The adoption of this approach has resulted in tolerance specifications for components which are undemanding by comparison with those normally associated with piezoelectric micro-positioning components.

10 CONCLUSIONS AND FUTURE WORK.

10.1 CONCLUSIONS.

It has been highlighted that despite enhancements and refinements to the electromagnetic family of actuators, the actuation times of such devices are never likely to fall below several milliseconds. This is due partly to electrical behaviour associated with the inductance of these devices, and partly to mechanical and magnetic factors associated with force coupling. Also, since a current must be maintained in some electromagnetic devices to hold position, power is often wasted when no physical work is done by the device. These inherent time response limitations of solenoids and similar devices have, until recently, created a barrier making it difficult to find engineering solutions for applications where higher speeds are required.

It is proposed that the adoption of an inherently 'faster' technology would not only potentiate performance enhancements to existing machine applications, but make certain machine systems possible which were not previously viable. Such an application is in the regulation of discrete motion drives, where cyclic motion is sequentially clutched by fast actuators onto a controlled component. In this mode of operation, high actuation speeds would result in low, or near zero relative velocities for the clutching surfaces, thus reducing the possibility or rate of wear. It was proposed that piezoelectric actuators could provide design solutions in this type of application.

The phenomenon of piezoelectricity was studied and a selection of actuator applications employing the converse piezoelectric effect was presented. The main characteristics of piezoelectric actuators and methods of their application were discussed. Some of these applications demonstrated the capability of piezoelectric ceramic actuator technology to produce devices which could operate at much higher speeds than electromagnetic devices. This indication necessitated a comprehensive literature survey, during which more applications of piezoelectric ceramic actuators were found. It was evident that the small movement that can be achieved with

piezoelectric actuators (stack-type) appears to have fostered several innovative and interesting methods of displacement amplification. Most of these were classified according to the mode of operation of the actuator, specifically; *Displacement/Force controllers, Wave (ultrasonic) motors, Inchworms (rotary/translational), Inertial pulse caterpillars (unique), Impulse transfer devices and Bi-stables.* There was, however, an absence of any application where these devices were used in clutching or gripping, and it is asserted that the reason for this is that the key to using piezoelectric actuators in clutching or gripping applications, lies in the ability to design efficient mechanical displacement amplifiers; to transform the movement which can be generated by an actuator, to a more practical, usable range. Evidence of the design of high-efficiency displacement amplifiers was not revealed in the data search.

The review also revealed devices based on the principle of impulse transfer; a technique which potentially offers very large displacements. Devices which operate as latches for the control of discrete motion drives were not found.

The requirements for an actuator which can control or regulate discrete motion drives, can be satisfied by monolithic (solid-state) displacement amplifying linkages, but for latching applications, the long displacement ranges and fast actuation times potentially offered by impulse transfer are attractive.

Several displacement amplification techniques were outlined and their merits discussed. Three promising displacement amplifying linkages are the simple lever (direct), the compressive flexural bridge and the hydraulic amplifier. Other methods exist but were rejected for a variety of reasons. The transverse simple lever topology can not produce structures which are as efficient as its direct counterpart, and the bimorph and multimorph approaches do not generate force / stroke characteristics in a suitable combination or with practical topologies. The hydraulic displacement amplifier is sophisticated compared to pivoting and flexure hinge based systems such as the simple lever and flexural bridge, and so its adoption could not be justified when other much simpler methods appear to offer satisfactory design solutions. The flexural bridge and simple beam displacement amplifier are mechanically simple, robust and

capable of high-speed (sub 1 ms) actuation.

Very high-gain amplifying structures were proposed, which used a two-stage lever system with a stack-type actuator. Using perspex models, movements of the order of 1 mm were found to be achievable, and whilst it is possible to design structures possessing higher gains in this way, the resulting structures exhibit lower electro-mechanical efficiencies, and accordingly longer response times, whereupon their speed advantage is lost. It is believed, however, that such structures offer potential in replacing electromagnetic devices in a wide range of applications.

A piezoelectrically driven displacement amplifying structure, known as the *strip-clutch*, was designed, constructed and tested. It employed simple levers and a flexural bridge structure, and demonstrated that this type of structure can perform well, both in terms of speed of response (typically less than 0.3 ms) and as a moderately efficient transformer of electrical energy into work done; the design was 25% efficient as a mechanical transformer. The device was later incorporated into a machine designed to demonstrate the principle of discrete motion control using piezoelectric ceramic actuators.

The natural ringing behaviour of such structures can be reduced or controlled by the inclusion of visco-elastic polymers (rubbers) within the amplifying structure. This technique makes it possible to design a mechanically simple displacement amplifying actuator which can be driven from a simple two-state electrical drive. Moreover, due to low design stressing (0.2 x yield stress) and the absence of friction generating surfaces, these devices offer the potential of great longevity.

In order to facilitate the design of simple lever (direct) amplifiers using flexure hinges, as used in the strip-clutch, an expert program called the *beam designer* was written. Given that the program is based on block modelling and interaction of different elements of the structure, the program performs moderately well and produces designs which demonstrate a good degree of correlation between the program itself, finite element modelling and measurements taken from the real devices as designed.

It is clear that for higher efficiency devices, assumptions concerning the rigidity of the host structure are not valid and lead to errors in predictions of device efficiency, but not in predictions of output displacement. The stresses predicted by the program are invariably conservative, and therefore the program is likely to produce designs which are more resistant to cyclic fatigue than expected. Overall, the program demonstrates that mechanical amplification by the (direct) simple lever method, involving the use of flexure hinges, with resulting efficiencies of upto 75%, is viable. Dynamic tests on devices designed in this way show that speeds of response of this class of device are typically less than 1 ms, even for devices with output displacements as high as 0.2 mm.

Combinations of mechanical damping and electronic wave shaping can certainly result in actuator transition behaviour which is conducive to operation of such devices at relatively high repetition rates; perhaps approaching 100 Hz, however, it is very likely that satisfactory performance can also be achieved solely by the use of mechanical damping.

A *bridge designer* expert program was also written and, through the application of the program to the 'top' section of the strip-clutch, and to a 'bridge only' displacement amplifier, demonstrated the potential for achieving displacement amplification in this way. It was demonstrated that single stage amplifiers with gains in the order of x 13 and efficiencies of 50% or higher are realistic.

The performance of the program was poorer than that of the beam designer, as for example, errors in predicted efficiency of the order of 11% were evident. Since agreement between the F.E. model and the program for the value of output displacement is quite good (<2%), it is possible that the poorer performance when comparing data with the real device is due to altering the specific geometry of the design, i.e. shifting the relative positions if the hinge and arm centroids, but this must remain a subject for investigation for further work. Although the designer program is not highly accurate, it does allow the semi-automatic design of such structures by computation. Again, like the beam designer, its accuracy in assessment of stress is

conservative and therefore the program is likely to succeed in producing statically fatigue robust designs providing the appropriate safety factor is chosen.

The discrete motion machine demonstrated that by using high-efficiency displacement amplification methods, piezo-electric ceramic actuators can be used to regulate discrete-motion drives. It was intentionally constructed as a technology demonstrator and was successful in this respect, despite some practical difficulties with the design of the strip clamps responsible for holding the strips in place.

It is unfortunate that the design's speed limitation was due to inertial load limiting of the two clutches and carriage, rather than the inherent speed of an individual clutching element. In this sense, the machine failed to demonstrate the true potential of piezoelectric clutching. Improved operating speed could be achieved by designing a system with no large reciprocating components, where the piezoelectric clutching elements are static, but offer a bearing surface for other, smaller clutching components.

The rotary micro-positioner, demonstrated the advantage of employing high-efficiency mechanical displacement amplifiers with piezoelectric ceramic actuators. Moreover, this is emphasized, since the latest development of this unit (now fitted with the amplifying linkages), is comparable to an earlier machine without linkages. The original unit was difficult to adjust for clutch clearance, and incapable of reproducing its stepping behaviour. The adoption of amplifying linkages has resulted in tolerance specifications for components which are undemanding by comparison with those normally associated with other piezoelectric micro-positioning components, such as the 'inch-worm'.

The aim of this thesis was to establish the feasibility of discrete motion control, using piezoelectric actuation and displacement amplifying linkages. It has been shown that this is feasible using an approach involving direct clutching, but it may also be possible to achieve regulation by latching; also through the use of solid-state amplifiers. However, the literature survey revealed some applications of piezoelectric multilayer actuators in the mode of operation described as impulse transfer, and the

study of this process here, has served to establish what can be achieved in terms of range of displacement and actuation speed, for example a 2 mm range can be typically traversed in 1 ms. This has been particularly valuable since the literature survey did not reveal any work concerned with predictive modelling.

The modelling also showed methods of electrical drive optimisation and the likely levels of electrical current stressing. Since the model predicts departure velocities for ballistic masses, it can be used as the basis of a design tool for the development of a practical actuator.

10.2 FUTURE WORK.

The work described in this thesis was sponsored by the S.E.R.C. and was principally addressed to the feasibility of using piezoelectric actuators to regulate discrete motion drives. This feasibility has been established by the demonstration of the principle through the discrete motion and rotary micropositioner mechanisms. Almost incidentally, the tools now exist (designer programs) which will facilitate quick and easy design to any realistic actuation specification, when specified in terms of required efficiency, displacement and output stiffness, and cyclic fatigue tolerance. Further refinements will be required for the designer programs to facilitate estimation of response time. Extension of study into the area of the ' response time / efficiency ' compromise, indicated in chapter 6, would be desirable, as this would facilitate the prediction of feasible actuation times for applications where the force-displacement requirement is well defined.

The two basic topologies developed for solid state displacement amplification are complementary in that one produces output movement along the same axis as the input, and the other transversely. This makes possible a family of compound amplifiers which can be designed and blended for a specific application. The design of such complex devices is possible with the software already developed.

This technology now seeks out real design problems. Many applications for this type of device exist, not only in new areas, but as performance enhancing alternatives to older families of device like the solenoid. The two machines described in this thesis demonstrate what is possible in terms of speed and displacement. Many systems already exist, the performance of which might be considerably enhanced by the design inclusion of piezoelectric type systems, such as in the existing 'electronic jacquard' for thread selection, knitting machinery and yarn tension control. Other applications include harmonic motors, micro-hydraulic pumps, flow controllers, and a wide range of systems which require displacements in the range order of 1 mm, but requiring greater forces than can be achieved with bimorph and multimorph topologies.

The work carried out on modelling the impulse transfer process points to the development of latching or two-state type devices, with large displacements in excess of 2 mm and low response times in the range of 1 ms. Push-pull type devices are possible using this technique. This work could be application led.

11 APPENDIX 1.

11.1 COMPLIANCE OF A TAPERED BEAM.

11.1.1 Analytical Modelling.

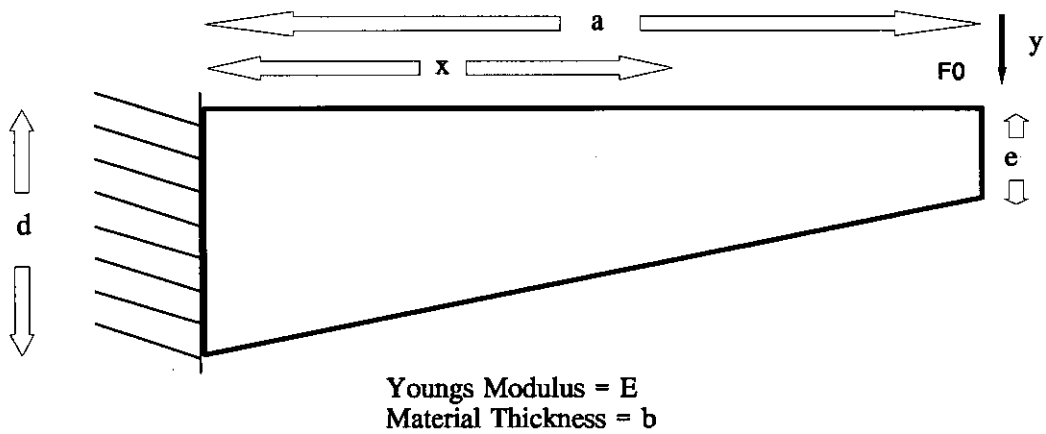

Figure 132: An Encastred Tapered Beam.

Figure 132 shows an end encastred tapered beam, experiencing a vertical force at the thin end. Classically, we can say;

$$I_z = \frac{3}{2}bp^3 \qquad \textbf{(177)}$$

where I_z is the moment of inertia at x, and p is half the beam height. Also;

$$EI_z\frac{d^2y}{dx^2} = M \qquad \textbf{(178)}$$

where M is the bending moment along x given by;

$$M = F(a - x) \tag{179}$$

by rearrangement and substitution, we get;

$$\frac{d^2y}{dx^2} = \gamma \frac{(a - x)}{(x + \delta)^3} \tag{180}$$

where;

$$\alpha = \frac{(e - d)}{2a} \tag{181}$$

and;

$$\gamma = \frac{3F}{2Eb\alpha^3} \tag{182}$$

Further substitution of;

$$\delta = \frac{\beta}{\alpha} \tag{183}$$

gives;

$$\frac{d^2y}{dx^2} = \frac{\gamma(a - x)}{(x + \delta)^3} \tag{184}$$

Integrating once and fitting $\frac{dy}{dx} = 0$ for $x = 0$ we get;

$$\frac{dy}{dx} = \frac{\gamma}{2}\left[\frac{1}{(x + \delta)} + \frac{(x - a)}{(x + \delta)^2} + \left(\frac{a}{\delta^2} - \frac{1}{\delta}\right)\right] \tag{187}$$

Integrating again, we get;

$$y = \frac{\gamma}{2}\left[2\ \ln(x + \delta) + \frac{(a - x)}{(x + \delta)} + \frac{x}{\delta}\left(\frac{a}{\delta} - 1\right) + k_2\right] \tag{188}$$

Setting a zero boundary condition and x=a, we get;

$$y_a = \frac{\gamma}{2}\left[2\ln\left(\frac{a+\delta}{\delta}\right) + \frac{a}{\delta}\left(\frac{a}{\delta} - 2\right)\right] \tag{189}$$

And since the output compliance is;

$$S_a = \frac{y_a}{F} \tag{190}$$

we get;

$$S_a = \frac{6a^3}{Eb(e-d)^3}\left[2\ln\frac{e}{d} + \left(\frac{e}{d} - 1\right)\left(\frac{e}{d} - 3\right)\right] \tag{191}$$

The maximum stress occurs at maximum vertical distance from the neutral axis and is given by;

$$\sigma_x = \frac{3F(a-x)}{2b(\alpha x + \beta)^2} \tag{192}$$

Using T as a dummy variable and setting;

$$T = \frac{(a-x)}{(x+\delta)^2} \tag{193}$$

and differentiating w.r.t. x to find a maximum, we get;

$$\frac{dT}{dx} = \frac{(x^2 - 2ax - \delta^2 - 2a\delta)}{(x+\delta)^2} \tag{194}$$

and setting this to zero, we solve the quadratic;

$$x^2 - 2ax - (\delta^2 + 2a\delta) = 0 \tag{195}$$

giving solutions for peak stress location as;

$$x_{peak} = a \pm \sqrt{a^2 + \delta^2 + 2a\delta} \tag{196}$$

Simplification shows two solutions at;

$$x_{peak} = \frac{ad}{(d-e)} \text{ and } x_{peak} = a\,\frac{(d-2e)}{(d-e)}$$

Inspection of valid space shows that the first solution always gives $x_{peak} > a$ which is meaningless, whereas the other solution is valid for $e < d/2$. For $e > d/2$, i.e. when the cross section approaches a uniform beam, there is no solution. This is because the maximum stress is not a peak value in the mathematical sense, and so cannot be solved using differentiation. The maximum stress will therefore occur at x=0 for $e > d/2$.

Substituting x_{peak} back into the peak stress equation, we get;

$$\sigma_{peak} = \frac{3F}{2(d-e)be^2} \tag{199}$$

unless $e>d/2$, in which case;

$$\sigma_{max} = \frac{24Fa^3}{bd^2(e-d)^2} \tag{200}$$

11.1.2 Finite Element Verification.

The following F.E.A. models are for Aluminium alloy with a Young's modulus of 7×10^{10} N/m^2 and dimensions a=0.05, b=0.0065, d=0.02 and e=0.01 or 0.005, representing two differing taper angles. The two cases have been chosen so that maximum stresses are predicted to occur at either x=0, or elsewhere along the beam.

Figure 133 shows the Von Mises stresses for a 1 N vertical load on the tip of the beam, with the left hand edge restrained encastre. This is the limiting case as in section 11.1.1. Apart from local stressing at the point load, the maximum value occurs at x=0. This value is 154 kPa. This is a simple load case, and it could be argued that the end face along *e* should be loaded as a distributed shear load. However, correlation as is shortly evident will justify this approach.

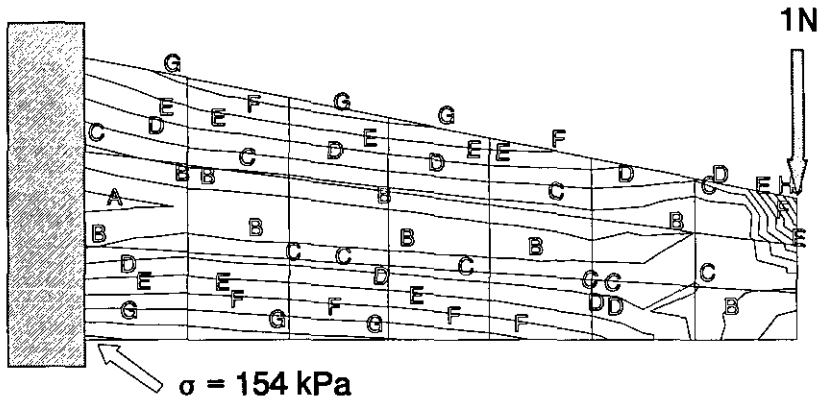

Figure 133: Von Mises Stress Distribution for a Tip Vertical Unit Load.

Figure 134 shows the deformation of the beam and in particular, the maximum displacement of the tip, giving a tip compliance of 0.253 μm/N, according to the F.E.A. The analytical value derived evaluates to 0.225 μm/N. This is a good match implying a sound analytical model, or both F.E. and analytical models are in error, which is unlikely.

Figure 135 shows the Von Mises stress plot for a thinner beam, where e = d/4. For this shape, the equations locate a peak stress (or maximum) at x = 2a/3. The F.E. model results in a maximum stress of 156 kPa. This is verified graphically and confirms the analytical model.

Figure 136 show the deformation of the same load as in Figure 135. The tip compliance is shown as 0.396 μm/N. The analytical model gives a value of 0.347 μm/N. Again, this is a fair match.

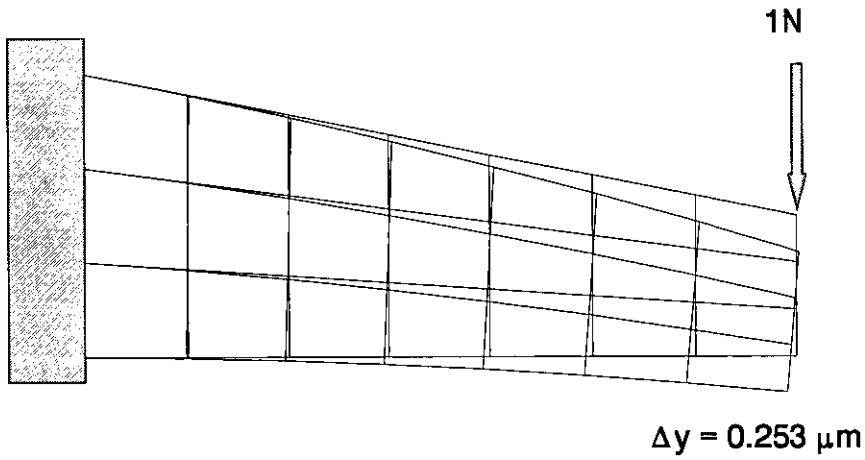

Figure 134: Magnified Beam Displacement.

11.2 COMPLIANCE OF AN ELLIPTICAL BEAM.

11.2.1 Analytical Modelling.

Figure 137 shows an end encastred tapered beam, experiencing a vertical force at the thin end. Classically, we can say;

$$I_z = \frac{bp^3}{12} \qquad \textbf{(201)}$$

where I_z is the moment of inertia at x, and p is the beam height along x. Also;

$$EI_z \frac{d^2y}{dx^2} = M \qquad \textbf{(202)}$$

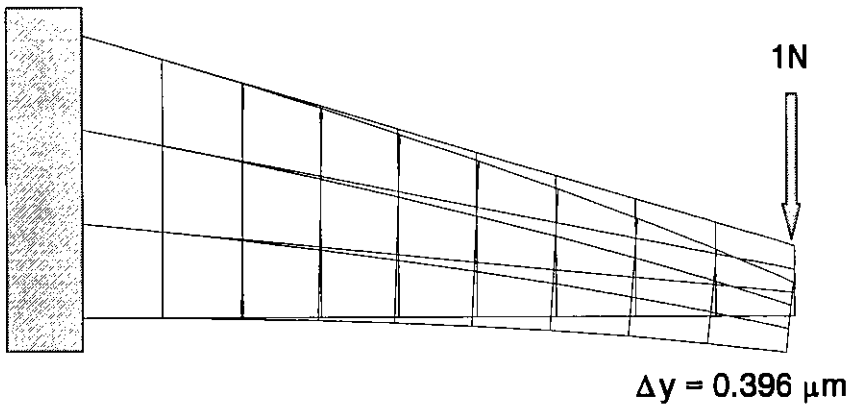

Figure 135: Magnified Beam Displacement.

where M is the bending moment along x given by;

$$M = F(a - x) \tag{203}$$

by rearrangement and substitution, we get;

$$\frac{d^2y}{dx^2} = \frac{\gamma(a - x)}{(\delta^2 - x^2)^{3/2}} \tag{204}$$

Since the curvature of the ellipse is given by;

$$d^2 = p^2 + k^2x^2 \tag{205}$$

where k is the factor of ellipsicity, given by;

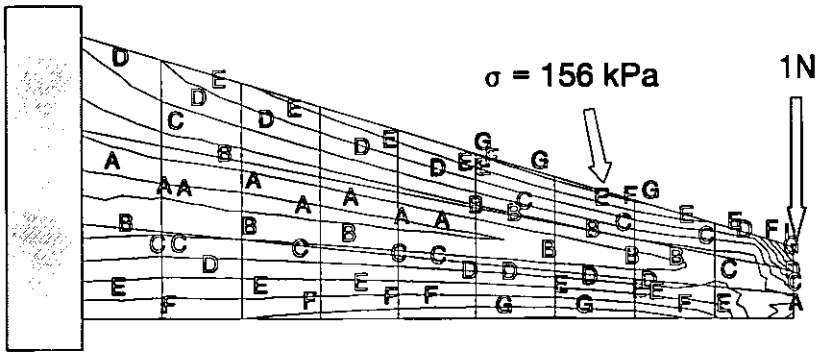

Figure 136: Von Mises Stress Distribution for a Tip Vertical Unit Load.

$$k = \frac{\sqrt{d^2 - e^2}}{a} \tag{206}$$

and;

$$\delta = \frac{d}{k} \tag{207}$$

with;

$$\gamma = \frac{12F}{Ebk^3} \tag{208}$$

By integration we get;

$$\frac{dy}{dx} = \gamma \int \frac{(a - x)}{(\delta^2 - x^2)^{3/2}} dx \tag{209}$$

Substitution of;

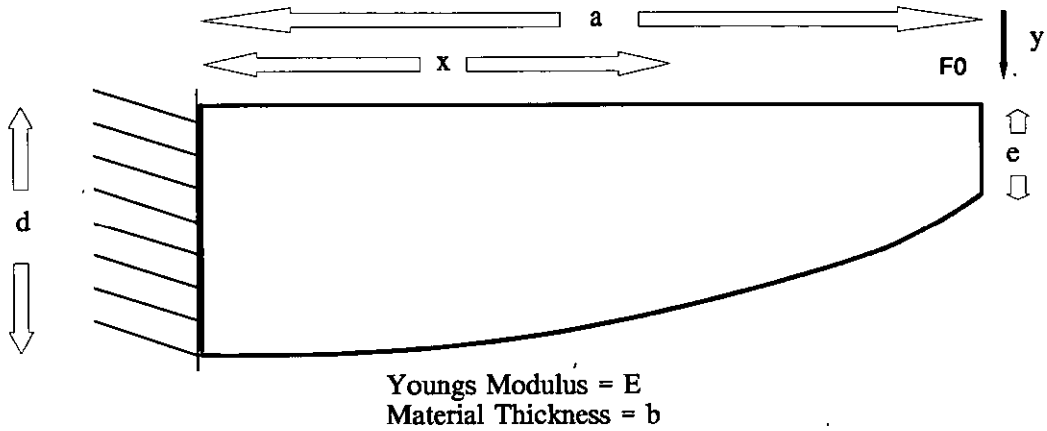

Figure 137: An Encastred Elliptical Beam.

$$\sin(z) = \frac{x}{\delta} \tag{210}$$

gives;

$$\frac{dy}{dx} = \gamma \left[\int \frac{(a - \delta \sin z)}{\delta^2 \cos^2 z} \partial z + k_1 \right] \tag{211}$$

and setting this to zero for x=0 (z=0) gives;

$$\frac{dy}{dx} = \gamma \left[\frac{a}{\delta^2} \tan z + \frac{(1 - \sec z)}{\delta} \right] \tag{212}$$

Since;

$$dx = \delta \cos z \, dz \tag{213}$$

On further integration to get y we get;

$$y = \gamma \left[\int \left(\frac{a}{\delta} \sin z + \cos z - 1 \right) dz + k_2 \right] \tag{214}$$

and setting this to zero for x=0 (z=0) gives;

$$y = \gamma \left[\frac{a}{\delta}(1 - \cos z) + \sin z - z \right] \tag{215}$$

Therefore the end beam compliance is given by;

$$S_a = \frac{12}{bEk^3} \left[\frac{a}{\delta}(1 - \cos z_a) + \sin z_a - z_a \right] \tag{216}$$

where;

$$z_a = \arcsin \left(\frac{a}{\delta} \right) \tag{217}$$

In consideration of the stress analysis results for the tapered beam, analysis for the elliptical beam is not considered necessary.

11.2.2 Finite Element Verification.

To verify the theory, a finite element mesh was constructed with overall size of;

$$d = 0.02,\ a = 0.065,\ b = 0.0065$$

Titanium was modelled, and variations of e and a values established by altering the lateral load point at different positions along the beam. Figure 138 graphically shows good correspondence between theoretical and finite element values. The only major variations occurring in the situation where the beam was loaded at the tip, and where the beam length a approaches the value for the beam depth d.

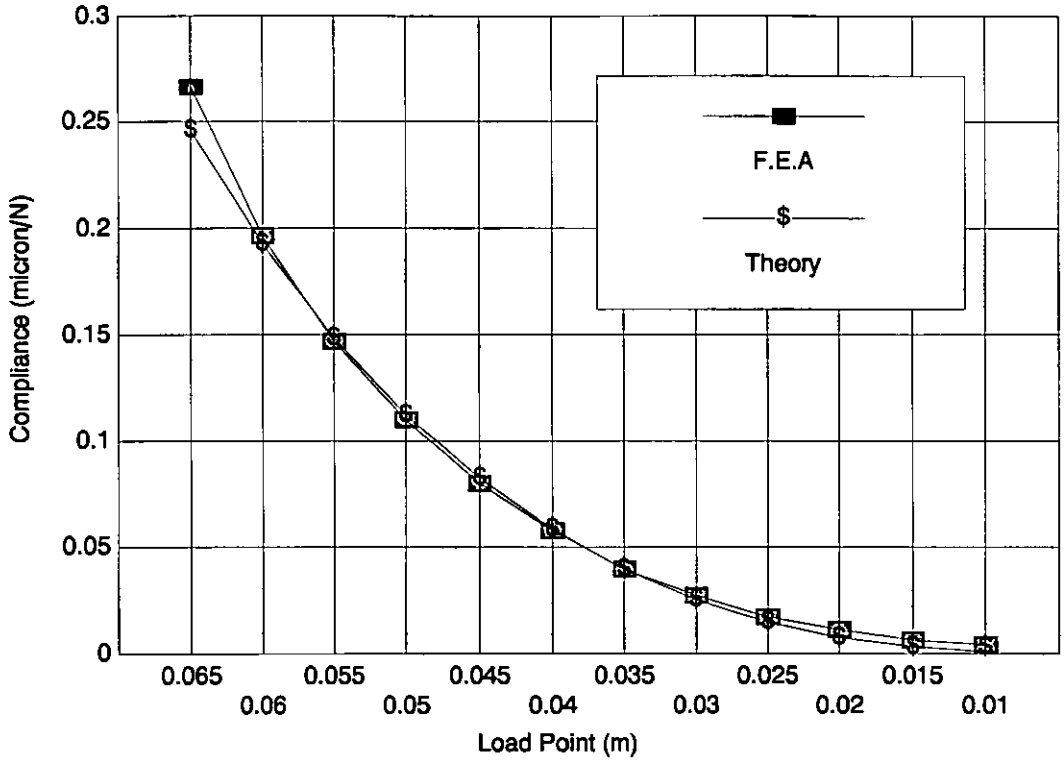

Figure 138 : Beam Compliance for various e and a values.

12 APPENDIX 2: BEAM DESIGNER PROGRAM LISTING.

The following program listing of the beam designer program is complete, and is provided so that the reader may appreciate the level of effort required to arrive at a working, easy to use program. It is written in Quick Basic 4.5, which is a fully structured language and can therefore be easily translated if desired to any other language of a similar structure, with only the graphical interface requiring significant alteration.

The portions of most interest, i.e. the Torsion algorithm and the Solution algorithm can be found in bold typeface starting on 243 and 248 respectively.

```
DECLARE SUB txt.dump ()
DECLARE SUB get.o.details ()
DECLARE SUB synthrightarc (d!, e!, l!)
DECLARE SUB synthleftarc (d!, e!, l!)
DECLARE SUB modstring (prompt$, value$)
DECLARE SUB sort.order ()
DECLARE SUB find.material (x$, pt%)
DECLARE SUB rationalise (xinput!, finput!, xoutput!, emat!, thickness!, a1!, a2!, l1!,
l2!, w1!, w2!, d!, e1!, e2!, foutput!, peak.stress!, stall.stress!)
DECLARE SUB disp.materials ()
DECLARE SUB position (x%, r%, c%)
DECLARE SUB pick.page (matpt%)
DECLARE FUNCTION structure.mass! (thickness!, a1!, a2!, l1!, l2!, w1!, w2!, d!, e1!,
e2!)
DECLARE FUNCTION arccos! (a!)
DECLARE FUNCTION beam.area! (a!, d!, e!)
DECLARE SUB choose.material (m$, em!, ys!, de!)
DECLARE SUB display.performance (efred!, free.stress!, stall.stress!, f.output!,
xout.free!, mass!)
DECLARE SUB centre (a$)
DECLARE SUB leader (a$, col%)
DECLARE SUB twait (seconds!)
DECLARE SUB elevate (xout!)
DECLARE FUNCTION arcsin! (a!)
DECLARE FUNCTION s.taper! (a!, b!, d!, e!, modulus!)
DECLARE FUNCTION password! ()
DECLARE SUB get.material ()
DECLARE SUB filing (a1!, a2!, l1!, l2!, w1!, w2!, d!, e1!, e2!)
DECLARE SUB read.mats ()
DECLARE SUB synthellipse (d!, e!, a!)
DECLARE SUB synthpillar (atx!, w!, l!)
DECLARE SUB syntharc (x!, y!, r!, sa!, ea!)
DECLARE SUB synthline (x1!, y1!, x2!, y2!)
DECLARE SUB create.dxf (a1!, a2!, l1!, l2!, w1!, w2!, d!, e1!, e2!)
DECLARE FUNCTION s.ellipse! (a!, b!, d!, e!, modulus!)
DECLARE SUB fmp (b!, a1!, modulus!, l1!, l2!, w1!, w2!, x!, f!, m!, p!)
DECLARE SUB solve (xin.free!, fin.stall!, xout.free!, modulus!, thickness!, a1!, a2!,
l1!, l2!, w1!, w2!, d!, e1!, e2!, fout.stall!, free.stress!, stall.stress!)
DECLARE FUNCTION hinge.stresses! (a1!, modulus!, thickness!, l1!, l2!, w1!, w2!, f!,
m!, p!)
DECLARE FUNCTION maxi! (a!, b!)
DECLARE SUB display.geometry (thickness!, a1!, a2!, l1!, l2!, w1!, w2!, d!, e1!, e2!)
DECLARE SUB linedisp (a$, aa!)
DECLARE SUB setup ()
DECLARE SUB draw.structure (a1!, a2!, l1!, l2!, w1!, w2!, d!, e1!, e2!)
DECLARE SUB pillar (w!, l!)
DECLARE FUNCTION efficiency! (xin.free!, fin.stall!, xout.free!, fout.stall!)
DECLARE SUB win1 ()
DECLARE SUB win2 ()
DECLARE FUNCTION keypress$ ()
DECLARE SUB show.commands ()
DECLARE SUB analyse (xin.free!, fin.stall!, xout.free!, modulus!, thickness!, a1!,
```

```
a2!, l1!, l2!, w1!, w2!, d!, e1!, e2!, fout.stall!, free.stress!, stall.stress!)
DECLARE SUB get.i.details ()
DECLARE SUB win3 ()
DECLARE SUB modvar (prompt$, value!)
DECLARE SUB win4 ()
DECLARE SUB display.parametrics ()
DECLARE SUB get.parametrics ()
DECLARE SUB get.geometry (a1!, a2!, l1!, l2!, w1!, w2!, d!, e1!, e2!)
DECLARE SUB standard.scale (factor!)
DECLARE SUB warp.geometry (a1!, a2!, l1!, l2!, w1!, w2!, d!, e1!, e2!)
DECLARE SUB title ()
DECLARE SUB display.help ()
DECLARE SUB win5 ()
COMMON SHARED match.factor.stall, safety.factor, yield.stress, material$
COMMON SHARED match.factor.rotate, max.stress, match.factor.beam, emat
COMMON SHARED stress.max, mass, dens
COMMON SHARED textmode%, graphmode%, toggle%, dscale
COMMON SHARED xinput, xoutput, finput, foutput, thickness, eff, eff.des
COMMON SHARED folin$, foang$, forad$, ver!
COMMON SHARED mats%, matpt%, num%
COMMON SHARED epower!, dpower!, ypower!, sort.mode$
num% = 100
DIM SHARED mat$(num%), emod!(num%), yield!(num%), density!(num%)
CONST pi! = 3.141592654#, true% = -1, false% = 0

ver = 4.5
SCREEN 12
WIDTH 80, 60
VIEW (160, 0)-(479, 239)
setup
CLS
title

solve xinput, finput, xoutput, emat, thickness, a1, a2, l1, l2, w1, w2, d, e1, e2,
foutput, peak.stress, stall.stress
analyse xinput, finput, xoutput, emat, thickness, a1, a2, l1, l2, w1, w2, d, e1, e2,
foutput, peak.stress, stall.stress
eff = efficiency(xinput, finput, xoutput, foutput)
mass = structure.mass(thickness, a1, a2, l1, l2, w1, w2, d, e1, e2)
display.geometry thickness, a1, a2, l1, l2, w1, w2, d, e1, e2
display.parametrics
display.performance eff, peak.stress, stall.stress, foutput, xoutput, mass
draw.structure a1, a2, l1, l2, w1, w2, d, e1, e2
    DO
        DO
            DO
                VIEW PRINT 57 TO 59
                show.commands
                k$ = INKEY$
                IF k$ <> "" THEN EXIT DO
            LOOP
            k$ = UCASE$(k$)
            LOCATE 57, 1
            PRINT SPACE$(LEN(c$))
            IF INSTR(CHR$(27) + "AGTHOEMDCRPFSQIW123456789", k$) <> 0 THEN EXIT DO
            PLAY "o0 l64 f"
        LOOP
        SOUND 500, 1
        SELECT CASE k$
            CASE "R"
                rationalise xinput, finput, xoutput, emat, thickness, a1, a2, l1, l2,
w1, w2, d, e1, e2, foutput, peak.stress, stall.stress
            CASE "F"
                filing a1, a2, l1, l2, w1, w2, d, e1, e2
            CASE "C"
                choose.material material$, emat, yield.stress, dens
                '   Analyse existing geometry if geometrically possible
'                IF d <> 0 THEN
 '                   analyse xinput, finput, xoutput, emat, thickness, a1, a2, l1, l2,
w1, w2, d, e1, e2, foutput, peak.stress, stall.stress
  '                   eff = efficiency(xinput, finput, xoutput, foutput)
   '                  mass = structure.mass(thickness, a1, a2, l1, l2, w1, w2, d, e1,
e2)
    '               END IF
            CASE "D"
                create.dxf a1, a2, l1, l2, w1, w2, d, e1, e2
            CASE "H"
                display.help
            CASE "I"
                '   input, output parameters
                win1
                CLS 2
                get.i.details
            CASE "O"
```

```
                '   output parameter
                win1
                CLS 2
                get.o.details
            CASE "A"
                '   Analyse existing geometry if geometrically possible
                IF d <> 0 THEN
                    analyse xinput, finput, xoutput, emat, thickness, a1, a2, l1, l2,
w1, w2, d, e1, e2, foutput, peak.stress, stall.stress
                    eff = efficiency(xinput, finput, xoutput, foutput)
                    mass = structure.mass(thickness, a1, a2, l1, l2, w1, w2, d, e1,
e2)
                END IF
            CASE "E"
                '   Elevate output movement
                IF d <> 0 THEN
                    elevate xoutput
                    solve xinput, finput, xoutput, emat, thickness, a1, a2, l1, l2,
w1, w2, d, e1, e2, foutput, peak.stress, stall.stress
                    analyse xinput, finput, xoutput, emat, thickness, a1, a2, l1, l2,
w1, w2, d, e1, e2, foutput, peak.stress, stall.stress
                    eff = efficiency(xinput, finput, xoutput, foutput)
                    mass = structure.mass(thickness, a1, a2, l1, l2, w1, w2, d, e1,
e2)
                END IF
            CASE "M"
                '   Select a material
                get.material
                mass = structure.mass(thickness, a1, a2, l1, l2, w1, w2, d, e1, e2)
            CASE "T"
                xinput = xoutput
                finput = foutput
                '   then re-check input, output parameters
                win1
                CLS 2
                get.i.details
            CASE "G"
                '   Edit Geometry
                get.geometry a1, a2, l1, l2, w1, w2, d, e1, e2
                mass = structure.mass(thickness, a1, a2, l1, l2, w1, w2, d, e1, e2)
            CASE "W"
                '   visually manipulate structure
                warp.geometry a1, a2, l1, l2, w1, w2, d, e1, e2
                analyse xinput, finput, xoutput, emat, thickness, a1, a2, l1, l2, w1,
w2, d, e1, e2, foutput, peak.stress, stall.stress
                eff = efficiency(xinput, finput, xoutput, foutput)
                mass = structure.mass(thickness, a1, a2, l1, l2, w1, w2, d, e1, e2)
            CASE "P"
                get.parametrics
                solve xinput, finput, xoutput, emat, thickness, a1, a2, l1, l2, w1,
w2, d, e1, e2, foutput, peak.stress, stall.stress
                analyse xinput, finput, xoutput, emat, thickness, a1, a2, l1, l2, w1,
w2, d, e1, e2, foutput, peak.stress, stall.stress
                eff = efficiency(xinput, finput, xoutput, foutput)
                mass = structure.mass(thickness, a1, a2, l1, l2, w1, w2, d, e1, e2)
            CASE "S"
                solve xinput, finput, xoutput, emat, thickness, a1, a2, l1, l2, w1,
w2, d, e1, e2, foutput, peak.stress, stall.stress
                analyse xinput, finput, xoutput, emat, thickness, a1, a2, l1, l2, w1,
w2, d, e1, e2, foutput, peak.stress, stall.stress
                eff = efficiency(xinput, finput, xoutput, foutput)
                mass = structure.mass(thickness, a1, a2, l1, l2, w1, w2, d, e1, e2)
            CASE "Q", CHR$(27)
                EXIT DO
            CASE "1" TO "9"
                dnum = VAL(k$)
                dscale = 2 ^ ((dnum - 5))
        END SELECT
        display.geometry thickness, a1, a2, l1, l2, w1, w2, d, e1, e2
        display.parametrics
        display.performance eff, peak.stress, stall.stress, foutput, xoutput, mass
        draw.structure a1, a2, l1, l2, w1, w2, d, e1, e2
    LOOP
END

SUB analyse (xin.free, fin.stall, xout.free, modulus, thickness, a1, a2, l1, l2, w1,
w2, d, e1, e2, fout.stall, free.stress, stall.stress)

STATIC req.gain, s.drive, s.input, aspect.ratio, f.stall, w, l
STATIC xstim, safety.factor.rotate, real.drive, f.drive, sin.total
STATIC s.stalled.input

'   NOTE xout.free , fout.free , free.stress , stall.stress are
'   MUTABLE. All others are INPUTS !!!
```

```
' First find free.stress

'   Input compliance ....

xstim = .000001
fmp thickness, a1, modulus, l1, l2, w1, w2, xstim, f, m, p
s.input = xstim / f
s.drive = xin.free / fin.stall

'   Find real input drive

sin.total = s.input + s.drive
f.drive = xin.free / sin.total
real.drive = f.drive * s.input

'   Find maximum stress in stalled hinges

fmp thickness, a1, modulus, l1, l2, w1, w2, real.drive, f, m, p
free.stress = hinge.stresses(a1, modulus, thickness, l1, l2, w1, w2, f, m, p)

'   Now find total stalled input compliance

s1 = l1 / modulus / w1 / thickness
s2 = l2 / modulus / w2 / thickness
sb1 = s.ellipse(a1, thickness, d, e1, modulus)
sb2 = s.ellipse(a2, thickness, d, e2, modulus)
s.stalled.input = s2 + (sb1 + s1) * a2 ^ 2 / (a1 + a2) ^ 2 + sb2 * a1 ^ 2 / (a1 + a2)
^ 2

'   Now find loading on drive

s.stat.total = s.stalled.drive + s.drive
f2 = xin.free / s.stat.total

'    Now find stresses

f1 = f2 * a2 / (a1 + a2)

sigma1 = f1 / w1 / thickness
sigma2 = f2 / w2 / thickness

stall.stress = maxi(sigma1, sigma2)

'   Now find output movement

xout.free = (a1 + a2) / a1 * real.drive

'   Now find output compliance of structure AND drive

s.out = (s1 + sb1) * a2 ^ 2 / a1 ^ 2 + (s2 + s.drive) * (a1 + a2) ^ 2 / a1 ^ 2 + sb2

'   Output stall force of ensemble

fout.stall = xout.free / s.out
END SUB

FUNCTION arccos (a)
    IF a = 0 THEN
        arccos = pi / 2
    ELSE
        arccos = ATN(SQR(1 - a * a) / a)
    END IF
END FUNCTION

FUNCTION arcsin (a)
        arcsin = ATN(a / SQR(1 - a * a))
END FUNCTION

FUNCTION beam.area (a, d, e)
    STATIC k, m, th1, th2, arg
    k = SQR(d * d - e * e) / a
    m = d / k
    th1 = arccos(0): th2 = arccos(a / m)
    arg = (th2 - th1) / 2 - (SIN(2 * th2) - SIN(2 * th1)) / 4
    beam.area = -k * m * m * arg
END FUNCTION

DEFINT A-Z
SUB centre (a$)
    STATIC l, s
    l = LEN(a$)
    s = 40 - l / 2
    PRINT TAB(s); a$;
END SUB
```

```
DEFSNG A-Z
SUB choose.material (m$, em, ys, de)
    win4
    CLS 2
    IF matpt% = 0 THEN matpt% = 1
    LOCATE 57, 1
    PRINT "CHOOSE MATERIAL"
    DO
        win4
        LOCATE 58, 1: PRINT "Select Material  "; mat$(matpt%); SPACE$(30);
        x$ = keypress$
        IF x$ = CHR$(13) THEN pick.page matpt%
        IF x$ = "6" AND matpt% < mats% THEN matpt% = matpt% + 1
        IF x$ = "7" THEN matpt% = 1
        IF x$ = "1" THEN matpt% = mats%
        IF x$ = "4" AND matpt% > 1 THEN matpt% = matpt% - 1
        m$ = mat$(matpt%): em = emod(matpt%): ys = yield(matpt%): de = density(matpt%)
        IF x$ = "5" OR x$ = CHR$(13) THEN EXIT DO
    LOOP
LOCATE 58, 1: PRINT SPACE$(70);
END SUB

SUB create.dxf (a1, a2, l1, l2, w1, w2, d, e1, e2)
STATIC file$, dr$, prime%, pw, pl
INPUT "Save DXF as file "; file$
INPUT "To which directory "; dr$
IF dr$ <> "" THEN dr$ = dr$ + "\"
IF file$ = "" THEN file$ = "beam"
CLS 2
OPEN "c:\beamodel\dxf.mid" FOR OUTPUT AS #1

'   shape segment here

    synthpillar -a1, w1, l1
    synthpillar 0, w2, l2
    synthline -a1 + w1, 0, -w2, 0
    synthline w2, 0, a2 + w2, 0
    synthleftarc d, e1, a1 + w1
    synthrightarc d, e2, a2 + w2
    PRINT "Press P for prime mover"
    p$ = keypress$
    IF p$ = "P" THEN
        INPUT "Width of Piezo (mm) ", pw
        pw = pw + 1
        pw = pw / 1000
        INPUT "Length of Piezo (mm) ", pl
        pl = pl / 1000
        CLS 2
        REM piezopad on hinge 2
        synthline -w2, -l2 - w2, -pw / 2, -l2 - w2 - pw / 2
        synthline w2, -l2 - w2, pw / 2, -l2 - w2 - pw / 2
        synthline -pw / 2, -l2 - w2 - pw / 2, pw / 2, -l2 - w2 - pw / 2
        REM beef on hinge 1
        synthline -a1 + w1, -l1 - w1, -pw / 2 - .001, -l1 - w1
        synthline -pw / 2 - .001, -l1 - w1, -pw / 2 - .001, -l2 - w2 - pw / 2 - pl
        synthline -pw / 2 - .001, -l2 - w2 - pw / 2 - pl, pw / 2 + .001, -l2 - w2 - pw
/ 2 - pl


    END IF
CLOSE #1
win5
SHELL "copy c:\beamodel\dxf.hdr+c:\beamodel\dxf.mid+c:\beamodel\dxf.end " + dr$ +
file$ + ".dxf"

CLS 2

END SUB

SUB disp.materials
    FOR j% = 1 TO mats%
        position j%, r%, c%
        LOCATE r%, c%
        COLOR 2 - 8 * (j% = matpt%)
        PRINT mat$(j%);
    NEXT j%
END SUB

    SUB display.geometry (thickness, a1, a2, l1, l2, w1, w2, d, e1, e2)
    win1
    centre "GEOMETRY STATUS": PRINT : PRINT
    toggle% = false%
    linedisp "Material thickness (b)", thickness
```

```
    linedisp "Hinge separation (a1)", a1
    linedisp "Output beam length (a2)", a2
    linedisp "Anchor hinge length (l1)", l1
    linedisp "Input hinge length (l2)", l2
    linedisp "Anchor hinge width (w1)", w1
    linedisp "Input hinge width (w2)", w2
    linedisp "Max beam width (d)", d
    linedisp "Min beam width 1 (e1)", e1
    linedisp "Min beam width 2 (e2)", e2
END SUB

SUB display.help
win5
COLOR 12
CLS
centre "H E L P   S C R E E N": PRINT : PRINT
PRINT "H     This page"
PRINT "I     Adjust input and output displacement and compliance"
PRINT "E     Elevate the output displacement incrementally, then re-solve"
PRINT "M     Adjust Material characteristics"
PRINT "C     Choose a material from the standard list, re-analyse"
PRINT "S     Determine the best geometry for the existing design parameters"
PRINT "P     Adjust matching parameters for various loss modes, then re-solve"
PRINT "G     Numerically adjust the geometry"
PRINT "W     Graphically adjust the geometry .. with dynamic analysis"
PRINT "A     Analyse the existing geometry"
PRINT "T     Transfer current output characteristics to input .. allows edit"
PRINT "D     Create a DXF file"
PRINT "F     Filing operations for geometry"
PRINT "Q     Really??!"
PRINT : PRINT
PRINT "                          Press a key"
kk$ = keypress$
CLS 2
END SUB

SUB display.parametrics
    win3
    toggle% = false%
    centre "PARAMETRICS STATUS": PRINT : PRINT
    linedisp "match.factor.stall", match.factor.stall
    linedisp "match.factor.rotate", match.factor.rotate
    linedisp "match.factor.beam", match.factor.beam
    linedisp "safety.factor", safety.factor
    linedisp "yield.stress", yield.stress
    linedisp "youngs modulus", emat
END SUB

SUB display.performance (efred, free.stress, stall.stress, f.output, xout.free, mass)
    win2
    PRINT "                                PERFORMANCE STATUS": PRINT
    linedisp "Efficiency", efred
    linedisp "free stress [MPa]", free.stress / 1000000!
    linedisp "stall stress [MPa]", stall.stress / 1000000!
    linedisp "output force", f.output
    linedisp "output movement", xout.free
    linedisp "mass [gram]", mass * 1000
END SUB

SUB draw.structure (a1, a2, l1, l2, w1, w2, d, e1, e2)
    STATIC th1, th2
    IF d <> 0 AND d > e1 AND d > e2 THEN
        standard.scale dscale
        CLS 1
        win5
        LOCATE 5, 5: PRINT material$; SPACE$(20);
        LOCATE 7, 5: PRINT USING "Scale = X ##.###"; dscale
        aa1 = a1 + w1: aa2 = a2 + w2
        COLOR 3
        PSET (0, 0): pillar w2, l2
        PSET (-a1, 0): pillar w1, l1
        LINE (-a1 + w1, 0)-(-w2, 0)
        LINE (w2, 0)-(aa2, 0)
        LINE (-aa1, 0)-STEP(0, e1)
        LINE (aa2, 0)-STEP(0, e2)
        k1 = SQR(d * d - e1 * e1) / aa1
        PSET (0, d)
        FOR x = 0 TO aa1 STEP aa1 / 25
            y = SQR(d ^ 2 - k1 ^ 2 * x ^ 2)
            LINE -(-x, y)
        NEXT x
        LINE -(-aa1, e1)
        k2 = SQR(d * d - e2 * e2) / aa2
        PSET (0, d)
```

```
        FOR x = 0 TO aa2 STEP aa2 / 25
            y = SQR(d ^ 2 - k2 ^ 2 * x ^ 2)
            LINE -(x, y)
        NEXT x
        LINE -(aa2, e2)
    ELSE
        PLAY "16f"
    END IF
END SUB

FUNCTION efficiency (xin.free, fin.stall, xout.free, fout.stall)
STATIC e.in, e.out
    e.in = xin.free * fin.stall
    e.out = xout.free * fout.stall
    efficiency = e.out / e.in
END FUNCTION

SUB elevate (xout)
    win4
    CLS 2
    LOCATE 57, 1
    PRINT "ELEVATE OUTPUT VALUE"
    xout = xout * 1000000!
    DO
        win4
        LOCATE 58, 1
        PRINT USING "Current output (micron) ####.#"; xout;
        x$ = keypress$
        IF x$ = "8" THEN xout = xout * 1.01
        IF x$ = "2" THEN xout = xout / 1.01
        IF x$ = "9" THEN xout = xout * 1.1
        IF x$ = "3" THEN xout = xout / 1.1
        IF x$ = "5" THEN EXIT DO
    LOOP
xout = INT(xout)
LOCATE 58, 1: PRINT SPACE$(70);
xout = xout / 1000000!
END SUB

SUB filing (a1, a2, l1, l2, w1, w2, d, e1, e2)
win4

DO
CLS 2
PRINT "Filing ... Save Load Dir Text Abort"
    DO
        kk$ = keypress$
        IF INSTR("SLTDA", kk$) <> 0 THEN
            EXIT DO
        ELSE
            PLAY "164a"
        END IF
    LOOP
        SELECT CASE kk$
            CASE "A"
                EXIT DO
            CASE "S"
                INPUT "Save filename "; sf$
                OPEN sf$ + ".STR" FOR OUTPUT AS #1
                PRINT #1, a1, a2, l1, l2, w1, w2, d, e1, e2
                CLOSE #1
            CASE "L"
                INPUT "Load filename "; lf$
                OPEN lf$ + ".STR" FOR INPUT AS #1
                INPUT #1, a1, a2, l1, l2, w1, w2, d, e1, e2
                CLOSE #1
            CASE "D"
                win5
                CLS 2
                FILES "*.str"
                PRINT "Press a key to continue"
                kkk$ = keypress$
                CLS 2
                win4
            CASE "T"
                txt.dump
        END SELECT
LOOP
CLS 2
END SUB

DEFINT A-Z
SUB find.material (x$, pt%)
    STATIC j, g$
```

```
    j = pt%
    DO
        j = j + 1
        IF j = mats% THEN j = 1
        g$ = LEFT$(mat$(j), 1)
        IF g$ = x$ THEN
            pt% = j
            EXIT DO
        END IF
        IF j >= mats THEN EXIT DO
    LOOP
END SUB

DEFSNG A-Z
SUB fmp (b, a1, modulus, l1, l2, w1, w2, x, f, m, p)
    STATIC de, ep
    STATIC r1, r2, s1, s2, t1, t2
    STATIC square, cube

    i1 = b * w1 ^ 3 / 12
    i2 = b * w2 ^ 3 / 12

    square = (l1 ^ 2 / i1 + l2 ^ 2 / i2)
    cube = (l1 ^ 3 / i1 + l2 ^ 3 / i2)

    de = -2 / 3 * cube / square
    ep = a1 * l1 ^ 2 / i1 / square

    r1 = modulus * i1 * x / a1
    r2 = modulus * i2 * x / a1
    s1 = l1 * (a1 - ep)
    s2 = l2 * ep
    t1 = (l1 / 2 + de) * l1
    t2 = (l2 / 2 + de) * l2

    f = (r1 * t2 + r2 * t1) / (s1 * t2 + s2 * t1)
    p = (s1 * f - r1) / t1
    m = de * p + ep * f

    m1 = f * a1 - m
    m2 = m

END SUB

SUB get.geometry (a1, a2, l1, l2, w1, w2, d, e1, e2)
STATIC e1rat, e2rat
    win3
    CLS 2
    e1rat = e1 / d: e2rat = e2 / d
    modvar "thickness", thickness
    draw.structure a1, a2, l1, l2, w1, w2, d, e1, e2
    modvar "a1", a1
    draw.structure a1, a2, l1, l2, w1, w2, d, e1, e2
    modvar "a2", a2
    draw.structure a1, a2, l1, l2, w1, w2, d, e1, e2
    modvar "l1", l1
    draw.structure a1, a2, l1, l2, w1, w2, d, e1, e2
    modvar "l2", l2
    draw.structure a1, a2, l1, l2, w1, w2, d, e1, e2
    modvar "w1", w1
    draw.structure a1, a2, l1, l2, w1, w2, d, e1, e2
    modvar "w2", w2
    draw.structure a1, a2, l1, l2, w1, w2, d, e1, e2
    modvar "d", d
    e1 = d * e1rat: e2 = d * e2rat
    draw.structure a1, a2, l1, l2, w1, w2, d, e1, e2
    modvar "e1", e1
    draw.structure a1, a2, l1, l2, w1, w2, d, e1, e2
    modvar "e2", e2
    draw.structure a1, a2, l1, l2, w1, w2, d, e1, e2
    win3
    CLS 2
END SUB

SUB get.i.details
    win3
    CLS 2
    IF xoutput < 2 * xinput THEN xoutput = 2 * xinput
    DO
        modvar "input free movement", xinput
        modvar "input stall force", finput
        IF xoutput > xinput THEN EXIT DO
        PLAY "l32g"
    LOOP
```

```
    win3
    CLS 2
END SUB

SUB get.material
STATIC ys, em, th
    win3
    CLS 2
    ys = yield.stress / 1000000!
    em = emat / 1E+09
    th = thickness * 1000!
    modvar "yield.stress [MPa]", ys
    modvar "youngs modulus [GPa]", em
    modvar "safety.factor", safety.factor
    modvar "billet thickness [mm]", th
    modvar "density [kg/m^3]", dens
    yield.stress = ys * 1000000!
    emat = em * 1E+09
    thickness = th / 1000
    win3
    CLS 2
END SUB

SUB get.o.details
    win3
    CLS 2
    IF xoutput < 2 * xinput THEN xoutput = 2 * xinput
    DO
        modvar "output free movement", xoutput
        IF xoutput > xinput THEN EXIT DO
        PLAY "l32g"
    LOOP
    win3
    CLS 2

END SUB

SUB get.parametrics
    win3
    CLS 2
    modvar "match.factor.stall", match.factor.stall
    modvar "match.factor.rotate", match.factor.rotate
    modvar "match.factor.beam", match.factor.beam
    CLS 2
END SUB

FUNCTION hinge.stresses (a1, modulus, thickness, l1, l2, w1, w2, f, m, p)
    STATIC m1, m2, sig1, sig2, bigsig, i1, i2
        '   PRINT f, m, p
        i1 = w1 ^ 3 * thickness / 12
        i2 = w2 ^ 3 * thickness / 12

        m1 = f * a1 - m
        m2 = m

        sig1 = (m1 - p * l1) * w1 / 2 / i1 + f / thickness / w1
        sig2 = (m2 + p * l2) * w1 / 2 / i2 - f / thickness / w2
        hinge.stresses = maxi(sig1, sig2)
END FUNCTION

DEFINT A-Z
FUNCTION keypress$
STATIC k, k$, tog
DO
    DO
        k$ = INKEY$
        IF k$ <> "" THEN EXIT DO
    LOOP
    k = ASC(k$)
    IF k >= 13 AND k < 128 THEN EXIT DO
LOOP
keypress$ = UCASE$(k$)
END FUNCTION

SUB leader (a$, col)
    STATIC l, tog, j, mark, char$
    l = LEN(a$)
    mark = 0
    FOR j = 1 TO l
        IF mark THEN
            COLOR col + 8
        ELSE
            COLOR col
        END IF
```

```
        char$ = MID$(a$, j, 1)
        mark = (char$ = " ")
        PRINT char$;
    NEXT j
END SUB

DEFSNG A-Z
SUB linedisp (a$, aa)
    al% = LEN(a$)
    f$ = "####.######"
    IF ABS(aa) >= 1000 THEN f$ = f$ + "^^^^"
    lead$ = STRING$(24 - al%, 46)
    IF toggle% THEN PRINT TAB(41);
    PRINT UCASE$(a$); lead$;
    IF toggle% THEN
        PRINT USING f$; aa
    ELSE
        PRINT USING f$; aa;
    END IF
    toggle% = NOT toggle%
END SUB

FUNCTION maxi (a, b)
STATIC ma, s
IF ABS(a) > ABS(b) THEN
    ma = a
    s = SGN(a)
ELSE
    ma = b
    s = SGN(b)
END IF
maxi = ma * s
END FUNCTION

DEFINT A-Z
SUB modstring (prompt$, value$)
    win3
    CLS 2
    PRINT UCASE$(prompt$); " ";
    PRINT USING " & "; value$;
    INPUT dummy$
    IF dummy$ <> "" THEN
        value$ = dummy$
    END IF
END SUB

DEFSNG A-Z
SUB modvar (prompt$, value)
    win3
    CLS 2
    PRINT UCASE$(prompt$); " ";
    PRINT USING "#####.####### "; value;
    INPUT dummy$
    IF dummy$ <> "" THEN
        value = VAL(dummy$)
    END IF
END SUB

FUNCTION password
STATIC p$, j%, thispass$
thispass$ = LEFT$(DATE$, 2) + MID$(DATE$, 4, 2)
FOR k = 1 TO 5
    FOR j = 8 TO 15
        COLOR j
        LOCATE 21, 1
        PRINT "                                    ========"
        PRINT "                                    PASSWORD"
        PRINT "                                    ========"
    NEXT j
NEXT k
'   thispass$ = "BBB"
p$ = ""
FOR j% = 1 TO LEN(thispass$)
    p$ = p$ + keypress$
NEXT j%
password = (p$ = thispass$)
END FUNCTION

SUB pick.page (matpt%)
    STATIC j%, r%, c%
    r% = 0: c% = 1
    VIEW PRINT
    CLS 2
    DO
```

```
        disp.materials
        x$ = keypress$
        IF x$ >= "A" AND x$ <= "Z" THEN find.material x$, matpt%
        IF x$ = CHR$(13) THEN EXIT DO
        IF x$ = "5" THEN
            sort.order
        END IF
        IF x$ = "7" THEN matpt% = 1
        IF x$ = "1" THEN matpt% = mats%
        IF x$ = "8" AND matpt% > 1 THEN matpt% = matpt% - 1
        IF x$ = "2" AND matpt% < mats% THEN matpt% = matpt% + 1
        IF x$ = "4" AND matpt% > 40 THEN matpt% = matpt% - 40
        IF x$ = "6" AND matpt% < mats% - 40 THEN matpt% = matpt% + 40
        m$ = mat$(matpt%): em = emod(matpt%): ys = yield(matpt%): de = density(matpt%)
    LOOP
    CLS 2
END SUB

SUB pillar (w, l)
    PSET STEP(w, 0)
    CIRCLE STEP(0, -w / 2), w / 2, , pi! / 2, pi!
    PSET STEP(-w / 2, 0)
    LINE -STEP(0, -l)
    CIRCLE STEP(w / 2, 0), w / 2, , pi!, 3 * pi! / 2
    PSET STEP(0, -w / 2)
    LINE -STEP(-2 * w, 0)
    CIRCLE STEP(0, w / 2), w / 2, , 3 * pi! / 2, 2 * pi!
    PSET STEP(w / 2, 0)
    LINE -STEP(0, l)
    CIRCLE STEP(-w / 2, 0), w / 2, , 0, pi! / 2
    PSET STEP(w, w / 2)
END SUB

DEFINT A-Z
SUB position (x, r, c)
    r = (x - 1) MOD 40 + 1
    c = 1 + 26 * INT((x - 1) / 40)
END SUB

DEFSNG A-Z
SUB quickfitscreen (a1, a2, l1, l2, d)
    STATIC lt, rt, up, dn, fit, asp, hrat, lmax, hh
    asp = 640 / 480
    fit = 2
    lt = -a1
    rt = a2
    lmax = maxi(l1, l2)
    hh = lmax + d
    hspan = rt - lt
    vspan = hspan / asp
    up = vspan * d / hh
    dn = -vspan * lmax / hh
    lt = lt * fit
    rt = rt * fit
    up = up * fit
    dn = dn * fit
    WINDOW (lt, dn)-(rt, up)
    REM CLS1
END SUB

SUB rationalise (xinput, finput, xoutput, emat, thickness, a1, a2, l1, l2, w1, w2, d,
e1, e2, foutput, peak.stress, stall.stress)
STATIC perf, lc%
    modvar "Desired efficiency", eff.des
    win5
    lc% = 0
    match.factor.stall = .02
DO
    lc% = lc% + 1
    solve xinput, finput, xoutput, emat, thickness, a1, a2, l1, l2, w1, w2, d, e1, e2,
foutput, peak.stress, stall.stress
    eff = efficiency(xinput, finput, xoutput, foutput)
    perf = 100 * eff / eff.des
    IF perf > 99.5 AND perf < 100.9 THEN EXIT DO
    match.factor.stall = match.factor.stall + .0071 * (perf - 100)
    p$ = STR$(INT(eff * 100 - 17))
    PLAY "L64N" + p$
    IF lc% > 13 OR ABS(match.factor.stall) > .8 THEN
        PLAY "O0 l8 a p8 l4 c+"
        EXIT DO
    END IF
    REM PRINT USING "  ###.###"; match.factor.stall; 100 * eff; 1000 * mass; perf
LOOP
analyse xinput, finput, xoutput, emat, thickness, a1, a2, l1, l2, w1, w2, d, e1, e2,
```

```
foutput, peak.stress, stall.stress
mass = structure.mass(thickness, a1, a2, l1, l2, w1, w2, d, e1, e2)
CLS 2

END SUB

SUB read.mats
STATIC j
OPEN "material.dat" FOR INPUT AS #1
INPUT #1, mats%
FOR j% = 1 TO mats%
    INPUT #1, mat$(j%)
    mat$(j%) = UCASE$(mat$(j%))
    INPUT #1, emod(j%)
    emod(j%) = emod(j%) * 1E+09
    INPUT #1, yield(j%)
    yield(j%) = yield(j%) * 1000000!
    INPUT #1, density(j%)
NEXT j%
CLOSE #1
END SUB

FUNCTION s.ellipse (a, b, d, e, modulus)
STATIC bracket, k, delta, za, fred
        '   d is max width
        '   a is beam length
        '   e is min width
        '   b is uniform thickness

        k = SQR(d * d - e * e) / a
        delta = d / k
        za = arcsin(a / delta)
        bracket = a / delta * (1 - COS(za)) + SIN(za) - za
        fred = ABS(12 * bracket / b / modulus / k ^ 3)
        '   PRINT e, fred
        s.ellipse = fred
END FUNCTION

FUNCTION s.taper (a, b, d, e, modulus)
STATIC bracket
        '   d is max width
        '   a is beam length
        '   e is min width
        '   b is uniform thickness

        bracket = 2 * LOG(e / d) + (e / d - 1) * (e / d - 3)
        s.taper = ABS(6 * a ^ 3 * bracket / modulus / b / ((e - d) ^ 3))
END FUNCTION

SUB setup
    xinput = .000015
    finput = 850
    xoutput = .00003
    thickness = .0065
    match.factor.stall = .1
    match.factor.rotate = .1
    eff.des = .7
    safety.factor = .15
    match.factor.beam = .1
    emat = 1.1E+11
    yield.stress = 4.8E+08
    dens = 4540
    textmode% = true%
    graphmode% = true%
    dscale = 1
    folin$ = "#####.######"
    foang$ = "#####.######"
    forad$ = "#####.######"
    material$ = "UN-SPECIFIED"
    read.mats
    matpt% = 1
    epower = 2
    ypower = 1
    dpower = -.5
    sort.mode$ = "N"
END SUB

SUB show.commands
STATIC coltog%, col%
    coltog% = NOT coltog%
    IF coltog% THEN
        col% = 4
    ELSE
        col% = 5
```

```
    END IF
    c$ = " Help Inpt Elev Matl Chse Solv Parm Ratn Geom Warp Anls Tran DXF File Quit"
    LOCATE 57, 1
    leader c$, col%
    twait .2
END SUB

SUB solve (xin.free, fin.stall, xout.free, modulus, thickness, a1, a2, l1, l2, w1, w2,
d, e1, e2, fout.stall, free.stress, stall.stress)
'   Complete solution algorithm
'   Solves for structure given; xin.free , fin.stall , xout.free
'   Note xout.free is MUTABLE

STATIC req.gain, s.drive, s.input, aspect.ratio, f.stall, w, l
STATIC xstim, safety.factor.rotate, real.drive
STATIC turn%, abort1%, abort2%, good%

req.gain = xout.free / xin.free


'   maximum stress is....
max.stress = yield.stress * safety.factor
stall.stress = max.stress

'   stall infinitely stiff arm, and assume h1 & h2 are very close
s.drive = xin.free / fin.stall

'   force input compliance to be a fraction of drive compliance
s.input = s.drive * match.factor.stall

'   assume l = 2 allows a solution of aspect ratio : aspect =l/w
aspect.ratio = s.input * thickness * modulus / 2

f.stall = xin.free / (s.input + s.drive)
w = f.stall / max.stress / thickness
w1 = w: w2 = w
l = w * aspect.ratio
l1 = l: l2 = l

'   now find a1 and a2 to minimise bending losses in free movement
'   start with a1 = 3 * w1
'   find solution so that input compliance is a factor of drive
'   compliance

xstim = .000001
a1 = 3 * w1

DO
    ' Performance check

    DO
        fmp thickness, a1, modulus, l1, l2, w1, w2, xstim, f, m, p
        s.input = xstim / f
        IF s.input >= s.drive / match.factor.rotate THEN
            EXIT DO
        END IF
        a1 = a1 * (1 + match.factor.rotate)

    LOOP

    '    now check stresses in hinges for these values....
    '   first find free operating point

    '   Stress check

    fin = xin.free / (s.drive + s.input)
    xin.real = fin * s.input

    '   now find f , m , p
        fmp thickness, a1, modulus, l1, l2, w1, w2, xin.real, f, m, p
        free.stress = hinge.stresses(a1, modulus, thickness, l1, l2, w1, w2, f, m, p)
        safety.factor.rotate = free.stress / max.stress
        '   PRINT safety.factor.rotate
    IF safety.factor.rotate > 1 THEN
        '   readjust a1 to obtain a lower safety.factor.rotate
        a1 = a1 * (1 + match.factor.rotate)
    ELSE
        EXIT DO
    END IF
LOOP

'    now find a2 based on loading of hinges and gain required

fmp thickness, a1, modulus, l1, l2, w1, w2, xstim, f, m, p
```

```
s.input = xstim / f
f.real = xin.free / (s.input + s.drive)
real.drive = f.real * s.input
real.gain = xout.free / real.drive
a2 = a1 * (real.gain - 1)

'   Now find beam geometry
'   Stage 1 is to find aan almost uniform thickness beam where
'    e1=.99 * d : e2 = e1
'   such that the input compliance is no more than necessary

'    linear compliances of the hinges ...

s1 = l1 / modulus / w1 / thickness
s2 = l2 / modulus / w2 / thickness

s.i.beam.req = match.factor.beam * (s.drive + s1 + s2)

'   Start with d = w2

d = w2
good% = false%
DO
    e1 = d * .99: e2 = e1
    sb1 = s.ellipse(a1, thickness, d, e1, modulus)
    sb2 = s.ellipse(a2, thickness, d, e2, modulus)
    s.i.beam = sb1 * (a2 / (a1 + a2)) ^ 2 + sb2 * (a1 / (a1 + a2)) ^ 2
    good% = ((s.i.beam / s.i.beam.req) < (1 - match.factor.beam))
    IF good% THEN
        REM PLAY "o6164f"
        EXIT DO
    ELSE
        d = d * 1.05
    END IF
LOOP


'   Best structure output compliance, including drive is ....

s.out.best = (s1 + sb1) * (a2 / a1) ^ 2 + (s2 + s.drive) * ((a1 + a2) / a1) ^ 2 + sb2
good% = false%
FOR turn% = 1 TO 2
    '   do e1 ane e2 in turn
    DO
        SELECT CASE turn%
            CASE 1
                e1 = e1 * .95
                e2 = d * .99
            CASE 2
                e2 = e2 * .95
                e1 = d * .99
        END SELECT
        sb1 = s.ellipse(a1, thickness, d, e1, modulus)
        sb2 = s.ellipse(a2, thickness, d, e2, modulus)
        s.out = (s1 + sb1) * (a2 / a1) ^ 2 + (s2 + s.drive) * ((a1 + a2) / a1) ^ 2 +
sb2
        abort1% = (e1 / d < match.factor.beam)
        abort2% = (e2 / d < match.factor.beam)
        good% = ((s.out / s.out.best) >= (1 + match.factor.beam / 10))
        REM IF abort1% OR abort2% THEN PLAY "o2164f"
        REM IF good% THEN PLAY "o6164f"
        IF good% OR abort1% OR abort2% THEN
            IF turn% = 1 THEN e1.found = e1
            IF turn% = 2 THEN e2.found = e2
            EXIT DO
        END IF
    LOOP
NEXT turn%
e1 = e1.found
e2 = e2.found

'    DESIGN NOW COMPLETE

'        display.geometry thickness, a1, a2, l1, l2, w1, w2, d, e1, e2
'        draw.structure a1, a2, l1, l2, w1, w2, d, e1, e2
        sb1 = s.ellipse(a1, thickness, d, e1, modulus)
        sb2 = s.ellipse(a2, thickness, d, e2, modulus)
        s.out.total = (s1 + sb1) * a2 ^ 2 / a1 ^ 2 + (s2 + s.drive) * (a1 + a2) ^ 2 /
a1 ^ 2 + sb2

fout.stall = xout.free / s.out.total
peak.stress = free.stress
END SUB
```

```
DEFINT A-Z
SUB sort.order
STATIC j, suc, ee1!, yy1!, dd1!, mm1$, ee2!, yy2!, dd2!, mm2$
    modstring "Sort Mode - N/E/Y/D/S", sort.mode$
    IF sort.mode$ = "" THEN
        sort.mode$ = "N"
    ELSE
        sort.mode$ = UCASE$(LEFT$(sort.mode$, 1))
    END IF
    IF sort.mode$ = "S" THEN
        modvar "Power of Young's Modulus", epower!
        modvar "Power of Yield Stress", ypower!
        modvar "Power of Density", dpower!
    END IF

    DO
        suc = 0
        FOR j = 1 TO mats - 1
        REM Take Note
        ee1! = emod!(j): yy1! = yield!(j): dd1! = density!(j): mm1$ = mat$(j)
        ee2! = emod!(j + 1): yy2! = yield!(j + 1): dd2! = density!(j + 1): mm2$ =
mat$(j + 1)

        SELECT CASE sort.mode$
            CASE "E"
                perf! = ee2! / ee1!
            CASE "Y"
                perf! = yy2! / yy1!
            CASE "D"
                perf! = dd2! / dd1!
            CASE "S"
                perf! = ((ee2! / ee1!) ^ epower!) * ((yy2! / yy1!) ^ ypower!) * ((dd2!
/ dd1!) ^ dpower!)
            CASE ELSE
                perf! = 0
        END SELECT


        IF perf! > 1! THEN
            suc = -1
            REM swap 'em
            emod!(j + 1) = ee1!: yield!(j + 1) = yy1!: density!(j + 1) = dd1!: mat$(j
+ 1) = mm1$
            emod!(j) = ee2!: yield!(j) = yy2!: density!(j) = dd2!: mat$(j) = mm2$
        END IF
        NEXT j
        IF suc = 0 THEN EXIT DO
    LOOP

    VIEW PRINT
    CLS 2
END SUB

DEFSNG A-Z
SUB standard.scale (factor)
    STATIC lt, rt, up, dn, fit, asp, hrat, lmax, hh
    across = 640
    down = 480
    fit = 2000 * 2.66666
    lt = -across / 2 / factor / fit
    rt = across / 2 / factor / fit
    up = down / 2 / factor / fit
    dn = -down / 2 / factor / fit
    WINDOW (lt, dn)-(rt, up)
END SUB

FUNCTION structure.mass (thickness, a1, a2, l1, l2, w1, w2, d, e1, e2)
    STATIC ab1, ab2, ah1, ah2, area
    ab1 = beam.area(a1, d, e1)
    ab2 = beam.area(a2, d, e2)
    ah1 = l1 * w1
    ah2 = l2 * w2
    area = ab1 + ab2 + ah1 + ah2
    structure.mass = area * thickness * dens
END FUNCTION

SUB syntharc (x, y, r, sa, ea)
    REM angles in degrees!!!
    REM convert to millimeters
    xx = x * 1000
    yy = y * 1000
    rr = r * 1000
    PRINT #1, "ARC"
    PRINT #1, "  8"
```

```
    PRINT #1, "0"
    PRINT #1, " 10"
        PRINT #1, USING folin$; xx
    PRINT #1, " 20"
        PRINT #1, USING folin$; yy
    PRINT #1, " 40"
        PRINT #1, USING forad$; rr
    PRINT #1, " 50"
        PRINT #1, USING foang$; sa
    PRINT #1, " 51"
        PRINT #1, USING foang$; ea
    PRINT #1, "  0"
END SUB

SUB synthellipse (d, e, a)
STATIC k, x1, y1, x2, y2, x, y
x1 = 0: y1 = d
k = SQR(d * d - e * e) / a
FOR x = 0 TO a STEP a / 20
    y = SQR(d * d - k * k * x * x)
    x2 = x: y2 = y
    synthline x1, y1, x2, y2
    x1 = x2: y1 = y2
NEXT x
IF a <> x1 THEN
    synthline x1, y1, a, e
END IF
END SUB

SUB synthleftarc (d, e, l)
STATIC f
IF l > (d - e) THEN
    f = (l ^ 2 + e ^ 2 - d ^ 2) / 2 / (d - e)
    ea = 90 + 180 / pi * ATN(l / (f + e))
    syntharc 0, -f, d + f, 90, ea
    synthline -l, e, -l, 0
ELSE
    syntharc 0, d - l, l, 90, 180
    synthline -l, d - l, -l, 0
END IF

END SUB

SUB synthline (x1, y1, x2, y2)
STATIC xx1, yy1, xx2, yy2, fo$
    REM convert to millimeters
    xx1 = x1 * 1000: xx2 = x2 * 1000
    yy1 = y1 * 1000: yy2 = y2 * 1000
    PRINT #1, "LINE"
    PRINT #1, "  8"
    PRINT #1, "0"
    PRINT #1, " 10"
        PRINT #1, USING folin$; xx1
    PRINT #1, " 20"
        PRINT #1, USING folin$; yy1
    PRINT #1, " 11"
        PRINT #1, USING folin$; xx2
    PRINT #1, " 21"
        PRINT #1, USING folin$; yy2
    PRINT #1, "  0"
END SUB

SUB synthpillar (atx, w, l)
    syntharc atx - w, -w / 2, w / 2, 0, 90
    synthline atx - w / 2, -w / 2, atx - w / 2, -w / 2 - l
    syntharc atx - w, -w / 2 - l, w / 2, 270, 0
    synthline atx - w, -w - l, atx + w, -w - l
    syntharc atx + w, -w / 2 - l, w / 2, 180, 270
    synthline atx + w / 2, -w / 2, atx + w / 2, -w / 2 - l
    syntharc atx + w, -w / 2, w / 2, 90, 180
END SUB

SUB synthrightarc (d, e, l)
STATIC f
IF l > (d - e) THEN
    f = (l ^ 2 + e ^ 2 - d ^ 2) / 2 / (d - e)
    sa = 90 - 180 / pi * ATN(l / (f + e))
    syntharc 0, -f, d + f, sa, 90
    synthline l, e, l, 0
ELSE
    syntharc 0, d - l, l, 0, 90
    synthline l, d - l, l, 0
END IF
```

```
END SUB

SUB title
    VIEW PRINT 10 TO 25
    LOCATE 10, 1
    centre "F L E X U R E   H I N G E   A M P L I F I Y I N G   L E V E R"
    PRINT : PRINT : PRINT
    centre "D E S I G N   S Y S T E M "
    PRINT : PRINT : PRINT
    centre "V e r s i o n  " + STR$(ver!)
    PRINT : PRINT : PRINT : PRINT : PRINT
'    IF NOT password THEN SYSTEM
centre "Press a key"
k$ = keypress$
    CLS 2
END SUB

SUB twait (seconds!)
    STATIC t!
    t! = TIMER + seconds!
    DO
    IF TIMER > t! THEN EXIT DO
    LOOP
END SUB

DEFINT A-Z
SUB txt.dump
STATIC x, y, a, l$
win4
CLS 2
INPUT "Dump File Name "; df$
IF df$ = "" THEN GOTO dennis
OPEN df$ FOR OUTPUT AS #1
    FOR y = 30 TO 57
    l$ = ""
        FOR x = 1 TO 80
             l$ = l$ + CHR$(SCREEN(y, x))
             REM PRINT a
        NEXT x
        PRINT #1, l$
    NEXT y
CLOSE #1
dennis:
CLS 2
END SUB

DEFSNG A-Z
SUB warp.geometry (a1, a2, l1, l2, w1, w2, d, e1, e2)
    '   Allow visual manipulation of geometry

    STATIC pt%, quit%, adjer, update%
    DIM v(10), v$(10)
    v$(1) = "thickness": v$(2) = "a1": v$(3) = "a2": v$(4) = "l1": v$(5) = "l2"
    v$(6) = "w1": v$(7) = "w2": v$(8) = "d": v$(9) = "e1": v$(10) = "e2"
    IF pt% = 0 THEN pt% = 1
    quit% = false%
    adjer = .1
    win4
    CLS 2
    LOCATE 57, 1
    PRINT "WARP GEOMETRY - (NUM LOCK ON)"
    DO
        update% = false%
        win4
        v(1) = thickness: v(2) = a1: v(3) = a2: v(4) = l1: v(5) = l2
        v(6) = w1: v(7) = w2: v(8) = d: v(9) = e1: v(10) = e2
        LOCATE 58, 1: PRINT "Select parameter (+/-/Ent)  "; v$(pt%); SPACE$(10);
        x$ = keypress$
        IF x$ = "6" AND pt% < 10 THEN pt% = pt% + 1
        IF x$ = "4" AND pt% > 1 THEN pt% = pt% - 1
        IF x$ = "7" THEN pt% = 1
        IF x$ = "1" THEN pt% = 10
        update% = (INSTR("82", x$) <> 0)
        IF x$ = "5" THEN EXIT DO
        IF x$ = "8" THEN v(pt%) = v(pt%) * (1 + adjer)
        IF x$ = "2" THEN v(pt%) = v(pt%) / (1 + adjer)
        thickness = v(1): a1 = v(2): a2 = v(3): l1 = v(4): l2 = v(5)
        w1 = v(6): w2 = v(7): d = v(8): e1 = v(9): e2 = v(10)
        IF e1 > d THEN e1 = d * .99
        IF e2 > d THEN e2 = d * .99
        IF update% THEN
            analyse xinput, finput, xoutput, emat, thickness, a1, a2, l1, l2, w1, w2,
d, e1, e2, foutput, peak.stress, stall.stress
            eff = efficiency(xinput, finput, xoutput, foutput)
```

```
            mass = structure.mass(thickness, a1, a2, l1, l2, w1, w2, d, e1, e2)
            display.geometry thickness, a1, a2, l1, l2, w1, w2, d, e1, e2
            display.parametrics
            display.performance eff, peak.stress, stall.stress, foutput, xoutput, mass
            draw.structure a1, a2, l1, l2, w1, w2, d, e1, e2
        END IF
    LOOP
LOCATE 58, 1: PRINT SPACE$(70);

END SUB

SUB win1
    VIEW PRINT 31 TO 40
    COLOR 6
    LOCATE 31, 1
END SUB

SUB win2
    VIEW PRINT 39 TO 44
    COLOR 2
    LOCATE 39, 1
END SUB

SUB win3
    VIEW PRINT 45 TO 50
    COLOR 3
    LOCATE 45, 1
END SUB

SUB win4
    VIEW PRINT 57 TO 59
    COLOR 4
    LOCATE 57, 1
END SUB

SUB win5
    VIEW PRINT 1 TO 29
    COLOR 5
    LOCATE 1, 1
END SUB
```

13 APPENDIX 3: 'DISTIME' PROGRAM LISTING.

The 'DISTIME' program is listed below was originated by the author in 1987 and has been the result of numerous additions and expansions over the last five years. It has been used for work throughout the project (which has been the source for this thesis), and has proven to be an easy-to-use tool for the modelling of dynamic systems in the time domain, particularly where linear modelling either breaks down or is inappropriate.

```
'
'     PC DISTIME
'
'     AUTHOR: J.K. THORNLEY
'
'     USABLE FUNCTIONS AND SUBROUTINES
'
DEFINT A-Z
DECLARE FUNCTION arccos! (b!)
DECLARE FUNCTION arcsin! (b!)
DECLARE FUNCTION atod% (infeed!, vlow!, vhigh!, bits%, noisevolts!)
DECLARE FUNCTION bound! (infeed!, upper!, lower!)
DECLARE FUNCTION clip! (feed!, level!)
DECLARE FUNCTION comparator! (infeed!, threshold!, uclamp!, lclamp!)
DECLARE FUNCTION convolution! (infeed1!, infeed2!, tloop!, tconv!, toffer!, hot%)
DECLARE FUNCTION counter! (hertz!, stepsize!, direc!, clipup!, clipdown!)
DECLARE FUNCTION deadband! (feed!, level!)
DECLARE FUNCTION delay! (time!, infeed!)
DECLARE FUNCTION delta% (time!)
DECLARE FUNCTION differ! (top!, bottom!)
DECLARE FUNCTION differentiate! (top!, bottom!, clipped!)
DECLARE FUNCTION dtoa! (infeed!, vlow!, vhigh!, bits%, noisevolts!)
DECLARE FUNCTION edge! (levelfrom!, levelto!, when!)
DECLARE FUNCTION frequency! (infeed!)
DECLARE FUNCTION highpass1! (gain!, tau!, infeed!, clipped!)
DECLARE FUNCTION hysteresis! (infeed!, slopp!)
DECLARE FUNCTION integ! (infeed!, withrespectto!)
DECLARE FUNCTION integrate! (infeed!, withrespectto!, clipped!, outoffset!, rst)
DECLARE FUNCTION lowpass1! (gain!, tau!, infeed!, clipped!)
DECLARE FUNCTION max! (a1!, a2!)
DECLARE FUNCTION min! (a1!, a2!)
DECLARE FUNCTION monostable% (period!, fire%)
DECLARE FUNCTION noise! (level!)
DECLARE FUNCTION nonlinear! (maxfeed!, semideviation!, infeed!)
DECLARE FUNCTION notch! (frequency!, q!, infeed!)
DECLARE FUNCTION peak! (infeed!, setter)
DECLARE FUNCTION positive! (infeed!)
DECLARE FUNCTION profile! (which%)
DECLARE FUNCTION pureintegrator! (tau!, infeed!)
DECLARE FUNCTION quantise! (infeed!, aperture!, bits%)
DECLARE FUNCTION realdifferentiator! (gain!, tau!, infeed!)
DECLARE FUNCTION rectify! (infeed!, datum!)
DECLARE FUNCTION resonance! (frequency!, damping!, infeed!)
DECLARE FUNCTION samplehold! (infeed!, tloop!, topen!, tclose!, hot%)
DECLARE FUNCTION sawtooth! (amplitude!, frequency!)
DECLARE FUNCTION secondorder! (frequency!, damping!, infeed!)
DECLARE FUNCTION sine! (amplitude!, frequency!)
DECLARE FUNCTION slewratelimit! (infeed!, rate!)
DECLARE FUNCTION square! (amplitude!, frequency!, duty!)
DECLARE FUNCTION srflipflop% (fset%, freset%)
DECLARE FUNCTION sweep! (flo!, fhi!)
DECLARE FUNCTION togval! (identity$, j%, trueval!, falseval!)
DECLARE FUNCTION triangle! (amplitude!, frequency!)
DECLARE FUNCTION trough! (infeed!, setter)
DECLARE FUNCTION zerocross% (infeed!)

DECLARE SUB adjust (vname$, present!)
```

```
DECLARE SUB adjust (vname$, present!)
DECLARE SUB aplot (variable!, title$)
DECLARE SUB datafile (var1!, var2!)
DECLARE SUB file (variable!)
DECLARE SUB file.event.pair (filename$, var$, var!)
DECLARE SUB flash ()
DECLARE SUB hold ()
DECLARE SUB initialise (t1!, x1!, nplotsmax%)
DECLARE SUB plot (variable!, scale!, title$, format$)
DECLARE SUB quattro.dump (filename$, time.interval!)
DECLARE SUB quattro.prn.1 (filename$, var1!)
DECLARE SUB quattro.prn.2 (filename$, var1!, var2!)
DECLARE SUB quattro.prn.3 (filename$, var1!, var2!, var3!)
DECLARE SUB quattro.prn.4 (filename$, var1!, var2!, var3!, var4!)
DECLARE SUB quattro.prn.5 (filename$, var1!, var2!, var3!, var4!, var5!)
DECLARE SUB readprofile (filename$)
DECLARE SUB reeset (param%)
DECLARE SUB sequence (x!)
DECLARE SUB set (param%)
DECLARE SUB steptrapif (condition1%, condition2%)
DECLARE SUB status (ISTR$)
DECLARE SUB switch (vname$, present%)
DECLARE SUB tick (c%)
DECLARE SUB timemark (c%, often!)
DECLARE SUB trigger (param%, trace%)

'-----------------------------------------------------------------------
'
'     USER TRANSPARENT FUNCTIONS AND ROUTINES
'     ********** DO NOT CALL ****************
'
DECLARE FUNCTION ctinc% ()
DECLARE FUNCTION keyin$ ()
DECLARE FUNCTION quitflag% ()
DECLARE FUNCTION paraedit% ()

DECLARE SUB aliascheck (frequency!, m$)
DECLARE SUB boxer ()
DECLARE SUB countmanager ()
DECLARE SUB datafilemanager ()
DECLARE SUB filemanager ()
DECLARE SUB helpmode (k$)
DECLARE SUB pause (seconds!)
DECLARE SUB scrinit ()
DECLARE SUB smodemod ()
DECLARE SUB stringadjust (vname$, present$)
DECLARE SUB timing (tspan!)
DECLARE SUB titles ()
DECLARE SUB tplot ()
DECLARE SUB timescale ()
DECLARE SUB xmagnify ()


DEFINT A-Z
COMMON SHARED t!, tmax!, td!, delt!, time!, ct, xmag!, oxmag!, helpon
COMMON SHARED pi!, wheight!, c, d, page, bon, pcol, autoscale, zeroscale
COMMON SHARED countloop, countloopmax, abort, paraset, wlock, smode, utrig%, dotrig%
COMMON SHARED filer, fstate, filename$, variabledirectory$
COMMON SHARED ttl1!, ttl0!, stat$, qplot, ident$, mode, mode$
COMMON SHARED datapoint, filedata, points, oldpoints, datadirectory$
COMMON SHARED micron$, qmode%, qhandle%, qlim%, qcount%, qstart!, qtime!, qtime$
CONST true = -1, false = 0, big! = 1E+25
CONST aspect! = 1.75
DIM SHARED dummy!(500), delays!(9, 500), dpoint(9)
DIM SHARED profiles!(9, 1, 100), lastprofindex(9)
DIM SHARED tog%(9), tog$(9)
REM MODE DECLARATION
mode = 9
'*************************************************************************

DEFSNG A-Z
      initialise 5, 1, 4

DO
   IF quitflag% THEN EXIT DO

LOOP
END

DEFINT A-Z
SUB adjust (vname$, present!)
STATIC nv$, nva!, prol, proc, grunt!
```

```
prol = 23
proc = 12

IF paraset THEN
      IF bon THEN PLAY "164f"
      LOCATE prol, proc
      PRINT UCASE$(vname$); "= "; present!; " New >";
      INPUT nv$
      IF nv$ = "" OR nv$ = "#" THEN
           nva! = present!
      ELSE
           IF INSTR(UCASE$(nv$), "I") > 0 THEN
               grunt! = present!
           ELSE
               grunt! = 0!
           END IF
           nva! = VAL(nv$) + grunt!
           IF UCASE$(vname$) = "TMAX" THEN
               timing nva!
           END IF

      END IF
      present! = nva!
      LOCATE prol, proc
      PRINT SPACE$(45);
      IF nv$ = "#" THEN paraset = false
END IF

IF qmode = 1 THEN
   WRITE #qhandle, vname$, present!
END IF

END SUB

SUB aliascheck (frequency!, m$)
   DO
      IF 5 * frequency! > 1 / delt! THEN
           status "ALIAS " + m$
           delt! = delt! / SQR(2!)
           xmag! = xmag! / SQR(2!)
           pause .1
           status "adjusting"
           pause .1
           status ""
      ELSE
         EXIT DO
      END IF
   LOOP
END SUB

SUB aplot (variable!, title$)
STATIC j, k, l, wup!, wdo!, height!, y!, vert, aperture!, form$, oldy!, pc, oldt!,
tscale!
j = ctinc
k = ctinc
l = ctinc
c = c + 1
   IF c > qplot THEN
      status "too many plots"
      GOTO enough
   END IF
   pc = pcol
   aperture! = aspect! * wheight! / qplot
   wup! = wheight! - aperture! * (c - 1)
   wdo! = wup! - aperture!
   fred! = (wup! + wdo!) / 2!
   scale! = dummy!(l)
   IF scale! = 0 OR zeroscale THEN
      scale! = 1E-12
      dummy!(l) = scale!
   END IF

   IF autoscale AND ABS(variable!) > scale! THEN
      scale! = ABS(variable!) * 1.05
      dummy!(l) = scale!
      pc = pcol + 2
   END IF

   y! = variable! / scale! * aperture! / 2 + fred!
   vert = (18 / qplot + .5) * c
   oldy! = dummy!(j)
   oldt! = dummy!(k)

   IF countloop = 1 OR countloop = 0 THEN
```

```
      LINE (0, fred!)-(tmax!, fred!), , , 255
      LINE (0, wup!)-(tmax!, wup!)
      LINE (0, wdo!)-(tmax!, wdo!)
      dummy!(j) = y!
      dummy!(k) = delt!
      LOCATE vert - 1, 2
      PRINT UCASE$(title$);
      maxscale$ = CHR$(240) + RIGHT$(SPACE$(9) + STR$(scale!), 7)
      LOCATE vert - 2, 2
      PRINT maxscale$;
   ELSE
      IF oldy! > wup! THEN pc = pcol + 1: oldy! = wup!
      IF oldy! < wdo! THEN pc = pcol - 1: oldy! = wdo!
      IF y! > wdo! AND y! < wup! THEN
         LINE (oldt!, oldy!)-(t!, y!)
         dummy!(j) = y!
         dummy!(k) = t!
      END IF

   END IF

   LOCATE vert, 2
   PRINT USING "+#.#^^^^"; variable!;
enough:
END SUB

DEFSNG A-Z
FUNCTION arccos (b)
   REM needs PI
   IF b <> 0 THEN
      arccos = ATN(SQR(1 - b * b) / b)
   ELSE
      arccos = pi / 2
   END IF
END FUNCTION

FUNCTION arcsin (b)
   REM needs PI
   IF ABS(b) <> 1 THEN
      arcsin = ATN(b / SQR(1 - b * b))
   ELSE
      arcsin = pi / 2 * SGN(b)
   END IF
END FUNCTION

DEFINT A-Z
FUNCTION atod (infeed!, vlow!, vhigh!, bits, vnoisevolts!)
STATIC fred, fred2, vnoise!
   levels = 2 ^ bits
   voltsperlevel! = ABS(vhigh! - vlow!) / levels
   vnoise! = (RND - .5) * vnoisevolts!
   fred = (infeed! - vlow! + vnoise!) / voltsperlevel!
   SELECT CASE fred
      CASE IS > levels - 1
         fred2 = levels - 1
      CASE IS < 0
         fred2 = 0
      CASE ELSE
         fred2 = fred
   END SELECT
atod = fred2
END FUNCTION

FUNCTION bound! (infeed!, upper!, lower!)
bound! = infeed!
IF infeed! > upper! THEN bound! = upper!
IF infeed! < lower! THEN bound! = lower!
END FUNCTION

SUB boxer
   CLS
   LOCATE 23, 12
   PRINT stat$;
   LOCATE 24, 30
   PRINT mode$; ident$;
   LINE (0, wheight!)-(tmax!, wheight!)
   LINE (0, -wheight!)-(tmax!, -wheight!)
   LINE (0, -wheight!)-(0, wheight!)
   LINE (tmax!, -wheight!)-(tmax!, wheight!)
   LINE (0, -wheight!)-(-tmax! / 7, -wheight!)
   LINE (0, wheight!)-(-tmax! / 7, wheight!)
   LINE (-tmax! / 7, -wheight!)-(-tmax! / 7, wheight!)
END SUB
```

```
FUNCTION clip! (feed!, level!)
IF ABS(feed!) > ABS(level!) THEN
      clip! = level! * SGN(feed!)
ELSE
      clip! = feed!
END IF
END FUNCTION

FUNCTION comparator! (infeed!, threshold!, uclamp!, lclamp!)
IF infeed! > threshold! THEN
      comparator! = ABS(uclamp!)
ELSE
      comparator! = -ABS(lclamp!)
END IF
END FUNCTION

FUNCTION convolution! (infeed1!, infeed2!, tloop!, tconv!, toffer!, hot)
IF tconv! > tloop! OR toffer! > tloop! THEN
      status "CONVOLUTION ERROR!"
      hold
      STOP
END IF
j = ctinc
k = ctinc
l = ctinc
tlocal! = dummy!(j)
sumvar! = dummy!(k)
sumtime! = dummy!(l)
tlocal! = tlocal! + delt!
IF tlocal! > tloop! THEN
      tlocal! = tlocal! - tloop!
      sumvar! = 0!
      sumtime! = 0!
END IF
IF tlocal! < tconv! AND tlocal! + delt! >= tconv! THEN
      convolution! = sumvar! / sumtime!
      hot = true
ELSE
      convolution! = 0!
      hot = false
END IF
IF tlocal! < tconv! THEN
      sumtime! = sumtime! + 1!
      sumvar! = sumvar! + infeed1! * infeed2!
END IF
dummy!(j) = tlocal!
dummy!(k) = sumvar!
dummy!(l) = sumtime!
END FUNCTION

FUNCTION counter! (hertz!, stepsize!, direc!, clipup!, clipdown!)
STATIC tlocal!, lastout!, period!
j = ctinc
k = ctinc
lastout! = dummy!(j)
tlocal! = dummy!(k)
period! = 1! / hertz!
tlocal! = tlocal! + delt!
IF tlocal! >= period! THEN
      tlocal! = tlocal! - period!
      lastout! = lastout! + ABS(stepsize!) * SGN(direc!)
      IF lastout! > clipup! THEN
           lastout! = clipup!
      END IF
      IF lastout! < clipdown! THEN
           lastout! = clipdown!
      END IF
END IF
counter! = lastout!
dummy!(j) = lastout!
dummy!(k) = tlocal!
END FUNCTION

SUB countmanager
      t! = t! + delt!
      time! = time! + delt!
      IF t! > tmax! THEN
           t! = t! - tmax!
           td! = td! + tmax!
           IF wlock THEN
               status "Press a key"
               hold
           END IF
           boxer
```

```
            countloop = 0

            IF autoscale THEN
              autoscale = false
              status "autoscale done"
            END IF
            delt! = tmax! / 280! * xmag!
        END IF
        IF zeroscale THEN
           zeroscale = false
           autoscale = true
           status "re-zero-activated autoscaling"
        END IF

        ct = 0
        tplot
countloop = countloop + 1
END SUB

FUNCTION ctinc
ctinc = ct
ct = ct + 1
END FUNCTION

SUB datafile (var1!, var2!)
STATIC frf
   IF filedata THEN
      SELECT CASE datapoint
         CASE 0
            status ""
            LOCATE 23, 12
            INPUT "Datafile name "; dfile$
            status ""
            IF dfile$ = "" THEN
              filedata = false
              EXIT SUB
            END IF

            LOCATE 23, 12
            INPUT "Maximum number of samples "; points
            status ""
            IF points = 0 THEN
              points = oldpoints
            END IF
            oldpoints = points
            status "Maximum set to " + STR$(points)
            pause 1

            dfile$ = datadirectory$ + "\" + dfile$ + ".DAT"
            frf = FREEFILE
            status "Data storage initiated as " + dfile$
            OPEN dfile$ FOR OUTPUT AS #frf
            datapoint = 1
         CASE points
            status "Data storage file " + dfile$ + " closed"
            CLOSE #frf
            filedata = false
            datapoint = 0
         CASE ELSE
            PRINT #frf, var1!
            PRINT #frf, var2!
            datapoint = datapoint + 1
      END SELECT
   END IF
END SUB

SUB datafilemanager
   IF filedata THEN

   ELSE
      datapoint = 0
      filedata = true
   END IF
END SUB

FUNCTION deadband! (feed!, level!)
IF ABS(feed!) < ABS(level!) THEN
      deadband! = 0
ELSE
      deadband! = feed! - level! * SGN(feed!)
END IF
END FUNCTION

FUNCTION delay! (time!, infeed!)
```

```
STATIC tloop, lastpoint, fred!
tloop = INT(time! / delt!)
IF tloop > 500 THEN
      status "long delay"
      hold
      END
END IF
lastpoint = dpoint(d)

fred! = delays!(d, lastpoint)
delays!(d, lastpoint) = infeed!
delay! = fred!
lastpoint = lastpoint + 1
IF lastpoint >= tloop THEN
      lastpoint = 0
END IF
dpoint(d) = lastpoint
d = d + 1
END FUNCTION

FUNCTION delta (time!)
STATIC fred, loctime!
j = ctinc
loctime! = dummy!(j) + delt!
IF loctime! > time! THEN
      loctime! = loctime! - time!
      fred = true
ELSE
      fred = false
END IF
delta = fred
dummy!(j) = loctime!
END FUNCTION

DEFSNG A-Z
FUNCTION differ! (top!, bottom!)
   differ! = differentiate!(top!, bottom!, big!)
END FUNCTION

DEFINT A-Z
FUNCTION differentiate! (top!, bottom!, clipped!)
STATIC fred!, clap!, j, k, deltop!, delbot!
   j = ctinc
   k = ctinc
   clap! = ABS(clipped!)
   deltop! = top! - dummy!(j)
   delbot! = bottom! - dummy!(k)
   IF delbot! <> 0 THEN
      fred! = deltop! / delbot!
   ELSE
      fred! = clap! * SGN(deltop!)
   END IF
   IF clap! = 0! THEN GOTO bypass
   IF fred! > clap! THEN fred! = clap!
   IF fred! < -clap! THEN fred! = -clap!
bypass:
   differentiate! = fred!
   dummy!(j) = top!
   dummy!(k) = bottom!
END FUNCTION

FUNCTION dtoa! (infeed!, vlow!, vhigh!, bits, vnoisevolts!)
STATIC fred!, fred2!, vnoise!, vspan!, fred3!
   levels = 2 ^ bits
   vspan! = ABS(vhigh! - vlow!)
   vnoise! = (RND - .5) * vnoisevolts!
   fred! = infeed! / levels
   fred2! = vlow! + vspan! * fred!
   SELECT CASE fred2!
      CASE IS < vlow!
         fred3! = vlow!
      CASE IS > vhigh!
         fred3! = vhigh!
      CASE ELSE
         fred3! = fred2!
   END SELECT
   dtoa! = fred3!
END FUNCTION

FUNCTION edge! (levelfrom!, levelto!, when!)
IF t! > when! THEN
      edge! = levelto!
ELSE
      edge! = levelfrom!
```

```
END IF
END FUNCTION

SUB file (variable!)
IF filer THEN
      IF fstate THEN
           INPUT #1, variable!
      ELSE
           PRINT #1, variable!
      END IF
END IF
END SUB

DEFSNG A-Z
SUB file.event.pair (filename$, var$, var)
   STATIC x%, first.data%
   x% = FREEFILE
   OPEN filename$ FOR APPEND AS #x%
      IF NOT first.data% THEN PRINT #x%, "Begins"
      WRITE #x%, "Time", time, var$, var
   CLOSE #x%
   first.data% = true%
END SUB

DEFINT A-Z
SUB filemanager
STATIC prol, proc
      prol = 23
      proc = 12
      LOCATE prol, proc

      IF fstate THEN
           REM import
           INPUT "Import data from "; filename$
      ELSE
           REM export
           INPUT "Export data to "; filename$
      END IF

      IF filename$ = "" THEN
           filer = false
           LOCATE prol, proc
           PRINT SPACE$(45);
           EXIT SUB
      END IF
      filename$ = variabledirectory$ + "\" + filename$ + ".dat"
      IF fstate THEN
           REM import
           OPEN filename$ FOR INPUT AS #1
           status "importing from " + filename$
           pause 1
      ELSE
           REM export
           OPEN filename$ FOR OUTPUT AS #1
           status "exporting to " + filename$
           pause 1
      END IF
END SUB

SUB flash
   STATIC state
   state = state + 1
   IF state = 9 THEN state = 1
   IF bon THEN PLAY "L64c"
   LOCATE 24, 2
   PRINT STRING$(8, 176);
   LOCATE 24, 1 + state
   PRINT CHR$(178);
END SUB

FUNCTION frequency! (infeed!)
   STATIC lastval!, lastdif!, nowval!, nowdif!, lastime!, top
   j = ctinc
   k = ctinc
   l = ctinc
   m = ctinc
   lastval! = dummy!(j)
   lastdif! = dummy!(k)
   lastime! = dummy!(l)
   lastfreq! = dummy!(m)
   nowval! = infeed!
   nowdif! = differentiate!(nowval!, time!, 1E+20)
   top = (lastdif! > 0 AND nowdif! <= 0)
   IF top THEN
```

```
      dummy!(l) = time!
      period! = time! - lastime!
      fr! = 1 / period!
      dummy!(m) = fr!
      frequency! = fr!
   ELSE
      frequency! = lastfreq!
   END IF
   dummy!(j) = infeed!
   dummy!(k) = nowdif!
END FUNCTION

SUB helpmode (k$)
STATIC m$
   SELECT CASE k$
         CASE CHR$(32)
           m$ = "freezes the display"
         CASE CHR$(27)
           m$ = "end program"
         CASE CHR$(13)
           m$ = "adjust or switch variables"
         CASE "A"
           m$ = "toggle autoscaling"
         CASE "Z"
           m$ = "re-zero autoscaling"
         CASE "B"
           m$ = "toggle beeps (sound)"
         CASE "W"
           m$ = "toggle screen wrap"
         CASE "R"
           m$ = "reset display"
         CASE "T"
           m$ = "adjust timescale"
         CASE "X"
           m$ = "adjust time resolution"
         CASE "S"
           m$ = "toggle step mode"
         CASE "I"
           m$ = "import variable values"
         CASE "E"
           m$ = "export variable values"
         CASE "D"
           m$ = "data output to file"
         CASE "H"
           m$ = "help mode off"
           helpon = false
         CASE ELSE
           m$ = ">>>>>not defined<<<<<"
           BEEP
   END SELECT
   status m$
END SUB

FUNCTION highpass1! (gain!, tau!, infeed!, clipped!)
STATIC tfrac!, fred!, clap!, j, k
   j = ctinc
   k = ctinc
   clap! = ABS(clipped!)
   tfrac! = tau! / delt!
   aliascheck 1! / tau!, "hp1"
   fred! = tau! / (tau! + delt!) * (infeed! - dummy!(j) + dummy!(k))
   IF fred! > clap! THEN fred! = clap!
   IF fred! < -clap! THEN fred! = -clap!
   highpass1! = fred! * gain!
   dummy!(j) = infeed!
   dummy!(k) = fred!
END FUNCTION

SUB hold
DO
      k$ = INKEY$
      IF k$ <> "" THEN EXIT DO
LOOP
IF UCASE$(k$) = "S" THEN
      smodemod
END IF
END SUB

FUNCTION hysteresis! (infeed!, slopp!)
STATIC slapp!, fred!
j = ctinc
slapp! = ABS(slopp!)
hysteresis! = dummy!(j)
IF infeed! > dummy!(j) + slapp! THEN
```

```
      fred! = infeed! - slopp!
      END IF
IF infeed! < dummy!(j) - slapp! THEN
      fred! = infeed! + slopp!
      END IF
hysteresis! = fred!
dummy!(j) = fred!
END FUNCTION

SUB initialise (t1!, x1!, nplotsmax)

REM    mode = 2: 'CGA
REM    mode = 3: 'HERCULES
REM    mode = 9: 'EGA,VGA

IF mode = 3 THEN mode$ = "HERC"
IF mode = 2 THEN mode$ = "CGA"
IF mode = 9 THEN mode$ = "EGA"

ident$ = "-DISTIME v3.22"
titles
countloop = 0
smode = false
abort = false
filedata = false
datapoint = 0
points = 50
oldpoints = points
datadirectory$ = "d:\Qpro\work"
REM datadirectory$ = "c:\qb45\distime"
variabledirectory$ = "\QB45\DATAFILE"
pi! = 4! * ATN(1)
wheight! = 10!
ttl1! = 2.4
ttl0! = .8
paraset = false
qplot = nplotsmax
timing t1!
xmag! = x1!
wlock = false
time! = 0!
FOR j = 0 TO 500
      dummy!(j) = 0!
NEXT j
REM timescale
REM xmagnify
oxmag! = xmag!
delt! = tmax! / 280 * xmag!
bon = false
page = 0
pcol = 12
micron$ = CHR$(230) + "m"
IF nplotsmax > 8 THEN
      status "plots exceeded"
      hold
      STOP
END IF
autoscale = false
zeroscale = false
FOR j = 0 TO 9
   tog(j) = 0
NEXT j

qmode = false
qjustset = false
qjustreset = false
qisnew = true
qtime$ = "1"

END SUB

FUNCTION integ! (infeed!, withrespectto!)
integ! = integrate!(infeed!, withrespectto!, 0, 0, 0)
END FUNCTION

FUNCTION integrate! (infeed!, withrespectto!, clipped!, outoffset!, rst)
STATIC fred!, clap!, j, k, lastout!, dx!
   j = ctinc
   k = ctinc
   IF clipped! = 0 THEN
      clap! = big!
   ELSE
      clap! = ABS(clipped!)
   END IF
```

```
   lastout! = dummy!(j)
   dx! = withrespectto! - dummy!(k)
   fred! = lastout! + infeed! * dx! + outoffset!
   IF rst THEN
      fred! = outoffset!
   END IF
   IF clap! <> 0 AND ABS(fred!) > clap! THEN
      fred! = clap! * SGN(fred!)
   END IF
   integrate! = fred!
   dummy!(j) = fred! - outoffset!
   dummy!(k) = withrespectto!

END FUNCTION

FUNCTION keyin$
STATIC x$
DO
x$ = UCASE$(INKEY$)
IF x$ <> "" OR x$ = CHR$(13) THEN EXIT DO
LOOP
keyin$ = x$
END FUNCTION

FUNCTION lowpass1! (gain!, tau!, infeed!, clipped!)
STATIC tfrac!, fred!, clap!
j = ctinc
clap! = ABS(clipped!)
tfrac! = delt! / tau!
aliascheck 1! / tau!, "lp1"
fred! = gain! * tfrac! * infeed! + dummy!(j) - (tfrac! * dummy!(j))
IF fred! > clap! THEN fred! = clap!
IF fred! < -clap! THEN fred! = -clap!
lowpass1! = fred!
dummy!(j) = fred!
END FUNCTION

FUNCTION max! (a1!, a2!)
IF a1! > a2! THEN
      max! = a1!
ELSE
      max! = a2!
END IF
END FUNCTION

FUNCTION min! (a1!, a2!)
IF a1! < a2! THEN
      min! = a1!
ELSE
      min! = a2!
END IF
END FUNCTION

FUNCTION monostable (period!, fire)
   STATIC j, lastime!, fred
   j = ctinc
   lastime! = dummy!(j)
   IF fire THEN
      lastime! = 0
   END IF
   lastime! = lastime! + delt!
   fred = (lastime! <= period!)
   monostable = fred
   dummy!(j) = lastime!
END FUNCTION

FUNCTION noise! (level!)
noise! = level! * (1 - 2 * RND)
END FUNCTION

FUNCTION nonlinear! (maxfeed!, semideviation!, infeed!)
STATIC synin, n!, infeed1!, muxfeed!
synin = SGN(infeed!)
muxfeed! = ABS(maxfeed!)
infeed1! = ABS(infeed! / muxfeed!)
n! = -1.442695041# * LOG(.5 - semideviation!)
nonlinear! = synin * muxfeed! * infeed1! ^ n!
END FUNCTION

DEFSNG A-Z
FUNCTION notch! (frequency!, q!, infeed!)
   STATIC j, k, l, m, om2!, d!, delt2!
   STATIC lastin1!, lastin2!, lastout1!, lastout2!
   STATIC fred!
```

```
   aliascheck frequency!, "notch"
      j = ctinc
      k = ctinc
      l = ctinc
      m = ctinc
      lastin1! = dummy!(j)
      lastin2! = dummy!(k)
      lastout1! = dummy!(l)
      lastout2! = dummy!(m)
   omega! = 2 * pi! * frequency!
   barg! = 1 / delt! ^ 2 + 2 * q! * omega! / delt! + omega! ^ 2
   sum! = infeed! - 2 * lastin1! + lastin2! + 2 * lastout1! - lastout2!
   fred! = (sum! / delt! ^ 2 + infeed! * omega! ^ 2 + 2 * q! * omega! / delt! *
lastout1!) / barg!

   notch! = fred!

   dummy!(m) = lastout1!
   dummy!(k) = lastin1!
   dummy!(j) = infeed!
   dummy!(l) = fred!

END FUNCTION

DEFINT A-Z
FUNCTION paraedit
END FUNCTION

SUB pause (seconds!)
STATIC t1!, t2!
t1! = TIMER
t2! = t1! + seconds!
DO
IF TIMER > t2! THEN EXIT DO
LOOP
END SUB

FUNCTION peak! (infeed!, setter)
STATIC j, k, lastin!, lastfred!, fred!
j = ctinc
k = ctinc
lastin! = dummy!(j)
lastfred! = dummy!(k)

IF (infeed! > lastfred!) AND setter = false THEN
      fred! = infeed!
END IF

IF setter = true THEN
      fred! = infeed!
END IF

peak! = fred!
dummy!(j) = infeed!
dummy!(k) = fred!
END FUNCTION

SUB plot (variable!, scale!, title$, format$)
STATIC fred!, wup!, wdo!, height!, y!, vert, aperture!
STATIC form$, oldy!, pc, oldt!, maxscale$
j = ctinc
k = ctinc
c = c + 1
   IF c > qplot THEN
      status "too many plots"
      GOTO abort
   END IF
   aperture! = aspect! * wheight! / qplot
   wup! = wheight! - aperture! * (c - 1)
   wdo! = wup! - aperture!
   fred! = (wup! + wdo!) / 2!
   y! = variable! / scale! * aperture! / 2.1 + fred!
   vert = (18 / qplot + .5) * c
   oldy! = dummy!(j)
   oldt! = dummy!(k)

   IF format$ = "" THEN
      form$ = "###.####"
   ELSE
      form$ = format$
   END IF

   IF countloop = 1 OR countloop = 0 THEN
      LINE (0, fred!)-(tmax!, fred!), , , 15
```

```
      LINE (0, wup!)-(tmax!, wup!)
      LINE (0, wdo!)-(tmax!, wdo!)
      dummy!(j) = y!
      dummy!(k) = delt!
      LOCATE vert - 1, 2
      PRINT UCASE$(title$);
      LOCATE vert - 2, 2
      PRINT USING form$; scale!;
      PRINT CHR$(127);
   ELSE
      IF qmode = 2 THEN
         pc = 15
      ELSE
         pc = pcol
      END IF
      IF oldy! > wup! THEN pc = pcol + 1: oldy! = wup!
      IF oldy! < wdo! THEN pc = pcol - 1: oldy! = wdo!
      IF y! > wdo! AND y! < wup! THEN
         LINE (oldt!, oldy!)-(t!, y!)
         dummy!(j) = y!
         dummy!(k) = t!
      END IF
   END IF

   LOCATE vert, 2
   PRINT USING form$; variable!;

   IF qmode = 3 THEN
      PRINT #qhandle, CHR$(34) + title$ + CHR$(34) + " , ";
   END IF

   IF qmode = 2 AND qcount = 0 THEN
      PRINT #qhandle, STR$(variable!) + " , ";
   END IF
abort:

END SUB

FUNCTION positive! (infeed!)
IF infeed! > 0! THEN
      positive! = infeed!
ELSE
      positive! = 0!
END IF
END FUNCTION

FUNCTION profile! (which)
STATIC timeout, pnt, t1!, t2!, p1!, p2!

pnt = lastprofindex(which)

DO
   timeout = (time! > profiles!(which, 0, pnt + 1))
   IF NOT timeout THEN EXIT DO
   pnt = pnt + 1
LOOP
lastprofindex(which) = pnt

t1! = profiles!(which, 0, pnt)
t2! = profiles!(which, 0, pnt + 1)
p1! = profiles!(which, 1, pnt)
p2! = profiles!(which, 1, pnt + 1)
profile! = p1! + (time! - t1!) * (p2! - p1!) / (t2! - t1!)
END FUNCTION

FUNCTION pureintegrator! (tau!, infeed!)
STATIC fred!
j = ctinc
fred! = dummy!(j) + infeed! * delt! / tau!
pureintegrator! = fred!
dummy!(j) = fred!
END FUNCTION

FUNCTION quantise! (infeed!, aperture!, bits)
STATIC resolution!, digger, numeral&, fred!
   numeral& = 2 ^ (bits - 1)
   resolution! = aperture! / numeral&
   fred! = infeed!
   IF fred! > ABS(aperture!) THEN fred! = ABS(aperture!)
   IF fred! < -ABS(aperture!) THEN fred! = -ABS(aperture!)
   fred! = fred! / resolution!
   quantise! = INT(fred!) * resolution!
END FUNCTION
```

```
SUB quattro.dump (filename$, time.interval!)
   IF qmode = 3 THEN
      qhandle = FREEFILE
      stringadjust "filename", filename$
      stringadjust "maximum time span", qtime$
      qtime! = VAL(qtime$)
      OPEN datadirectory$ + "\" + filename$ + ".prn" FOR OUTPUT AS #qhandle
      status "Quattro dumper open as " + filename$
      WRITE #qhandle, "Distime Plot Dump"
      WRITE #qhandle, DATE$
      qlim = INT(time.interval! / delt!)
      qcount = 0
      qstart! = time!
      pause 1
      PRINT #qhandle, CHR$(34) + "Time" + CHR$(34) + " , ";
   END IF
   IF qmode = 2 AND qcount = 0 THEN
      PRINT #qhandle,
      PRINT #qhandle, STR$(time!) + " , ";
   END IF
   IF qmode = 1 THEN
      CLOSE #qhandle
      status "Quattro dumper closed"
   END IF
END SUB

DEFSNG A-Z
SUB quattro.prn.1 (filename$, var1)
   STATIC x%
   x% = FREEFILE
   OPEN filename$ FOR APPEND AS #x%
      WRITE #x%, var1
   CLOSE #x%
END SUB

SUB quattro.prn.2 (filename$, var1, var2)
   STATIC x%
   x% = FREEFILE
   OPEN filename$ FOR APPEND AS #x%
      WRITE #x%, var1, var2
   CLOSE #x%
END SUB

SUB quattro.prn.3 (filename$, var1, var2, var3)
   STATIC x%
   x% = FREEFILE
   OPEN filename$ FOR APPEND AS #x%
      WRITE #x%, var1, var2, var3
   CLOSE #x%
END SUB

SUB quattro.prn.4 (filename$, var1, var2, var3, var4)
   STATIC x%
   x% = FREEFILE
   OPEN filename$ FOR APPEND AS #x%
      WRITE #x%, var1, var2, var3, var4
   CLOSE #x%
END SUB

SUB quattro.prn.5 (filename$, var1, var2, var3, var4, var5)
   STATIC x%
   x% = FREEFILE
   OPEN filename$ FOR APPEND AS #x%
      WRITE #x%, var1, var2, var3, var4, var5
   CLOSE #x%
END SUB

DEFINT A-Z
FUNCTION quitflag
STATIC decide
countmanager

IF qmode = 1 THEN qmode = 0
IF qmode = 3 THEN qmode = 2

IF qmode = 2 AND (time! >= qtime! + qstart!) THEN
   qmode = 1
   WRITE #qhandle,
   WRITE #qhandle,
END IF


IF qcount < qlim THEN qcount = qcount + 1
```

```
IF qcount = qlim THEN
   qcount = 0
END IF

paraset = false
decide = 0
IF filer THEN
      status "closing file"
      pause 1
      status ""
      CLOSE #1
END IF
filer = false
dotrig = false
c = 0
d = 0
k$ = INKEY$
IF k$ = "" THEN GOTO fred
k$ = UCASE$(k$)
IF helpon THEN
   helpmode k$
ELSE
   SELECT CASE k$
         CASE "+"
           utrig = true
           dotrig = true
         CASE "-"
           utrig = false
           dotrig = true
         CASE "*"
           utrig = NOT utrig
           dotrig = true
         CASE CHR$(32)
             IF bon THEN PLAY "L32ceg"
             status "HELD"
             hold
             status ""
             decide = 0
         CASE CHR$(27)
             decide = -1
         CASE CHR$(13)
             paraset = true
         CASE "A"
             autoscale = NOT autoscale
             IF autoscale THEN
               status "autoscaling active"
             ELSE
               status "autoscale off"
             END IF
         CASE "Z"
           zeroscale = true
           status "re-zeroing"
           pause .5
           status ""
         CASE "B"
             bon = NOT bon
             IF bon THEN
                  status "BEEP ON"
                  PLAY "L32cdefg"
             ELSE
                  status "BEEP OFF"
                  PLAY "L32gec"
             END IF
         CASE "W"
             wlock = NOT wlock
             IF wlock THEN
                  status "wrap off"
             ELSE
                  status "wrap on"
             END IF
         CASE "R"
             td! = td! + t!
             t! = 0!
             autoscale = false
             status "autoscale inactive"
             scrinit
         CASE "T"
             timescale
         CASE "X"
             xmagnify
         CASE "S"
             smodemod
         CASE "I"
             filer = true
```

```
            fstate = true
            filemanager
        CASE "E"
            filer = true
            fstate = false
            filemanager
        CASE "D"
            datafilemanager
        CASE "H"
            helpon = true
            status "help mode active"
        CASE "0" TO "9"
          tpt = VAL(k$)
          tog(tpt) = NOT tog(tpt)
          ss$ = tog$(tpt)
          IF tog(tpt) THEN
            ss$ = ss$ + " set  "
            SOUND 400, 2
          ELSE
            ss$ = ss$ + " reset"
            SOUND 300, 2
          END IF
          status ss$
        CASE "Q"
          IF qmode = 2 THEN
            qmode = 1
            WRITE #qhandle,
            WRITE #qhandle,
          END IF
          IF qmode = 0 THEN qmode = 3
        CASE ELSE
            IF bon THEN BEEP
   END SELECT
END IF
fred:
quitflag = decide OR abort

IF smode THEN
      hold
END IF
END FUNCTION

SUB readprofile (filename$)
   STATIC whichpoint, x, tpoint
   x = FREEFILE
   tpoint = 0
   OPEN filename$ FOR INPUT AS #x
   DO
      IF EOF(x) THEN EXIT DO
      INPUT #x, profiles!(whichpoint, 0, tpoint)
      IF EOF(x) THEN EXIT DO
      INPUT #x, profiles!(whichpoint, 1, tpoint)
      tpoint = tpoint + 1
   LOOP
   CLOSE #x
   whichpoint = whichpoint + 1
   IF whichpoint > 9 THEN
      status "TOO MANY PROFILES"
      END
   END IF
END SUB

FUNCTION realdifferentiator! (gain!, tau!, infeed!)
STATIC fred!, tco!
   j = ctinc
   k = ctinc
   tco! = 1! + delt! / tau!
   fred! = (gain! * (infeed! - dummy!(j)) + dummy!(k)) / tco!
   realdifferentiator! = fred!
   dummy!(j) = infeed!
   dummy!(k) = fred!
END FUNCTION

FUNCTION rectify! (infeed!, datum!)
STATIC erv!
erv! = ABS(infeed! - datum!)
rectify! = datum! + erv!
END FUNCTION

SUB reeset (param)
   param = false
END SUB

FUNCTION resonance! (frequency!, damping!, infeed!)
```

```
STATIC omega!, a!, b!, c!, fred!
j = ctinc
k = ctinc
l = ctinc
omega! = 2! * pi! * frequency!
a! = omega! * omega! * delt!
b! = 2! * damping! * omega! * delt!
c! = a! * delt!
fred! = (a! * (infeed! - dummy!(l)) + dummy!(k) * (2! + b!) - dummy!(j)) / (1! + b! +
c!)
resonance! = fred!
dummy!(j) = dummy!(k)
dummy!(k) = fred!
dummy!(l) = infeed!
END FUNCTION

FUNCTION samplehold! (infeed!, tloop!, topen!, tclose!, hot)
STATIC tlocal!, lastval!, fred!
j = ctinc
k = ctinc
lastval! = dummy!(k)
tlocal! = dummy!(j)
tlocal! = tlocal! + delt!
IF tclose! > tloop! OR topen! >= tclose! THEN
      status "sample error"
      hold
      STOP
END IF
IF tlocal! > tloop! THEN
      tlocal! = tlocal! - tloop!
END IF
IF (tlocal! < topen! AND tlocal! + delt! > topen!) OR (tlocal! < tclose! AND tlocal! +
delt! > tclose!) THEN
      hot = true
ELSE
      hot = false
END IF
IF tlocal! < topen! THEN
      fred! = lastval!
END IF
IF tlocal! >= topen! AND tlocal! <= tclose! THEN
      fred! = infeed!
END IF
IF tlocal! > tclose! THEN
      fred! = lastval!
END IF
samplehold! = fred!
lastval! = fred!
dummy!(j) = tlocal!
dummy!(k) = lastval!
END FUNCTION

FUNCTION sawtooth! (amplitude!, frequency!)
STATIC omega!, fred!, phase!
j = ctinc
aliascheck 2 * frequency!, "SAW"
omega! = 2! * pi! * frequency!
phase! = dummy!(j) + omega! * delt!
IF phase! > 2! * pi! THEN phase! = phase! - 2! * pi!
sawtooth! = amplitude! * phase! / 2! / pi!
dummy!(j) = phase!
END FUNCTION

SUB scrinit
countloop = 0
SCREEN mode
WINDOW (-tmax! / 7, -wheight!)-(tmax! * 1.01, wheight!)
boxer
      SELECT CASE mode
            CASE 3
                VIEW SCREEN (90, 0)-(715, 325)
            CASE 2
                VIEW SCREEN (80, 0)-(635, 187)
            CASE 9
                VIEW SCREEN (80, 0)-(635, 327)
            CASE ELSE
                status "screen mode undefined"
                END
      END SELECT
END SUB

FUNCTION secondorder! (frequency!, damping!, infeed!)
STATIC alpha!, beta!, gamma!, a!, b!, bot!, taunatural!, fred!
j = ctinc
```

```
k = ctinc
taunatural! = 1 / 2 / pi! / frequency!
a! = 2 * damping! * taunatural! / delt!
b! = (taunatural! / delt!) ^ 2
bot! = (1 + a! + b!)
alpha! = 1 / bot!
beta! = (a! + 2 * b!) / bot!
gamma! = b! / bot!
fred! = alpha! * infeed! + beta! * dummy!(j) - gamma! * dummy!(k)
secondorder! = fred!
dummy!(k) = dummy!(j)
dummy!(j) = fred!
END FUNCTION

DEFSNG A-Z
SUB sequence (x)
   lx = INT(LOG(x) / LOG(10))
   xn = x / 10 ^ lx
REM    PRINT x, lx, xn
   IF xn >= 10 THEN
      lx = lx + 1
      xn = xn / 10
   END IF
   SELECT CASE xn
      CASE .95 TO 1.05
         xm = 1.5
      CASE 1.45 TO 1.55
         xm = 2.25
      CASE 2.15 TO 2.35
         xm = 5
      CASE 4.95 TO 5.05
         xm = 7.5
      CASE 7.45 TO 7.55
         xm = 10
   CASE ELSE
      PRINT "sequencer error"
      END
   END SELECT
   x = xm * 10 ^ lx
END SUB

DEFINT A-Z
SUB servicecounter

END SUB

SUB set (param)
   param = true
END SUB

FUNCTION sine! (amplitude!, frequency!)
   STATIC omega!, phase!
   j = ctinc
   aliascheck 3 * frequency!, "SINE"
   omega! = 2 * pi! * frequency!
   phase! = dummy!(j) + omega! * delt!
   IF phase! > 2! * pi! THEN phase! = phase! - 2! * pi!
   dummy!(j) = phase!
   sine! = amplitude! * SIN(phase!)
END FUNCTION

FUNCTION slewratelimit! (infeed!, rate!)
STATIC jump!, direc
j = ctinc
jump! = ABS(rate! * delt!)
direc = SGN(infeed! - dummy!(j))
IF ABS(infeed! - dummy!(j)) > jump! THEN
      fred! = dummy!(j) + jump! * direc
ELSE
      fred! = infeed!
END IF
slewratelimit! = fred!
dummy!(j) = fred!
END FUNCTION

SUB smodemod
smode = NOT smode
IF smode THEN
      status "step on"
ELSE
      status "step off"
END IF
END SUB
```

```
FUNCTION square! (amplitude!, frequency!, duty!)
STATIC threshold!, omega!, bwave!, fred!
j = ctinc
aliascheck 3 * frequency!, "SQUARE"
omega! = 2! * pi! * frequency!
threshold! = SIN(pi! * (duty! - .5))
phase! = dummy!(j) + omega! * delt!
IF phase! > 2! * pi! THEN phase! = phase! - 2! * pi!
bwave! = SIN(phase!)
fred! = amplitude!
IF bwave! > threshold! THEN
      fred! = -fred!
END IF
square! = fred!
dummy!(j) = phase!
END FUNCTION

FUNCTION srflipflop (fset, freset)
   STATIC j, fred
   j = ctinc
   fred = dummy!(j)
   IF fset THEN fred = true
   IF freset THEN fred = false
   srflipflop = fred
   dummy!(j) = fred
END FUNCTION

SUB status (ISTR$)
STATIC fred$
   stat$ = UCASE$(ISTR$)
   fred$ = LEFT$(stat$ + SPACE$(60), 60)
   LOCATE 23, 12
   PRINT fred$
   IF bon AND ISTR$ = "" THEN PLAY "L32cdg"
END SUB

SUB steptrapif (condition1%, condition2%)
      IF condition1% AND condition2% THEN
           smode = true
           status "trapped.. s continues"
      END IF
END SUB

DEFSNG A-Z
SUB stringadjust (vname$, present$)
STATIC nv$, nva$, prol, proc, grunt!
prol = 23
proc = 12
      IF bon THEN PLAY "164f"
      LOCATE prol, proc
      PRINT UCASE$(vname$); "= "; present$; " New >";
      INPUT nv$
      IF nv$ <> "" THEN
         present$ = nv$
      END IF
      LOCATE prol, proc
      PRINT SPACE$(45);
END SUB

DEFINT A-Z
FUNCTION sweep! (flo!, fhi!)
STATIC frequency!, p!, m!, c!, omega!
p! = 10 ^ (t! / tmax!)
m! = (fhi! - flo!) / 9!
c! = flo! - m!
frequency! = m! * p! + c!
sweep! = frequency!
END FUNCTION

SUB switch (vname$, present)
STATIC nv$, prol, proc
prol = 23
proc = 12
IF paraset THEN

      IF bon THEN BEEP
   DO
      LOCATE prol, proc
      PRINT UCASE$(vname$);

      IF present THEN
           PRINT " YES";
      ELSE
           PRINT " NO ";
```

```
      END IF

      DO
          nv$ = keyin$
           nv$ = LEFT$(nv$, 1)
           IF nv$ = CHR$(13) OR nv$ = "+" OR nv$ = "-" OR nv$ = "#" THEN EXIT DO
           BEEP
      LOOP
      IF nv$ = "#" THEN paraset = false: EXIT DO
      IF nv$ = CHR$(13) THEN EXIT DO
      IF nv$ = "+" THEN present = true
      IF nv$ = "-" THEN present = false
   LOOP
      LOCATE prol, proc
      PRINT STRING$(45, 32);

END IF

END SUB

SUB tick (c)
STATIC fred!, height!, aperture!
      aperture! = aspect! * wheight! / qplot
      wup! = wheight! - aperture! * (c - 1)
      wdo! = wup! - aperture!
      fred! = (wup! + wdo!) / 2!
      wup! = (wup! + 2! * fred!) / 3!
      wdo! = (wdo! + 2! * fred!) / 3!
      vert = (18 / qplot + .5) * c
      LINE (t!, wdo!)-(t!, wup!), 12
      LOCATE 25, 10 * c + 2
      PRINT USING "##.#####"; time!;

END SUB

SUB timemark (c, often!)
   STATIC j, since!, fred!, height!, aperture!
   j = ctinc
   since! = dummy!(j) * delt!
   er! = ABS(since! - often! + delt!)
   IF er! <= delt! THEN
      aperture! = aspect! * wheight! / qplot
      wup! = wheight! - aperture! * (c - 1)
      wdo! = wup! - aperture!
      fred! = (wup! + wdo!) / 2!
      wup! = (wup! + 2! * fred!) / 3!
      wdo! = (wdo! + 2! * fred!) / 3!
      LINE (t!, wdo!)-(t!, wup!), 10
      LOCATE 25, 2
      PRINT USING "##.#####"; time!;
      dummy!(j) = 0
      SOUND 100, 1
   ELSE
      dummy!(j) = dummy!(j) + 1
   END IF

END SUB

SUB timescale
paraset = true
adjust "time window", tmax!
paraset = false
timing tmax!
END SUB

SUB timing (tspan!)
tmax! = tspan!
delt! = tmax! / 280! * xmag!
scrinit
END SUB

DEFSNG A-Z
SUB titles
DEFINT A-Z
IF fpause THEN
      CLS
      LOCATE 3, 20
      PRINT mode$ + ident$
      LOCATE 5, 20
      PRINT "Author : J.K.THORNLEY"
      pause 2
      CLS
      fpause = false
END IF
```

```
CLS
END SUB

FUNCTION togval! (identity$, j, trueval!, falseval!)
   STATIC fred!, ptp
   tog$(j) = identity$
   IF tog(j) THEN
      fred! = trueval!
   ELSE
      fred! = falseval!
   END IF
   togval! = fred!
   REM status identity$ + " set to " + STR$(fred!)
END FUNCTION

SUB tplot
LOCATE 24, 55
PRINT USING "####.######"; t! + td!;
IF countloop = 1 THEN
page = page + 1
      LOCATE 24, 50
      PRINT "TIME";
      LOCATE 24, 69
      PRINT USING "Pg ###"; page;
END IF
END SUB

SUB trap (variable!, level!, tolerance!, trapset, events)
STATIC lo!, hi!
lo! = level! - tolerance!
hi! = level! + tolerance!
IF trapset AND events > 0 AND variable! >= lo! AND variable! <= hi! THEN
      trapset = 0
      IF bon THEN BEEP
      status "TRAPPED"
      hold
      status ""
END IF
END SUB

FUNCTION triangle! (amplitude!, frequency!)
STATIC omega!, fred!, phase!, locphase!
j = ctinc
aliascheck 3 * frequency!, "TRIANG"
omega! = 2! * pi! * frequency!
phase! = dummy!(j) + omega! * delt!
IF phase! > 2! * pi! THEN phase! = phase! - 2! * pi!
locphase! = phase! / pi! * 2!
SELECT CASE locphase!    ' 0 to 4
      CASE 0 TO 1
           fred! = locphase!
      CASE 1 TO 3
           fred! = 2! - locphase!
      CASE 3 TO 4
           fred! = locphase! - 4!
END SELECT
triangle! = fred! * amplitude!
dummy!(j) = phase!
END FUNCTION

SUB trigger (param, trace)
   IF dotrig% THEN
      param = utrig%
      IF trace > 0 THEN
         tick trace
      END IF
   END IF
END SUB

FUNCTION trough! (infeed!, setter)
STATIC j, k, lastin!, lastfred!, fred!
j = ctinc
k = ctinc
lastin! = dummy!(j)
lastfred! = dummy!(k)

IF (infeed! < lastfred!) AND setter = false THEN
      fred! = infeed!
END IF

IF setter = true THEN
      fred! = infeed!
END IF
```

```
trough! = fred!
dummy!(j) = infeed!
dummy!(k) = fred!

END FUNCTION

SUB xmagnify
paraset = true
adjust "time definition", xmag!
oxmag! = xmag!
paraset = false
delt! = tmax! / 280! * xmag!
END SUB

FUNCTION zerocross (infeed!)
STATIC lastval!
      j = ctinc
      lastval! = dummy!(j)
      zerocross% = (SGN(lastval!) <> SGN(infeed!))
      dummy!(j) = infeed!
END FUNCTION
```

14 APPENDIX 4: BRIDGE DESIGNER PROGRAM LISTING.

The following program listing of the bridge designer program is complete, and is provided so that the reader may appreciate the level of effort required to arrive at a working, easy to use program. It is written in Quick Basic 4.5, which is a fully structured language and can therefore be easily translated if desired to any other language of a similar structure, with only the graphical interface requiring significant alteration.

The central algorithm 'design' is shown in bold type on page 280.

```
DECLARE FUNCTION second.moment! (dep!, wid!)
DECLARE FUNCTION omega! ()
DECLARE FUNCTION gamma! ()
DECLARE FUNCTION max! (x!, y!)
DECLARE SUB design ()
DECLARE SUB millform (a$, a!)
DECLARE FUNCTION unity% (x!)
DECLARE SUB microform (a$, a!)
DECLARE SUB stressform (a$, a!)
DECLARE SUB unityform (a$, a!)
DECLARE SUB forceform (a$, a!)
DECLARE SUB percent (a$, a!)
DECLARE SUB angleform (a$, a!)
DECLARE SUB stripset ()
DECLARE SUB display.geometry ()
DECLARE SUB linedisp (a$, aa!)
DECLARE SUB win1 ()
DECLARE SUB win2 ()
DECLARE SUB analyse ()
DECLARE SUB win3 ()
DECLARE SUB win4 ()
DECLARE SUB display.parametrics ()
DECLARE SUB display.performance ()
DECLARE SUB display.help ()
DECLARE SUB win5 ()
DECLARE SUB create.dxf ()
DECLARE SUB choose.material ()
DECLARE SUB centre (a$)
DECLARE SUB pick.page (matpt%)
DECLARE SUB position (x%, r%, c%)
DECLARE SUB disp.materials ()
DECLARE FUNCTION maxi! (a!, b!)
DECLARE SUB setup ()
DECLARE FUNCTION keypress$ ()
DECLARE SUB show.commands ()
DECLARE SUB modvar (prompt$, value!)
DECLARE SUB get.geometry ()
DECLARE SUB get.material ()
DECLARE SUB standard.scale (factor!)
DECLARE SUB read.mats ()
DECLARE SUB filing ()
DECLARE FUNCTION password! ()
DECLARE SUB elevate (xout!)
DECLARE SUB twait (seconds!)
DECLARE SUB leader (a$, col%)
DECLARE SUB draw.structure ()
DECLARE SUB find.material (x$, pt%)
DECLARE SUB sort.order ()
DECLARE SUB modstring (prompt$, value$)
DECLARE SUB get.i.details ()
DECLARE SUB get.o.details ()
DECLARE SUB txt.dump ()
```

```
DECLARE SUB warp.geometry ()
DECLARE SUB title ()
DECLARE SUB set.constraints ()
DECLARE SUB synthline (x1!, y1!, x2!, y2!)
DEFSNG A-Z
COMMON SHARED d1, d2, d3, d13, dmin
COMMON SHARED l1, l2, l3, l13
COMMON SHARED l, r, w
COMMON SHARED x1, x2, x3
COMMON SHARED a1, a2, a3
COMMON SHARED i1, i2, i3
COMMON SHARED e, f, b, theta
COMMON SHARED youngs, sigmax, safety, max.stress, bending.stress
COMMON SHARED free.stress, stalled.stress, real.safety
COMMON SHARED pfree, pstalled
COMMON SHARED efficiency
COMMON SHARED ver, mic$, texlen%
COMMON SHARED fd, kd, xd, yo.set, yo.real, kout
COMMON SHARED sd, sif, sis, sif.req, sis.req
COMMON SHARED gamma.req, omega.req
COMMON SHARED g, gain, real.gain
COMMON SHARED qstalled, fd.out, fd.in, wstalled
COMMON SHARED min.asp, max.asp
COMMON SHARED ldes, w.eff.drop

COMMON SHARED material$
COMMON SHARED emat
COMMON SHARED mass, dens
COMMON SHARED textmode%, graphmode%, toggle%, dscale
COMMON SHARED folin$, foang$, forad$
COMMON SHARED mats%, matpt%, num%
COMMON SHARED epower!, dpower!, ypower!, sort.mode$

num% = 100
DIM SHARED mat$(num%), emod!(num%), yield!(num%), density!(num%)


CONST pi = 3.141592654#, true% = -1, false% = 0

ON ERROR GOTO errtrap
setup

ver = 2.6
SCREEN 12
WIDTH 80, 60
VIEW (160, 0)-(479, 239)

CLS 0
title
restart:

REM give it something to chew on

    stripset
    display.geometry
    display.parametrics
    display.performance
    draw.structure

    DO
        DO
            DO
                VIEW PRINT 57 TO 59
                show.commands
                k$ = INKEY$
                IF k$ <> "" THEN EXIT DO
            LOOP
            k$ = UCASE$(k$)
            LOCATE 57, 1
            PRINT SPACE$(LEN(c$))
            IF INSTR(CHR$(27) + "AGTHOEMDCPFSQIW123456789", k$) <> 0 THEN EXIT DO
            PLAY "o0 l64 f"
        LOOP
        SOUND 100, 1
        SELECT CASE k$
            CASE "P"
                REM new coercion routine
                set.constraints
            CASE "F"
                filing
            CASE "C"
                choose.material
                analyse
            CASE "D"
```

```
            create.dxf
        CASE "H"
            display.help
        CASE "I"
            '   input, output parameters
            win1
            CLS 2
            get.i.details
        CASE "O"
            '   output parameter
            win1
            CLS 2
            get.o.details
        CASE "A"
                analyse
        CASE "E"
            '   Elevate output movement
                elevate yo.set
                design
                analyse
        CASE "M"
            '   Select a material
            get.material
        CASE "T"
            xinput = xoutput
            finput = foutput
            '   then re-check input, output parameters
            win1
            CLS 2
            get.i.details
        CASE "G"
            '   Edit Geometry
            get.geometry
        CASE "W"
            '   visually manipulate structure
            warp.geometry
            analyse
        CASE "P"
            design
            analyse
        CASE "S"
            design
            analyse
        CASE "Q", CHR$(27)
            EXIT DO
        CASE "1" TO "9"
            dnum = VAL(k$)
            dscale = 2 ^ ((dnum - 5))
    END SELECT
    display.geometry
    display.parametrics
    display.performance
    draw.structure
LOOP
END

errtrap:
BEEP
RESUME restart

SUB analyse
'   Assumes a complete geometry defined by d1-3, l , r, b, youngs, theta
'   Also known are xd, kd, but recalculates yo.set
'
    d1 = d13
    d2 = w * d13
    d3 = d13
    l1 = r * l
    l2 = (1 - 2 * r) * l
    l3 = r * l
    l13 = l1
    e = l * SIN(theta)
    f = l * COS(theta)
sd = 1 / kd
sif = (e * e * omega + 4 * gamma) / 4 / youngs
sis = gamma / youngs * (1 + e * e / f / f)
pfree = xd / (sd + sif)
pstalled = xd / (sd + sis)
qstalled = pstalled * TAN(theta)
wstalled = pstalled / COS(theta)
xi = xd * sif / (sd + sif)
yo.real = xi / TAN(theta)

fd.out = yo.real * qstalled
```

```
    fd.in = kd * xd ^ 2

    kout = qstalled / yo.real
    efficiency = fd.out / fd.in
    free.stress = pfree * (d13 + 3 * e) / b / d13 ^ 2
    stalled.stress = pstalled / b / d13: REM  * SQR(1 + e * e / f / f)
    real.safety = max(free.stress, stalled.stress) / sigmax
    real.gain = yo.real / xd
END SUB

SUB angleform (a$, a)
    PRINT RIGHT$(SPACE$(texlen%) + a$, texlen%);
    PRINT USING "   ####.### " + CHR$(248); a * 180 / pi
END SUB

DEFINT A-Z
SUB centre (a$)
    STATIC l, s
    l = LEN(a$)
    s = 40 - l / 2
    PRINT TAB(s); a$;
END SUB

DEFSNG A-Z
SUB choose.material
    win4
    CLS 2
    IF matpt% = 0 THEN matpt% = 1
    LOCATE 57, 1
    PRINT "CHOOSE MATERIAL"
    DO
        win4
        LOCATE 58, 1: PRINT "Select Material  "; mat$(matpt%); SPACE$(30);
        x$ = keypress$
        IF x$ = CHR$(13) THEN pick.page matpt%
        IF x$ = "6" AND matpt% < mats% THEN matpt% = matpt% + 1
        IF x$ = "7" THEN matpt% = 1
        IF x$ = "1" THEN matpt% = mats%
        IF x$ = "4" AND matpt% > 1 THEN matpt% = matpt% - 1
        material$ = mat$(matpt%)
        youngs = emod(matpt%)
        sigmax = yield(matpt%)
        dens = density(matpt%)
        IF x$ = "5" OR x$ = CHR$(13) THEN EXIT DO
    LOOP
LOCATE 58, 1: PRINT SPACE$(70);
END SUB

SUB create.dxf
STATIC file$, dr$, prime%, pw, pl, c, s
STATIC x1, x2, x3, y1, y2, y3, xs, ys
DIM x(20), y(20)
    INPUT "Save DXF as file "; file$
    INPUT "To which directory "; dr$
    IF dr$ <> "" THEN dr$ = dr$ + "\"
    IF file$ = "" THEN file$ = "beam"
    CLS 2
    c = COS(theta)
    s = SIN(theta)
    h = (d2 - d13) / 2
    xs = d13 * s
    ys = d13 * c

    REM prepare coordinate system

    x(0) = 0
    x(1) = 5 * d13
    x(2) = x(1)
    x(3) = x(2) + l13 * c
    x(4) = x(3) + h * s
    x(5) = x(4) + l2 * c
    x(6) = x(5) - h * s
    x(7) = x(6) + l13 * c
    x(8) = x(7)
    x(9) = x(8) + 5 * d13

    x(20) = 0
    x(19) = x(20)
    x(18) = x(1) - xs
    x(17) = x(18)
    x(16) = x(3) - xs
    x(15) = x(16) - h * s
    x(14) = x(15) + l2 * c
    x(13) = x(6) - xs
```

```
    x(12) = x(7) - xs
    x(11) = x(12)
    x(10) = x(9)

    y(0) = 0
    y(1) = y(0)
    y(2) = y(1) + 2 * d13
    y(3) = y(2) + l13 * s
    y(4) = y(3) - h * c
    y(5) = y(4) + l2 * s
    y(6) = y(5) + h * c
    y(7) = y(6) + l13 * s
    y(8) = y(7) - 2 * d13
    y(9) = y(8)

    y(20) = y(0)
    y(17) = y(2) + ys
    y(18) = y(17) + 2 * d13
    y(19) = y(18)
    y(16) = y(3) + ys
    y(15) = y(16) + h * c
    y(13) = y(6) + ys
    y(14) = y(13) + h * c
    y(12) = y(7) + ys
    y(11) = y(12) + 2 * d13
    y(10) = y(11)

    OPEN "c:\beamodel\dxf.mid" FOR OUTPUT AS #1

'   shape segment here
    FOR j% = 0 TO 19
        synthline x(j%), y(j%), x(j% + 1), y(j% + 1)
    NEXT j%

CLOSE #1
win5
SHELL "copy c:\beamodel\dxf.hdr+c:\beamodel\dxf.mid+c:\beamodel\dxf.end " + dr$ +
file$ + ".dxf"
CLS 2

END SUB

SUB design
REM
REM LDES is a required design length
REM For a free choice this must be sen to 0 from main program
REM
REM w.eff.drop is the acceptible drop in efficiency ratio of minimising
REM d2 dimension, typically 0.025. Can be zero in the main program, which
REM causes this default value.
REM
REM dmin is the minimum acceptable d13 value (machinability)
REM
STATIC rnew, fail%, way, edrop, did, cycle%

REM immutables & switches

    way = 0
    gain = yo.set / xd
    sd = 1 / kd
    w = 1000

    IF ldes = 0 THEN
        l = 500 * xd
    ELSE
        l = ldes
    END IF

    IF w.eff.drop <= .005 THEN
        edrop = .005
        w.eff.drop = .005
    ELSE
        edrop = w.eff.drop
    END IF


REM first approximation

    sis = 0
    sif = sd * 100
    cycle% = 0

RERUN:
```

```
    fail% = false%
    theta = ATN((sif) / gain / (sd + sif))
    did = xd / b / max.stress / COS(theta) / (sd + sis)
    d13 = max(did, dmin)
    r = d13 / l * min.asp

REM Begin calcs
    DO
        theta = ATN((sif) / gain / (sd + sif))
        did = xd / b / max.stress / COS(theta) / (sd + sis)
        d13 = max(did, dmin)
        cycle% = cycle% + 1

        REM Geometry
        d1 = d13
        d2 = w * d13
        d3 = d13
        l1 = r * l
        l2 = (1 - 2 * r) * l
        l3 = r * l
        l13 = l1
        e = l * SIN(theta)
        f = l * COS(theta)

    REM Calc compliances
        sif = (e * e * omega + 4 * gamma) / 4 / youngs
        sis = gamma / youngs / (COS(theta)) ^ 2

    REM stall stress is self optimising through manipulation of d13
        stalled.stress = xd / (sd + sis) / b / d13 / COS(theta)
    REM manipulate free stress by altering r
        free.stress = xd * (d + 3 * e) / (sd + sif) / b / d13 ^ 2

        rnew = r * free.stress / max.stress
        IF unity(r / rnew) THEN
                EXIT DO
        END IF

        r = rnew

        IF r < d13 / l * min.asp THEN
            r = d13 / l * min.asp
            way = -1
            fail% = true%
            EXIT DO
        END IF

        IF r > d13 / l * max.asp THEN
            r = d13 / l * max.asp
            way = 1
            fail% = true%
            EXIT DO
        END IF
        IF cycle% = 1000 THEN
            fail% = true%
            BEEP: BEEP
            EXIT SUB
        END IF
    LOOP

    IF ldes = 0 AND fail% THEN
        l = l * (1 + way / 10)
        GOTO RERUN
    END IF

REM Calculate the reduction in W to achieve an acceptible efficiency loss

    analyse
    peak.efficiency = efficiency

    DO
        analyse
        efrat = efficiency / peak.efficiency / (1 - edrop)
        w = w / efrat
        IF unity(efrat) THEN EXIT DO
    LOOP
END SUB

SUB disp.materials
    FOR j% = 1 TO mats%
        position j%, r%, c%
        LOCATE r%, c%
        COLOR 2 - 8 * (j% = matpt%)
        PRINT mat$(j%);
```

```
    NEXT j%
END SUB

    SUB display.geometry
    win1
    centre "GEOMETRY STATUS": PRINT : PRINT
    toggle% = false%
    linedisp "Material Width [mm]", b * 1000
    linedisp "Thin Hinge length [mm]", l13 * 1000
    linedisp "Thick Hinge length [mm]", l2 * 1000
    linedisp "Flexor thickness [mm]", d13 * 1000
    linedisp "Bracer thickness [mm]", d2 * 1000
    linedisp "overall length [mm]", l * 1000
    linedisp "ground shadow [mm]", l * 1000 * COS(theta)
    linedisp "Incline [deg]", 180 / pi * theta
END SUB

SUB display.help
win5
COLOR 12
CLS
centre "H E L P   S C R E E N": PRINT : PRINT
PRINT "H     This page"
PRINT "I     Adjust input displacement and compliance"
PRINT "E     Elevate the output displacement incrementally, then re-solve"
PRINT "M     Adjust Material characteristics"
PRINT "C     Choose a material from the standard list, re-analyse"
PRINT "S     Determine the best geometry for the existing design parameters"
PRINT "P     Adjust matching parameters for various loss modes, then re-solve"
PRINT "G     Numerically adjust the geometry"
PRINT "W     Graphically adjust the geometry .. with dynamic analysis"
PRINT "A     Analyse the existing geometry"
PRINT "T     Transfer current output characteristics to input .. allows edit"
PRINT "D     Create a DXF file"
PRINT "F     Filing operations for geometry"
PRINT "Q     Really??!"
PRINT : PRINT
PRINT "                          Press a key"
kk$ = keypress$
CLS 2
END SUB

SUB display.parametrics
    win3
    toggle% = false%
    centre "PARAMETRICS STATUS": PRINT : PRINT
    linedisp "required safety factor", safety
    linedisp "yield stress [mpa]", sigmax * .000001
    linedisp "youngs modulus [gpa]", youngs * 1E-09
END SUB

SUB display.performance
    win2
    centre "PERFORMANCE STATUS": PRINT : PRINT
    toggle% = false%
    linedisp "Efficiency [%]", INT(efficiency * 100)
    linedisp "free stress [MPa]", free.stress / 1000000!
    linedisp "stall stress [MPa]", stalled.stress / 1000000!
    linedisp "real safety factor", real.safety
    linedisp "output force [N]", qstalled
    linedisp "output movement [" + mic$ + "]", yo.real * 1000000!
    linedisp "output stiffness [n/" + CHR$(230) + "m]", kout * .000001
    linedisp "real gain", real.gain
END SUB

SUB draw.structure
    STATIC c, s
        standard.scale dscale
        CLS 1
        win5
        COLOR 7
        LOCATE 5, 5: PRINT material$; SPACE$(20);
        LOCATE 7, 5: PRINT USING "Scale = X ##.###"; dscale
        c = COS(theta): s = SIN(theta)
        COLOR 12
        h = (d2 - d13) / 2
        LINE (-d2 * s / 2 - l2 * c / 2, d2 * c / 2 - l2 * s / 2)-STEP(l2 * c, l2 * s)
        LINE -STEP(-h * s, h * c)
        LINE -STEP(l13 * c, l13 * s)
        LINE -STEP(-d13 * s, d13 * c)
        LINE -STEP(-l13 * c, -l13 * s)
        LINE -STEP(-h * s, h * c)
        LINE -STEP(-l2 * c, -l2 * s)
        LINE -STEP(h * s, -h * c)
```

```
        LINE -STEP(-l13 * c, -l13 * s)
        LINE -STEP(d13 * s, -d13 * c)
        LINE -STEP(l13 * c, l13 * s)
        LINE -(-d2 * s / 2 - l2 * c / 2, d2 * c / 2 - l2 * s / 2)
END SUB

SUB elevate (xout)
    win4
    CLS 2
    LOCATE 57, 1
    PRINT "ELEVATE OUTPUT VALUE"
    xout = xout * 1000000!
    DO
        win4
        LOCATE 58, 1
        PRINT USING "Current output (micron) ####.#"; xout;
        x$ = keypress$
        IF x$ = "8" THEN xout = xout * 1.01
        IF x$ = "2" THEN xout = xout / 1.01
        IF x$ = "9" THEN xout = xout * 1.1
        IF x$ = "3" THEN xout = xout / 1.1
        IF x$ = "5" THEN EXIT DO
    LOOP
xout = INT(xout)
LOCATE 58, 1: PRINT SPACE$(70);
xout = xout / 1000000!
END SUB

SUB filing
win4

DO
CLS 2
PRINT "Filing ... Save Load Dir Text Abort"
    DO
        kk$ = keypress$
        IF INSTR("SLTDA", kk$) <> 0 THEN
            EXIT DO
        ELSE
            PLAY "l64a"
        END IF
    LOOP
        SELECT CASE kk$
            CASE "A"
                EXIT DO
            CASE "S"
                INPUT "Save filename "; sf$
                OPEN sf$ + ".bri" FOR OUTPUT AS #1
                PRINT #1, b, d13, d2, l13, l2, theta
                CLOSE #1
            CASE "L"
                INPUT "Load filename "; lf$
                OPEN lf$ + ".bri" FOR INPUT AS #1
                INPUT #1, b, d13, d2, l13, l2, theta
                CLOSE #1
                d1 = d13
                d3 = d13
                l1 = l13
                l3 = l13
                l = l2 + 2 * l13
                r = l13 / l
                w = d2 / d13
            CASE "D"
                win5
                CLS 2
                FILES "*.bri"
                PRINT "Press a key to continue"
                kkk$ = keypress$
                CLS 2
                win4
            CASE "T"
                txt.dump
        END SELECT
LOOP
CLS 2
END SUB

DEFINT A-Z
SUB find.material (x$, pt%)
    STATIC j, g$
    j = pt%
    DO
        j = j + 1
        IF j = mats% THEN j = 1
```

```
        g$ = LEFT$(mat$(j), 1)
        IF g$ = x$ THEN
            pt% = j
            EXIT DO
        END IF
        IF j >= mats THEN EXIT DO
    LOOP
END SUB

DEFSNG A-Z
SUB forceform (a$, a)
    PRINT RIGHT$(SPACE$(texlen%) + a$, texlen%);
    PRINT USING "   ####.##  N  "; a
END SUB

FUNCTION gamma
    a1 = b * d1
    a2 = b * d2
    a3 = b * d3
    gamma = l1 / a1 + l2 / a2 + l3 / a3
END FUNCTION

SUB get.geometry
STATIC bs, d13s, d2s, l13s, l2s, thetas
    win3
    CLS 2
    bs = b * 1000
    d13s = d13 * 1000
    d2s = d2 * 1000
    l13s = l13 * 1000
    l2s = l2 * 1000
    thetas = theta * 180 / pi
    modvar "b [mm]", bs
    draw.structure
    modvar "d13 [mm]", d13s
    draw.structure
    modvar "d2 [mm]", d2s
    draw.structure
    modvar "l13 [mm]", l13s
    draw.structure
    modvar "l2 [mm]", l2s
    draw.structure
    modvar "theta [" + CHR$(233) + "]", thetas
    draw.structure

    b = bs / 1000
    d13 = d13s / 1000
    d2 = d2s / 1000
    l13 = l13s / 1000
    l2 = l2s / 1000
    theta = thetas / 180 * pi
    l = 2 * l13 + l2
    r = l13 / l
    w = d2 / d13
    win3
    CLS 2
END SUB

SUB get.i.details
STATIC xds, kds
    xds = xd * 1000000!
    kds = kd * .000001
    win3
    CLS 2
        modvar "input free movement [" + mic$ + "]", xds
        modvar "input stiffness [N/" + mic$ + "]", kds
    win3
    CLS 2
    xd = xds * .000001
    kd = kds * 1000000!
END SUB

SUB get.material
STATIC ys, em, th
    win3
    CLS 2
    ys = sigmax / 1000000!
    em = youngs / 1E+09
    th = b * 1000!
    modvar "yield.stress [MPa]", ys
    modvar "youngs modulus [GPa]", em
    modvar "safety.factor", safety
    modvar "billet thickness [mm]", th
    modvar "density [kg/m^3]", dens
```

```
    sigmax = ys * 1000000!
    youngs = em * 1E+09
    b = th / 1000
    win3
    CLS 2
END SUB

SUB get.o.details
    yos = yo.set * 1000000!
    win3
    CLS 2
        modvar "output free movement [" + mic$ + "]", yos
    win3
    CLS 2
    yo.set = yos * .000001
END SUB

DEFINT A-Z
FUNCTION keypress$
STATIC k, k$, tog
DO
    DO
        k$ = INKEY$
        IF k$ <> "" THEN EXIT DO
    LOOP
    k = ASC(k$)
    IF k >= 13 AND k < 128 THEN EXIT DO
LOOP
keypress$ = UCASE$(k$)
END FUNCTION

DEFSNG A-Z
SUB keystep
DO
    IF INKEY$ <> "" THEN EXIT DO
LOOP
END SUB

DEFINT A-Z
SUB leader (a$, col)
    STATIC l, tog, j, mark, char$
    l = LEN(a$)
    mark = 0
    FOR j = 1 TO l
        IF mark THEN
            COLOR col
        ELSE
            COLOR col + 1
        END IF
        char$ = MID$(a$, j, 1)
        mark = (char$ = " ")
        PRINT char$;
    NEXT j
END SUB

DEFSNG A-Z
SUB linedisp (a$, aa)
    al% = LEN(a$)
    f$ = "####.######"
    IF ABS(aa) >= 1000 THEN f$ = f$ + "^^^^"
    lead$ = STRING$(24 - al%, 46)
    IF toggle% THEN PRINT TAB(41);
    PRINT UCASE$(a$); lead$;
    IF toggle% THEN
        PRINT USING f$; aa
    ELSE
        PRINT USING f$; aa;
    END IF
    toggle% = NOT toggle%
END SUB

FUNCTION max (x, y)
    STATIC big
    big = x
    IF y > big THEN big = y
    max = big
END FUNCTION

FUNCTION maxi (a, b)
STATIC ma, s
    IF ABS(a) > ABS(b) THEN
        ma = a
        s = SGN(a)
    ELSE
```

```
        ma = b
        s = SGN(b)
    END IF
    maxi = ma * s
END FUNCTION

SUB microform (a$, a)
    PRINT RIGHT$(SPACE$(texlen%) + a$, texlen%);
    PRINT USING " ######.#   " + CHR$(230) + "m"; a * 1000000
END SUB

SUB millform (a$, a)
    PRINT RIGHT$(SPACE$(texlen%) + a$, texlen%);
    PRINT USING "    ###.### mm"; a * 1000
END SUB

DEFINT A-Z
SUB modstring (prompt$, value$)
    win3
    CLS 2
    PRINT UCASE$(prompt$); " ";
    PRINT USING " & "; value$;
    INPUT dummy$
    IF dummy$ <> "" THEN
        value$ = dummy$
    END IF
END SUB

DEFSNG A-Z
SUB modvar (prompt$, value)
    win3
    CLS 2
    PRINT UCASE$(prompt$); " ";
    PRINT USING "#####.####### "; value;
    INPUT dummy$
    IF dummy$ <> "" THEN
        value = VAL(dummy$)
    END IF
    CLS 2
END SUB

FUNCTION omega
    STATIC omega1, omega2, omega3
    i1 = second.moment(b, d1)
    i2 = second.moment(b, d2)
    i3 = second.moment(b, d3)
    x1 = l1
    x2 = x1 + l2
    x3 = x2 + l3
    omega1 = x1 / i1 + (x2 - x1) / i2 + (x3 - x2) / i3
    omega2 = -2 / l * (x1 ^ 2 / i1 + (x2 ^ 2 - x1 ^ 2) / i2 + (x3 ^ 2 - x2 ^ 2) / i3)
    omega3 = 4 / 3 / l ^ 2 * (x1 ^ 3 / i1 + (x2 ^ 3 - x1 ^ 3) / i2 + (x3 ^ 3 - x2 ^ 3)
/ i3)
    omega = omega1 + omega2 + omega3
END FUNCTION

FUNCTION password
STATIC p$, j%, thispass$
thispass$ = LEFT$(DATE$, 2) + MID$(DATE$, 4, 2)
FOR k = 1 TO 5
    FOR j = 8 TO 15
        COLOR j
        LOCATE 21, 1
        PRINT "                                    ========"
        PRINT "                                    PASSWORD"
        PRINT "                                    ========"
    NEXT j
NEXT k
'   thispass$ = "BBB"
p$ = ""
FOR j% = 1 TO LEN(thispass$)
    p$ = p$ + keypress$
NEXT j%
password = (p$ = thispass$)
END FUNCTION

SUB percent (a$, a)
    PRINT RIGHT$(SPACE$(texlen%) + a$, texlen%);
    PRINT USING "   ####.##  %  "; a * 100
END SUB

DEFSNG A-Z
SUB pick.page (matpt%)
    STATIC j%, r%, c%
```

```
    r% = 0: c% = 1
    VIEW PRINT
    CLS 2
    DO
        disp.materials
        x$ = keypress$
        IF x$ >= "A" AND x$ <= "Z" THEN find.material x$, matpt%
        IF x$ = CHR$(13) THEN EXIT DO
        IF x$ = "5" THEN
            sort.order
        END IF
        IF x$ = "7" THEN matpt% = 1
        IF x$ = "1" THEN matpt% = mats%
        IF x$ = "8" AND matpt% > 1 THEN matpt% = matpt% - 1
        IF x$ = "2" AND matpt% < mats% THEN matpt% = matpt% + 1
        IF x$ = "4" AND matpt% > 40 THEN matpt% = matpt% - 40
        IF x$ = "6" AND matpt% < mats% - 40 THEN matpt% = matpt% + 40
        m$ = mat$(matpt%): em = emod(matpt%): ys = yield(matpt%): de = density(matpt%)
    LOOP
    CLS 2
END SUB

SUB piezodrive
    xd = .000015 / 2
    sd = xd / 850
    kd = 1 / sd
    fd = kd * xd
    yo.set = .0002
END SUB

DEFINT A-Z
SUB position (x, r, c)
    r = (x - 1) MOD 40 + 1
    c = 1 + 26 * INT((x - 1) / 40)
END SUB

DEFSNG A-Z
SUB quickfitscreen (a1, a2, l1, l2, d)
    STATIC lt, rt, up, dn, fit, asp, hrat, lmax, hh
    asp = 640 / 480
    fit = 2
    lt = -a1
    rt = a2
    lmax = maxi(l1, l2)
    hh = lmax + d
    hspan = rt - lt
    vspan = hspan / asp
    up = vspan * d / hh
    dn = -vspan * lmax / hh
    lt = lt * fit
    rt = rt * fit
    up = up * fit
    dn = dn * fit
    WINDOW (lt, dn)-(rt, up)
    REM CLS1
END SUB

SUB read.mats
STATIC j
OPEN "material.dat" FOR INPUT AS #1
INPUT #1, mats%
FOR j% = 1 TO mats%
    INPUT #1, mat$(j%)
    mat$(j%) = UCASE$(mat$(j%))
    INPUT #1, emod(j%)
    emod(j%) = emod(j%) * 1E+09
    INPUT #1, yield(j%)
    yield(j%) = yield(j%) * 1000000!
    INPUT #1, density(j%)
NEXT j%
CLOSE #1
END SUB

SUB reveal.geometry
    PRINT "GEOMETRY"
    millform "b", b
    millform "L", l
    millform "d1", d1
    millform "d2", d2
    millform "d3", d3
    angleform "Theta", theta
    millform "l1", l1
    millform "l2", l2
    millform "l3", l3
```

```
    unityform "Hinge aspect", l1 / d1

END SUB

SUB reveal.performance
PRINT : PRINT "PERFORMANCE"
    microform "xd", xd
    microform "yo", yo.set
    stressform "Free stress", free.stress
    stressform "Stalled stress", stalled.stress
    percent "Efficiency", efficiency
    forceform "Output Stall Force", qstalled
    forceform "Input Stall Force", kd * xd
END SUB

FUNCTION second.moment (dep, wid)
    second.moment = dep * wid ^ 3 / 12
END FUNCTION

SUB set.constraints
STATIC ldesw, weffer, dmins
    ldesw = ldes * 1000
    weffer = w.eff.drop * 100
    dmins = dmin * 1000!
    modvar "Overall length [mm] (0 releases constraint)", ldesw
    modvar "Centre width efficiency wasting [%]", weffer
    modvar "Minimum flexor thickness [mm]", dmins
    ldes = ldesw * .001
    w.eff.drop = weffer / 100
    dmin = dmins * .001
END SUB

SUB setup
    texlen% = 20
    mic$ = CHR$(230) + "m"
    min.asp = 3
    max.asp = 8
    w = 100


    youngs = 1.1E+11
    sigmax = 4.8E+08
    safety = .2
    max.stress = safety * sigmax
    b = .0065
    dmin = 0

    ldes = 0
    w.eff.drop = .01

    xd = .000015 * 4
    kd = 56000000 / 4
    yo.set = .0002

    textmode% = true%
    graphmode% = true%
    dscale = 1
    folin$ = "#####.######"
    foang$ = "#####.######"
    forad$ = "#####.######"
    material$ = "UN-SPECIFIED"
    read.mats
    matpt% = 1
    epower = 2
    ypower = 1
    dpower = -.5
    sort.mode$ = "N"
END SUB

SUB show.commands
STATIC coltog%, col%
    coltog% = NOT coltog%
    IF coltog% THEN
        col% = 4
    ELSE
        col% = 4 + 8
    END IF
    c$ = " Help Inpt Elev Matl Chse Solv Prog Geom Warp Anls Tran DXF File Quit"
    LOCATE 57, 1
    leader c$, col%
    twait .2
END SUB

DEFINT A-Z
```

```
SUB sort.order
STATIC j, suc, ee1!, yy1!, dd1!, mm1$, ee2!, yy2!, dd2!, mm2$
    modstring "Sort Mode - N/E/Y/D/S", sort.mode$
    IF sort.mode$ = "" THEN
        sort.mode$ = "N"
    ELSE
        sort.mode$ = UCASE$(LEFT$(sort.mode$, 1))
    END IF
    IF sort.mode$ = "S" THEN
        modvar "Power of Young's Modulus", epower!
        modvar "Power of Yield Stress", ypower!
        modvar "Power of Density", dpower!
    END IF

    DO
        suc = 0
        FOR j = 1 TO mats - 1
        REM Take Note
        ee1! = emod!(j): yy1! = yield!(j): dd1! = density!(j): mm1$ = mat$(j)
        ee2! = emod!(j + 1): yy2! = yield!(j + 1): dd2! = density!(j + 1): mm2$ =
mat$(j + 1)

        SELECT CASE sort.mode$
            CASE "E"
                perf! = ee2! / ee1!
            CASE "Y"
                perf! = yy2! / yy1!
            CASE "D"
                perf! = dd2! / dd1!
            CASE "S"
                perf! = ((ee2! / ee1!) ^ epower!) * ((yy2! / yy1!) ^ ypower!) * ((dd2!
/ dd1!) ^ dpower!)
            CASE ELSE
                perf! = 0
        END SELECT


        IF perf! > 1! THEN
            suc = -1
            REM swap 'em
            emod!(j + 1) = ee1!: yield!(j + 1) = yy1!: density!(j + 1) = dd1!: mat$(j
+ 1) = mm1$
            emod!(j) = ee2!: yield!(j) = yy2!: density!(j) = dd2!: mat$(j) = mm2$
        END IF
        NEXT j
        IF suc = 0 THEN EXIT DO
    LOOP

    VIEW PRINT
    CLS 2
END SUB

DEFSNG A-Z
SUB standard.scale (factor)
    STATIC lt, rt, up, dn, fit, asp, hrat, lmax, hh
    across = 640
    down = 480
    fit = 2000 * 2.66666
    lt = -across / 2 / factor / fit
    rt = across / 2 / factor / fit
    up = down / 2 / factor / fit
    dn = -down / 2 / factor / fit
    WINDOW (lt, dn)-(rt, up)
END SUB

SUB stressform (a$, a)
    PRINT RIGHT$(SPACE$(texlen%) + a$, texlen%);
    PRINT USING "   ####.##  MPa"; a / 1000000!
END SUB

SUB stripset
    xd = 2.189E-05
    sd = 2.889E-07
    kd = 1 / sd
    fd = kd * xd
    yo.set = .00011
END SUB

SUB syntharc (x, y, r, sa, ea)
    REM angles in degrees!!!
    REM convert to millimeters
    xx = x * 1000
    yy = y * 1000
    rr = r * 1000
```

```
    PRINT #1, "ARC"
    PRINT #1, "  8"
    PRINT #1, "0"
    PRINT #1, " 10"
        PRINT #1, USING folin$; xx
    PRINT #1, " 20"
        PRINT #1, USING folin$; yy
    PRINT #1, " 40"
        PRINT #1, USING forad$; rr
    PRINT #1, " 50"
        PRINT #1, USING foang$; sa
    PRINT #1, " 51"
        PRINT #1, USING foang$; ea
    PRINT #1, "  0"
END SUB

SUB synthline (x1, y1, x2, y2)
STATIC xx1, yy1, xx2, yy2, fo$
    REM convert to millimeters
    xx1 = x1 * 1000: xx2 = x2 * 1000
    yy1 = y1 * 1000: yy2 = y2 * 1000
    PRINT #1, "LINE"
    PRINT #1, "  8"
    PRINT #1, "0"
    PRINT #1, " 10"
        PRINT #1, USING folin$; xx1
    PRINT #1, " 20"
        PRINT #1, USING folin$; yy1
    PRINT #1, " 11"
        PRINT #1, USING folin$; xx2
    PRINT #1, " 21"
        PRINT #1, USING folin$; yy2
    PRINT #1, "  0"
END SUB

SUB title
    COLOR 15
    VIEW PRINT 10 TO 25
    LOCATE 10, 1
    centre "F L E X U R E   H I N G E   A M P L I F I Y I N G   B R I D G E"
    PRINT : PRINT : PRINT
    centre "D E S I G N   S Y S T E M "
    PRINT : PRINT : PRINT
    centre "V e r s i o n  " + STR$(ver!)
    PRINT : PRINT : PRINT : PRINT : PRINT
'    IF NOT password THEN SYSTEM
centre "Press a key"
k$ = keypress$
    CLS 2
END SUB

SUB twait (seconds!)
    STATIC t!
    t! = TIMER + seconds!
    DO
    IF TIMER > t! THEN EXIT DO
    LOOP
END SUB

DEFINT A-Z
SUB txt.dump
STATIC x, y, a, l$
win4
CLS 2
INPUT "Dump File Name "; df$
IF df$ = "" THEN GOTO dennis
OPEN df$ FOR OUTPUT AS #1
    FOR y = 30 TO 57
    l$ = ""
        FOR x = 1 TO 80
            l$ = l$ + CHR$(SCREEN(y, x))
            REM PRINT a
        NEXT x
        PRINT #1, l$
    NEXT y
CLOSE #1
dennis:
CLS 2
END SUB

FUNCTION unity (x!)
    STATIC xx!
    xx! = ABS(LOG(ABS(x!)))
    unity = xx! < .00001
```

```
END FUNCTION

DEFSNG A-Z
SUB unityform (a$, a)
    PRINT RIGHT$(SPACE$(texlen%) + a$, texlen%);
    PRINT USING "     ##.#######    "; a
END SUB

SUB warp.geometry
    '   Allow visual manipulation of geometry

    STATIC pt%, quit%, adjer, update%
    DIM v(10), v$(10)
    v$(1) = "b": v$(2) = "d13": v$(3) = "d2": v$(4) = "l13": v$(5) = "l2"
    IF pt% = 0 THEN pt% = 1
    quit% = false%
    adjer = .02
    win4
    CLS 2
    LOCATE 57, 1
    PRINT "WARP GEOMETRY - (NUM LOCK ON)"
    DO
        update% = false%
        win4
        v(1) = b: v(2) = d13: v(3) = d2: v(4) = l13: v(5) = l2: v(6) = theta
        LOCATE 58, 1: PRINT "Select parameter (+/-/Ent)  "; v$(pt%); SPACE$(10);
        x$ = keypress$
        IF x$ = "6" AND pt% < 6 THEN pt% = pt% + 1
        IF x$ = "4" AND pt% > 1 THEN pt% = pt% - 1
        IF x$ = "7" THEN pt% = 1
        IF x$ = "1" THEN pt% = 6
        update% = (INSTR("82", x$) <> 0)
        IF x$ = "5" OR x$ = "Q" THEN EXIT DO
        IF x$ = "8" THEN v(pt%) = v(pt%) * (1 + adjer)
        IF x$ = "2" THEN v(pt%) = v(pt%) / (1 + adjer)
        b = v(1): d13 = v(2): d2 = v(3): l13 = v(4): l2 = v(5): theta = v(6)
        IF update% THEN
            l = (l2 + 2 * l13)
            r = l13 / l
            w = d2 / d13
            analyse
            display.geometry
            display.parametrics
            display.performance
            draw.structure
        END IF
    LOOP
LOCATE 58, 1: PRINT SPACE$(70);
END SUB

SUB win1
    VIEW PRINT 31 TO 40
    COLOR 6
    LOCATE 31, 1
END SUB

SUB win2
    VIEW PRINT 39 TO 46
    COLOR 2
    LOCATE 39, 1
END SUB

SUB win3
    VIEW PRINT 47 TO 52
    COLOR 3
    LOCATE 47, 1
END SUB

SUB win4
    VIEW PRINT 57 TO 59
    COLOR 4
    LOCATE 57, 1
END SUB

SUB win5
    VIEW PRINT 1 TO 29
    COLOR 5
    LOCATE 1, 1
END SUB
```

15 APPENDIX 5: CUSTOM INSTRUMENTATION.

This appendix contains circuit diagrams of two units of test equipment used during the project which were not available as commercial equipment, either due to non-existence or other reasons of non-availability such as cost. These were designed by the author.

15.1 GENERAL PURPOSE TEST AMPLIFIER.

The test amplifier was designed and constructed due to an essential requirement for a completely versatile medium voltage driver for use with piezoelectric multilayer actuators working at up to 150 V d.c.. It comprises a power supply, a high slew-rate d.c. coupled amplifier, based on Hex-FET technology, and a bi-state precision level generator, which can be driven by TTL/CMOS input. Additionally, either AC or DC analogue input can be used as a signal source.

The full amplitude bandwidth of the amplifier was broad enough to achieve electrical response times of less than 20 μs, unloaded.

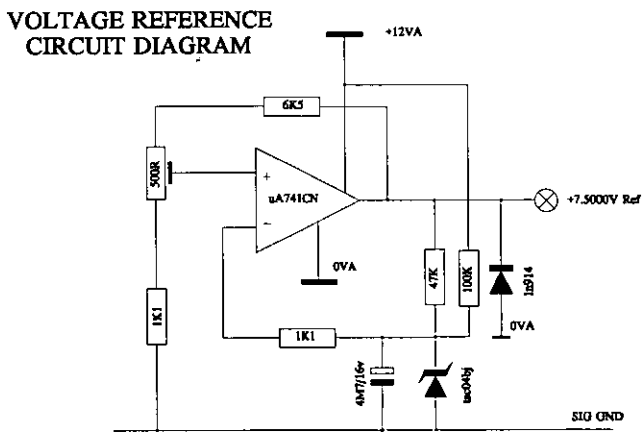

Figure 140: Precision Voltage Reference.

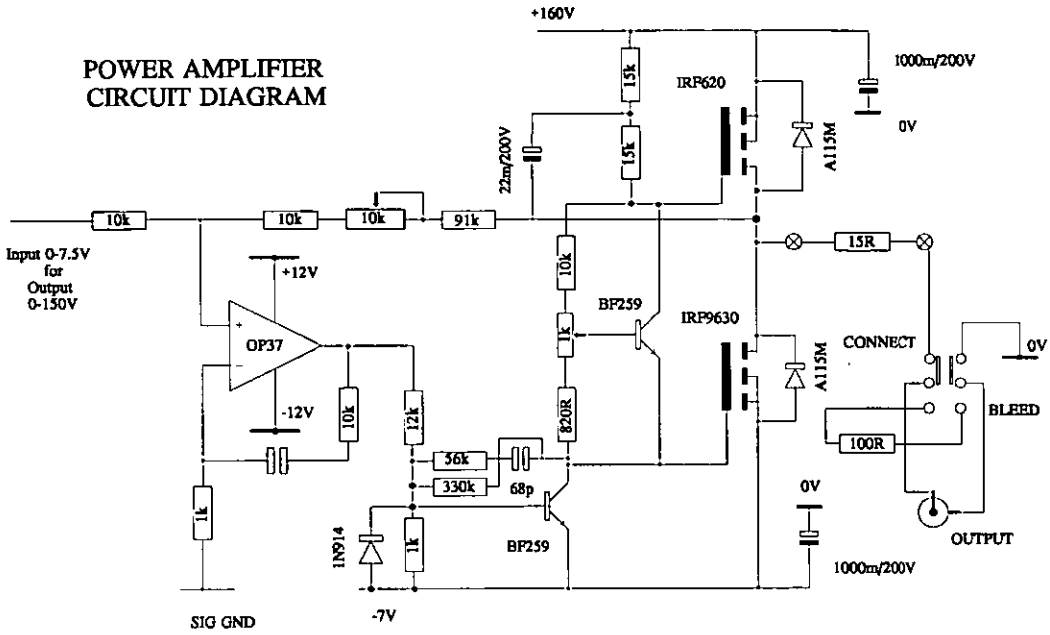

Figure 139: Test Amplifier Power Output Stage.

15.2 LOW-PASS FILTER.

The experiments with drive bandwidth cut-off required an active brick wall filter. This was designed around the MF6 series charge-pump filter circuit. The cut-off frequency (-3dB) of this filter is controlled by the frequency of a clock generated from a simple R-C oscillator, facilitated by the chip. The frequency ratio of clock to cut-off is fixed at 50:1 for this device. The unit was calibrated for dial-position against cut-off frequency.

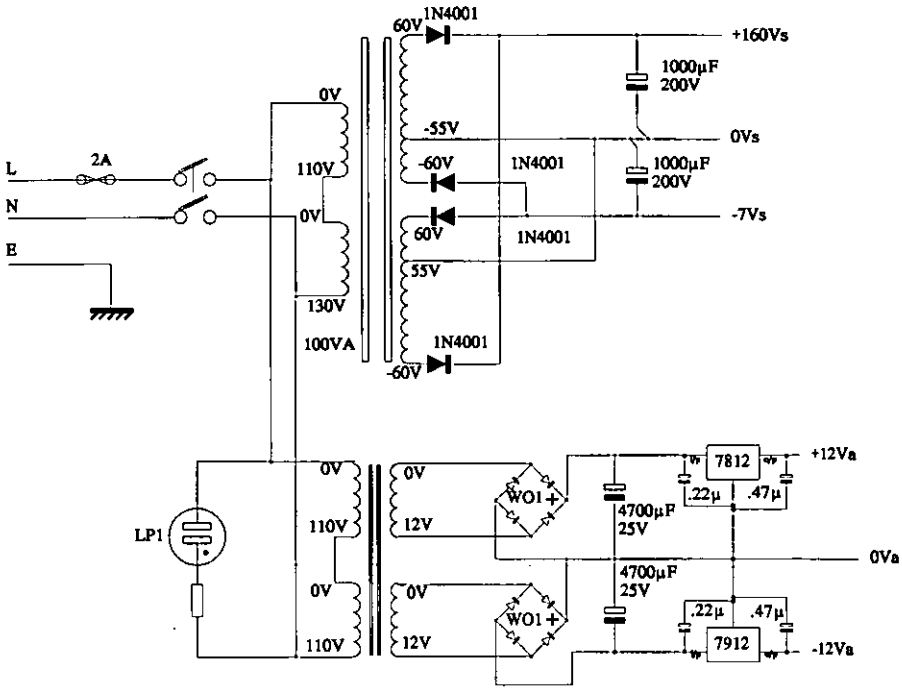

Figure 141: Power Supply for the Test Amplifier.

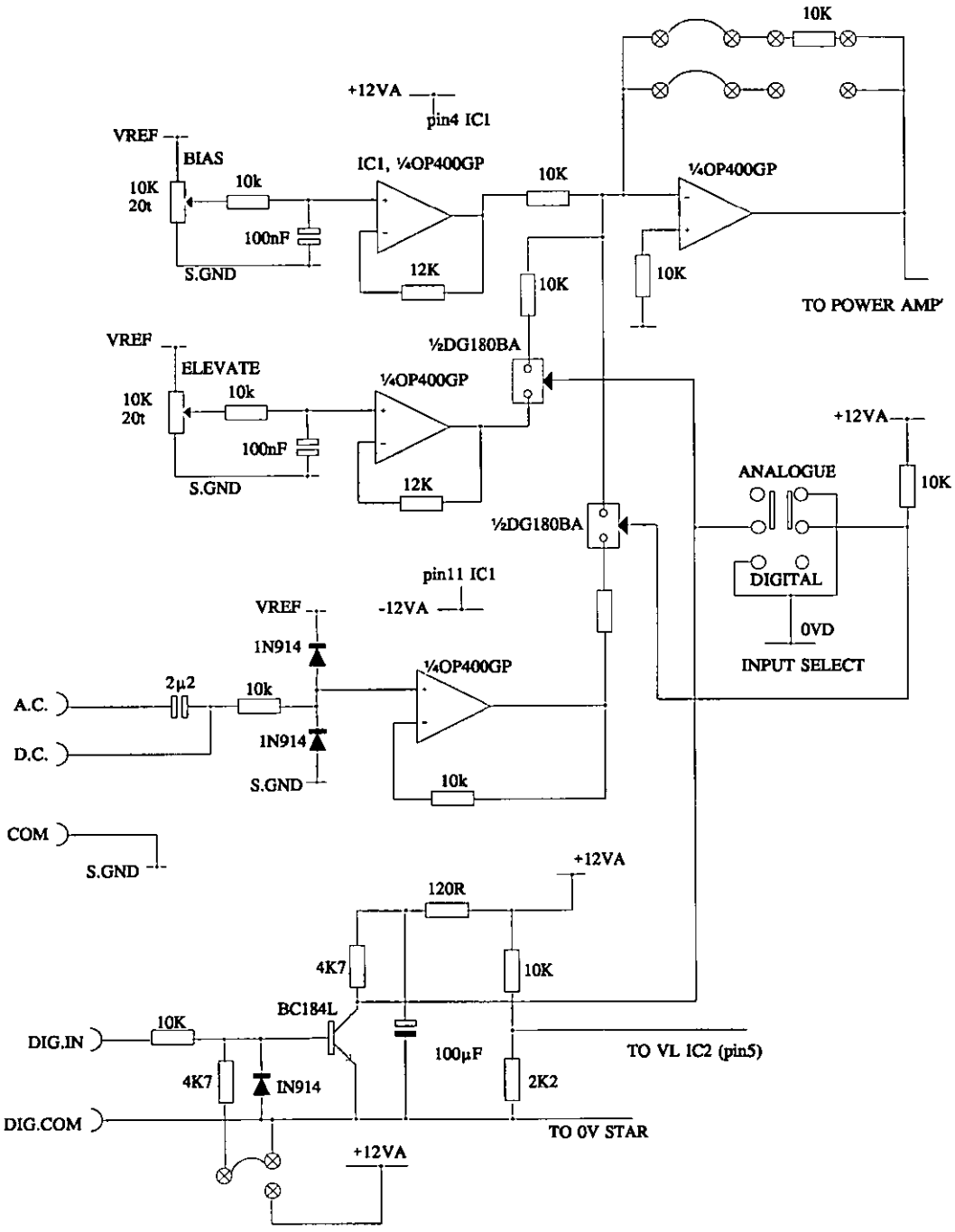

Figure 142: Drive Signal Conditioning Circuit.

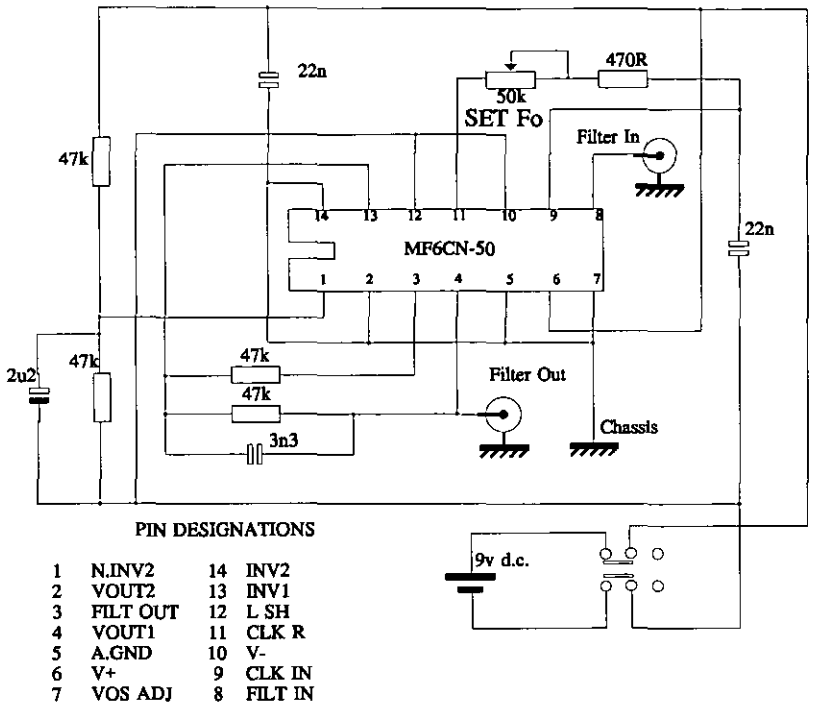

Figure 143: 6 th Order Butterworth Active Filter.

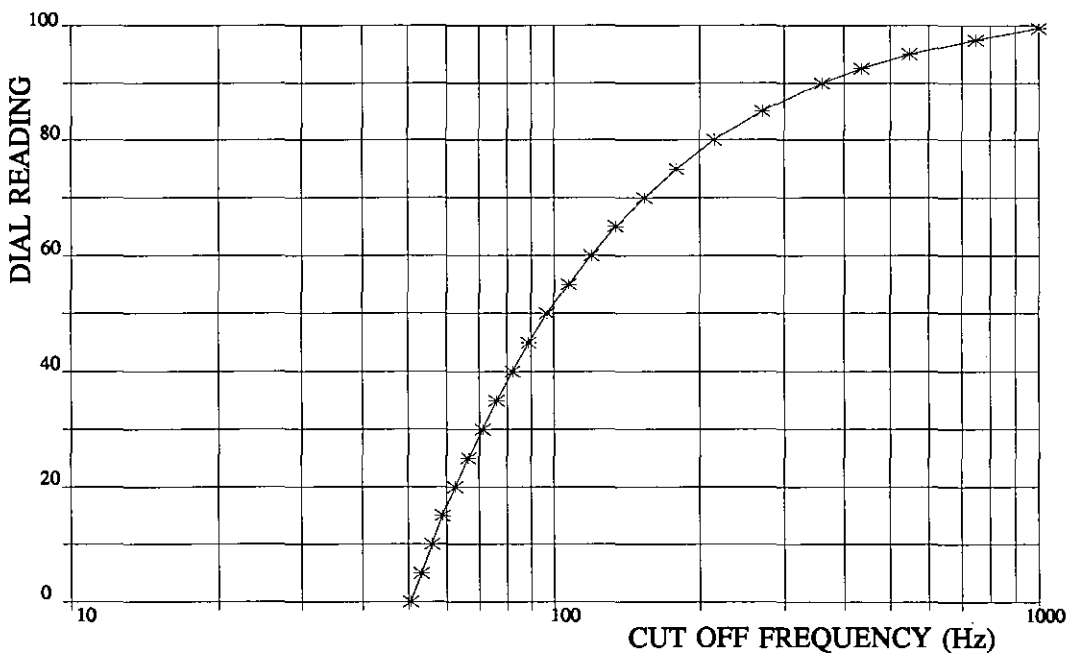

Figure 144: Calibration Curve for the Filter Circuit.

16 PLATES.

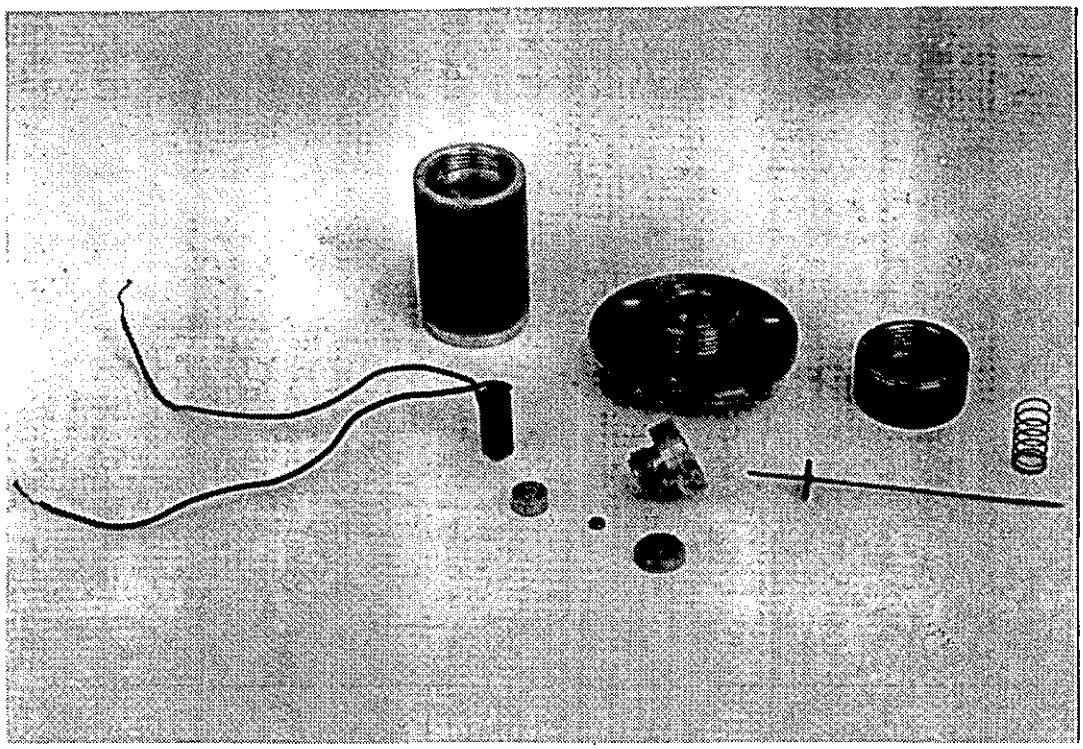

Plate 1: Component Parts of the Hydraulic Amplifier.

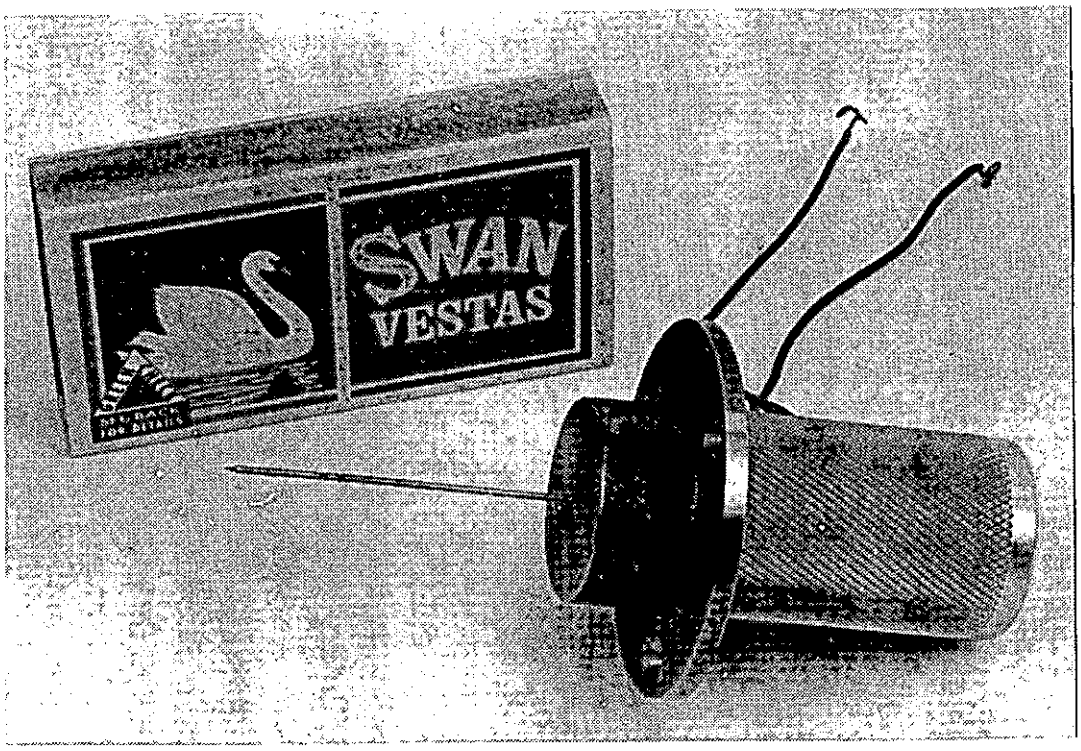

Plate 2: Assembled Hydraulic Amplifier.

Plate 3: A Complete Strip-Clutch Element, shown with a scale reference.

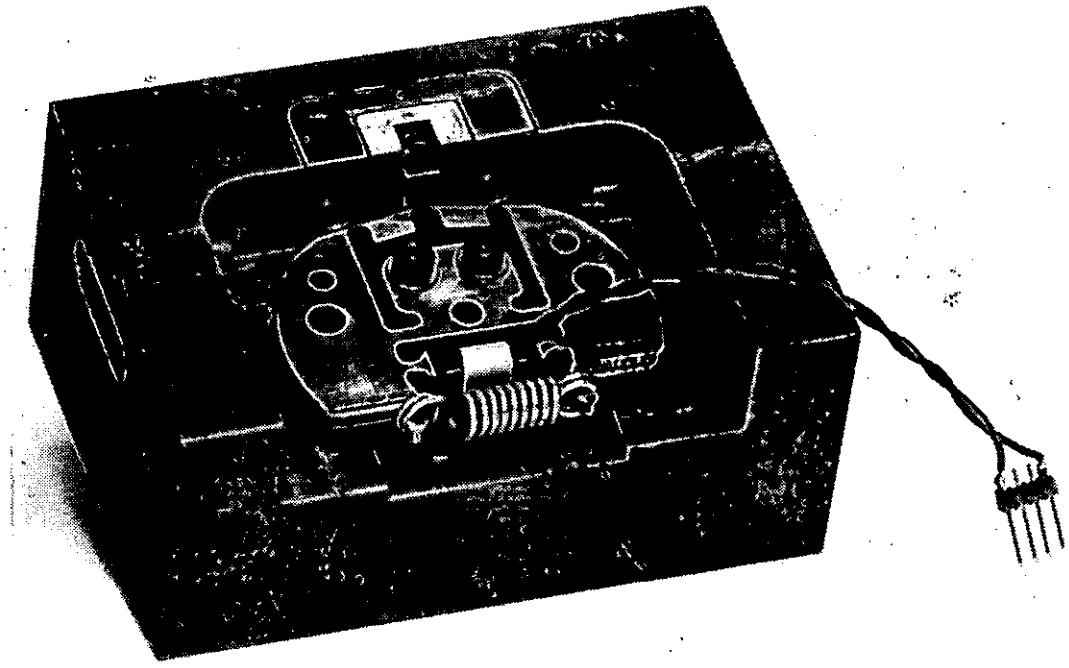

Plate 4: Strip-Clutch Element mounted on a jig for preliminary slip tests.

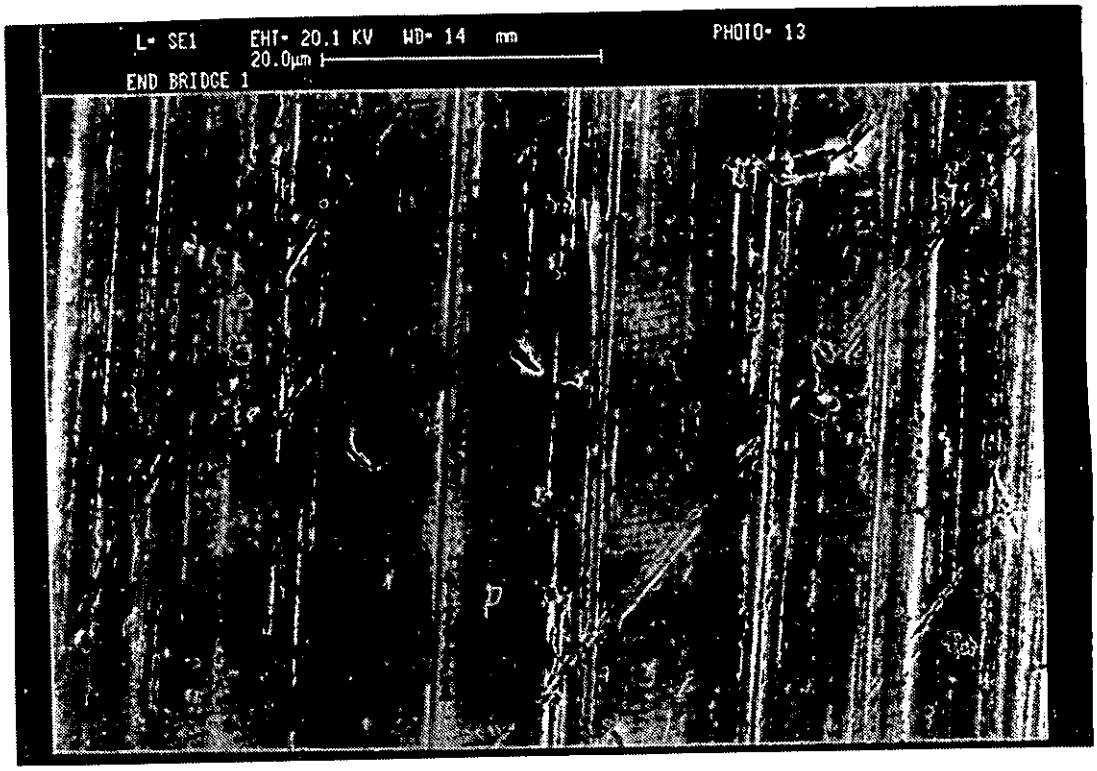

Plate 5: A Scanning Electron Micrograph of Zone 4 of the Strip-Clutch.

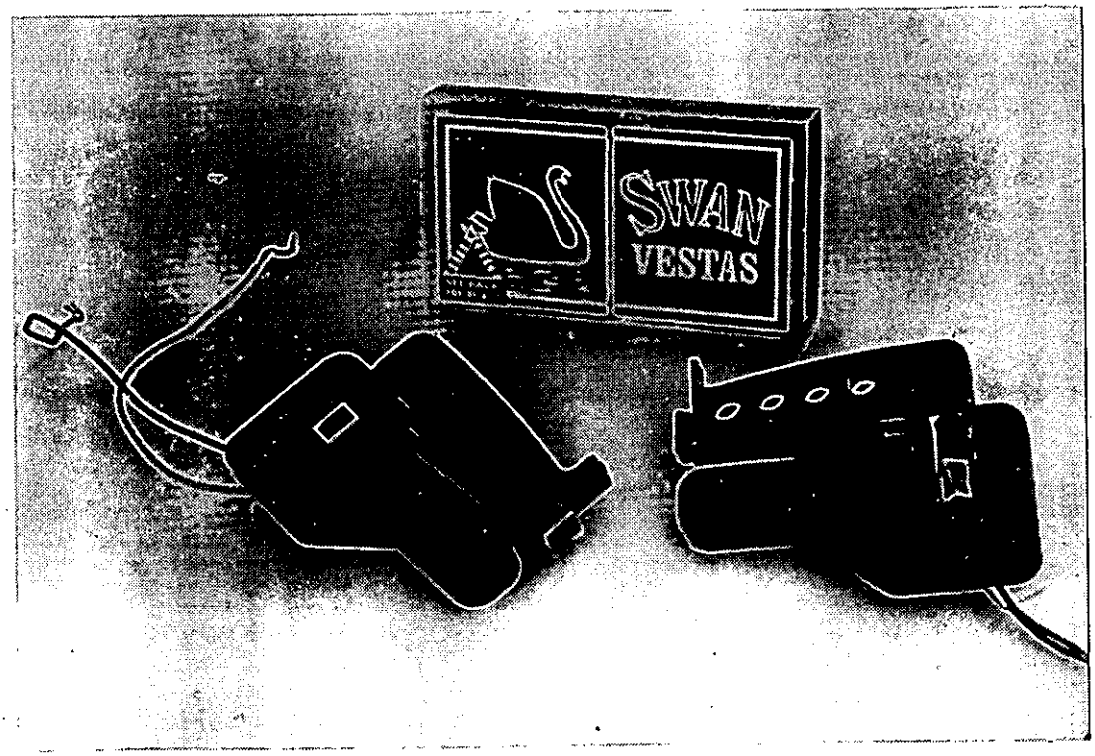

Plate 6: Two Simple Beam Amplifiers (200µm Output).

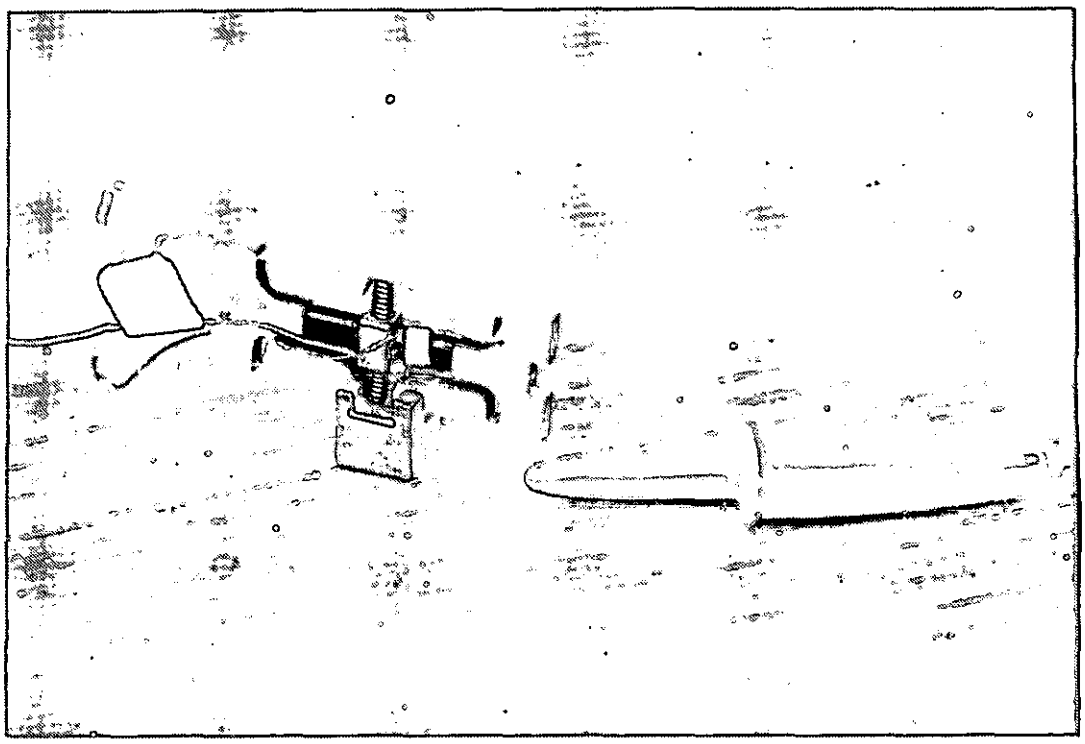

Plate 7: The Bilateral (200μm Output) Flexure Bridge Amplifier.

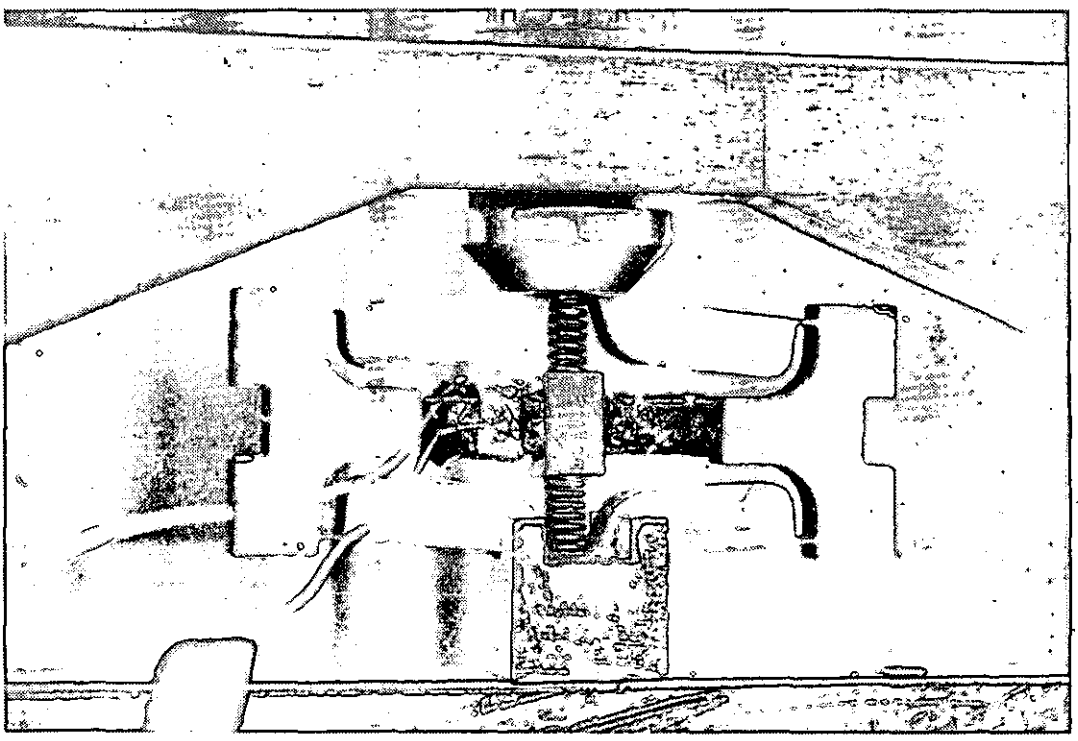

Plate 8: Bilateral Amplifier Compliance Measurement.

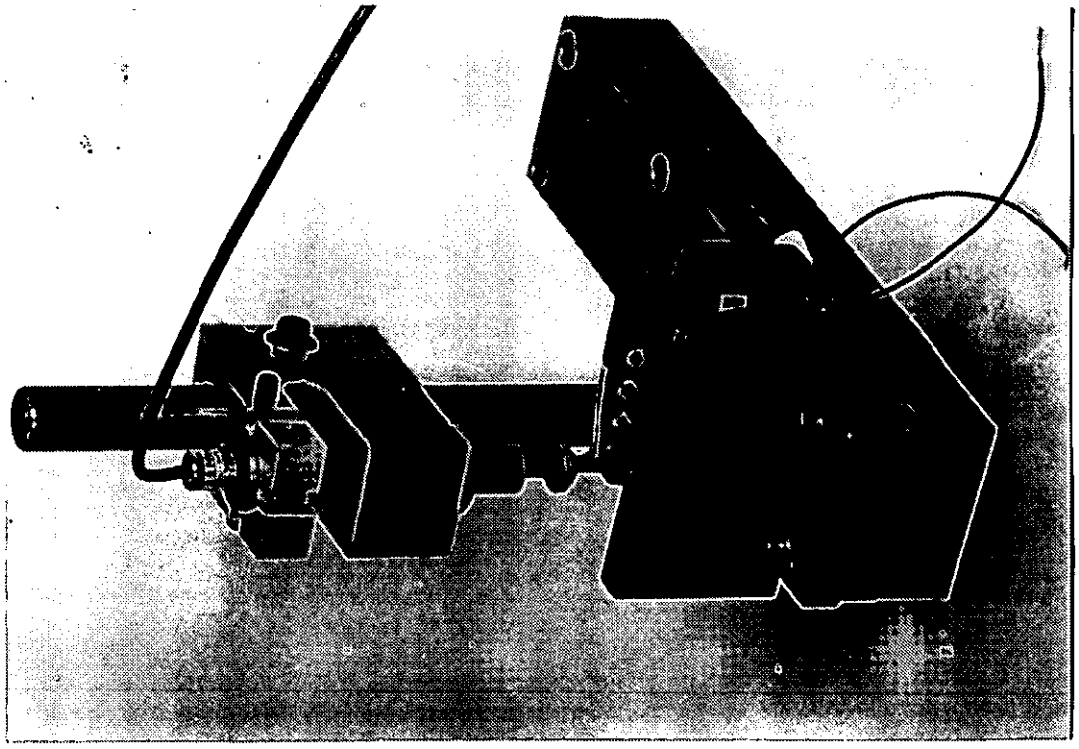

Plate 9: Simple Beam Amplifier on the Test Apparatus.

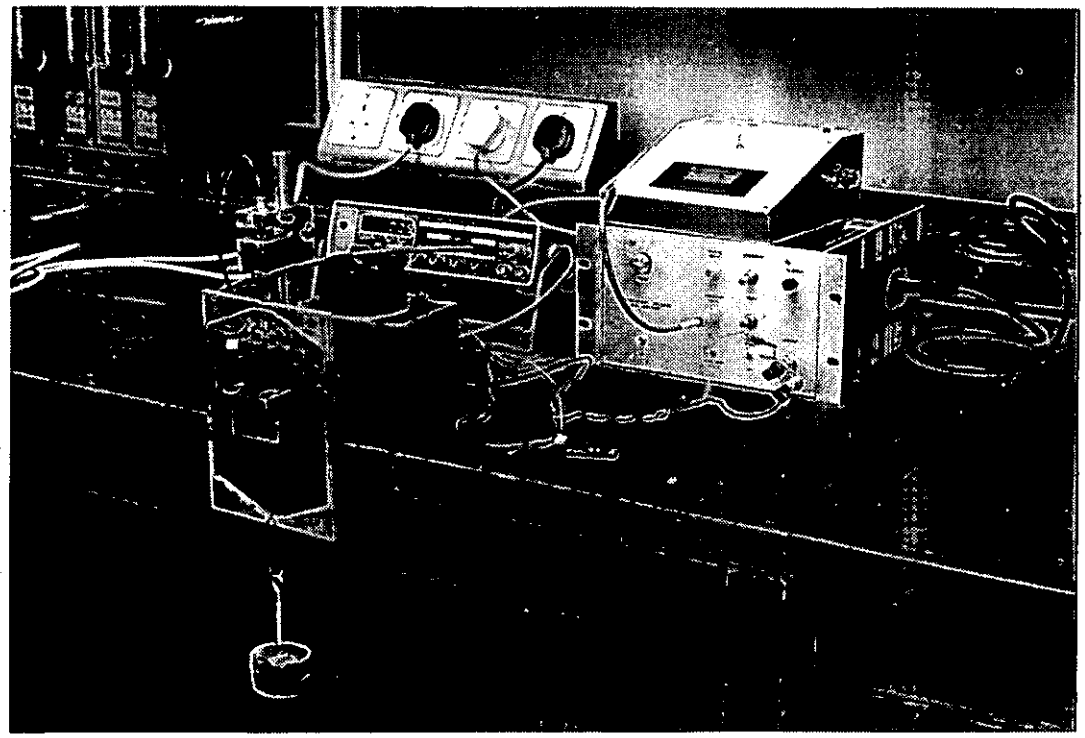

Plate 10: Complete Static Test Apparatus.

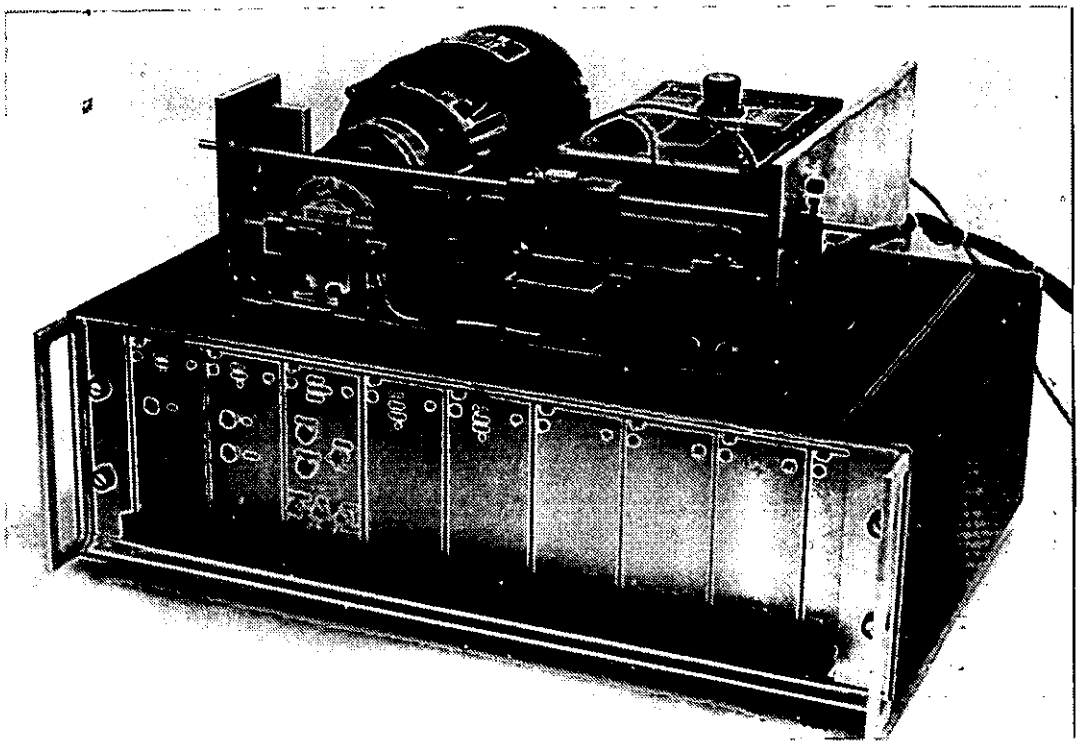

Plate **11**: Discrete Motion Machine complete with Drive Electronics.

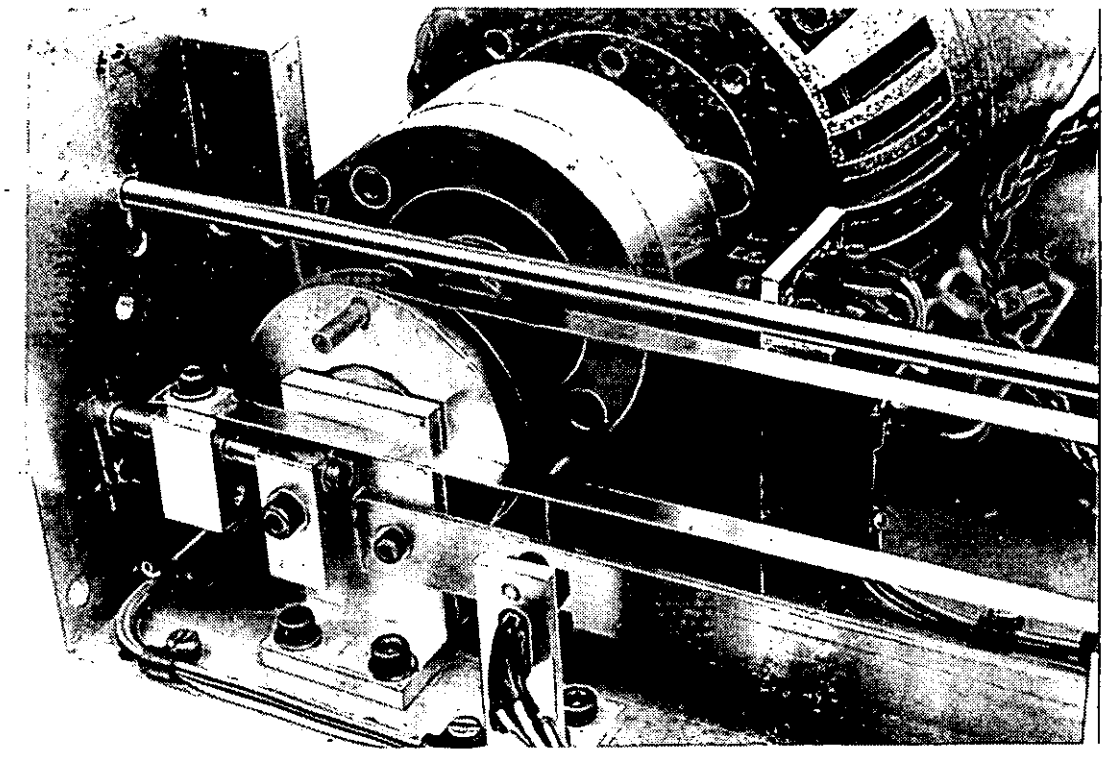

Plate **12**: Detail showing; Motor, Slot Cam, Rocker, Opto-switches and Strips.

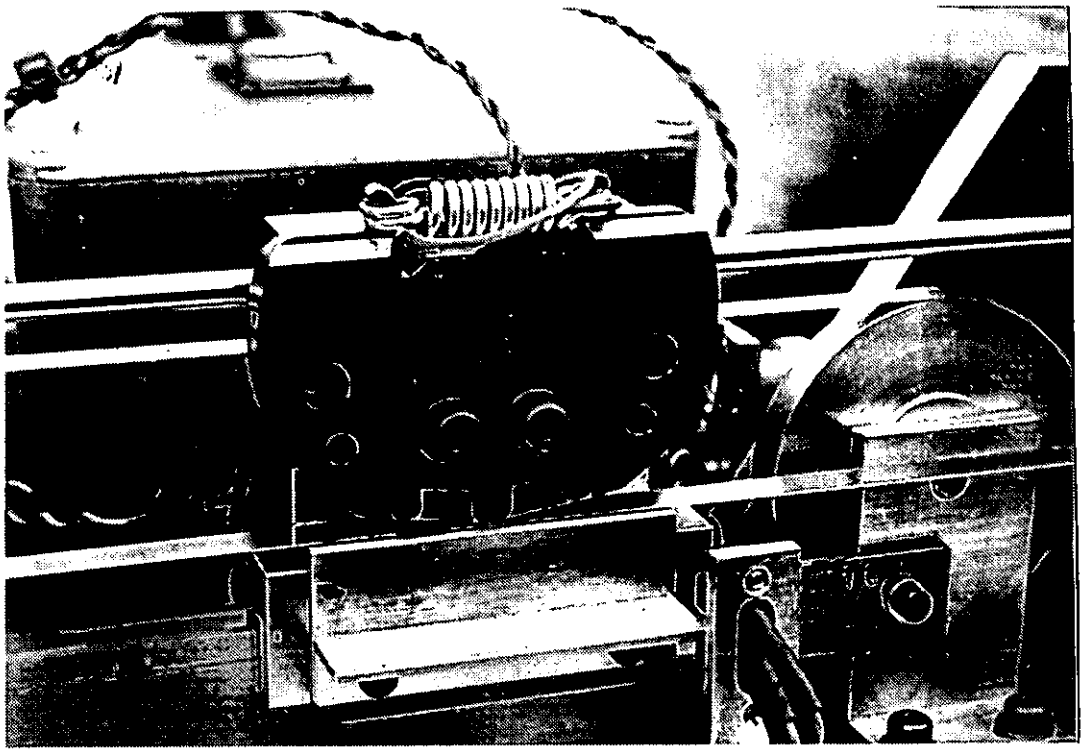

Plate **13**: One Strip-Clutch mounted on the Machine Carriage.

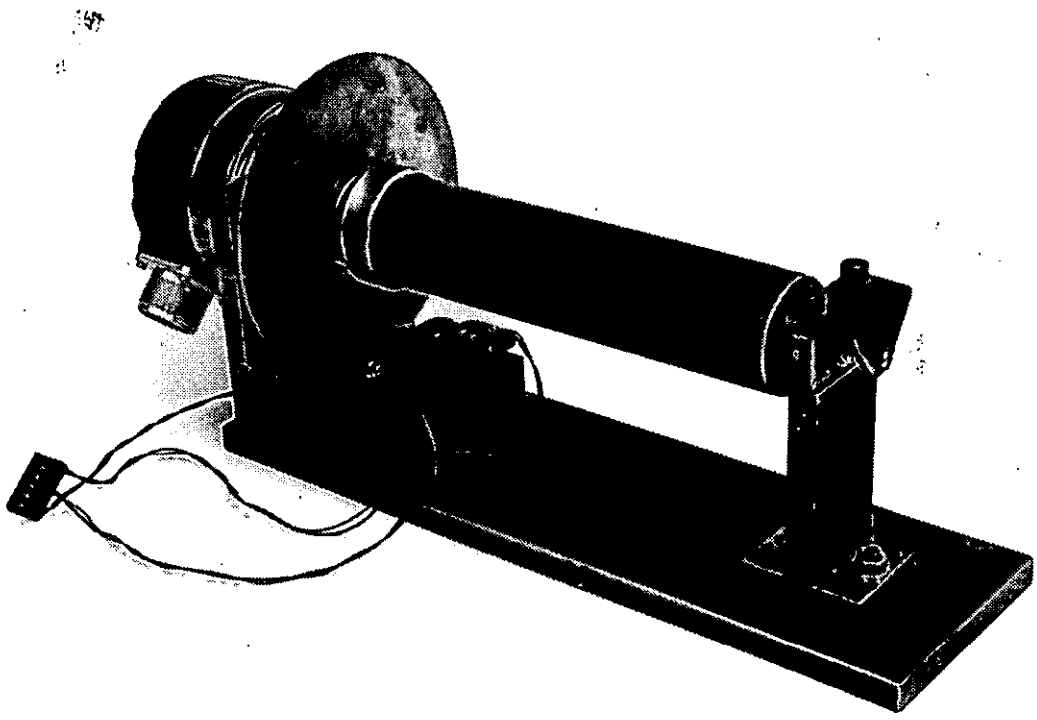

Plate **14**: Mechanics for the Rotary Micro-positioner.

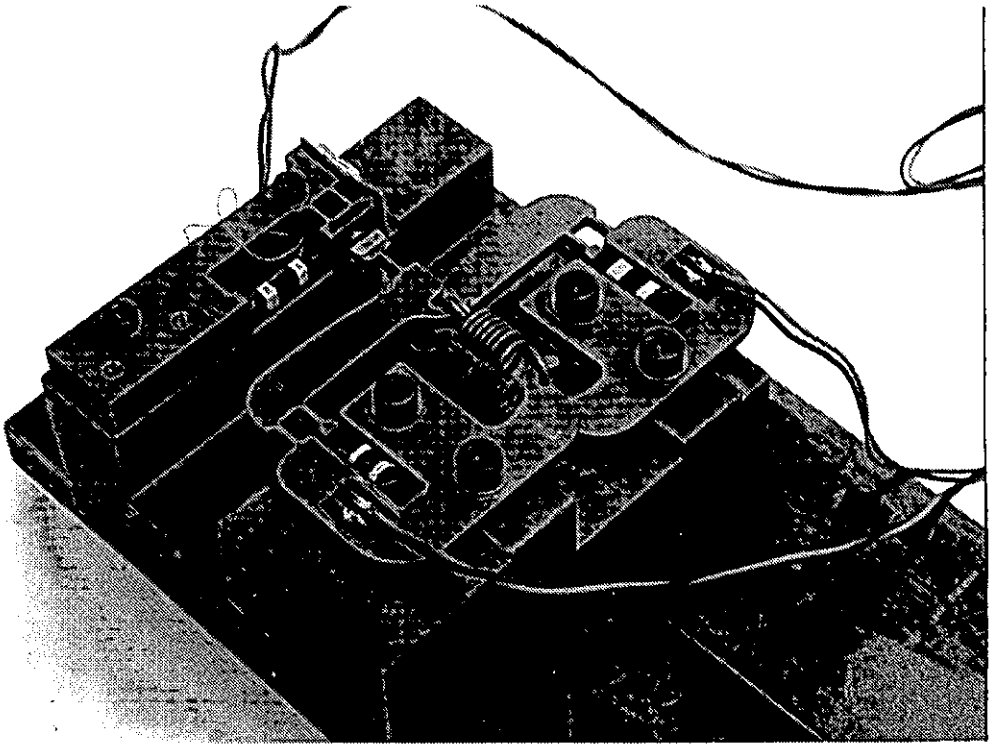

Plate **15**: Close-up of the Clutching and Extending Mechanism.

17 REFERENCES.

1 Seilly, A.H., Fast-acting helical solenoid actuators, IEE Proceedings D (Control Theory and Applications), vol.127, no.6, pp.245-9

2 Jaffe, Cooke and Jaffe, Piezoelectric Ceramics, Academic Press, 1971

3 Piezoelectric Ceramic Products Literature, Morgan Matroc, Unilator Division, Clwyd, UK

4 Herbert, J.M., Ferroelectric Transducers and Sensors, Gordon and Breach, 1982

5 Piezoelectric Technology for Designers, Vernitron Piezoelectric Division, Ohio, USA

6 Ikebe, Y., et. al., Load Insensitive Electro-Hydraulic Servo-system, ASME J. Dynamic Systems Meas Control, 103, 1981, 361

7 Takahashi S., Yano T., Fukui I., Sato E., Multilayer Piezoelectric Actuator with Varying Thickness Layers, Proc. of the 5th Meet. on Ferroelectric Materials and Their Applications, Kyoto 1985, Jap. J. of Appl. Phys., Vol. 24 (1985), Suppl. 24-3, pp. 206-208

8 Takahashi S., Multilayer Piezoelectric Ceramic Actuators and Their Applications, Proc. of the 6th Int. Meet. on Ferroelectricity, Kobe 1985, Jap. J. of Appl. Phys., Vol. 24 (1985), Suppl. 24-2, pp. 41-45

9 Panasonic Ultrasonic Motor, Technical Leaflet from Matsushita Electric Industrial Company Ltd., Japan

10 "The Piezo Book", Burleigh Instruments Inc. New york, USA

11 Gee, A.E., A Micro-Incher Machine Carriage Drive with Automatic Feed-Back Control of Step-Pitch, Step-Phase and Inter-Step Positioning, Precision Engg, 4, 2, 1982, pp. 85-91

12 Catalogue of Physik Instrumente GmbH & Co., W.Germany

13 Thornley J.K., et.al., Piezoelectric and Electrostrictive Actuators: Device Selection and Application Techniques, IMechE, Eurotech Direct - Machine Systems, 2-4 July 1991, NEC, Birmingham U.K., paper C414/057, pp. 115-119.

14 Kusaka C., Tomikawa Y., Narita K., Driving Voltage Waveform for High Speed Operation of a Piezoelectric Actuator, Proc. of 9th Symp. on Ultrasonic Electronics, Sendai 1988, Jap. J. of App. Phys., Vol. 28 (1989), Suppl. 28-1, pp. 97-99

15 Tamaru, N., Piezoelectric Bimorph Actuator Control Using a Kalman Filter, Trans. Soc. Instrum Control Eng., 1987, Vol 23, Pt. 8, pp. 873-5

16 Mitsuhashi, S., et. al., Relay Using Multilayer Piezoelectric Actuator, Proc. of the 5 th Meeting on Ferrorelectric Materials and Their Applications, Kyoto 1985, Jap. J. of Appl. Phys., Vol 24 (1985) Suppl. 24-3, pp. 190-192

17 Schmeisser F., Piezoelectric Actuators: powerful and fast, Electronik, 1984, Vol. 33, Part 8, pp. 92-96

18 Kaizuka H., Siu B., A Simple Way to Reduce Hysteresis and Creep When Using Piezoelectric Actuators, Jap. J. of Appl. Phys., Vol. 27, No. 5, May 1988, pp. L773-L776

19 Okazaki Y., A micro-positioning tool post using a piezoelectric actuator for diamond turning machines,Precision Engineering, July 1990, Vol. 12, No.3, pp.

151 -156

20 Atherton P., Micropositioning Using Piezoelectric Translators, Photonics Spectra, December 1987, pp. 51-54

21 Shimizu H., Takeuchi Y., et. al., A Basic Study on the Development of a Highly Accurate Rotational Positioning Acutator, Nippon Kikai Gakkai Ronbunshu, Hen-Tra, Vol. 55, Pt. 517, pp. 2371-2375

22 Nakajima Y., Hayashi T., Hayashi I., Uchino K., Electrostrictive Properties of a PMN Stacked Actuator, Jap. J. of Appl. Phys., Vol. 24, No. 2, February 1985, pp. 235-238

23 Ogawa T., Ando A., Wakino K., Electrostrictive Properties of Monolithic Bimorphous Actuator, Ferroelectrics, 1986, Vol. 68, pp. 249-256

24 Tomikawa Y., Masamura K., Sugawara S., Konno M., Fundamental Consideration of Piezoelectric Ceramic Multi-Morph Actuators, Proc. of the 6th Int. Meet. on Ferroelectricity, Kobe 1985, Jap. J. of Appl. Phys., Vol. 24 (1985), Suppl. 24-2, pp. 457-459

25 Kondo M., Ohya K., Effects of One-Dimensional Compressive Stress on the Properties of Multilayer Piezoelectric Ceramic Actuator, NEC Res. & Develop., Vol. 32, No. 2, April 1991

26 Fujii H., Ohnishi Y., On the Responsibility of Piezoelectric Actuator, Proc. of the 6th Meet. on Ferroelectric Materials and Their Applications, Kyoto 1987, Jap. J. of App. Phys., Vol. 26 (1987), Suppl. 26-2 pp. 177-179

27 Kato T., Imai A., Measurements of Equivalent Circuit Parameters of Piezoelectric Ceramic Resonators, Proc. of the 6th Meet. on Ferroelectric Materials and Their Applications, Kyoto 1987, Jap. J. of App. Phys., Vol. 26

(1987), Suppl. 26-2 pp. 191-194

28 Kramarov S.O., Beliaev A.V., Grekov A.A., Katsnelson L.M., Strength Characteristics and Microstructure of Some Piezoceramic Composites, Ferroelectrics, 1986, Vol. 68, pp. 45-52

29 Ochi A., Takahashi S., Tagami S., Temperature Characteristics for Multilayer Piezoelectric Ceramic Actuator, Proc. of the 5th Meet. on Ferroelectric Materials and Their Applications, Kyoto 1985, Jap. J. of Appl. Phys., Vol. 24 (1985), Suppl. 24-3, pp. 209-212

30 Ohuchi H., Nakano K., Uchino K., Endoh H., Fukumoto H., High-Speed Electro-hydraulic Servovalves using Electrostrictive Ceramic PMN Actuators, Fluid Control & Measurement, 1986, Vol. 1, pp.157-162

31 DeMeis, R., Piezoelectric Damping for Space Structures, Aerospace America, Sept 1985, pp. 32-3

32 Gaffard, J.P., et. al., Adaptive Optics with segmented mirror of deformable mirror, J. de Physique Colloque, vol.41, no.C-9, pp. C9/269-73, Nov. 1980

33 Fuschetto, A., Three-actuator defirmable water-cooled mirror, Optical Engg., vol.20, no.2, pp. 310-15

34 Albertinetti, N.P., et. al., Deformable mirrors with bimorph actuators, Proc. of the Soc. of Photo-Optical Instrum. Engineers, vol.179, Adaptive Optical Components II, pp.28-31

35 Lloyd J., La Comb, Jr., Quate C.F., Piezodriven Scanner for Cryogenic Applications, Rev. Sci. Instrum. 59 (9), Spet. 1988, pp. 1906-1910

36 Okayama, S., et.al., High resolution piezoelectric actuator for STM, J. Jap. Soc.

of Prec. Eng., vol.54, no.5, pp.817-21

37 Blackford B.L., Dahn D.C., Jericho M.H., High-Stability Bimorph Scanning Tunneling Microscope, Rev. Sci. Instrum., 58(8), August 1987, pp. 1343-1348

38 Kobayashi, M., et.al., Noiseless trick-play techniques using Piezoelectric Ceramic Actuator for VTRs, Wireless Res. Lab., Matsushita Electric Industrial Co. Ltd., Osaka, Japan, National Tech. Report, vol. 28, no 3, pp.419-27, 1982

39 Tojo T., Sugihara K., Piezoelectric driven Turntable with High Positioning Accuracy, Bull. Jap. Soc. of Prec. Engg, Vol. 19, No. 2, June 1985, pp. 135-137

40 Higuchi T., Watanabe M., Kudou K., Precise Positioner Utilising Rapid Deformations of a Piezoelectric Element, J. Jpn. Soc. of Prec. Engg., 1988, Vol. 54, Part 11, pp. 2107-2112

41 Lee F.C., PZT Printing Applications, Technologies, New Devices, Ultrasonics Symposium (1988), pp. 693-697

42 Yoshida K., Yoshiura T., Shimada Y., Ceramic Green Sheet Puncher Using Multilayer Piezoelectric Actuator, Proc. of the 6th Meet. on Ferroelectric Materials and Their Applications, Kyoto 1987, Jap. J. of App. Phys., Vol. 26 (1987), Suppl. 26-2 pp. 186-187

43 Schmeisser F., Piezoelectric Actuators: powerful and fast, Electronik, 1984, Vol. 33, Part 8, pp. 92-96

44 Takahashi, S., Piezoelectric actuator and its applications, Fundamental Res. Labs., NEC Corp. Tokyo, Japan, Oyo Buturi, vol.54, no.6, pp.587-8

45 Crawley, E.F., Development of piezoelectric technology for applications in

control of intelligent structures, Proc. of the 1988 American Control Conference, pp. 1890-6, vol3., 1988

46 Tanuma C., Yoshida S., Yamashita Y., Piezoelectric Materials for Low Hysteresis Actuators, Proc. of the 6th Meet. on Ferroelectric Materials and Their Applications, Kyoto 1987, Jap. J. of App. Phys., Vol. 26 (1987), Suppl. 26-2 pp. 174-176

47 Higuchi T., State and Future Trend of Solid Element Actuator, J. Jpn. Soc. Precis. Eng., 1987, Vol. 53, Part 5, pp. 683-685

48 Nomura, S., Uchino, K., Recent Applications of PMN-based electrostrictors, Ferroelectrics, vol.50, no.1-4, pp. 523-8, Nov. 1983

49 Spanner, K., Marth, H., Precise Positioning with Piezoelectric Translators, Lasers & Applications, August 1983, pp. 61-63

50 Paros J.M., Weisbord L., How to design Flexure Hinges, Machine Design, 1965, November 25, pp. 151-156

51 Tsutsumi, Y., et. al., Development of Piezo TEMS (Toyota Electronic Modulated Suspension), SAE Technical Paper Series 901745

52 Heywood R.B., `Designing Against Fatigue', Chapman & Hall Ltd, London, 1962

18 PUBLICATIONS.

1 Thornley J.K., et.al., Piezoelectric and Electrostrictive Actuators: Device Selection and Application Techniques, IMechE, Eurotech Direct - Machine Systems, 2-4 July 1991, NEC, Birmingham U.K., paper C414/057, pp. 115-119.

2 Thornley J.K., Preston M.E., King T.G., A Fast Electro-mechanical Clutch Clement using a Piezoelectric Multilayer Actuator, Colloquium on `Robot Actuators', IEE, 7 October 1991, Savoy Place, London, Dig. Ref 1991/146, pp. 1-4.

3 Thornley J.K., Preston M.E., King T.G., A Very High-speed Piezoelectrically Actuated Clutching Device., Mechatronics, Spec. Ed. - Actuators. Publication Accepted.

4 Thornley J.K., Preston M.E., King T.G., A Piezoelectrically-Controlled Rotary Micropositioner for Applications in Surface Finish Metrology, IFToMM-jc International Symposium on Theory of Machine and Mechanisms, Sept. 1992, Nagoya, Japan..

5 Thornley J.K., Preston M.E., King T.G., The Design of Mechanical Amplifiers using Piezoelectric Multilayer Devices for use as Fast Actuators., International Conference: Mechatronics, University of Dundee, Scotland, 22nd Sept. 1992.

PIEZOELECTRIC AND ELECTROSTRICTIVE ACTUATORS: DEVICE SELECTION AND APPLICATION TECHNIQUES

Mr.J.K.Thornley, Dr.M.E.Preston, Dr.T.G.King
Department of Mechanical Engineering
Loughborough University of
Technology, U.K.

ABSTRACT.

This paper offers a simple methodology for the selection of piezoelectric or electrostrictive devices for fast two-state actuator applications. Specifically, the paper discusses the factors of response time, hysteresis, displacement, and movement amplification techniques, and asserts that the maximum mechanical strain energy density value for an actuator is a practical figure of merit for device selection.

1. INTRODUCTION.

Despite the commercial appearance of piezoelectric devices some 40 years ago, it is only within the last few years that interest in these devices has been rekindled. The reasons for this are many, but must include the emergence of new materials, and manufacturing techniques, fostering devices of unprecedented performance. The employment of manufacturing techniques common to the production of multilayer capacitors has meant improvements in device operating voltage, reliability and range of application. These techniques currently allow multilayer devices to be cheaply assembled with layer thicknesses of less than 50 μm, and this is expected to fall to even lower figures. [1]

Because piezoelectric devices have been applied extensively in the fields of sonar and non destructive testing, it is inevitable that the data will reflect the requirements of these areas. Now that a new generation of devices is available, which lend themselves to power actuation, and in particular, two-state operation, the existing data form only a nucleus from which more useful information can be extracted.

It is the intent of the authors to present a methodology, with suggestions of useful techniques, whereby application specific requirements may be quickly arrived at, based on existing manufacturers data.

2. STRAIN ENERGY DENSITY AS A FIGURE OF MERIT.

Whatever form an actuator assumes, to produce movement from one position to another requires an energy input. In many applications, little or no work output is required, and in those cases, the philosophies presented here will be of little interest. It is with cases where the **efficiency** of the device is important, that we are concerned here.

Taking the case of a clutching mechanism involving some mechanical amplifying device, it is clear that within such a mechanical system, there has to be a minimum working clearance, or gap between the clutching surfaces. In addition, it might be expected that the clutch plates would be held together with a certain pressure or force, when clutching action occurs. The required constraints of clutching force and clearance can be expressed as an function of energy. (Despite the fact that with a perfect clutch no work is done, in practice the whole mechanism is compliant and therefore gives rise to work being done by the actuator against this compliance). Further, one might reason as follows;

Specifying the clutching action to begin at 50% of the actuator's free full travel (X_{max} at full electrical drive), this would result in a developed force of precisely half that of the isometrically developed force (F_{max}), when the actuator is taken to full electrical drive. Thus a work function can be expressed as;

$$W = \frac{F_{max} . X_{max}}{4}$$

There are many systems which can be subjected to this rationale and in general, the ability of an actuator/amplifying mechanism to do useful work can always be related back to the output stiffness and its maximum free extension. The precise coupling coefficients will vary from system to system.

For a linear amplifying system, this function must relate to the ability of the actuator to do work. It can be shown that this is related to the maximum stored energy of the free actuator, which is;

$$W = \frac{V.E.\epsilon^2_{max}}{4}$$

where V is device volume, E is elastic modulus and ε_{max} is the maximum safe electrically-inducible strain.

Since E and ε_{max} are essentially constants for a particular material and construction technique, the approximate volume of ceramic required can be calculated. Simplistically, rearrangement shows an energy/unit volume figure is calculable, thus making it possible to calculate the amount of material required for a device in a given application.

As an example, if a 100N clamping force was required at a range or clearance of 50 micron, W = 1.25 mJ. Using materials such as those used in actuators from Group 1 of Figure 1, we can calculate a collective effective Modulus of 5.66 GPa, and a required volume of $1.73 \times 10^{-6} m^3$. As a direct coupled actuator this would imply an actuator length of 70 mm. This is not entirely practical, although devices of similar length exist.

Although for a specific system, it is important to more fully understand the dynamics, simple calculations can quickly show, to within a half order of magnitude, the size and characteristics of the required actuator.

Using this approach, by calculating the W/V value for a range of actuators, manufactured with differing materials and by differing processes, a figure of merit can be adopted to assist in choosing the actuator most suitable for an application. Some examples are shown in Fig 1. Whilst this is probably one of the most useful approaches, the criterion must be tempered with other factors, such as hysteresis and speed of response.

Each group contains devices of similar construction but of differing size. Note that the devices in group 1 are constructed from a material with similar bulk composition, but are constructed as stacks, using adhesives, whereas the remainder are of multilayer construction.

The low figures, produced by these older style stacks (Group 1) are dwarfed by multi-layer piezoelectric devices (Groups 3,4 and 5), and still further by new generation electrostrictors (Group 2).

Fig.2 illustrates the basic difference between multilayer and stack construction. The smaller active zone of the stack on the left consists of piezoelectric, electrode and bonding materials, all of which contribute to the mechanical characteristics of the device. Note that the electrodes and bond zones are exposed to shear stress. With the multilayer device, the electrodes are effectively thin conductive zones in the bulk ceramic; the whole device contributes to extension and to its' mechanical properties.

To summarize, the basic approach is that;

An actuation application requires a certain (maximum) energy, which must be coupled through a lossy medium.

In electrostrictors or piezoelectric devices, an energy function can be assigned, which must match the actuation and loss criteria for a given application. Materials are preferred where the product $k.\varepsilon_{max}^2$ is high as this quantity implies a reduction of the mass of the device required.

3. DISPLACEMENT.

For many applications, the output movement of the actuator must be amplified, and therefore to reduce the burden of amplification placed up on an external device, the maximisation of actuator displacement and hence choice of device can be primary.

When considering the output movement of an actuator, the coefficient often cited as of high importance for stacks and multilayer devices is the d_{33} value, (or

strain/applied electric field). Whilst this figure is valuable, its use must be tempered with the maximum allowed electric field and therefore the resultant maximum strain obtainable.

For Lead Zirconate Titanate materials, typical values of d_{33} vary from 150 x 10^{-12} to over 600 x 10^{-12} mV^{-1}. The higher values are generally associated with lower Curie temperatures, lower maximum strains, lower Young's modulus and higher hysteresis; the materials with these characteristics are called *Soft PZTs*.

Data on most multilayer actuators currently available usually indicates the free output movement of the actuator.

4. HYSTERESIS.

For positioning applications such as those found in optics and, in particular, systems where there is no closed loop control, hysteresis parameters will undoubtedly be critical in determining material selection. This usually rules out soft piezos since a 15% hysteresis value is typical for these materials.

Electrical drive techniques have been proposed by Kaizuka, et al.[3] which claim to reduce creep and hysteresis significantly, at the expense of device sensitivity.

In two-state systems however, hysteresis principally affects the energy lost in one complete actuation cycle, which will ultimately appear in device heating. Fig.3 shows an idealised piezoelectric actuator stress/strain curve for a device with 15% hysteresis.

For an actuator under minimal loading, the energy loss per cycle, due to hysteresis, although dependent on the shape of the stress/strain characteristic, can be approximated to;

$$E_h = E_s . p . h_{max}$$

where E_h is the energy lost/unit volume/cycle, E_s is the strain energy/unit volume, h_{max} is the maximum hysteresis, and p is a unitless shape factor whose value depends on the hysteresis curve and usually falls in the range;

$$0.5 \leq p \leq 0.8$$

5. RESPONSE TIME.

Whilst it is tempting to think that in high-speed machines, the response time of the actuator is a vital factor for device selection, this is often **not** the case. Most, but not all, practical systems employ some kind of amplification device, to produce useful movement, and it is these structures which usually dominate the response

characteristics of the ensemble.

However, in applications where no mechanism exists and/or the actuator is lightly loaded, the response of the system can be obviously simplified into two basic components, i.e. the electrical and mechanical factors.

To consider electrical and mechanical factors in isolation is entirely inappropriate with piezoelectric devices, by their very nature. However, careful design of well damped or pulse-tailored drive amplifiers will aid in minimising response times. [2]

a. ELECTRICAL RESPONSE.

This factor is principally dependent on how the device is electrically driven, possibly by a simple solid-state switch or by techniques involving current or charge dumping. For a simple switch, the response time (90% full response) is given by;

$$t_{res}=(2.30).R_{eff}C_{act}$$

where R_{eff} is sum of the effective drive resistance and the effective series resistance of the actuator, and C_{act} is the effective capacitance of the actuator. It will be seen that this term dominates mechanical response for most practical systems. As an example, a multilayer actuator 18 mm x 5 mm square would typically possess a capacitance of 5 μF. If the drive amplifier (or switch circuit) resistance is say 1 Ω, this gives a t_{res} of 11.5μs. To reduce t_{res}, the resistance must be lowered, but in doing so, the inrush current is proportionally raised.

Charge dumping techniques can be effective in improving this figure, but techniques such as this modify the voltage/current/time profile and can result in excessive voltage and current stress in the device. [4]

b. MECHANICAL RESPONSE.

The dynamic response of a stack or multilayer actuator to a pulse or step change in drive level, must be considered in relation to how the device is mechanically constrained. The breadth of potential applications makes it impossible to exhaustively cover these here. However, there are two cases which cover these applications. These are;

1 One end *fixed* with the other end practically uncoupled, as in a no-work positioning application.

2 One end *fixed* with the other end coupled into a linear compliance.

In either case, the velocity of longitudinal waves in the bulk material is given by [5];

$$c_L^2 = \frac{\lambda + 2.\mu}{\rho}$$

where ρ is density, and λ together with μ are Lame's elastic constants (μ is the transverse rigidity), related to Young's Modulus Y by;

$$Y = \lambda + 2.\mu - 2.\lambda.\nu$$

where ν is Poissons ratio and B is the bulk modulus.

$$B = \lambda + \frac{2}{3}.\mu = \frac{Y}{3(1-2.\nu)}$$

The longitudinal and transverse acoustic phase velocities are given by;

$$c_L = \sqrt{\frac{B + \frac{4}{3}.\mu}{\rho}}$$

and

$$c_T = \sqrt{\frac{\mu}{\rho}}$$

Considering devices as before, of 5mm square section and 18mm length, the zero order resonance will occur at 58 Khz. Given 5 periods to damp out, settling will occur within less than 100 μs.

Case 1 is the simplest. Each element in the ensemble simultaneously experiences identical electrical excitation, and quickly develops strain accordingly. Wave propagation then occurs and partial reflections occur from both ends. Ultimately, the transients will dissipate within a time depending upon the geometry of the actuator, its intrinsic damping (although most devices in the multilayer family are relatively low loss), and the acoustic impedance matching of the interface at the fixed end.

Case 2 is more complex since there is a transmission of energy into the compliance.

6. AMPLIFICATION TECHNIQUES.

Since most applications require output movements much larger than those offered directly by stacks or multilayer devices, some amplifying linkage is required. Two practical approaches are offered by;

a) using flexural hinges (or solid state pivots) in elaborate lever structures to achieve high mechanical advantage or gain e.g. x15 or higher[6].

and

b) the use of impulse transfer into a dynamic system.

a. FLEXURE HINGES.

Such lever systems have the intrinsic advantage of zero backlash, coupled with the possibility of using the spring forces in the structure to pre-load the actuator. Since the movements of the actuator are small (usually <20μm), the range of alternative amplifying techniques is understandably restricted. Flexure hinges made from aluminium alloys such as 2014A (NE15) can be highly stressed whilst potentially offering a long fatigue life.

Flexure hinges are not new[7], but they are ideally suited for adoption by piezo-actuators.

b. IMPULSE TRANSFER.

This technique involves the conversion of the available electro-mechanical energy (or a fraction thereof) into the kinetic energy of another body, usually one of lower mass. This need not involve a direct collision as such, since the energy transfer can occur via an elastic medium already in intimate contact. One advantage of this technique is that the actuator as a whole can deliver an energy impulse at comparatively long range. Existing applications of this principle are embodied in devices such piezo-driven print heads[8] and green-sheet punchers[9]. The projected mass can be a fluid as in the case of ink-jet print heads[10].

Since this approach is a dynamic one, certain applications will necessitate careful timing.

7. CONCLUSIONS.

The maximum mechanical strain energy density value for an actuator is a practical figure of merit for device selection. This figure alone establishes the superiority of multilayer devices over disc stacks.

For two-state operation, electrostrictive actuators may offer an advantage over piezoelectric devices of similar construction, in terms of available work output.

Flexure hinge mechanisms offer a simple and reliable way of amplifying actuator output, particularly for applications requiring static positioning. In addition, the employment of impulse transfer can be combined to achieve comparatively longer ranges for applications not requiring position holding, such as printing, ink-jets and punches.

8. REFERENCES.

1 Piezoelectric and Electrostrictive Materials for Actuators, Bell A.J., School of Materials, University of Leeds, U.K.

2 Driving Voltage Waveform for High-speed Operation of a Piezoelectric Actuator, Kusakabe C. et al, Jap. J. Appl. Phys., Vol 28 (1989) Suppl. 28-1.

3 A Simple way to Reduce Hysteresis and Creep When Using Piezoelectric Actuators, Kaizuka H., Siu B., Jap. J. Appl. Phys., Vol 27, No.5, 1988.

4 Piezoelectric actuators: Powerful and Fast, Schmeisser F., Elektronik (Germany) 1984, Vol 33., Pt. 8.

5 The Physics of Vibrations and Waves, Pain H.J., Wiley and Sons

6 Piezodriven scanner for cryogenic applications, Lloyd J., et.al., Rev. Sci Instrum. 59(9), September 1988.

7 J.M.Paros and L.Weisbord, Mach. Des. 37, 151 (1965).

8 Multilayer Piezoelectric Ceramic Actuators and Their Applications, Takahashi S., Proc. of the sixth Int. Meet. on Ferroelectricity, Jap. J. of Appl. Phys., Vol 24 (1985), Suppl. 24-2.

9 Ceramic Green Sheet Puncher Using Multilayer Piezoelectric Actuator., Yoshida K. et al., Proc. of the 6 th Meeting on Ferroelectric Materials and Their Applications, Jap. J. Appl. Phys., Vol 26 (1987), Suppl. 26-2.

10 PZT Printing Applications, Technologies, New Devices, Lee F., 1988 Ultrasonics Symposium.

A FAST ELECTRO-MECHANICAL CLUTCH ELEMENT USING A PIEZOELECTRIC MULTILAYER ACTUATOR.

Thornley J.K., Preston M.E., King T.G.

SYNOPSIS

Piezoelectric multilayer actuators can rapidly generate very large stall forces. A typical device measuring 18 mm long by 5 mm square will produce an 800 Newton stall force in less than 100 µs, however the small output movement obtained, typically 15 µm, is almost unusable in medium or low precision machines. Efficient amplification or transformation of such movement, with optimisation of the force-displacement product at the output, makes it advantageous to employ piezoelectric multilayer actuators in lower precision, lower cost high-speed machines, such as those involving clutching or gripping.

The mechanism described in this paper is one design in a series of monolithically constructed devices designed around flexure hinges. It generates a 30 Newton stall force, with an unrestrained movement of over 110 µm, derived from a piezoelectric device which only extends by 15 µm. Although the device can not be considered as highly efficient, it transforms the output movement up to a level which can be used directly with components produced to moderate degrees of surface finish. This paper describes a prototype device whose purpose is to rapidly clutch a thin metal strip. This paper details the device and shows performance data including speed of response, electrical clutching energy and mechanical performance.

The efficient displacement amplification of piezoelectric devices is seen as a gateway to many differing applications, currently dominated by the solenoid. Many potential applications exist in the field of Robot Actuation.

1 INTRODUCTION

For many years, techniques of electro-mechanical actuation have been extensively dominated by electro-magnetic devices such as solenoids and rotary motors, and many configurations have emerged. However, the middle to late 1980's saw an upsurgence of interest in the application of piezoelectric and electrostrictive devices, particularly since the advent of the application of multilayer capacitor manufacturing techniques to the production of piezoelectric devices. This has been most in evidence in Japan. In addition, the conversion of manufacturing from the labour intensive stack approach, to the multilayer approach, has meant not only a reduction in unit cost, but a vast improvement of such device parameters as stiffness, speed, reliability, robustness and very importantly, reductions in operating voltage.

Although the output movement directly obtainable from piezoelectric ceramic

multilayer actuators is relatively small, they offer significant advantages over electromagnetic devices in terms of electrical drive speed and mechanical response, of well over an order of magnitude faster than electromagnetic alternatives. In addition they require almost no power to remain in any required state.

Many applications where larger movements are required, necessitate a displacement amplifying linkage of some sort. Solutions to this requirement have been many and varied.

2 DISPLACEMENT AMPLIFICATION

Inspection of piezoelectric actuator bibliography reveals that the amplification techniques used so far, can be broadly categorised into four groups. These are;

1) Hydraulic systems
2) Lever systems
3) Impulse transfer systems
4) Integration systems

2.1 HYDRAULIC SYSTEMS

Applications have emerged where displacement amplification is achieved with piston and bore assemblies where use is made of the properties of two pistons with dissimilar areas in a common hydraulically filled cavity. Two examples of this approach are;

- Ink jet printer heads
- Automotive damper control

There are several problems which can arise with this technique, particularly if the fluid system is closed. This is due to the types of fluids normally used, an their associated thermal bulk expansivity. This can be manifest as large drift in the output movement of the system with temperature. This problem is soluble by selection of different fluids, in combination with thermal matching of the fluid housing.

Further problems can arise from the deformation of seals, but these can be partially overcome by designing the system to operate at quasi-constant pressure, through pre-loading. This approach also allows the bulk rigidity of the fluid housing to be a less dominant design factor.

2.2 LEVER SYSTEMS

This technique, perhaps the most obvious, has been exploited in many areas, and principally involves lever arms of dissimilar lengths to achieve movement amplification. However, simple pivots employing bearing surfaces and knife edges generally tend to suffer from problems associated with high peak stressing and backlash. Since most piezoelectric actuator stacks only deform by a factor of 700 p.p.m., many designers resort to a modified technique involving flexural hinges.

Flexure hinges are simply ligaments which are purposely allowed to distort to facilitate lever action. This technique often solves peak stressing and backlash problems but diminishes the efficiency of the structure, since the hinge absorbs strain energy as a result of deformation. If these losses can be tolerated, then it is possible to design an amplifier with almost unlimited life, provided that great care is taken to ensure that stress concentrations are kept to a low value, typically 10% - 20% of either the U.T.S. or yield strength (where appropriate) of the material.

2.3 IMPULSE TRANSFER SYSTEMS

This category of amplifiers includes such devices as print flight hammers and punchers. The process usually involves rapid deformation of the multilayer device, and the resulting strain energy is coupled to an elastic mechanism. In this process, the energy of deformation is coupled into kinetic energy of the mechanism via a collision. Comparatively large displacements are achievable. This technique lends itself to applications involving a periodic actuation rather than those of steady state.

2.4 INTEGRATION SYSTEMS

This term describes systems in which larger movement is achieved by summing the discrete movements of smaller increments.

Inch-worms and ultrasonic motors fall into this category. They generally produce actuation characteristics with low compliance, low aggregate speed and often discrete motion, and are ideal for stiff, high resolution and long range actuation, e.g. in micropositioning applications.

In addition, there are devices which fall between this category and those described in section 2.3, and can loosely described as inertial caterpillars. These exploit the high speed of extension possible with piezoelectric ceramic actuators.

3 THE CLUTCHING APPLICATION

The design of machine systems in the textiles manufacturing area; knitting, weaving and so-on, has often generated a need for the fast selection and movement of individual threads. The solution to this need has often involved a sometimes undesirable compromise by way of thread grouping, to reduce the number of actuators required. Electronic jacquards often employ a solenoid to latch a reciprocating metal strip to achieve control over a group of warp threads within a loom. A reduction in size of the jacquard would result in the feasibility of one actuator per thread, and hence complete thread control with increased freedom of pattern production. The realisation of such an application might involve the use of a piezoelectric bimorph, whose deformation could steer the path of reciprocating components on to latches.

This is one application of a small high-speed device, and there are many others where a small low-power high-speed device would be advantageous.

4 PERFORMANCE

4.1 STATIC

Having an electro-mechanical nature, the performance of the device is more easily considered from potential energy conversion data. From manufacturers data and structure performance data we have;

PARAMETER	VALUE
Full operating Voltage	100 V
Electrical Capacitance	5 μF
Piezo Free Movement	15 μm
Piezo Stall Force	830 N
Output Free movement	110 μm
Output Stall Force	30 N

Table 2: Device and structure data for the Tokin NLA 5x5x18 / Strip Clutch

4.2 DYNAMIC

The actuator and structure are lightly damped. The highly resonant response, which would be problematic when fast settling is required, is partially damped by the introduction of a visco-elastic polysulphide rubber, moulded into the internal void of

the structure. The E' (complex modulus) coefficient can be tuned by the compound/cure volumetric ratio, to achieve the desired damping response for the ensemble.

A response time of less than 250 μs from the start of rise of the electrical drive, to zero velocity of the first cycle is evident. The resonant frequency of the structure is 2.5 kHz.

5 CONCLUSIONS

A piezoelectrically driven flexural amplifying structure has been designed, constructed and tested, and has shown that structures so designed can perform well, both in terms of speed of response and with respect to the transformation ratio of electrical energy to useful work.

Whilst the design discussed is intended primarily for two state actuation, it is an inherently linear device, which extends it's application to areas where a linearly controllable displacement with high stiffness is required, for example, in high precision gripping applications.

It is possible to design structures possessing even higher gains, but with lower electro-mechanical efficiencies.

It is believed that such structures offer great potential in replacing electromagnetic devices in a wide range of applications. They also offer the potential of high longevity, due to low design stressing and the absence of friction generating surfaces.

A VERY HIGH-SPEED PIEZOELECTRICALLY ACTUATED CLUTCHING DEVICE.

THORNLEY J.K., PRESTON M.E., KING T.G.
Department of Mechanical Engineering
Loughborough University of
Technology, U.K.

SYNOPSIS

Piezoelectric multilayer actuators can rapidly generate very large stall forces. A typical device measuring 18 mm long by 5 mm square will produce an 800 Newton stall force in less than 100 μs, however the small output movement obtained, typically 15 μm, is almost unusable in medium or low precision machines. Efficient amplification or transformation of such movement, with optimisation of the force-displacement product at the output, makes it advantageous to employ piezoelectric multilayer actuators in lower precision, lower cost high-speed machines, such as those involving clutching or gripping.

The mechanism described in this paper is one design in a series of monolithically constructed devices designed around flexure hinges. It generates a 30 Newton stall force, with an unrestrained movement of over 110 μm, derived from a piezoelectric device which only extends by 15 μm. Although the device can not be considered as highly efficient, it transforms the output movement up to a level which can be used directly with components produced to moderate degrees of surface finish. This paper describes a prototype device whose purpose is to rapidly clutch a thin metal strip. This paper details the device and shows performance data including speed of response, electrical clutching energy and mechanical performance.

The efficient displacement amplification of piezoelectric devices is seen as a gateway to many differing applications, currently dominated by the solenoid. Many potential applications exist in the field of Robot Actuation.

1 INTRODUCTION.

For many years, techniques of electro-mechanical actuation have been extensively dominated by electro-magnetic devices such as solenoids and rotary motors, and many configurations have emerged. However, the middle to late 1980's saw an upsurge of interest in the application of piezoelectric and electrostrictive devices[1], particularly since the advent of the application of multilayer capacitor manufacturing techniques to the production of piezoelectric devices[2]. This has been most in evidence in Japan. In addition, the conversion of manufacturing from the labour intensive stack approach, to the multilayer approach, has meant not only a reduction in unit cost, but a vast improvement of such device parameters as stiffness, speed, reliability, robustness and very importantly, reductions in operating voltage[3].

Although the output movement directly obtainable from piezoelectric ceramic multilayer actuators is relatively small, they offer significant advantages over electromagnetic devices in terms of electrical drive speed and mechanical response, of well over

an order of magnitude faster than electromagnetic alternatives. In addition they require almost no power to remain in any required state.

Many applications where larger movements are required, necessitate a displacement amplifying linkage of some sort. Solutions to this requirement have been many and varied.

2 DISPLACEMENT AMPLIFICATION.

Inspection of piezoelectric actuator bibliography reveals that the amplification techniques used so far, can be broadly categorised into four groups. These are;

1) Hydraulic systems
2) Lever systems
3) Impulse transfer systems
4) Integration systems

2.1 Hydraulic Systems.

Applications have emerged where displacement amplification is achieved with piston and bore assemblies where use is made of the properties of two pistons with dissimilar areas in a common hydraulically filled cavity. Two examples of this approach are;

- Ink jet printer heads[4]
- Automotive damper control

There are several problems which can arise with this technique, particularly if the fluid system is closed. This is due to the types of fluids normally used, an their associated thermal bulk expansivity. This can be manifest as large drift in the output movement of the system with temperature. This problem is soluble by selection of different fluids, in combination with thermal matching of the fluid housing.

Further problems can arise from the deformation of seals, but these can be partially overcome by designing the system to operate at quasi-constant pressure, through pre-loading. This approach also allows the bulk rigidity of the fluid housing to be a less dominant design factor.

2.2 Lever Systems.

This technique, perhaps the most obvious, has been exploited in many areas, and principally involves lever arms of dissimilar lengths to achieve movement amplification. However, simple pivots employing bearing surfaces and knife edges generally tend to suffer from problems associated with high peak stressing and backlash. Since most piezoelectric actuator stacks only deform by a factor of 700 p.p.m., many designers resort to a modified technique involving flexural hinges[5].

Flexure hinges are simply ligaments which are purposely allowed to distort to facilitate lever action. This technique often solves peak stressing and backlash problems but diminishes the efficiency of the structure, since the hinge absorbs strain energy as a result of deformation. If these losses can be tolerated, then it is possible to design an amplifier with almost unlimited life, provided that great care is taken to ensure that stress concentrations are kept to a low value, typically 10% - 20% of either the U.T.S. or yield strength (where appropriate) of the material.

2.3 Impulse Transfer Systems.

This category of amplifiers includes such devices as print flight hammers and punchers[4]. The process usually involves rapid deformation of the multilayer device, and the resulting strain energy is coupled to an elastic mechanism. In this process, the energy of deformation is coupled into kinetic energy of the mechanism via a collision. Comparatively large displacements are achievable. This technique lends itself to applications involving a periodic actuation

rather than those of steady state.

2.4 Integration Systems.

This term describes systems in which larger movement is achieved by summing the discrete movements of smaller increments.

Inch-worms and ultrasonic motors fall into this category[6]. They generally produce actuation characteristics with low compliance, low aggregate speed and often discrete motion, and are ideal for stiff, high resolution and long range actuation, e.g. in micropositioning applications.

In addition, there are devices which fall between this category and those described in section 2.3, and can loosely described as inertial caterpillars. These exploit the high speed of extension possible with piezoelectric ceramic actuators[7].

3 THE CLUTCHING APPLICATION.

The design of machine systems in the textiles manufacturing area; knitting, weaving and so-on, has often generated a need for the fast selection and movement of individual threads. The solution to this need has often involved a sometimes undesirable compromise by way of thread grouping, to reduce the number of actuators required. Electronic jacquards often employ a solenoid to latch a reciprocating metal strip to achieve control over a group of warp threads within a loom. A reduction in size of the jacquard would result in the feasibility of one actuator per thread, and hence complete thread control with increased freedom of pattern production. The realisation of such an application might involve the use of a piezoelectric bimorph, whose deformation could steer the path of reciprocating components on to latches.

This is one application of a small high-speed device, and there are many others where a small low-power high-speed device would be advantageous.

4 DEVICE DESIGN.

4.1 Overview.

Device simplicity was taken as an axiom. For this reason, a flexure hinge approach was adopted, since a flexure device can be manufactured monolithically by either milling or E.D.M.. The clutching application specification required a free movement of >100μm and a stall force in excess of 20N. This constitutes an energy coupling of 2mJ. Manufacturers data suggested a compatible actuator would be the Tokin NLA-5x5x18, which produces a free extension of 15μm and a stall force of 830N. This would allow for losses of up to 75% in coupling efficiency.

4.2 Design Techniques.

Mathematical and finite element modelling had shown that the required gain (in excess of x 6) could be achieved with a single lever stage, but that a faster, slightly less efficient design was possible with a two stage system. This design is shown schematically in Figure 1, manufactured from 6mm thick Titanium.

4.3 Materials.

Titanium was chosen in deference to others because of a combination of several properties and are discussed in this section.

4.3.1 Fatigue Strain.

The material must be able to strain to a high a level as possible with low probability of fatigue. This implies a high yield strength, and or U.T.S. We can define a useful parameter;
which should be maximised as far as possible. Note

$$\epsilon_w = \frac{n\sigma_{yield}}{E} \qquad (1)$$

that **n** is a safety factor associated with the structure.

4.3.2 Young's Modulus.

This should be maximised because increasing values of E imply a smaller geometry and hence greater speed of response; see para 4.3.3. From a static design view point, it is difficult to arrive at a high gain design with lower E values since this implies thicker hinges to achieve direct stress stiffness, which in turn increases torsional hinge stiffness, (according to a cubic relationship) which is undesirable.

4.3.3 Speed Of Response.

Simple modelling shows that for a given geometry, a structure's resonant frequency is related to E and density by;
We can therefore write a speed factor for material

$$f_{res} \propto \sqrt{\frac{E}{\rho}} \qquad (2)$$

as;

$$t = \sqrt{\frac{\rho}{E}} \qquad (3)$$

This factor requires minimisation.

4.3.4 Surface Hardness.

This importance of this factor depends on whether the structure itself will perform clutching directly. This is so in this case, and therefore materials such as aluminium alloys are unattractive in this respect. Materials such as titanium and various steels are more suitable for this application.

4.4 Design Method.

ZONE	FREE	STALLED
1	18 MPa	10 MPa
2	38 MPa	34 MPa
3	94 MPa	16 MPa
4	93 MPa	10 MPa

Table 1: Maximum principal stresses within the structure.

This design was developed using a combination of analytical beam modelling and intelligent tuning algorithms, with verification and refinements achieved through finite element analysis.

The design techniques used to produce this structure are complex and will be covered in a future paper. The salient points of the design are that;

1) Under no situation is there more that 20% yield strength stress level, either in normal operation or complete stall or off-load condition. This leads to a long device life with good fatigue characteristics.

2) Each flexure hinge is optimised for high normal and shear stiffness, in combination with a low bending stiffness. This results in an optimised energy coupling factor.

4.5 Finite Element Analysis.

Figure 2 and Figure 3 show the F.E. mesh used for analysis. The graphical output from the analyses is voluble and so the peak principal stresses realized in the four critical zones 1 - 4 are tabulated below.

As stated in para 4.4, the static principal stress levels in the structure are limited by design to within 20% of the material's yield strength. This gives a maximum stress level of 96 MPa, and maximum levels occur exclusively in the thin (0.3mm) flexural hinges (flexors) at the top of the structure. The stress levels in the zones identified in Figure 1 are shown in table 1.

The dynamic stresses in response to device switching are difficult to estimate, but it is unlikely that these will rise by a factor of 2 above those values in table 1.

4.6 Fabrication.

Conventional N.C. milling techniques were used to fabricate the device, however, electric discharge machining does offer certain advantages, and has shown to be a more direct route requiring less sophisticated machine programming. Since the device flexes and generates certain zones where the stress is tensile, surface finish becomes an important factor in reducing the probability of induced fatigue.

5 PERFORMANCE.

5.1 Static.

Having an electro-mechanical nature, the performance of the device is more easily considered from potential energy conversion data. From manufacturers data and structure performance data we know that the piezoelectric force-displacement product is 12.45 mJ, and from measurements, the output force-displacement product is 3.3 mJ, giving a structural energy efficiency of 26.5%.

Note that the electrical energy and the force-displacement product can not be directly compared without considering the energy transformation process; for linear structures such as this one the best coefficient for electrical to mechanical conversion would be 0.5.

Figure 4 shows the output displacement of the structure against excitation voltage for a range of applied loads at the output. The bowing of the curves is directly attributable to non-linearity in the characteristics of the soft piezoelectric material.

5.2 Dynamic.

The actuator and structure are lightly damped. It's ensemble response to a 20% step change in full drive voltage is shown in Figure 5. The highly resonant response, which would be problematic

PARAMETER	VALUE
Full operating Voltage	100 V
Electrical Capacitance	5 μF
Piezo Free Movement	15 μm
Piezo Stall Force	830 N
Output Free movement	110 μm
Output Stall Force	30 N

Table 2: Device and structure data for the Tokin NLA 5x5x18 / Strip Clutch.

when fast settling is required, is partially damped by the introduction of a visco-elastic polysulphide rubber, moulded into the internal void of the structure. The E' (complex modulus) coefficient can be tuned by the compound/cure volumetric ratio, to achieve the desired damping response for the ensemble. A typical result is shown in Figure 6.

Inspection of Figure 6 reveals a response time of less than 250 μs from the start of rise of the electrical drive, to zero velocity of the first cycle. The resonant frequency of the structure is 2.5 kHz.

6 CONCLUSIONS.

A piezoelectrically driven flexural amplifying structure has been designed, constructed and tested, and has shown that structures so designed can perform well, both in terms of speed of response and with respect to the transformation ratio of electrical energy to useful work.

Whilst the design discussed is intended primarily for two state actuation, it is an inherently linear device, which extends it's application to areas where a linearly controllable displacement with high stiffness is required, for example, in high precision gripping applications.

It is possible to design structures possessing even higher gains, but with lower electro-mechanical efficiencies.

It is believed that such structures offer great potential in replacing electromagnetic devices in a wide range of applications. They also offer the potential of high longevity, due to low design stressing and the absence of friction generating surfaces.

7 REFERENCES.

1 King T.G., et. al., Piezoelectric Ceramic Actuators: A Review of Machinery Applications, *Prec. Engg., July 1990, Vol 12, No 3, pp. 131-136*

2 Wersing W., Schnoller M., Wahl H., Monolithic Multilayer Piezoelectric Ceramics, *Ferroelectrics, 1986, Vol. 68, pp. 145-156*

3 Thornley J.K., et.al., Piezoelectric and electrostrictive actuators: device selection and application techniques, *Eurotech Direct '91, Birmingham U.K., Conf. on Machine Systems, Drives and Actuators, Sess. 4, Part 2.*

4 Lee F.C., PZT Printing Applications, Technologies, New Devices, *Ultrasonics Symposium (1988), pp. 693-697*

5 Lloyd J., La Comb, Jr., Quate C.F., Piezodriven Scanner for Cryogenic Applications, *Rev. Sci. Instrum. 59 (9), Sept. 1988, pp. 1906-1910*

6 Schadebrodt G., et. al., The piezo travelling wave motor, *Design Engg., January 1991, pp. 36-40*

7 Higuchi T., Watanabe M., Kudou K., Precise Positioner Utilising Rapid Deformations of a Piezoelectric Element, *J. Jpn. Soc. of Prec. Engg., 1988, Vol. 54, Part 11, pp. 2107-2112*

8 FIGURES.

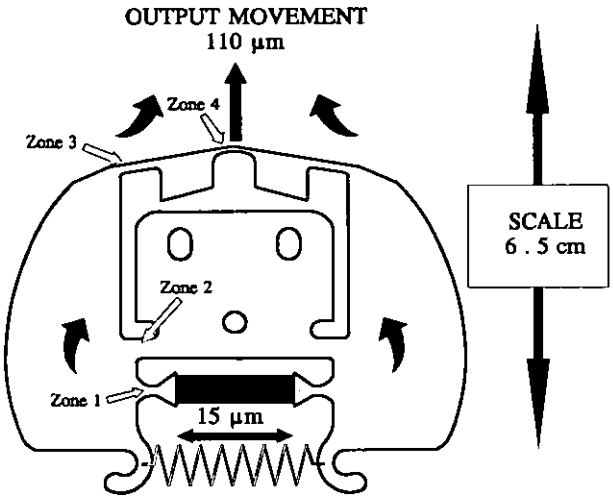

Figure 1 : Clutching Element Schematic.

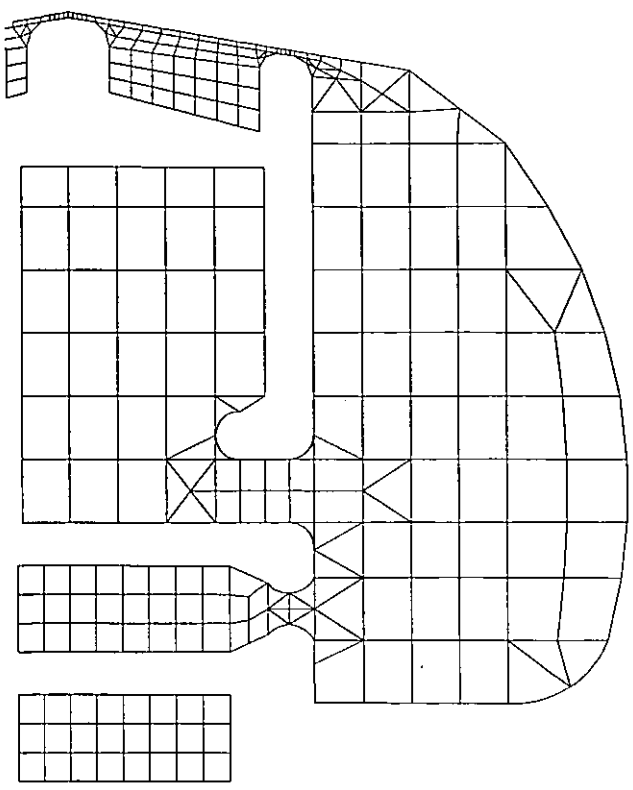

Figure 2 : Finite Element Mesh, Half Structure Shown.

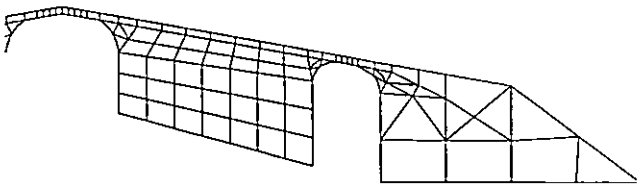

Figure 3: Finite Element Mesh, Bridge Structure Detail.

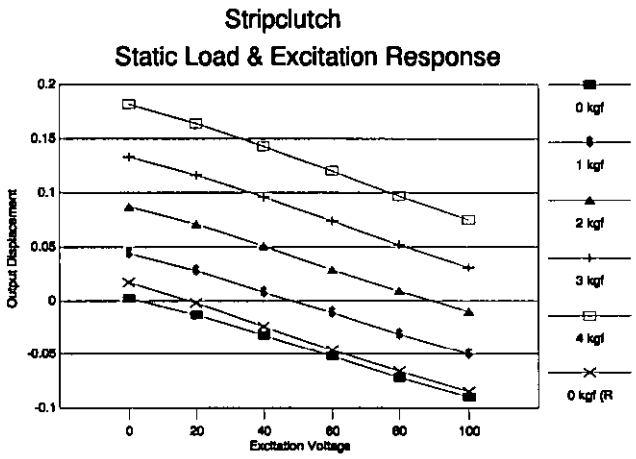

Figure 4: Displacement against excitation voltage.

PIEZOELECTRIC STRIP-CLUTCH
DYNAMIC RESPONSE

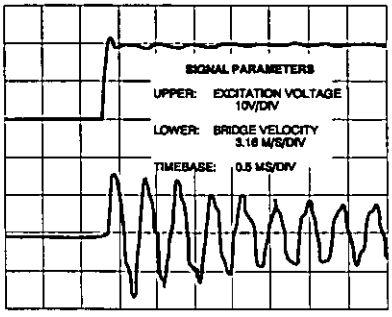

Figure 5: Dynamic response, Output Bridge Velocity for an undamped structure.

PIEZOELECTRIC STRIP-CLUTCH
DYNAMIC RESPONSE

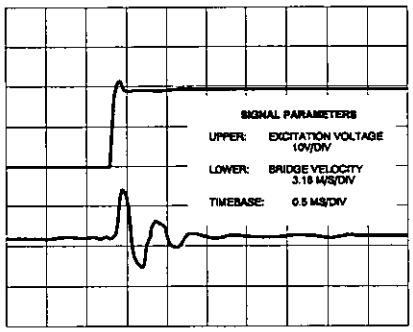

Figure 6: Output Bridge Velocity for a damped structure.

A PIEZOELECTRICALLY-CONTROLLED ROTARY MICROPOSITIONER FOR APPLICATIONS IN SURFACE FINISH METROLOGY.

Mr.J.K.Thornley, Dr.T.G.King, Dr. M.E. Preston
Dept. of Mechanical Engineering
Loughborough University of Technology
Loughborough, Leics, LE11 3TU, England

Abstract: A piezoelectrically-controlled rotary micropositioner is described and evaluated. The device is an application of piezoelectric actuation and clutching, using two simple beam mechanical displacement amplifiers for clutches, each of which generate a free displacement of 100 μm, and a direct acting 15μm actuator to develop incremental extension. The control electronics is dealt with in sufficient detail to allow an appreciation of the overall system, however, the mechanical components specifically designed for clutching and extension are discussed thoroughly. Of particular interest is the design of the piezoelectric displacement amplifiers, which are of monolithic design with force-displacement efficiencies of approximately 70%. In principle, the device is similar to a rotary 'inchworm', but has the added advantage that the rotor components can be manufactured to a much lower tolerance than those required by the inchworm [1].

1. INTRODUCTION.

The device described in this paper was developed for a surface metrology application in which maps of the surface microgeometric deviations of cylindrical test pieces are produced by repeated axial tracing of the test piece (using a stylus instrument), followed by a minute incremental test piece rotation. This procedure enables a 'raster scan' of the specimen surface to be built up. It is important for this application that the rotational increment is both repeatable and finely adjustable and that the mechanism is backlash free, with adequate positional stiffness to maintain the position of the specimen precisely during measurement.

The system described here is of closed loop architecture, with the ability to move or return to a prescribed angular position with repeatability of within 0.001°. The system requirements above demand two essential components. Firstly, a shaft encoder with a high angular resolution and secondly, a motor system capable of the required resolution and stiffness. Both these requirements are met.

2. BASIC DESIGN.

The basic principle by which rotation is produced is analogous to that of the linear 'Inchworm' actuator. In the Inchworm design two clamping collars are alternately clamped to a shaft whilst an extending element between them can vary their separation along the shaft axis. By controlling the sequence of actuation of the clamping and extending elements the device can be 'walked' along the shaft, rather like the caterpillar from which it takes its name. The operation of our rotary device might perhaps be likened to feeding the steering wheel from hand to hand when driving a car. A cross section of the basic machine is shown in Figure 1. The rotor disc is located on the same axis of rotation as the component under investigation, and the motion of the disc is governed by the extension and contraction of three special piezoelectric actuator devices. Two of these devices are clamps with a clamping range of 0.1 mm, the third actuator develops a displacement of 15 μm, tangential to the disk. Despite a very slight arcuate error, sequential stepping and clamping produces discrete rotary motion of the disk. The stepping sequence is shown in Figure 2. Since the radial position of the clamps and extender is at 6.5 cm from the centre, the angular step size on the prototype is approximately 50 seconds of arc. The use of a stainless steel rotor disc allows the clamping mechanisms to be 'single acting' since the disc is easily deflected laterally by the moving clamping surfaces to take up the running clearance between it and fixed clamping surfaces on the opposite side of the disc.

The design described here follows from an earlier prototype which used pre-packaged piezo pushers (Burleigh PZO-015-0) without mechanical amplification. In the previous version, which was of generally similar configuration, the piezo devices used as clamping elements acted directly on the rotor disc. Although this configuration was capable of

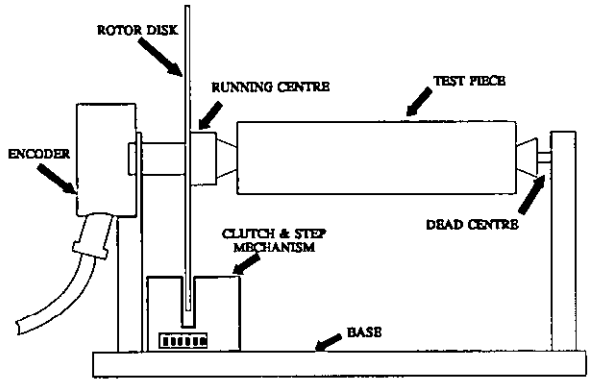

Figure 1: Basic Design of the Rotary Micropositioner.

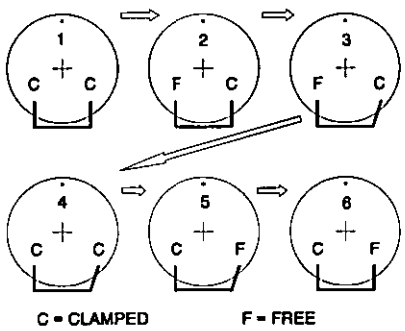

Figure 2: Sequencing of the Clamps and Extender.

generating considerable clamping forces, setting up the clamp clearances to give satisfactory operation was difficult due to the very small displacements available (15 μm). This made it impossible to achieve reliable sustained operation of the device once a small amount of wear and surface damage had taken place on the rotor disc. The second generation device therefore incorporates mechanical amplification of the clamp displacements to overcome these problems.

2.1 MECHANICAL.

The operation is essentially similar to an inchworm except that the mechanical clearances are much greater for the clamping elements, since these are specifically designed to have an operational range of approximately 0.1 mm. This movement is derived from standard *off the shelf* actuators and is transformed by a gain of x6.7 by the structure shown in Figure 3. The actuator dimensions are 2 x 3 x 18 mm.

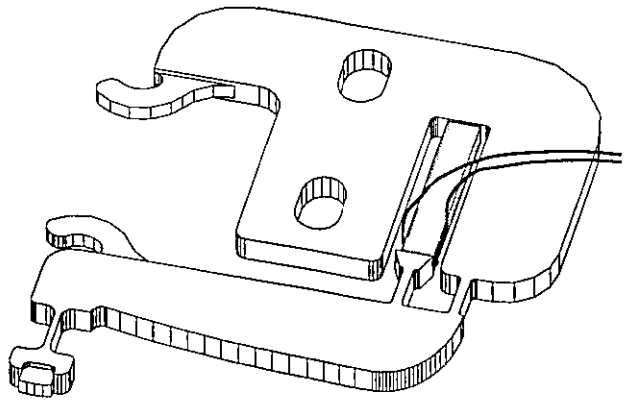

Figure 3: One of the Clamping Amplifiers.

These are custom designed amplifiers [2] which are highly efficient (70% based on force-displacement product) structures with exceptional fatigue characteristics. They are capable of developing maximum stall force of approximately 20 N, but since some of their movement must allow for clearance, only half of this value can practicably generated. Additionally, they are capable of developing this force in approximately 1 ms. The detailed design approach can be found in another paper[2].

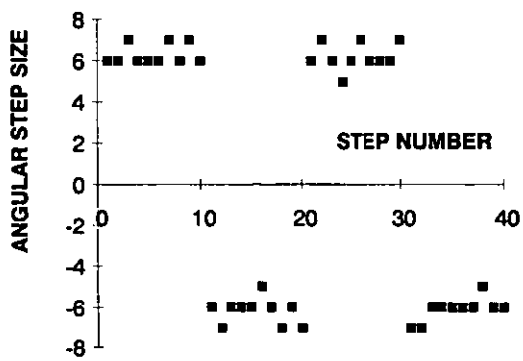

Figure 4: Step Size Variation.

The extender mechanism houses the same type of piezoelectric device as the clamps, but requiring no displacement magnification, the mechanism simply provides

a gripping surface which is very stiff in the direction of the clamping force, but compliant in the direction of the extending actuator. the design of this flexural mechanism is shown in Figure 5. Both the clamps and the extender mechanisms were manufactured using a Wire E.D.M. process.

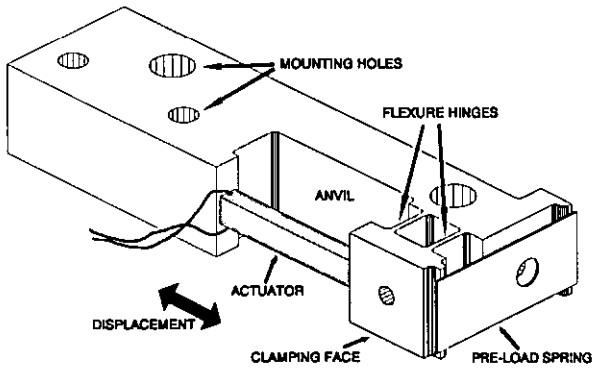

Figure 5: Perspective View of the Extender Mechanism.

2.2 ELECTRICAL.

The overall prototype system is quite simple as can be seen in Figure 6, and details of the electronics have been omitted for clarity. The system is controlled by an IBM compatible personal computer, containing an I/O board with 3 output lines plus several interface lines for the shaft encoder electronics. The system is therefore under software control and can therefore execute any control sequence according to the operators intent.

Because of the variable moment of inertia presented by the mechanism and the mounted test piece, the speed of operation of the extender can not be fully exploited. Devices such as the actuator used, can respond (but not necessarily settle) in less than 0.15 ms. In this application, the clamping force of approximately 10 N would be insufficient to guarantee to avoid shearing against the disk, and so the extender drive is intentionally lagged by a simple resistor to result in a drive rise time of approximately 2 ms (10%-90%). Since there are six phases of operation (see Figure 2), and clamping phases take approximately 1 ms each, this poses a theoretical maximum cycle frequency of 125 Hz; much slower that an inch-worm for example.[1]

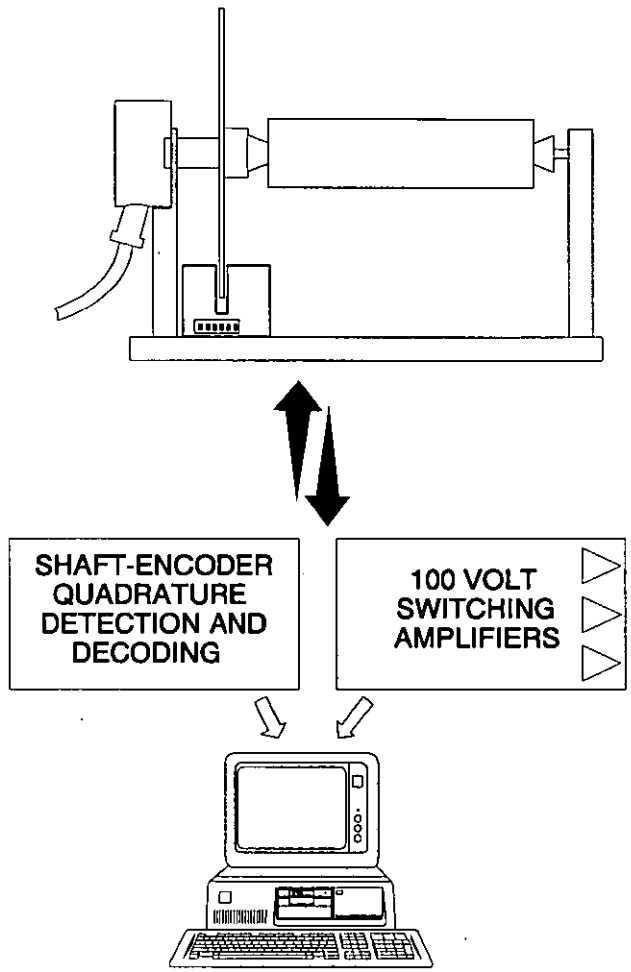

Figure 6: Schematic of the Rotary Micropositioner Control System.

3. PERFORMANCE.

The purpose of the prototype was to establish the feasibility of the control of angular position in this way. There are many factors which could influence the possibility of a design such as this being successful from the point of view of component wear or failure. The long term performance has not been investigated at this time, but its repeatability has been established.

Since the system is intended to be operated in a closed loop architecture, repeatability over many steps - is

unimportant, from the control performance and stability view point. Stiction, deviations from overall linearity, or any variations from repeatability at the step-size level are problematic, but as Figure 6 shows, this does not appear to be a problem. This figure shows step to step variation in the angular variation for 30 successive increments, with two changes in direction. Scatter within ±1 count has been achieved and is acceptable. (This corresponds to a rotational uncertainty of ±25 seconds of arc. The device has been successfully operated up to a' complete-cycle' frequency of 30 Hz resulting in an angular frequency of approximately 500×10^{-6} rad/s. It can sustain a static torque of 0.3 Nm, with no slippage.

4. CONCLUSIONS.

Functionally, this device is comparable with a rotary inch-worm. It is slow however, and in its present form can rotate at only 1½ minutes of arc per second. In the no-slip condition, the angular stiffness of the system is extrememly high and this lends itself to rotary positioning in surface metrology where variability in torque loading could result in shifting of the point of interest.

The prototype has established the feasibility of using displacement amplifiers in this configuration for high-speed clamping or clutching. The adoption of this approach has resulted in tolerance specifications for components which are undemanding by comparison with those normally associated with piezoelectric micro-positioning components; this must bring cost benefits.

5. REFERENCES.

[1] "The Piezo Book", Burleigh Instruments Inc. New York, USA.

[2] Thornley J.K., Preston M.E., King T.G., The Design of Mechanical Amplifiers using Piezoelectric Multilayer Devices for use as Fast Actuators, Conference on 'Mechatronics - The Integration of Engineering Design', IMechE, 22-24 September 1992, University of Dundee.

THE DESIGN OF MECHANICAL AMPLIFIERS USING PIEZOELECTRIC MULTILAYER DEVICES FOR USE AS FAST ACTUATORS.

by Mr.J.K.Thornley, Dr.T.G.King, Dr.M.E.Preston

Dept. of Mechanical Engineering
Loughborough University of Technology
Loughborough, Leics, LE11 3TU, Tel (0509) 263171
Fax (0509) 232029

SYNOPSIS.

The design process leading to the development of a family of mechanical amplifiers which use piezoelectric multilayer actuators as prime movers is described. This includes consideration of choice of materials and the use of finite element and analytical design techniques to arrive at and optimise the design, and ascertain its performance.

It is clear that in the field of actuators, the components available to engineers involved in a Mechatronic design process are mostly of the electromagnetic type, such as solenoids and many variants of the electric motor. Efficient force and displacement transformation is seen as the key to unlocking the potential of applications for modern piezoelectric devices in the Mechatronic sphere. Piezoelectric multilayer actuators can rapidly generate very large stall forces. A typical device measuring 18 mm long by 2 x 3 mm section, will produce a stall force of 200 N in less than 0.2 ms. However, the small, free output movement obtained, typically 15 μm, is almost unusable in medium or low precision machines. Efficient amplification or transformation of such movement, with optimisation of the force-displacement product (at the output), makes it possible to include piezoelectric multilayer actuators into lower precision, lower cost, high-speed machines.

A typical mechanism is described in this paper which generates a 20 Newton stall force, with an unrestrained movement of 100 μm, derived from a piezoelectric device which only produces 15 μm displacement. The device was manufactured and its performance compared to predictions made by a 'designer' program, and is just one in a series of monolithically constructed designs. Although it can not be considered as highly efficient (69%), it transforms the output movement up to a level which can be utilised for applications such as clutching, gripping and latching.

1 INTRODUCTION.

Since piezoelectric multilayer actuators develop maximum displacements in accordance with the electrically producible maximum strain, (typically within the range 600 p.p.m. to 850 p.p.m.), displacement amplification of some type is often advantageous.

The simplest solution to this problem is the obvious one of using a lever system. However, closer inspection of the problem reveals hidden pitfalls associated with hysteresis and wear in bearing surfaces; factors which must be considered when contemplating using pivots with lever systems. The small displacements, typically 10 - 20 μm, and the large potential forces, typically around 100 kgf, eliminate bearing type pivots. However, flexural hinges do not suffer from these problems and can be adopted by the designer in order to facilitate the rotations necessary in lever systems.

2 THE GENERIC SOLUTION.

Figure 1 shows a generalised representation of a flexure hinged displacement amplifier which indicates the topology of the structure, and the variables for which solutions need to be found. The diagram shows linearly tapered beams, and their use is possible, but some justification can be made for the beneficial effect of using beams of elliptical shape. Although this argument is not discussed here, the program was configured to assume elliptical beams.

The design process is as follows;

1) Determine the required output force /

displacement characteristics.

2) Choose an actuator.

3) Select a suitable material and billet thickness.

4) Solve geometry for;

4.1) l_1, l_2, w_1, w_2
4.2) a_1, a_2
4.3) d, e_1, e_2

The aim of the design process is to achieve;

i) A high work efficiency, i.e. the ratio of the force displacement product of the output, to that of the input by the prime mover.

ii) Low stressing in all operational modes to maximise fatigue life.

iii) Minimum size and hence mass and therefore maximum speed of response.

The design procedures outlined in this text have been implemented as a `beam designer' CAD program. This program assists the designer to find an efficient solution based on the following parameters;

i) The material's elastic modulus, billet thickness, yield stress and stress safety factor.

ii) The input parameters of compliance, displacement.

iii) The output displacement required.

iv) Tuning factors associated with compliance matching between various structural zones, selected by the designer, which affect the force displacement efficiency and actuation speed of the design.

3 DESIGN METHODOLOGY.

3.1 OUTPUT FORCE / DISPLACEMENT CHARACTERISTICS.

The requirement of output characteristics is entirely application specific, however it is possible to define a loose working envelope. Firstly, the generic topology can not exist for gains of less than x1. Gains greater than x2 are favoured, with a practical upper limit of approximately x20. In combination with the selection of an actuator, the output displacement determines the gain factor.

The envelope for output force is intimately linked with displacement. A useful criterion for such structures is the force displacement product (See para. 3.2).

3.2 CHOICE OF ACTUATOR.

It is shown later that overall device efficiencies between 50% and 85% are possible, with practical values between 60% and 70%. These figures can be used to select a suitable actuator, also based on the required output characteristics. If the minimum required output force has been determined, in conjunction with the output displacement, this can be referred back to the actuator through the efficiency value. It is conservative initially to select an efficiency of 55% to 60%, and base the actuator selection on this value. For efficiency η, the relationship between input and output forces and displacements is;

$$\eta F_{act} x_{act} = F_{out} x_{out} \qquad (1)$$

3.3 CHOICE OF MATERIAL AND BILLET THICKNESS.

A determining factor for the thickness of material is that of actuator geometry. Billet thicknesses less than the actuator thickness are possible but not recommended. Efficient structures favour thick billets with thin hinges, but extremes here are usually impractical. For reasons associated with stress loading and actuator/billet elastic modulus, values of billet thickness of approximately 120% of the actuator thickness are practical.

3.4 SOLUTION OF GEOMETRY.

The structure is considered in two modes of deformation, specifically;

1) The structure is free at the output, with the input fully driven.

2) The output is stalled or vertically constrained, with the input fully driven.

In both modes, the input is driven through an external compliance. This compliance will usually be associated with the compliance of the actuator.

The finite element analysis of structures of this type has shown that maximum stressing always occurs in

the flexure hinges, as expected. For this reason, the 'beam designer' does not check for stresses in the elliptical beam members.

3.4.1 SOLUTION OF l_1, l_2, w_1, w_2.

Figure 3 indicates the technique employed to find the widths and lengths of the flexure hinges. The vertical compliances of the main beam are considered to be zero. This is a good working approximation and facilitates an effective isolation of l_1, l_2, w_1, w_2. In mode 2, the response of the structure will be approximately manifested as direct stress in both hinges. These stresses can only be determined by knowing the input compliance of the structure in its currently modelled state. The compliance of the drive is given by;

$$s_d = \frac{x_{i_{free}}}{f_{i_{stall}}} \tag{2}$$

The input compliance in mode 2 will be given by;

$$s_i = \frac{\left(\frac{l_1}{w_1} + \frac{l_2}{w_2}\right)}{Eb} \tag{3}$$

For coupling maximum energy into the structure, the perfect situation would be for the input compliance to be zero. This is impossible, so a *tuning factor* is introduced;

$$k_{stall} = \frac{s_i}{s_d} \tag{4}$$

which should be minimised as far as possible, to achieve an acceptable overall efficiency, without the geometry becoming unwieldy. This factor is set in the 'beam designer' program. Typical values lie in the range **0.10** to **0.25**. Should the resulting design be too inefficient, the design process can be repeated.

It can be seen that the aspect ratio of the hinges is deterministic for this relation, in;

$$r_{aspect} = \frac{s_i}{Eb} \tag{5}$$

and this can be chosen to satisfy the stall-stress relation. To solve this, the stall force must be determined by;

$$f_{stall} = \frac{x_{i_{free}}}{(s_i + s_d)} \tag{6}$$

Assuming that the hinges have equal width, and are of equal length, then the widths are fixed by;

$$w_1 = w_2 = \frac{f_{stall}}{b\sigma_{max}} \tag{7}$$

where;

$$\sigma_{max} = n\sigma_{yield} \tag{8}$$

Therefore;

$$l_1 = l_2 = r_{aspect} w_1 \tag{9}$$

3.4.2 SOLUTION OF a_1 AND a_2.

The geometry a_1, l_1, l_2, w_1, w_2, b and Young's Modulus E, will determine the structural loading on the input drive (usually an actuator) in mode 1. This loading must be minimised to optimise efficiency. The only remaining variable to achieve this is $\mathbf{a}_1$. In addition, the selection of this variable must be tempered with the criterion of stress loading.

The relation between input displacement, input force, input compliance and maximum stress is complex and is determined by the solution of simultaneous equations of the third order.

Figure 2 shows the idealised deformation of the flexors at full piezo extension, but with no output load (mode 1). Although this is simplified, we can calculate the maximum stresses due to bending, which will naturally occur at the periphery of flexors, assuming that the stiffness of the main beam remains far greater than that of the flexors.

We know that the extension of the drive component is given by;

$$x_{i_{true}} = x_{i_{free}} \cdot \frac{s_{rot}}{(s_{rot} + s_d)} \tag{10}$$

where $\mathbf{s}_{rot}$ is the input compliance of the structure, and therefore;

$$\theta = \frac{x_{i_{true}}}{a_1} \tag{11}$$

If the beam is sufficiently stiff over the length a_1, we can assume that the top end of the flexors undergo the same angular deflection. Thus;

$$\theta = \frac{x_{i_{true}}}{a_1} = \frac{-Pl_1^2}{2EI_1} + \frac{Ml_1}{EI_1} = \frac{Pl_2^2}{2EI_2} + \frac{(Fa_1 - M)l_2}{EI_2} \tag{12}$$

By a similar argument, the lateral deflection of both

flexors must be approximately equal. And so;

$$\frac{Pl_1^3}{3EI_1} - \frac{Ml_1^2}{2EI_1} = \frac{-Pl_2^3}{3EI_2} - \frac{(Fa_1 - M)l_2^2}{2EI_2} \qquad (13)$$

These equations can be solved to find **F**, **M** and **P** and therefore the input compliance s_{rot} from;

$$s_{rot} = \frac{x_{i_{rot}}}{F} \qquad (14)$$

The maximum stresses within the structure can be estimated by considering the individual contributions from direct force **F**, lateral force **P** and bending moment **M**. The peak stress zones are indicated in Figure 2.

Finding a value for a_1 is achieved by testing solutions for increasing values, and terminating when a value is found which results in a good matching efficiency. This matching value is given by;

$$k_{rot} \leq \frac{s_{rot}}{s_d} \qquad (15)$$

This solution is then tested for stress safety by re-calculating the newly found input compliance. Re-running the torsion algorithm checks for the maximum stress obtained in mode 1, and increases a_1 until the stress value is acceptable.

The final value of a_1 and the input compliance is used to re-calculate the real input movement, as before, and thence the value of a_2, necessary to generate the required output of the structure. The gain is given by;

$$g = \frac{x_o}{x_{i_{rot}}} \qquad (16)$$

and therefore;

$$a_2 = a_1(g-1) \qquad (17)$$

3.4.3 SOLUTION OF **d, e₁, e₂.**

To arrive at an appropriate geometry for this section of the structure, a value for the main beam input compliance must be chosen. There is little point in choosing an excessively low value. For this reason, an input compliance for the beam structure is sought, simply supported at both ends, and measured from the top of hinge 2. The value of this is set to;

$$s_{i_{beam}} = k_{beam}(s_d + s_1 + s_2) \qquad (18)$$

and is found iteratively by locking e_1 = .99 d and $e_2 = e_1$.

Values of **d** beyond this imply geometries which are unnecessarily bulky. It is effectively the sum of the compliances of the two half-beams of the structure, reflected through appropriate pivotal centres. Each component therefore has a *weighting factor* associated with it, derived from geometrical values. The individual components considered are;

i) Compliances due to linear extension/compression of the hinges (flexors) s_{f1} and s_{f2}.

ii) Compliance due to the bending of the two beam structures to the left and right of the axis of the piezo; s_{b1} and s_{b2}.

(Note that stiffness due to the bending of the hinges is ignored.)

If hinge 2 is in compression and the drive experiences the same force, by assuming rotation about h_1 we can say;

$$s_{of2} = s_{f2}\left(\frac{a_2 + a_1}{a_1}\right)^2 \qquad (19)$$

where s_{of2} is the output compliance solely due to hinge 2 compressing. Similarly, by pivoting about hinge 2, we get the effective output compliance due to hinge 1 extension as;

$$s_{of1} = s_{f1}\left(\frac{a_2}{a_1}\right)^2 \qquad (20)$$

The compliances of each hinge s_{f1} and s_{f2} are simply given by;

$$s_{f1} = \frac{l_1}{Ebw_1} \qquad s_{f2} = \frac{l_2}{Ebw_2} \qquad (21)$$

The output compliance of the structure can now be calculated for the case when e_1 and e_2 are nearly d. This compliance is;

$$s_{o_{beam}} = (s_1 + s_{b1})\left(\frac{a_2}{a_1}\right)^2 + (s_2 + s_d)\left(\frac{a_1 + a_2}{a_1}\right)^2 + s_{b2} \qquad (22)$$

From this point, the e_1 and e_2 values are iteratively decreased to reduce mass, and the output compliance allowed to rise, again according to a programmable tuning parameter, i.e.;

$$\frac{s_o}{s_{o_{beam}}} = 1 + k_{beam} \qquad (23)$$

The overall force-displacement efficiency is defined as;

$$\eta_{fd} = \frac{x_{o_{free}} f_{o_{act}}}{x_{i_{free}} f_{i_{act}}} \quad (24)$$

4 A WORKED EXAMPLE.

As an example the program was used to find a solution to the problem of generating a high force output with 100μm displacement, from a Tokin Corp. NLA 2x3x18 Actuator employing a single stage amplifier. The ensuing design was manufactured using an Electric Discharge Machining Process, and assessed for output displacement and output stiffness.

It must be stated that the program does not produce a unique solution for a particular problem since there are many degrees of freedom to solve. Additionally, many design parameters exist which the program calculates but does not solve for, such as device mass.

A piece of 2.5mm thick SAE 4340 steel was chosen as the billet from which the device could be manufactured.

A typical family of solutions is shown in Figure 5. The program control parameter of device efficiency was used to generate this group, and as can be seen, devices approaching 80% efficient can be designed, but with the penalty of increasing device mass. Generally, the resonant frequency and hence speed of response of such a family of devices, can be related to the function;

$$f(m) \propto \frac{1}{\sqrt{m}} \quad (25)$$

and this relationship is shown in Figure 6.

A compromise between response speed and efficiency would normally be resolved by particular factors in a real design problem. For the purpose of the design study, the 70% efficient device was chosen. A screen-dump of the program, running the example is shown in Figure 7. The geometrical data generated by the beam designer program is shown in Table 1.

These values were used to construct a finite element mesh using PIGS 4.2, via the DXF output option of the beam designer. The results obtained from the F.E. analysis are shown in Table 2, along with the values predicted by the beam designer program, and measurements taken from the device. Stress measurements on the device itself were not possible.

Most parameters from either the program or the real device fall within a 12% band of those generated by F.E. analysis. The stress values obtained by the beam designer program were all conservative by this standard, i.e. the actual stresses predicted by the F.E. technique were slightly lower than those predicted by the program. The discrepancies produced are believed by the authors to be mostly due to inadequacies in the modelling which fail to take account of *local* distortions and stresses generated in the beams by the hinges, for example, within the hinge fillets. The `beam designer' modelling also fails to account for distortions of the host structure at the `static' end of the actuator. Most seriously, the F.E.A. prediction of output displacement is poor by comparison with the `beam designer'.

5 CONCLUSIONS.

A methodology has been offered for the design of simple linear displacement amplifiers for use with piezoelectric multilayer actuators. Finite Element Analysis of a structure proposed by the designer program indicated an acceptable degree of correlation between the F.E.A. results, the performance and stressing data generated by the program, and real data obtained by experimental measurement of the real device.

Theoretical results show that highly efficient designs (80%+) are possible, but result in bulky structures. The relationship between device efficiency and device mass is one of diminishing returns, favouring compromises in the region of 50% to 70% force displacement efficiency. This results in device geometry of comparable size to the prime mover.

6 FIGURES.

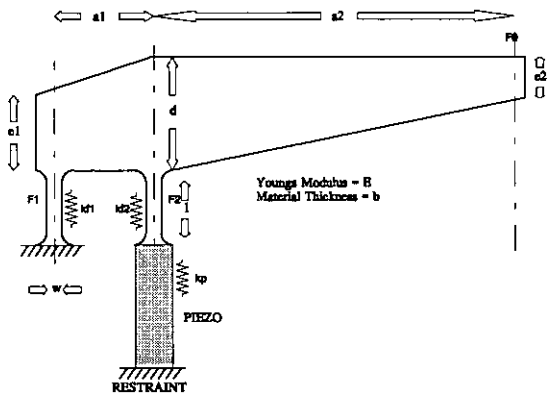

Figure 1: One type of displacement amplifier using flexural hinges.

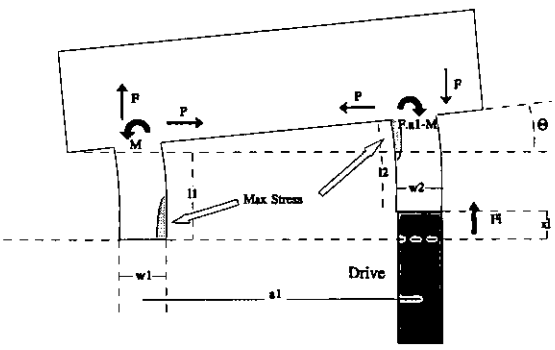

Figure 2: Solution of Hinge Separation.

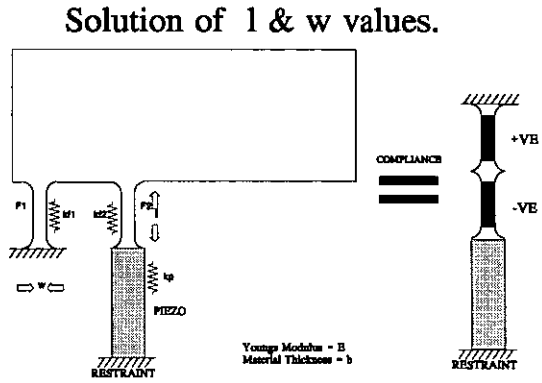

Figure 3: Solution of the Hinge Dimensions.

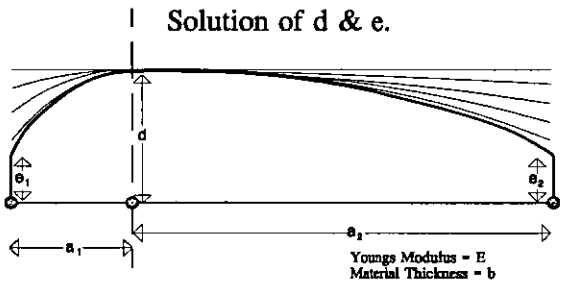

Figure 4: Iterative Solution of **d**, $\mathbf{e}_1$ and $\mathbf{e}_2$ values.

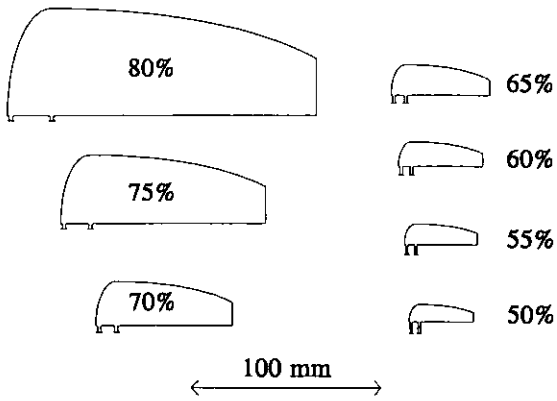

Figure 5: Family of solutions for the 100μm amplifier. Percentages shown refer to structural efficiency.

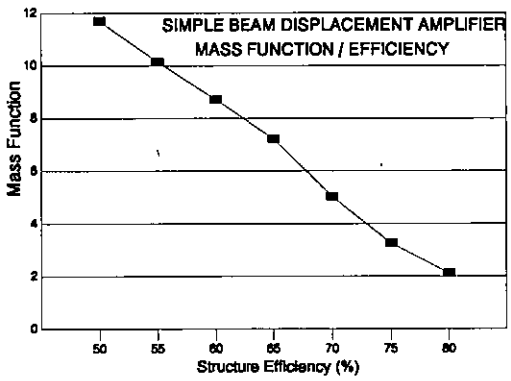

Figure 6: Mass function against efficiency for the 100μm amplifier.

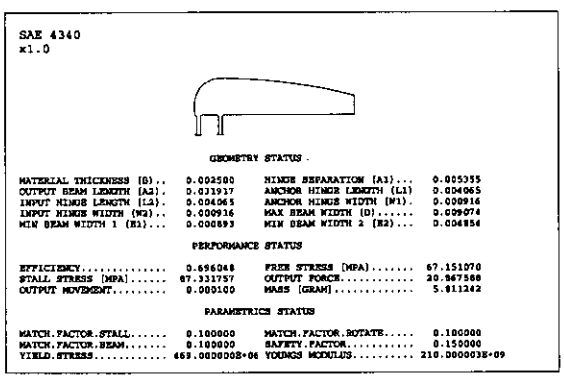

SAE 4340
x1.0

GEOMETRY STATUS

MATERIAL THICKNESS [D]..	0.002500	HINGE SEPARATION [A3]...	0.005355
OUTPUT BEAM LENGTH [A2].	0.031937	ANCHOR HINGE LENGTH [L1]	0.004065
INPUT HINGE LENGTH [L2].	0.004065	ANCHOR HINGE WIDTH [W1].	0.000916
INPUT HINGE WIDTH [W2]..	0.000916	MAX BEAM WIDTH [D].....	0.009074
MIN BEAM WIDTH 1 [R1]...	0.000893	MIN BEAM WIDTH 2 [R2]...	0.004854

PERFORMANCE STATUS

EFFICIENCY.....	0.696048	FREE STRESS [MPA].....	67.151070
STALL STRESS [MPA].....	67.331757	OUTPUT FORCE.....	20.867560
OUTPUT MOVEMENT.....	0.000100	MASS [GRAM].....	5.811242

PARAMETRICS STATUS

MATCH.FACTOR.STALL.....	0.100000	MATCH.FACTOR.ROTATE.....	0.100000
MATCH.FACTOR.BEAM.....	0.100000	SAFETY.FACTOR.....	0.150000
YIELD.STRESS.....	469.0000008+06	YOUNGS MODULUS.....	210.0000038+09

Figure 7: Screen-dump of the Beam Designer program.

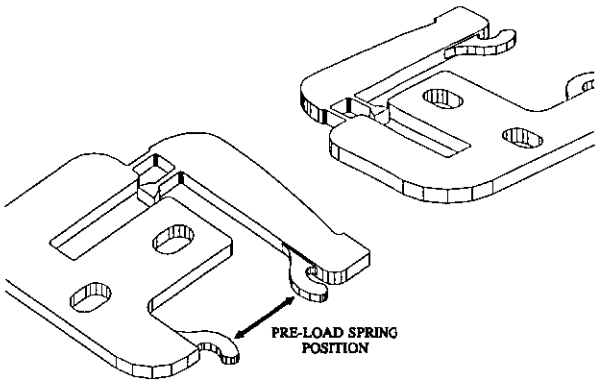

Figure 8: Two Views of the Displacement Amplifier.

Table I: Geometrical data produced by the Beam Designer Program.

DIMENSION	VALUE(mm)
a_1	5.36
a_2	31.90
l_1	4.07
l_2	4.07
w_1	0.92
w_2	0.92
d	9.07
e_1	0.89
e_2	4.85
b	2.50

Table II: Comparison of Modelling Performance with F.E.A. and a Manufactured Device.

PARAM	DESIGN	F.E.A.	REAL
Displacement	100 μm	92 μm	101μm
Stall Force	20.8 N	18.6 N	18.2 N
Stall Stress	87 MPa	72 MPa	-----
Free Stress	67 MPa	59 MPa	-----
Efficiency	69 %	57 %	61%